

METABOLIC ACTIVATION AND DNA-DAMAGING
PROPERTIES OF CARCINOGENIC N-NITROSAMINES

A DISSERTATION
SUBMITTED TO THE FACULTY OF THE GRADUATE
SCHOOL OF THE UNIVERSITY OF MINNESOTA
BY

ERIK STEPHEN CARLSON

IN PARTIAL FULFILLMENT OF THE REQUIREMENTS FOR
THE DEGREE OF DOCTOR OF PHILOSOPHY

ADVISOR: DR. STEPHEN S. HECHT

May 2019

Acknowledgements

My academic journey to a Ph.D. has been made possible by many exceptional people. First, I thank my thesis advisor, Dr. Stephen S. Hecht, for his generous guidance and support during my graduate education. Under his mentorship, I learned many valuable lessons in how to design experiments, accurately interpret data, draw valid conclusions, craft compelling research stories, and learn from both failure and success. Additionally, I appreciate the freedom he gave me in conducting my projects and also being a safety net when I inevitably stumbled over roadblocks. Overall, it is a great privilege to be a part of his prolific career and I hope to extend that legacy with my own independent career.

Next, I want to thank the remainder of the thesis committee: Dr. Jill Siegfried, Dr. Lisa Peterson, and Dr. Steven Patterson. Their insightful comments and critiques helped mold me into the scientist I am today. Individually, I thank Dr. Siegfried for leadership as committee chair and Department Head, Dr. Peterson for her rigorous approach towards science, and Dr. Patterson for providing me my first experiences with organic synthesis and pushing me to think like a chemist. Likewise, I thank the Department of Pharmacology faculty for their academic influences, particularly Dr. Colin Campbell who continually changes the way I view science through his memorable sayings.

Other mentors who were critical to my success are Dr. Silvia Balbo, Dr. Pramod Upadhyaya, and Dr. Ronald Brisbois. Dr. Balbo facilitated my initial training in the Hecht lab and continued to advocate and open doors for me throughout the rest of my graduate career. I look forward to staying connected as cross-country collaborators. Dr. Upadhyaya has shown consistent care, kindness, and day-to-day guidance that I wish all graduate students could experience. Lastly, I thank Dr. Brisbois for demonstrating how to effectively teach students in the classroom and showcasing the ideals of a professor at a primarily undergraduate institution. It was truly inspiring to see him so easily connect with students and positively impact their college experience in and out of the classroom. My short time in his classroom at Macalester gave me insights to academia I could get nowhere else.

I also express gratitude to all past and present Hecht lab members for building a welcoming environment to learn and perform research. Important among them are Dr. Adam Zarth, Dr. Anna Michel, Dr. Bin Ma, Dr. Yupeng Li, Makenzie Pillsbury, Viviana Paiano, Alisa Heskin, Ben Ransom, Brad Hochalter, Steve Carmella, Guang Cheng, Mei-Kuen Tang, and Menglan Chen. I especially want to thank Dr. Zarth for his insightful discussions and willingness to help at any given notice, Dr. Michel for troubleshooting many synthetic difficulties together, Dr. Ma for his proficiency in assay design and implementation, and Dr. Li for his scientific ambition, which will bring abundant success as he carries the torch forward. Additionally I need to thank many members of the Balbo, Stepanov, and Murphy labs including Dr. Alessia Stornetta, Dr. Laura Maertens, Dr. Andrea Carra, Valeria Guidolin, Anshu Jain, Dr. Vipin Jain, Dr. Linda von Weymarn, and Chris Sipe, who have been excellent collaborators, friends, baking partners, and, in one case, bus buddies. Lastly, Robert (Bob) Carlson is the well-oiled machine that keeps the Hecht lab and the rest of CCRB afloat and was critical to my ability to perform and present quality research.

Almost all the work presented herein would be impossible without the instrumentation and expertise of the Analytical Biochemistry Core facility and staff. Dr. Peter Villalta, Xun Ming, Makenzie Pillsbury, and Dr. Yingchun Zhao work tirelessly to ensure all users, including me, receive the highest quality data and almost never leave wondering “where is my peak?”.

I also extend thanks to critical professors and advisors from the University of Minnesota Duluth who prepared me for success in graduate school. Dr. Victor Nemykin and Dr. Viktor Zhdankin sparked my passion for chemistry, Dr. Anne Hinderliter changed the way I think about chemistry, and Dr. Robert Carlson convinced me that a Ph.D. was actually achievable. Lastly, I thank Dr. Joseph Johnson for introducing me to primary metabolism and advising my undergraduate research, an experience that led me to pursue graduate school.

Outside of the lab, I need to first thank my parents for their endless support and encouragement in all aspects of life. Any and all achievements I have or may have in the future are a reflection of their parenting. I also thank other immediate and extended

family members: Lindsey, Ben, Callie, Corrie, Roarie, Rylie, Brooks, Shabba, and Reggie. Additionally, I have been blessed with a great squad of friends throughout Minneapolis and St. Paul including Felipe Pelaez, my best friend for over 20 years, and Nick Boon who have been my roommates over the last 5 years. Similarly, I've had the pleasure of completing my degree alongside many talented classmates who have impacted me more than they know.

Last, but not least, I want to thank my wonderful girlfriend Megan McKeehan. Megan has always supported and lifted me up when I've needed it most, and humbled me when I need to be brought back to earth. She's been there to celebrate many milestones of my academic career including my first publication and I know she will be there to celebrate my last.

Dedication

To my wonderful parents, Kristine and Steven Carlson, whose never-ending support and love make it possible to follow my dreams and accomplish more than I ever imagined.

Abstract

Upon entry into a host, carcinogens are subjected to a variety of Phase I and Phase II metabolic pathways that result in bioactivation or detoxification. The bioactivation pathways are of particular importance because they often generate DNA-damaging compounds. It would stand to reason that fully understanding these activation pathways, their outcomes, and their differences amongst individuals would aid in combating cancer. This dissertation focuses on the metabolic activation of two tobacco carcinogens: 4-(methylnitrosamino)-1-(3-pyridyl)-1-butanone (NNK) and *N'*-nitrosornicotine (NNN). Concepts pertinent to this work such as tobacco carcinogenesis, chemistry of *N*-nitroso compounds, cytochrome P450 metabolism, and tobacco-specific nitrosamines are reviewed.

The first study of this dissertation evaluates a hypothesized metabolic pathway for *N*-nitrosamines: processive P450 oxidation of NNK and NNN to *N*-nitrosamides. In this study, the three corresponding *N*-nitrosamides were synthesized, tested for stability, and monitored for formation *in vitro*. This study shows for the first time that *N*-nitrosamides are direct products of *N*-nitrosamine metabolism by cytochrome P450s. While these compounds were minor metabolites, their relative stability and DNA-damaging properties could impart biological relevance. Determining the generality of this metabolic pathway requires future work.

The second study sought after the structures and abundance of stable 2'-deoxyadenosine (dAdo) damage (DNA adducts) induced by NNK bioactivation. This was accomplished by synthesizing hypothetical dAdo-adduct structures based on known reactivity and applying them to *in vitro* and *in vivo* assays. *In vitro* data indicates that *N*⁶- and *N*¹-adducts are formed, however, *in vivo* data only shows *N*⁶-adduct formation, indicating extensive repair of *N*¹-adducts. The relative abundance of these adducts were determined in rat liver and lung for three different treatment groups. The biological activity of these adducts requires future study.

The last study measured direct biomarkers for human NNN metabolic activation for the first time by using [pyridine-D₄]NNN-enriched tobacco. The deuterium-labelling

allows NNN metabolites to be selectively measured by mass spectrometry and removes all interference by competing nicotine metabolites. This study is ongoing but current data suggests metabolic activation of NNN varies among individuals and is at least partially due to the activity of P450 2A6, the dominant enzyme for NNN bioactivation.

Table of Contents

<i>List of Tables</i>	<i>x</i>
<i>List of Figures</i>	<i>xi</i>
<i>List of Schemes</i>	<i>xiv</i>
<i>List of Abbreviations</i>	<i>xvi</i>
Chapter 1 <i>Overview of Tobacco Carcinogenesis and Bioactivation of N-Nitroso Species</i>	1
1.1 Overview of Tobacco Carcinogenesis	2
1.1.1 Tobacco and Its Relation to Cancer	2
1.1.2 Tobacco-related Chemicals and Carcinogens.....	3
1.1.3 Metabolic Mechanisms of Carcinogen Activation and Detoxification	5
1.1.4 DNA Adducts Resulting from Tobacco Carcinogens	8
1.1.5 Repair of DNA Adducts	10
1.1.6 Mutations, Cancer Initiation and Progression	13
1.2 Chemistry and Carcinogenicity of N-Nitroso Compounds	13
1.2.1 Brief History of N-Nitrosamines and N-Nitrosamides	13
1.2.2 Preparation and Reactivity of N-Nitroso Compounds	14
1.2.3 Exogenous and Endogenous Sources of N-Nitroso Compounds.....	18
1.3 Metabolism of N-Nitrosamines by Cytochrome P450s	20
1.3.1 Structure and Properties of Cytochrome P450s.....	20
1.3.2 General Catalytic Cycle of Cytochrome P450s	21
1.3.3 α , β , and ω -Oxidation of N-Nitrosamines	22
1.3.4 P450 2A6 and 2A13.....	24
1.4 Tobacco-Specific Nitrosamines	26
1.4.1 Overview.....	26
1.4.2 NNN.....	27
1.4.3 NNK.....	33
Chapter 2 <i>N-Nitrosamides are Minor Oxidation Products in N-Nitrosamine Metabolism</i>	40
2.1 Introduction	41

2.2	Experimental Procedures	45
2.2.1	Chemicals and Enzymes	45
2.2.2	General Synthetic Procedures	45
2.2.3	Synthesis of Chemical Standards	46
2.2.4	Determination of $t_{1/2}$ of <i>N</i> -Nitrosamides	53
2.2.5	<i>In vitro</i> detection of CH ₂ -oxo-NNK using P450 2A13	54
2.2.6	<i>In vitro</i> detection of NNC using P450 2A6	55
2.2.7	<i>in vitro</i> Methylation of dGuo by CH ₂ -oxo-NNK	55
2.2.8	<i>in vitro</i> Methylation of calf thymus DNA by CH ₂ -oxo-NNK	56
2.3	Results	57
2.3.1	Synthesis of <i>N</i> -Nitrosamides	57
2.3.2	Stability of <i>N</i> -Nitrosamides	58
2.3.3	<i>In vitro</i> Cytochrome P450-catalyzed Metabolism of NNK to CH ₂ -oxo-NNK	61
2.3.4	<i>In vitro</i> Cytochrome P450-catalyzed metabolism of NNN to NNC	63
2.3.5	<i>In vitro</i> Methylation of dGuo and DNA by CH ₂ -oxo-NNK	64
2.4	Discussion	66
2.5	Conclusion	71
Chapter 3	<i>Formation and Quantitation of 2'-Deoxyadenosine Adducts resulting from NNK Bioactivation in vitro and in vivo</i>	72
3.1	Introduction	73
3.2	Experimental Procedures	76
3.2.1	Chemicals and Enzymes	76
3.2.2	General Synthetic Procedures	76
3.2.3	Synthesis of Chemical Standards	77
3.2.4	<i>In vitro</i> Detection of POB-DNA Adducts using NNKOAc	84
3.2.5	<i>In vivo</i> Detection and Quantitation of POB- and PHB-DNA Adducts in Rat Liver and Lung Tissues	86
3.3	Results	88
3.3.1	Synthesis of DNA Adduct Standards	88
3.3.2	<i>In vitro</i> Detection of 2'-Deoxyadenosine-derived POB adducts	90
3.3.3	<i>In vivo</i> Detection and Quantification of 2'-dAdo Adducts	91
3.4	Discussion	94

3.5	Conclusion.....	100
Chapter 4 Measurement of N'-Nitrosornicotine Bioactivation in Humans Using Deuterium-Labeled Analogs..... 101		
4.1	Introduction.....	102
4.2	Experimental Procedures	104
4.2.1	Chemicals and Enzymes	104
4.2.2	Rat Study	104
4.2.3	Production of [Pyridine-D ₄]NNN-enriched Chewing Tobacco.....	105
4.2.4	Subject Recruitment and Urine Collection	106
4.2.5	Analysis of [Pyridine-D ₄]hydroxy Acid in Tobacco Users' Urine.....	106
4.2.6	Analysis of [Pyridine-D ₄]NNN in Tobacco Users' Urine	107
4.2.7	Cotinine and 3'-Hydroxycotinine	108
4.3	Results	110
4.3.1	Rat Study	110
4.3.2	Tobacco Enrichment and Production.....	110
4.3.3	Urinary Analysis of [Pyridine-D ₄]hydroxy Acid and [Pyridine-D ₄]keto Acid.....	111
4.3.4	Urinary Analysis of Total [Pyridine-D ₄]NNN.....	114
4.3.5	Comparison of "Metabolic Activation Ratio" to "Nicotine Metabolite Ratio".....	116
4.4	Discussion.....	118
4.5	Conclusion.....	123
Bibliography.....		124

List of Tables

Table 3-1: Levels of DNA adducts in lung and liver DNA from rats chronically treated with NNK, (*S*)-NNAL, or (*R*)-NNAL (5 ppm in their drinking water) for 50 weeks. Values are the average of three replicates and their standard deviations. 97

Table 4-1: Accuracy and uniformity of [pyridine-D₄]NNN-enriched tobacco..... 111

List of Figures

Figure 1-1: Chemical structures of nicotine and its major metabolites (A) and several Group 1 carcinogens (B) found in tobacco.....	4
Figure 1-2: General <i>N</i> - and <i>O</i> -glucuronidation of alcohols and amines by UGTs.	6
Figure 1-3: Examples of metabolic activation of carcinogens by Phase I and II metabolism. (A) α -hydroxylation of <i>N</i> -nitrosamines. (B-C) Epoxidation of benzene and benzo[a]pyrene. (D) <i>N</i> -hydroxylation and <i>N</i> -acetylation of PhIP. NAT = <i>N</i> -acetyltransferase, Nu = nucleophile, PhIP = 2-amino-1-methyl-6-phenylimidazo[4,5-b]pyridine.	8
Figure 1-4: (A) Types of DNA adducts and (B) sites of DNA alkylation (denoted in red).	9
Figure 1-5: (A) The general structure of <i>N</i> -nitrosamines and <i>N</i> -nitrosamides. (B) Mechanisms of <i>N</i> -nitrosation by NaNO ₂ , nitrosyl esters, and nitrosyl halides. (C) A formaldehyde catalyzed <i>N</i> -nitrosation mechanism under basic conditions.	15
Figure 1-6: The general catalytic cycle of cytochrome P450 oxidation. This representation is based on a previous reviews ^{135,138,139}	21
Figure 1-7: Chemical structures of known TSNA.	26
Figure 1-8: Chemical structures of NNN-derived adducts measured <i>in vivo</i>	31
Figure 1-9: Chemical structures of POB- and PHB-adducts found in NNK- and NNAL-treated rats.....	37
Figure 2-1: HPLC-UV chromatograms of the decay of (A) NNC, (B) CH ₂ -oxo-NNK, and (C) CH ₃ -oxo-NNK in assay buffer at 37 °C. Chromatograms are the 15-min, 25-min, and 10-min time point for NNC, CH ₂ -oxo-NNK, and CH ₃ -oxo-NNK, respectively. All decomposition products are noted if their identity was supported by a synthetic standard.	59
Figure 2-2: Stability of CH ₂ -oxo-NNK (blue diamonds), CH ₃ -oxo-NNK (green triangles), and NNC (red squares) in reaction buffer at 37 °C. The half-lives were determined to be 35.5, 6.7, and 12.3 min, respectively, by HPLC-UV. Nitrosamide peak areas were normalized to the 0-min peak area and fit to a first-order exponential. Relative amounts of each nitrosamide were determined at each time point in triplicate with error bars denoting the standard deviation.....	60
Figure 2-3: LC-NSI-HRMS chromatograms resulting from the NNK-P450 2A13 incubations. For all sections, the top chromatogram is the accurate parent mass extracted from full scan for CH ₂ -oxo-NNK and CH ₃ -oxo-NNK. The middle and bottom chromatogram is the accurate product ion masses extracted from MS ² fragmentation for CH ₂ -oxo-NNK and CH ₃ -oxo-NNK, respectively. Sections are as follows: (A) CH ₂ -oxo-NNK standard, (B) CH ₃ -oxo-NNK standard, and NNK-P450 2A13 incubations containing all relevant enzymes and cofactors with incubation times of (C) 1 min, (D) 5 min, (E) 10 min, and (F) 60 min. RT = retention time; MA = Mass Area.....	62
Figure 2-4: LC-NSI ⁺ -HRMS chromatograms resulting from the NNN-P450 2A6 incubations. For all sections, the top chromatogram is the accurate parent mass extracted from full scan for NNC. The middle and bottom chromatograms are two accurate product ion masses extracted from MS ²	

fragmentation for NNC. Sections are as follows: (A) NNC standard, and NNC-P450 2A6 incubations containing all relevant enzymes and cofactors with incubation times of (B) 1 min, (C) 5 min, and (D) 10 min. RT = retention time; MA = Mass Area. 64

Figure 2-5: LC-MS/MS chromatograms resulting from in vitro methylation of dGuo and DNA by CH₂-oxo-NNK. For all sections, the top and middle chromatogram are the characteristic SRM transition for 7-meGua (eluting first) and O⁶meGua (eluting second). The bottom chromatogram showcases the SRM transition for the internal standard, [D₃]-O⁶meGua. Chromatograms are as follows: CH₂-oxo-NNK:dGuo type reactions containing (A) no CH₂-oxo-NNK or dGuo, (B) only dGuo, (C) CH₂-oxo-NNK with dGuo; CH₂-oxo-NNK-DNA type reactions containing (D) no CH₂-oxo-NNK or DNA, (E) calf thymus DNA, (F) CH₂-oxo-NNK with calf thymus DNA. 65

Figure 2-6: ¹H-NMR spectra for compound **2.20a** and **2.20b**. The top spectra is of the open-chain conformer, while the bottom spectra is of the lactam conformer 68

Figure 3-1: Structures and fragmentation patterns for the monitored N⁶-dAdo and N¹-dIno adducts. dR: 2'-deoxyribose 86

Figure 3-2: Representative LC-ESI⁺-MS/MS chromatograms for in vitro formation of N⁶-POB-dAdo and N¹-POB-dIno. In each case, the top two channels are monitoring separate transitions for the N¹-POB-dIno adducts (*m/z* 400 → *m/z* 284, 148). The bottom two channels are monitoring the N⁶-POB-dAdo adduct (*m/z* 399 → *m/z* 265) and its isotopically-labeled internal standard (*m/z* 403 → *m/z* 269). 90

Figure 3-3: Representative chromatograms obtained from the LC-ESI⁺-MS/MS analyses of (A) POB- and (B) PHB-DNA adducts in the lungs of rats chronically treated with 5 ppm NNK for 50 weeks. In each case, the top two channels are monitoring separate transitions for the N¹-dIno adducts (POB: *m/z* 400 → *m/z* 284, 148; PHB: *m/z* 402 → *m/z* 286, 132). The bottom two channels are monitoring the N⁶-dAdo adducts (POB: *m/z* 399 → *m/z* 265; PHB: *m/z* 401 → *m/z* 132) and its isotopically-labeled internal standard (POB: *m/z* 403 → *m/z* 269; PHB: *m/z* 406 → *m/z* 132). 91

Figure 3-4: Levels of N⁶-POB-dAdo and N⁶-PHB-dAdo in the liver and lung DNA of rats treated with NNK-, (S)-NNAL, and (R)-NNAL at a dose of 5 ppm in their drinking water for 50 weeks. Values are the average of three replicates and error bars denote their standard deviation. POB- and PHB-adducts are represented in blue and red, respectively. Liver and lung tissue is differentiated by light and dark hues, respectively. 92

Figure 3-5: Representative chromatograms obtained from the LC-NSI⁺-HRMS/MS analyses of POB- and PHB-DNA adducts in the lungs of rats chronically treated with 5 ppm NNK, (S)-NNAL, or (R)-NNAL for 50 weeks. Each channel is monitoring the two most abundant product ions from MS²-fragmentation of a particular DNA adduct. Adduct identity and product ions are the following: (A) N¹-POB-dIno (400 → 283.1300, 265.1194), (B) N¹-PHB-dIno (402 → 286.1296, 268.1191), (C) N⁶-POB-dAdo (399 → 283.1300, 265.1194), (D) [D₄]N⁶-POB-dAdo (403 → 285.1456, 267.1350), (E)

N^6 -PHB-dAdo (401 → 287.1550, 269.1445), (F) [$^{15}N_5$] N^6 -PHB-dAdo (406 → 290.1307, 272.1202).	93
Figure 4-1: Total hydroxy acid levels in the urine of rats treated with 1 nmol of NNN or [pyridine-D ₄]NNN. Blue and red bars indicate [pyridine-D ₄]hydroxy acid and hydroxy acid concentration, respectively. Values are the average of three replicates and error bars denote their standard deviation.	110
Figure 4-2: Urinary levels of total hydroxy acid for each subject. Blue, red, and green bars denote Day 1, Day 2, and Day 3 urine collections. N.D. – Not detectable	111
Figure 4-3: Representative LC-ESI ⁺ -MS/MS chromatograms for total hydroxy acid. In each case, the top two channels are monitoring separate transitions for derivatized [pyridine-D ₄]hydroxy acid (m/z 298 → m/z 182, 148). The bottom two channels are monitoring derivatized $^{13}C_6$ - 4.9 (m/z 300 → m/z 184, 124).	112
Figure 4-4: Urinary total hydroxy acid plotted against estimated [pyridine-D ₄]NNN dose.....	113
Figure 4-5: Comparison of Total Hydroxy Acid levels with and without NaBH ₄ reduction during the assay.	114
Figure 4-6: Representative LC-ESI ⁺ -MS/MS chromatograms for total [pyridine-D ₄]NNN. In each case, the top two channels are monitoring separate transitions for [pyridine-D ₄]NNN (m/z 182 → m/z 152, 124). The bottom two channels are monitoring [$^{13}C_6$]NNN (m/z 184 → m/z 154, 126).....	115
Figure 4-7: Urinary levels of total [pyridine-D ₄]NNN in each subject. Blue, red, and green bars denote Day 1, Day 2, and Day 3 urine collections. N.D. – Not detectable	115
Figure 4-8: Metabolic Activation Ratio (total hydroxy acid/ total [pyridine-D ₄]NNN) for each subject arranged in ascending order. Based on error bars, three potential activation groups are denoted: low, medium, and high.....	116
Figure 4-9: Metabolic Activation Ratio plotted against Nicotine Metabolite Ratio, a phenotypic marker for P450 2A6 activity. The red data point is Subject 1 whom had abnormally high Day 2-[pyridine-D ₄]hydroxy acid excretion.	117

List of Schemes

Scheme 1-1: Mechanism and downstream outcomes of nucleobase depurination.	10
Scheme 1-2: Representative reactions of N-nitrosamines. N-nitrosamines can be nitrosated with conc. HCl, alkylated with strong base and electrophiles, reduced, and oxidized. E ⁺ = halides, aldehydes, ketones, esters, α,β -unsaturated ketones, and other electrophiles.	16
Scheme 1-3: (A) General mechanism for hydrolysis of N-nitrosamides. (B) Thermal decomposition of N-nitrosamides by a [1,3] sigmatropic rearrangement resulting in an N ₂ -separated ion pair.	17
Scheme 1-4: Mechanisms of (A) α -hydroxylation, (B) β -oxidation and decomposition of N-nitrosodipropylamine, and (C) tandem ω -oxidation-Knoop-type β -oxidation of even-chained N-nitrosomethylalkylamines to N-nitroso-3-carboxypropylamine. n = any even number	23
Scheme 1-5: Overall metabolism of NNN	29
Scheme 1-6: Metabolism of NNK and NNAL <i>in vivo</i>	34
Scheme 2-1: (A) Established <i>in vivo</i> metabolism of NNK (2.1) and NNN (2.2) by P450 2A13- or P450 2A6-mediated oxidation, respectively. Oxidation results in unstable α -hydroxynitrosamines (2.3 – 2.6) which spontaneously decompose to diazohydroxides (2.7 – 2.9). These either hydrolyze to products excreted in the urine (2.10 – 2.12) or react with DNA to form adducts. (B) Proposed P450-mediated oxidation of NNK (2.1) and NNN (2.2) to N-nitrosamides (2.13 – 2.15) through retention of the α -hydroxynitrosamines 2.3, 2.4, and 2.6 within the P450 active site.	42
Scheme 2-2: Synthesis of Nitrosamides (A) Methyl Acrylate, NaCN, DMF, 40 °C, 4h; (B) NaOH, H ₂ O, RT, 3h; (C) EDAC, NHS, MeNH ₂ •HCl, DMSO, RT, 22h; (D) NaNO ₂ , Ac ₂ O:HOAc, 0 °C, 4h; (E) HS(CH ₂) ₃ SH, BF ₃ •OEt ₂ , THF, 80 °C, 24h; (F) (i) n-BuLi, TMEDA, THF, -78 °C, 1h; (ii) 27, THF, -78 °C to RT, 16h; (G) 25% TFA, CH ₂ Cl ₂ , RT, 3h; (H) HCO ₂ Me, Et ₃ N, MeOH, 55 °C, 4h; (I) AgNO ₃ , NCS, MeCN:H ₂ O (1:1), 0 °C, 30 min; (J) Boc ₂ O, Et ₃ N, CH ₂ Cl ₂ , RT, 30 min; (K) I ₂ , PPh ₃ , Im., CH ₂ Cl ₂ , 0 °C-RT, 22h	57
Scheme 2-3: (A) Mechanism of hydrolysis of nitrosamides. Hydrolysis results in a carboxylic acid and an alcohol via a transient diazohydroxide that decomposes to a diazonium ion. (B) The hypothesized decomposition products of CH ₂ -oxo-NNK, CH ₃ -oxo-NNK, and NNC in assay buffer (pH = 7.4) at 37 °C.	60
Scheme 3-1: Overview of NNK (3.2) and NNAL (3.3) metabolism and DNA adduct formation <i>in vivo</i> . NNK is in enzymatic equilibrium with NNAL, which is commonly glucuronidated. Both NNK and NNAL can alternatively be oxidized to α -hydroxynitrosamines 3.4 or 3.5. These further decompose to diazonium ions 3.8 or 3.9 and ultimately hydrolyze to 3.10 or 3.11, or form DNA adducts.	73
Scheme 3-2: Proposed mechanism for dAdo adduct formation. After initial N ¹ -alkylation, the resulting cationic intermediate either undergoes Dimroth rearrangement or deamination to yield N ⁶ -dAdo (3.20-3.21) or N ¹ -dIno (3.22-3.23) DNA adducts, respectively.	75

Scheme 3-3: Synthetic route for N^6 -PHB-dAdo and N^6 -POB-dAdo. dAdo = 2'-deoxyadenosine, TFA = trifluoroacetic acid, NCS = <i>N</i> -chlorosuccinimide.....	88
Scheme 3-4: Synthetic Scheme for (A) N^1 -POB-dIno and (B) N^1 -PHB-dIno. TBSCl = <i>tert</i> -butyldimethylsilyl chloride, Imid = imidazole, Pyr = pyridine, DMF = <i>N,N</i> -dimethylformamide, DCM = dichloromethane, TMEDA = <i>N,N,N,N</i> -tetramethylethylenediamine, TBAF = tetra- <i>n</i> -butylammonium fluoride.....	89
Scheme 4-1: Convergent metabolism of NNN and nicotine <i>in vivo</i>	102
Scheme 4-2: Metabolism of [pyridine- D_4]NNN and nicotine. Due to the deuterium-labeling, metabolites are distinguishable by LC-MS analysis.....	104
Scheme 4-3: Known metabolism of NNN in patas monkeys.....	122

List of Abbreviations

5-HC	5'-hydroxycotinine
11 β -HSD1	11-beta-hydroxysteroid dehydrogenase 1
7-Me-dGuo	<i>N</i> ⁷ -methyl-2'-deoxyguanosine
7-POB-dGuo	<i>N</i> ⁷ -(4-oxo-4-(3-pyridyl)-1-butyl)-2'-deoxyguanosine
7-POB-Gua	<i>N</i> ⁷ -(4-oxo-4-(3-pyridyl)-1-butyl)guanine
7-PHB-Gua	<i>N</i> ⁷ -(4-hydroxy-4-(3-pyridyl)-1-butyl)-guanine
A ₂₅₄	Absorbance at 254 nm
AGT	<i>O</i> ⁶ -alkylguanine DNA alkyltransferase
AKR	aldo-keto reductase
AP	apurinic
APE1	AP endonuclease 1
B _{1p} (POB)B ₂	B _{1p} (4-oxo-4-(3-pyridyl)-1-butyl)B ₂
B _{1p} (PHB) _s B ₂	B _{1p} (4-hydroxy-4-(3-pyridyl)-1-butyl)B ₂ (s = straight)
B _{1p} (PHB) _b B ₂	B _{1p} (4-hydroxy-4-(3-pyridyl)-1-butyl)B ₂ (s = branched)
BER	base excision repair
Boc	<i>tert</i> -butylcarbamate
bs	broad singlet
CH ₂ -oxo-NNK	4-(methylnitrosamino)-1-(3-pyridyl)-1-butanedione
CH ₃ -oxo-NNK	4-(nitrosoformamido)-1-(3-pyridyl)-1-butanone
CID	collision-induced dissociation
CR	carbonyl reductase
CV	coefficient of variation
d	doublet
dAdo	2'-deoxyadenosine
dCyd	2'-deoxycytidine
dGuo	2'-deoxyguanosine
DCM	dichloromethane
dd	doublet of doublets
ddd	doublet of doublets of doublets

DIPEA	<i>N,N'</i> -diisopropylethylamine
DLPC	dilauroylphosphatidylcholine
DMF	<i>N,N'</i> -dimethylformamide
DMSO	dimethylsulfoxide
dR	2'-deoxyribose
dt	doublet of triplets
EDAC	1-ethyl-3-(3-dimethylaminopropyl)carbodiimide
eV	electronvolts
FAD	flavin adenine dinucleotide
FMN	flavin mononucleotide
GABA	gamma-aminobutyric acid
GMP	good manufacturing practice
HCD	Higher-energy collisional dissociation
HEPA	high-efficiency particulate air
HPB	4-oxo-4-(3-pyridyl)-butanol
HPLC	high performance liquid chromatography
HRMS	high resolution mass spectrometry
IARC	International Agency for Research on Cancer
Im/Imid.	imidazole
LC-ESI ⁺ -MS/MS	liquid chromatography-positive electrospray ionization-tandem mass spectrometry
LC-MS/MS	liquid chromatography-tandem mass spectrometry
LC-NSI ⁺ -HRMS/MS	liquid chromatography-positive nanoelectrospray ionization-high resolution tandem mass spectrometry
Lactol	5-(3-pyridyl)-2-hydroxytetrahydrofuran
LDA	lithium diisopropylamide
LOD	limit of detection
<i>m/z</i>	mass to charge ratio
MA	mass area
<i>N</i> ¹ -POB-dIno	<i>N</i> ¹ -(4-oxo-4-(3-pyridyl)-1-butyl)-2'-deoxyinosine

<i>N</i> ¹ -POB-dIno	<i>N</i> ¹ -(4-hydroxy-4-(3-pyridyl)-1-butyl)-2'-deoxyinosine
<i>N</i> ³ -POB-dCyd	<i>N</i> ³ -(4-oxo-4-(3-pyridyl)-1-butyl)-2'-deoxycytidine
<i>N</i> ⁴ -POB-dCyd	<i>N</i> ⁴ -(4-oxo-4-(3-pyridyl)-1-butyl)-2'-deoxycytidine
<i>N</i> ⁶ -PHB-dAdo	<i>N</i> ⁶ -(4-hydroxy-4-(3-pyridyl)-1-butyl)-2'-deoxyadenosine
<i>N</i> ⁶ -POB-dAdo	<i>N</i> ⁶ -(4-oxo-4-(3-pyridyl)-1-butyl)-2'-deoxyadenosine
NAB	<i>N</i> '-nitrosoanabasine
NADP ⁺	nicotinamide adenine dinucleotide phosphate
NADPH	nicotinamide adenine dinucleotide phosphate (reduced)
NAT	<i>N</i> '-nitrosoanatabine
NCS	<i>N</i> -chlorosuccinimide
NDMA	<i>N</i> '-nitrosodimethylamine
NEIL1	endonuclease VIII-like 1
NER	nucleotide excision repair
NHS	<i>N</i> '-hydroxysuccinimide
NNA	4-(methylnitrosamino)-4-(3-pyridyl)butanal
NNAL	4-(methylnitrosamino)-1-(3-pyridyl)-1-butanol
NNC	<i>N</i> '-nitrosonorcotinine
NNK	4-(methylnitrosamino)-1-(3-pyridyl)-1-butanone
NNKOAc	4-(acetoxynitrosamino)-1-(3-pyridyl)-1-butanone
NNN	<i>N</i> '-nitrosonornicotine
NO _x	nitric oxide species
nts	nucleotides
Nu	nucleophile
<i>O</i> ² -POB-Cyt	<i>O</i> ² -(4-oxo-4-(3-pyridyl)-1-butyl)-cytosine
<i>O</i> ² -POB-dCyd	<i>O</i> ² -(4-oxo-4-(3-pyridyl)-1-butyl)-2'-deoxycytidine
<i>O</i> ² -POB-Thd	<i>O</i> ² -(4-oxo-4-(3-pyridyl)-1-butyl)-thymidine
<i>O</i> ² -PHB-dThd	<i>O</i> ² -(4-hydroxy-4-(3-pyridyl)-1-butyl)-thymidine
<i>O</i> ⁶ -Me-dGuo	<i>O</i> ⁶ -methyl-2'-deoxyguanosine
<i>O</i> ⁶ -MeGua	<i>O</i> ⁶ -methyl-guanine

<i>O</i> ⁶ -POB-dGuo	<i>O</i> ⁶ -(4-oxo-4-(3-pyridyl)-1-butyl)-2'-deoxyguanosine
<i>O</i> ⁶ -PHB-dGuo	<i>O</i> ⁶ -(4-hydroxy-4-(3-pyridyl)-1-butyl)-2'-deoxyguanosine
OGG1	8-oxo-guanine glycosylase 1
PAH	polyaromatic hydrocarbon
PBS	phosphate buffered saline
PHB	pyridylhydroxybutyl
PhIP	2-amino-1-methyl-6-phenylimidazo[4,5-b]pyridine
POB	pyridyloxobutyl
POR	NADPH-cytochrome P450 oxidoreductase
ppm	parts per million
Py-Py	pyridyl-pyrrolidine
Py-Py-dIno	2-(2-(3-pyridyl)- <i>N</i> -pyrrolidinyl)-2'-deoxyinosine
Py-Py-dNeo	6-(2-(3-pyridyl)- <i>N</i> -pyrrolidinyl)-2'-deoxynebularine
q	quartet
RT	retention time
s	singlet
SPE	solid-phase extraction
SRM	selected reaction monitoring
t	triplet
<i>t</i> _{1/2}	half life
TBAF	tetra- <i>n</i> -butylammonium fluoride
TBS-Cl	<i>tert</i> -butyldimethylsilyl chloride
TFA	trifluoroacetic acid
Thd	thymidine
THF	tetrahydrofuran
TLC	thin-layer chromatography
TMEDA	<i>N,N,N,N</i> '-tetramethylethylenediamine
TSNA	tobacco-specific nitrosamine
UGT	uridine-diphosphate glucuronosyltransferases
UV	ultraviolet

Chapter 1 Overview of Tobacco Carcinogenesis and Bioactivation of *N*-Nitroso Species

The following chapter gives background and context to the studies carried out in this dissertation. Principles of tobacco carcinogenesis, properties of *N*-nitroso compounds, and mechanisms of *N*-nitrosamine metabolism, in the context of *N'*-nitrosonornicotine (NNN) and 4-(methylnitrosamino)-1-(3-pyridyl)-1-butanone (NNK), will be discussed.

1.1 Overview of Tobacco Carcinogenesis

1.1.1 Tobacco and Its Relation to Cancer

America has a long and painful history with tobacco¹. As early as 1 B.C., tobacco was smoked by Native American tribes for ceremonial and, ironically, medicinal purposes. The tobacco plant was later given to Christopher Columbus as a gift during his famous 1492 voyage to the New World, and brought back to Europe where it became one of the world's most desired commodities. This transformed tobacco into one of America's first cash crops and even a colonial currency in Virginia. It wasn't until the 1900s, however, that tobacco began being sold in the form of cigarettes we see today². Near the peak of tobacco use in the early 1960's, when 53% of men and 33% of women were regular smokers, over 4,000 per capita cigarettes were smoked annually³. This great rise in cigarette use was driven foremost by nicotine addiction, but also fueled by misleading advertisement campaigns and limited evidence directly linking tobacco to adverse health effects⁴. In 1964, the perception of tobacco changed with the release of the Surgeon General Report where it was noted that "cigarette smoking is causally related to lung cancer ... and is a health hazard of sufficient importance in the United States to warrant appropriate remedial action"⁵. Due to the objective and authoritative approach of this report and the other Surgeon General Reports released in subsequent years⁴, health scientists and legislators began implementing changes to product labeling, advertising, taxation, and tar content while also executing plans to limit involuntary exposure and aid in cessation. Meanwhile, other types of tobacco and routes of exposure, such as smokeless products and second-hand smoke, were shown to cause cancer. These and many other public policies over the last 50 years have dramatically decreased the amount of tobacco users in the United States and overall in the world⁴; however, the amount remaining is not trivial.

As of 2016, an estimated 38,000,000 adults in the United States were smokers, while ~1,000,000,000 adults smoked worldwide⁶. The statistics are significantly less with smokeless tobacco (9,000,000 U.S⁷; ~350,000,000 worldwide⁸) but still notable due to its known carcinogenic properties⁹. This persistent tobacco use causes 480,000 deaths

annually in the U.S.⁴, maintaining its status as the leading preventable cause of death. Of these deaths, 160,000 are cancer-related which accounts for 32% of all U.S. cancer deaths¹⁰. While it is known that tobacco causes ~90% of all lung cancers¹¹, tobacco smoking has also been linked to cancers of the larynx, pharynx, oral cavity, esophagus, pancreas, nasal cavity, stomach, bladder, liver, cervix, and colorectum⁴. Together, this illustrates that while we have made significant progress since 1964, tobacco-related cancer is still a significant health concern that requires continued study to understand the over-arching health impacts of tobacco, identify cancer-susceptible individuals, and elucidate the chemical mechanisms of tobacco carcinogenesis.

1.1.2 Tobacco-related Chemicals and Carcinogens

Tobacco smoke is known to contain >7000 chemicals including carbon monoxide, ammonia, lead, arsenic, and polycyclic aromatic hydrocarbons¹². One of the most important, non-carcinogenic species in tobacco is nicotine (**Figure 1-1**), the addictive compound that encourages tobacco users to repeatedly use the product. On average, one cigarette contains 7 – 14 mg of nicotine which is ~2% of the dry weight of tobacco¹³. While the complex mechanisms of nicotine addiction are outside the scope of this thesis, it is generally accepted that nicotine releases dopamine in the ventral tegmental region of the brain via nicotinic acetylcholine receptor signaling¹⁴. Glutamate¹⁵ and gamma-aminobutyric acid (GABA)^{16,17} have been shown to be upregulated and contribute to the rewarding effects of nicotine as well. Chronic activation of these receptors and release of dopamine^{18,19} ultimately leads to the hallmark phenotypes of psychological and physical dependence to nicotine, which are demonstrated during withdrawal. It is these aspects of nicotine that are particularly troubling as this addiction is remarkably hard to break whether at a young or adult age. For that reason, many who begin using tobacco are unable to quit in their lifetime and forced into repeated exposure to carcinogens.

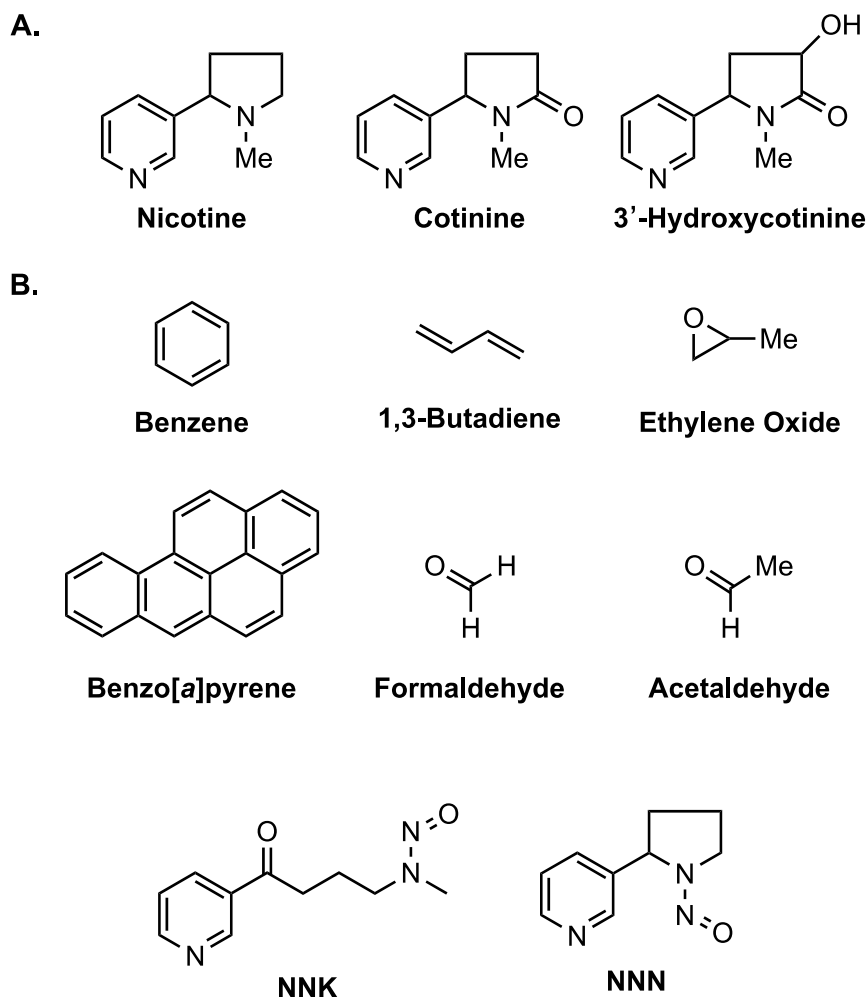


Figure 1-1: Chemical structures of nicotine and its major metabolites (A) and several Group 1 carcinogens (B) found in tobacco smoke

To date, at least 70 chemical carcinogens have been identified in tobacco smoke. **Figure 1-1** displays a few of these including two tobacco-specific nitrosamines: 4-(methylnitrosamino)-1-(3-pyridyl)-1-butanone (NNK) and *N'*-nitrosornicotine (NNN), which will be more thoroughly discussed in **Section 1.4**. All of these compounds have been evaluated as carcinogenic to humans, or Group 1 carcinogens, by the International Agency for Research on Cancer (IARC). In comparison to nicotine, these compounds are generally much less abundant; however, still exhibit strong tumorigenic effects. For example, chronic administration of NNK at 5 ppm in drinking water induces tumors in rats²⁰. Many of these substances alkylate or intercalate DNA where NNK and benzo[*a*]pyrene are prominent examples, respectively. While some tobacco carcinogens

act directly, many require metabolic activation to exert their effects, which is often counteracted by a variety of detoxification pathways.

1.1.3 Metabolic Mechanisms of Carcinogen Activation and Detoxification

Humans have evolved many enzymatic routes to metabolize and eliminate foreign chemical entities broadly referred to as xenobiotics. Xenobiotics can include any compound originating outside the body such as medicines, vitamins, metals, and carcinogens. Metabolism of these compounds is traditionally divided into two main categories: Phase I and Phase II. While outside the scope of this dissertation, Phase III metabolism, recognized as further enzymatic processing of metabolites like that seen in the mercapturic acid pathway²¹, and human microbial metabolism^{22,23} are also important areas of research.

Phase I metabolism is generally defined as enzyme-mediated oxidation, reduction, and hydrolysis for the purpose of increasing polarity and introducing functional handles for Phase II metabolism. A key example of Phase I metabolism is oxidation by cytochrome P450s. This class of enzymes can perform a diverse set of reactions including carbon and heteroatom hydroxylation, *O*-, *N*-, and *S*-dealkylation, epoxidation, and structural rearrangements²⁴. These enzymes and their mechanisms will be more thoroughly discussed in **Section 1.3**. Other examples of Phase I metabolism pertinent to this thesis includes alcohol oxidation²⁵, carbonyl reduction²⁶, and ester hydrolysis²⁷.

Phase II metabolism is generally thought to be enzyme-mediated conjugation chemistry²⁸. Similar to Phase I metabolism, these transformations typically increase the polarity of the xenobiotic, which aids in its urinary excretion. Examples of this include sulfation²⁹, acetylation³⁰, methylation³¹, glutathione conjugation³², and *O*- and *N*-glucuronidation³³, which is most relevant to this dissertation.

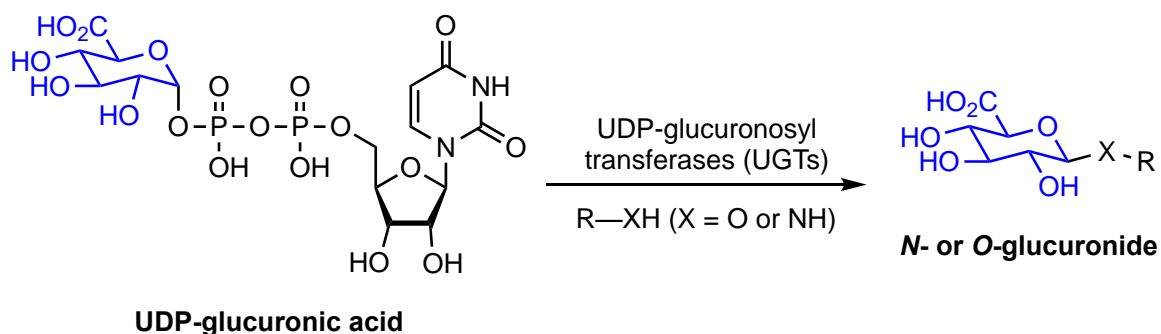


Figure 1-2: General *N*- and *O*-glucuronidation of alcohols and amines by UGTs.

Glucuronidation is the transfer of a glucuronosyl group from uridine-5'-phosphoglucuronic acid to a free alcohol or amine (**Fig. 1-2**), which may have been introduced via Phase I metabolism. The overall reaction is mediated by uridine-diphosphate glucuronosyltransferases (UGTs) which are mainly found in the liver, however, are known to be expressed in many tissues including the kidneys, spleen, thymus, and brain³⁴. The importance of this family of enzymes can be exemplified with the antibiotic chloramphenicol, which if not glucuronidated, will accumulate and lead to adverse effects including hypotension, abnormal respiration, cardiogenic shock, and gray skin color³⁵. These effects are often seen in chloramphenicol-treated newborns, who do not yet express UGTs, and colloquially known as “gray baby syndrome”. Lastly, it should be noted that Phase I and Phase II metabolism occur simultaneously and do not necessarily precede each other.

These two types of metabolism are a critical focus in this thesis as the chemistry performed by these enzymes both detoxify and activate tobacco carcinogens. *N*- and *O*-glucuronidation is the primary detoxification pathway explored in this thesis. As stated earlier, addition of this large, polar group typically aids in xenobiotic elimination by keeping the molecule within the bloodstream, outside of cells, and protected from further activating enzymes. This logic is consistent for other conjugative transformations like glutathione transfer, sulfation, and acetylation. In some cases, P450 oxidation can be a detoxification route. An example relevant to this thesis is the metabolism of nicotine³⁶. P450 2A6, which activates *N*-nitrosamines, sequentially oxidizes nicotine to cotinine (**Fig. 1-1A**)^{37,38}; the analogous reaction for *N'*-nitrosonornicotine is the subject of

Chapter 2. Cotinine can be further oxidized by P450 2A6 to 3'-hydroxycotinine³⁶, which if normalized to cotinine, is a phenotypic biomarker for enzymatic activity^{39,40}. Because both cotinine and 3'-hydroxycotinine have reduced activity at nicotinic receptors, this is viewed as detoxification.

The most important activation pathway for this thesis is Phase I α -hydroxylation of *N*-nitrosamines by cytochrome P450s. As shown in **Scheme 1-3A**, α -hydroxylation results in *N*-dealkylation and production of a highly reactive diazonium ion. This outcome is in direct contrast to nicotine, where identical chemistry lead to a detoxification product. Cytochrome P450s can also activate carcinogens to alkylating agents through epoxidation as seen with benzene and benzo[*a*]pyrene (**Scheme 1-3B & C**)⁴¹. Phase II enzymes can also activate xenobiotics as shown with PhIP (**Scheme 1-3D**)⁴². After initial *N*-oxidation, the new hydroxylamine can be acetylated or sulfated. These compounds can spontaneously lose acetate or sulfate to form highly electrophilic nitrenium ions. Due to the high reactivity of all the mentioned compounds and the aqueous environment of a cell, most activated carcinogens are hydrolyzed and eventually excreted in the urine. The hydrolyzed forms can then serve as biomarkers of carcinogen activation; **Chapter 4** demonstrates this by measuring activation biomarkers of NNN. If hydrolysis does not occur, these compounds can alkylate a variety of biomolecules such as DNA in the form of DNA adducts. It is ultimately these adducts that give the discussed carcinogens their robust activity and is a major focus of tobacco carcinogenesis.

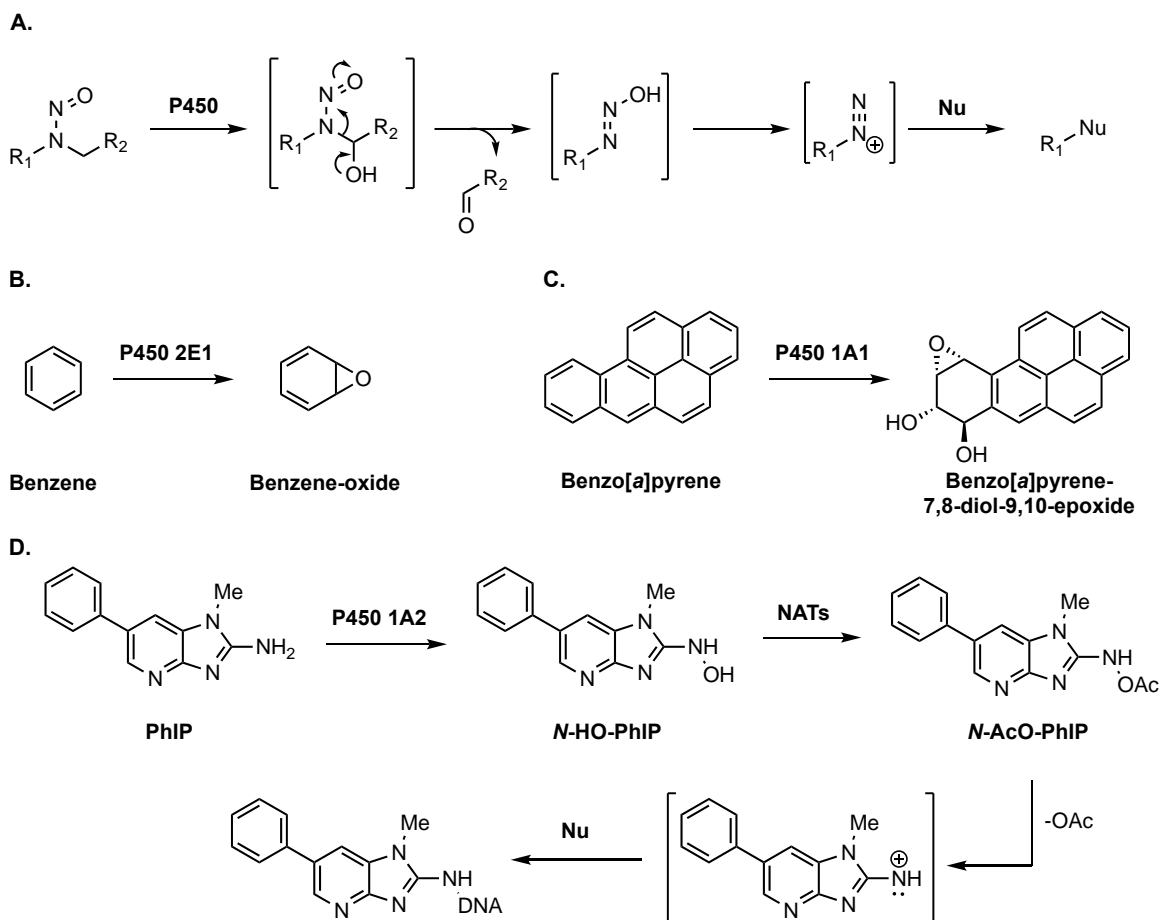


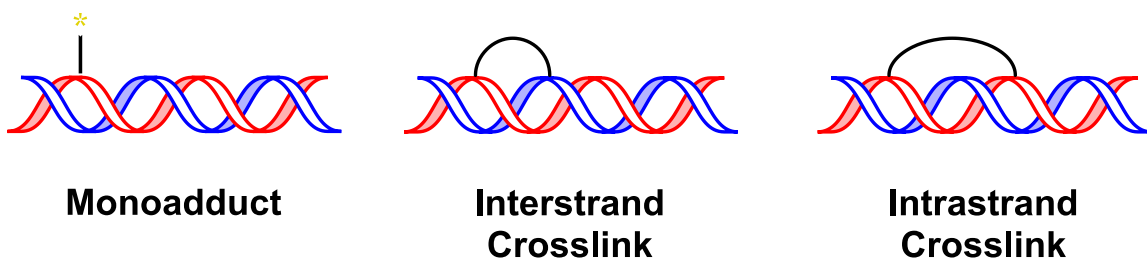
Figure 1-3: Examples of metabolic activation of carcinogens by Phase I and II metabolism. (A) α -hydroxylation of *N*-nitrosamines. (B-C) Epoxidation of benzene and benzo[a]pyrene. (D) *N*-hydroxylation and *N*-acetylation of PhIP. NAT = *N*-acetyltransferase, Nu = nucleophile, PhIP = 2-amino-1-methyl-6-phenylimidazo[4,5-b]pyridine.

1.1.4 DNA Adducts Resulting from Tobacco Carcinogens:

DNA damage is produced from many sources including ultraviolet (UV) light⁴³, ionizing radiation⁴⁴, reactive oxygen species^{45,46}, and alkylating agents⁴⁷. While some of the physical agents directly produce single and double-strand breaks, chemical agents typically modify the structure of DNA, which then leads to a variety of downstream effects. The tobacco carcinogens discussed in this thesis alkylate nucleobases to produce covalent addition products referred to as DNA adducts (**Figure 1-4**). These come in multiple forms depending on the location and connectivity of the alkylation. We characterize monoadducts, or nucleotides with a single modification, by the site of alkylation as shown in **Figure 1-4B**. Important for work in **Chapter 3** is various

alkylation sites of 2'-deoxyadenosine (dAdo), namely N^1 , N^3 , N^6 , and N^7 . Alkylating agents with two electrophilic sites can bind two nucleotides to produce a DNA crosslink⁴⁸ (**Fig. 1-4A**). These can either be intrastrand or interstrand and often lead to DNA strand breaks. These types of chemical agents are also known to bind proteins to form DNA-protein crosslinks⁴⁹. Similar to monoadducts, crosslinks can all be uniquely defined by the alkylation sites on the nucleobases involved. Besides nucleobase adducts, recent data is beginning to show that DNA phosphate adducts are quite abundant and may have important biological consequences⁵⁰⁻⁵².

A.



B.

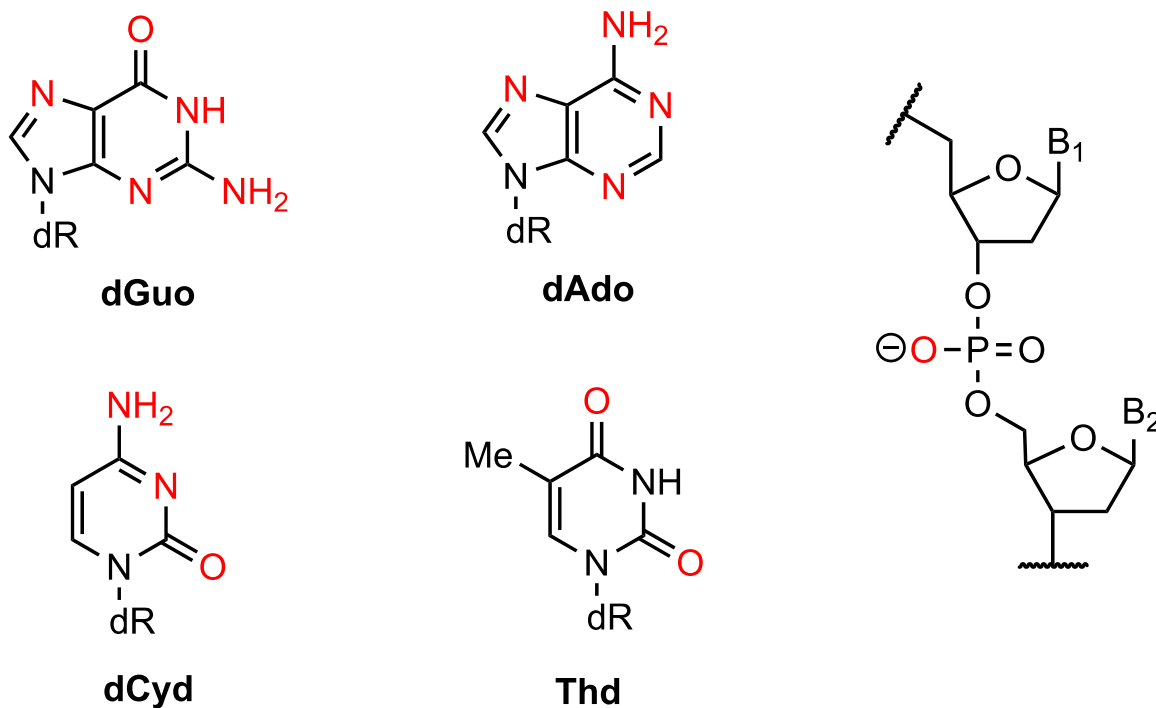
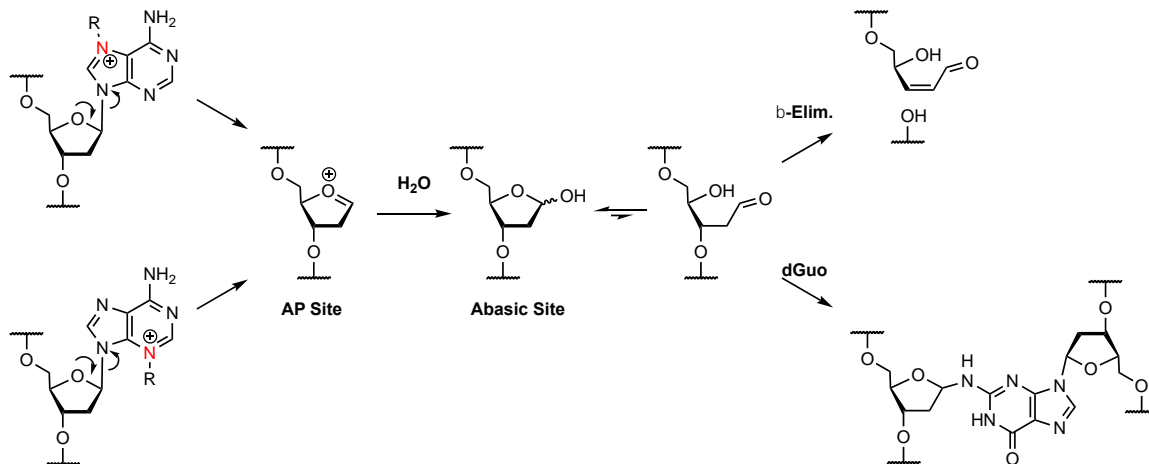


Figure 1-4: (A) Types of DNA adducts and (B) known sites of DNA alkylation (denoted in red).

The fates of these adducts are quite diverse. Alkylation of the N^3 or N^7 position of either guanine or adenine typically results in abasic sites through base depurination (**Scheme 1-1**). Alkylation at these positions creates a delocalized cationic charge that destabilizes the glycosidic bond and ultimately releases the damaged nucleobase⁵³. If left unrepaired, the newly formed abasic site can lead to a single-strand break via β -elimination of the 3'-phosphate⁵⁴. Abasic sites can also cause interstrand crosslinks with guanine or adenine via stabilized Schiff base interactions⁵⁵. Alkylation of most other sites including the N^2 and O^6 positions of guanine, N^4 of cytosine, and O^2 and O^4 position of thymine are generally stable and remain in DNA until encountered by repair enzymes. Lastly, alkylation of some sites such as the N^1 of adenine can lead to structural rearrangements and will be explored more in depth in **Chapter 3**.



Scheme 1-1: Mechanism and downstream outcomes of nucleobase depurination.

1.1.5 Repair of DNA Adducts

The formation of DNA adducts can pose many problems to a cell and thus many DNA repair pathways have been evolved to combat these lesions. While the entirety of DNA repair is outside the scope of this dissertation, base excision repair, nucleotide excision repair, and direct repair will be discussed.

Base excision repair (BER) mechanistically mirrors the process of base depurination discussed in the previous section (**Scheme 1-1**), but utilizes a host of enzymes to perform this action in a controlled fashion⁵⁶. First, the damaged nucleotide is

recognized by a DNA glycosylase and moved into the active site through a “base flipping” mechanism⁵⁷. As an example, alkyladenine DNA glycosylase performs this action by intercalating Tyr162 into the minor groove, which pushes the entire nucleotide outside of the helix via the major groove⁵⁸. This structural rearrangement additionally kinks the phosphate backbone and coordinates a water molecule towards the C1' of the 2'-deoxyribose sugar. Once in the active site, the glycosidic bond is polarized and cleaved which releases the damaged nucleobase and produces an apurinic (AP) site. Enzymes that perform this action include uracil DNA N-glycosylase, thymine DNA glycosylase, alkyladenine glycosylase, 8-oxo-guanine glycosylase 1 (OGG1), and endonuclease VIII-like 1 (NEIL1). Interestingly, recent reports have identified AlkD as a “non-base-flipping” glycosylase, indicating that “base flipping” is not always necessary⁵⁹. With an AP site now present, the phosphate backbone is cleaved at the 5'-position by AP endonuclease 1 (APE1) to produce a 5'-deoxyribose phosphate and an opposing 3'-OH, which DNA polymerase β and others use as a handle for nucleotide gap filling⁵⁶. This can be done in either a short-patch or long-patch manner, but both arrive in the same outcome of 5'-deoxyribose phosphate removal, gap filling, and strand ligation⁶⁰. Apurinic sugars can sometimes be removed in reverse order due to glycosylases such as OGG1 and NEIL1 inherently possessing 3'-endonuclease activity⁶¹. In this case, 3'-cleavage occurs directly after rupture of the glycosidic bond. This is then followed by 5'-cleavage by APE1 and gap filling as previously discussed. Common substrates for BER include oxidized bases, small alkylated bases, and deaminated bases such as uracil and hypoxanthine, which will become important in **Chapter 3**.

Nucleotide excision repair (NER) acts most commonly on bulky DNA damage such as UV-pyrimidine dimers, benzo[*a*]pyrene adducts, and DNA crosslinks^{62,63}. The DNA damage is initially recognized by either transcription-coupled NER or global genome NER. Both pathways detect major distortions to the DNA helix and recruit the transcription factor IIIH complex to the site of damage. Proteins including XPB, XPD, RPA, XPA, and XPG help to open the DNA helix, check for DNA damage, and stabilize the complex before proceeding further. Once all the necessary proteins are in place, dual incision of the damaged strand takes place and a 24 – 32 nucleotide region containing the

damaged nucleotide and protein complex is released. At this time, the large gap can be filled by a variety of DNA polymerases and ligases.

Compared to BER and NER, direct repair is relatively simple as all repair occurs at the nucleobase and does not involve cleavage of the DNA phosphate backbone. Two enzymes important to tobacco-related DNA adducts are *O*⁶-alkylguanine DNA alkyltransferase (AGT)^{64,65} and AlkB oxygenases⁶⁶. AGT is well known for repairing highly mutagenic *O*⁶-methyl guanine adducts, but can also accommodate other *O*⁶-alkylguanine and *O*⁴-alkylthymine adducts. Unlike the enzymes in BER and NER, this enzyme works in a stoichiometric fashion and facilitates only one turnover. This is a result of the repair mechanism where the alkyl group is transferred to a highly active cysteine within the active site through S_N2-type chemistry⁶⁴. After alkyl transfer, the enzyme releases an unmodified nucleotide but can no longer function and must be turned over. This makes AGT-based repair relatively slow and has major clinical implications for individuals who either lack or possess downregulated AGT. For example, mice lacking AGT form more colon tumors than wild type when given azoxymethane⁶⁷. Similarly, the anticancer drug Temozolomide is less effective against tumors with upregulated AGT as the resulting *O*⁶-methylguanine damage is quickly repaired, allowing the tumor cells to survive⁶⁸.

AlkB is an α -ketoglutarate-dependent hydroxylase and repairs DNA alkylation through an oxidative mechanism. α -Hydroxylation of the alkyl group relative to the *N*- or *O*-position of the nucleobase produces a highly unstable structure that releases an aldehyde and the native base^{66,69}. This type of reactivity is reminiscent of cytochrome P450s and will be revisited in **Section 1.3**. While monoalkylated adducts are the most common substrates, exocyclic-bridging adducts such as 1,*N*²-etheno-dGuo are also repaired by AlkB through a similar mechanism⁷⁰. Analogous to AGT, AlkB-mediated repair also seems to have clinical implications, although the mechanisms are not entirely elucidated. Together, it is clear that DNA repair is imperative for host cells to maintain genomic integrity but can also be used to resist chemotherapy.

1.1.6 Mutations, Cancer Initiation and Progression

As noted in the previous section, human cells devote high amounts of energy to repairing DNA adducts. The reason for this is that accumulation and persistence of DNA adducts lead to mutations within the genome that change cellular functions. Mutations occur because DNA adducts often stray from traditional Watson-Crick base pairing. For example, it is believed that O^6 -methylguanine mimics the hydrogen bonding of adenine and readily accepts thymine during replication, leading to a GC to AT transition. DNA adducts can also adapt Hoogsteen base pairs where the purine base rotates into a *syn* conformation and hydrogen bonds through the O/N^6 and N^7 positions.

If a mutation within onco- or tumor suppressor genes, such as *KRAS* and *TP53*, cell growth can be dysregulated and initiate tumor formation. Additional mutations can aid in tumor progression, where changes that promote survival occur. Typical hallmarks associated with survival include changes to metabolism, angiogenesis, nutrient acquisition, and genome maintenance. After sufficient DNA-adduct induced changes, a tumor can become self-sufficient and invasive leading to all the health effects of cancer which are outside the scope of this dissertation. Based on the fact that these changes are the result of DNA adducts, often formed by metabolically activated carcinogens, understanding the nature of DNA adducts and carcinogen activation are important for understanding tobacco carcinogenesis.

1.2 Chemistry and Carcinogenicity of *N*-Nitroso Compounds

1.2.1 Brief History of *N*-Nitrosamines and *N*-Nitrosamides

N-nitroso compounds are any compounds containing the structure shown in **Fig. 1-5A**. The first *N*-nitrosamine to be investigated for human toxicity was also the simplest: *N*-nitrosodimethylamine (NDMA). In the early 1950s, two researchers using NDMA as an industrial solvent reported cirrhosis of the liver 10 months after the chemical was introduced to the plant. In response, Barnes and Magee evaluated the effects of NDMA in animals and found LD₅₀ values of 26.5, 15, and 50 mg/kg for rats, rabbits, and dogs⁷¹. In all cases, the liver showed morphological changes and extensive hemorrhaging into the

gut lumen. In 1965, Magee and Barnes confirmed in their landmark study that NDMA also produces hepatic tumors when administered at 50 ppm in the diet⁷². This finding established that, at least in one case, *N*-nitrosamines are potent carcinogens and encouraged efforts to characterize other *N*-nitroso species. By 1984, more than 300 *N*-nitroso compounds were examined and over 90% were found to be carcinogenic and have organ specificity regardless of route of administration⁷³. For example, symmetrical dialkyl nitrosamines target the liver while many methylalkyl nitrosamines target the esophagus; however, if the second alkyl chain is an even carbon length greater than 6, the bladder becomes the major target organ. Cyclic nitrosamines generally have broad specificity with *N*-nitrosoproline actually exhibiting no carcinogenicity⁷⁴ for reasons discussed in **Section 1.3.3**.

N-Nitrosamides (**Fig. 1-5A**) have been similarly investigated for carcinogenic potential. In 1960, Schoental was evaluating the effects of macromolecule methylation and decided to use *N*-nitroso-*N*-methylurethane as a surrogate for diazomethane. High oral dose treatments (20% solution v/v) resulted in fatal damage to the lungs, liver, and stomach after 2 – 3 days. In low dose treatments (2.5% solution v/v), rats generally survived but in some cases developed squamous cell carcinomas of the stomach⁷⁵. Other related *N*-nitrosamides were later evaluated and shown to induce stomach tumors in rats, indicating that it is the common *N*-nitrosamide functional group initiating these effects⁷⁶. More broadly, it has now been established that the common *N*-nitroso group^{77,78} unifies the action of both *N*-nitrosamines and *N*-nitrosamides and continues to be of interest to health science.

1.2.2 Preparation and Reactivity of *N*-Nitroso Compounds

N-nitrosamines and *N*-nitrosamides can be prepared through nitrosation of amines or amides with NaNO₂, nitrosyl esters and nitrosyl halides under acidic conditions (**Fig 1-5B**). All of these reagents converge with the formation of HNO₂, which either dimerizes to form N₂O₃ or loses water to form NO⁺. Both species can then be attacked by the nucleophilic nitrogen of the desired amine or amide to form a *N*-nitroso species. Amides may be more complicated though as computational evidence supports initial *O*-alkylation

followed by a pseudopericyclic 1,3-sigmatropic rearrangement⁷⁹. A mechanism under basic conditions using formaldehyde as a catalyst has also been shown and is depicted in **Fig. 1-5C**⁷³. This could potentially have biological relevance as certain bacterial strains can perform nitrosation under basic conditions^{80,81}; however, recent insights into streptozotocin biosynthesis imply nitrosation is much more complex⁸². Nitrosation is most well understood for primary and secondary amines and amides, but tertiary amines⁸³ can also be nitrosated and has major implications for tobacco^{84,85} as discussed in **Section 1.4**.

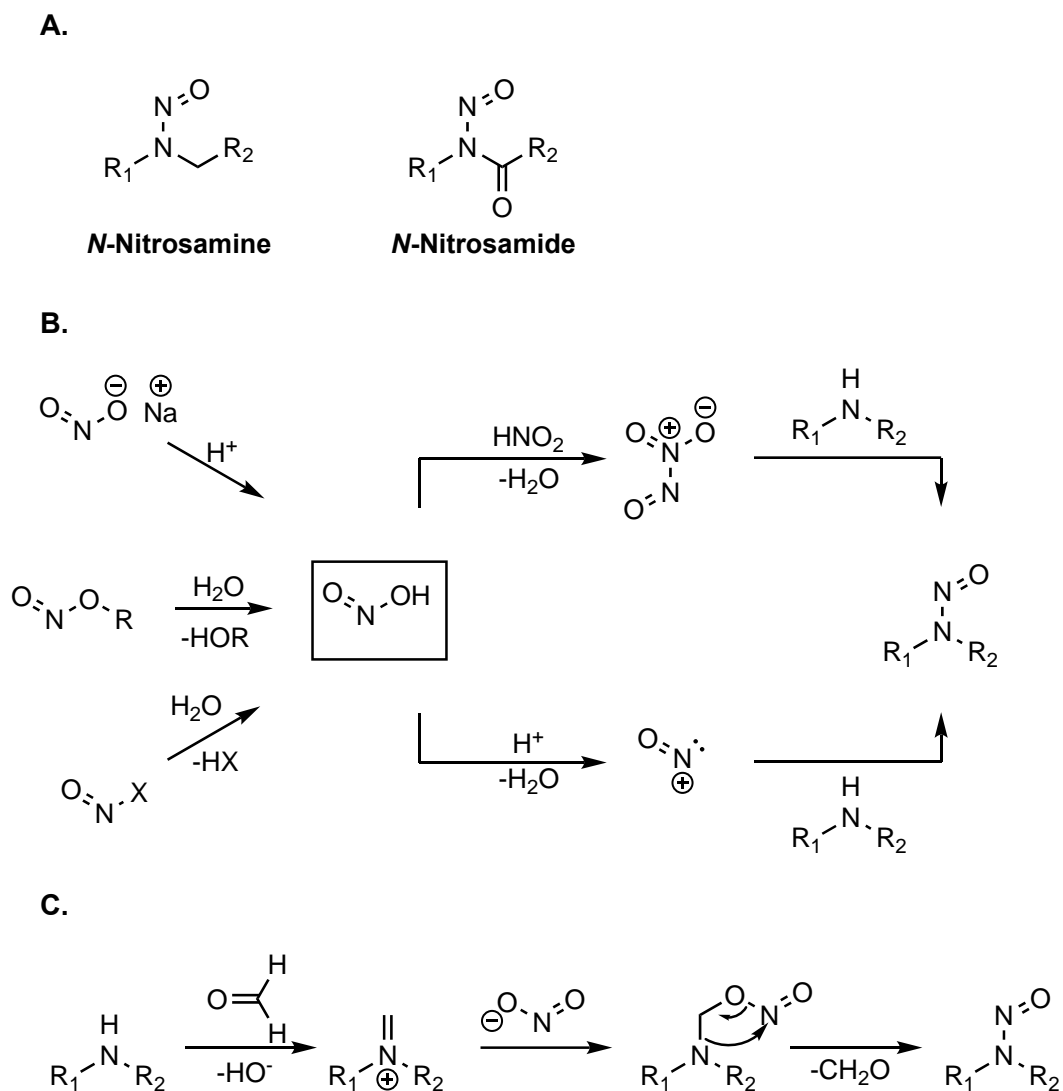
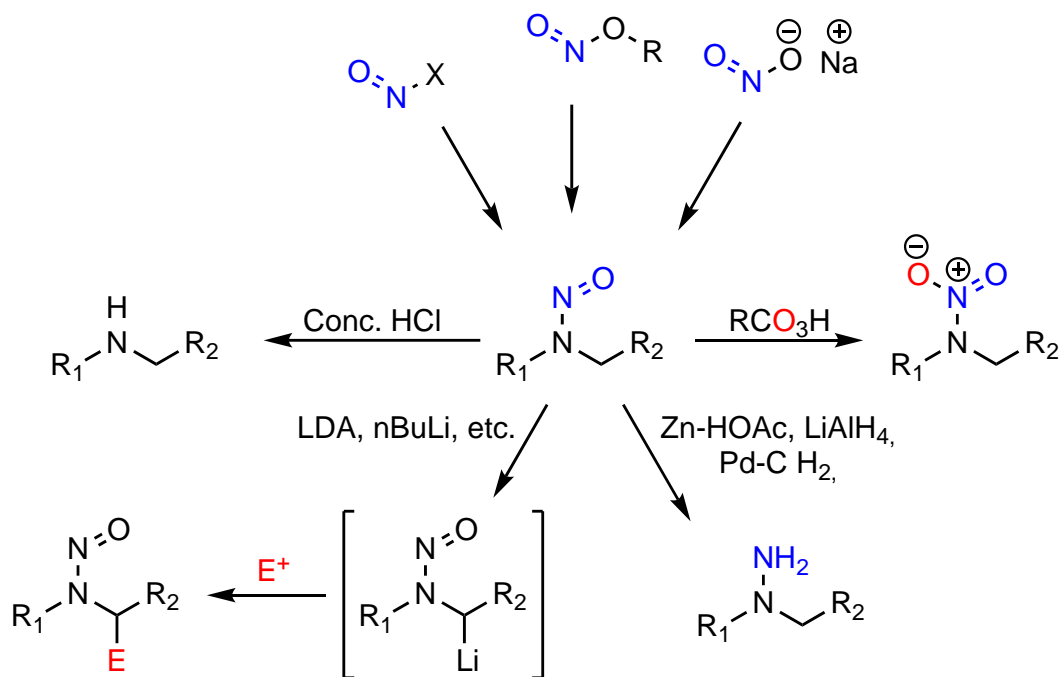


Figure 1-5: (A) The general structure of *N*-nitrosamines and *N*-nitrosamides. (B) Mechanisms of *N*-nitrosation by NaNO_2 , nitrosyl esters, and nitrosyl halides. (C) A formaldehyde catalyzed *N*-nitrosation mechanism under basic conditions.

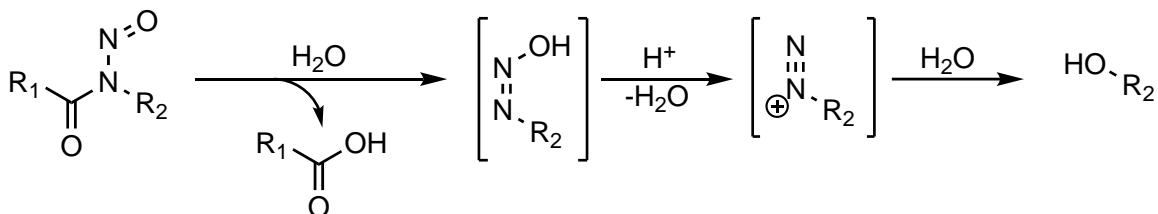
Once formed, *N*-nitrosamines are generally quite stable unless exposed to strongly acidic, basic, reducing, or oxidizing conditions. In the presence of concentrated HCl, denitrosation can occur through a debated mechanism^{86,87}. Under strongly basic conditions such as LDA or *n*-BuLi, *N*-nitrosamines display classical umpolung reactivity and are deprotonated at their α -carbons (**Scheme 1-2**)⁸⁸. The resulting carbanions can then react with halides, aldehydes, ketones, esters, α,β -unsaturated ketones, and various hetero-electrophiles to form α -substituted products⁸⁹. Some of the products (e.g. β -hydroxy-, β -keto, and β -carboxynitrosamines) have been reported to be unstable and decompose via retroaldol cleavage. If not for their carcinogenicity, *N*-nitrosamines would be excellent synthons for formal α -functionalization of secondary amines. The redox properties of *N*-nitrosamines can be summarized with a few representative examples. Zn dust in acetic acid⁹⁰ was the first method to reduce *N*-nitrosamines to hydrazines, but other common reducing agents like lithium aluminum hydride⁹¹ and catalytic hydrogenation⁹² have also been used. Oxidation to *N*-nitroamines is also possible using *m*-chloroperoxybenzoic acid or trifluoroperoxyacetic acid⁹³.



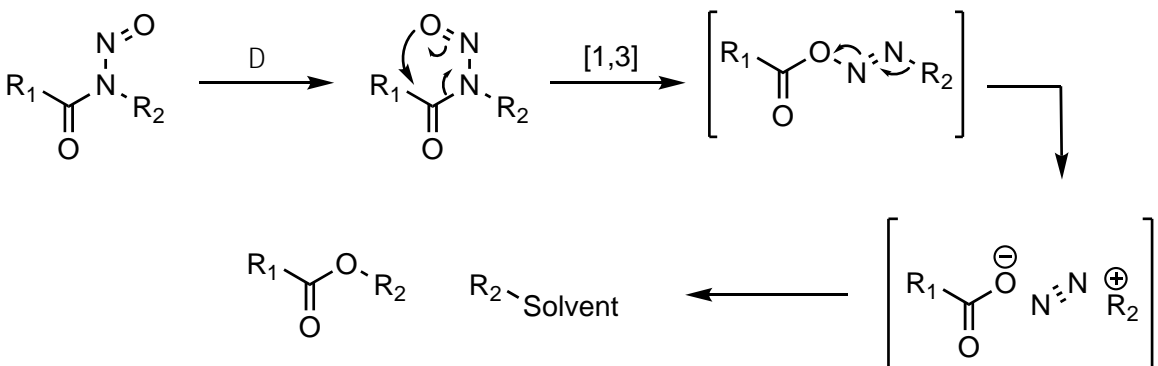
Scheme 1-2: Representative reactions of *N*-nitrosamines. *N*-nitrosamines can be nitrosated with conc. HCl, alkylated with strong base and electrophiles, reduced, and oxidized. E⁺ = halides, aldehydes, ketones, esters, α,β -unsaturated ketones, and other electrophiles.

In comparison to *N*-nitrosamines, *N*-nitrosamides are quite unstable. Due to the electron-withdrawing effects of the nitroso group, the amide bond is particularly unstable and easily cleaved in water (**Scheme 1-3A**). This releases a carboxylic acid and a diazohydroxide that loses water to form a diazonium ion. Under these conditions, an alcohol is formed with release of N_2 ⁹⁴. In addition to hydrolytic instability, Emil White demonstrated that *N*-nitrosamides undergo thermal 1,3-sigmatropic rearrangements to give diazoesters (**Scheme 1-3B**)^{95,96}. These ultimately decompose to an acid-carbocation ion pair that is transiently separated by N_2 ⁹⁷. The cation is remarkably strong and alkylates not only the acid to make esters, but also solvents such as benzene, toluene^{98,99}, pyrrole, *N*-methylpyrrole, and furan¹⁰⁰. Under physiological conditions, the hydrolytic mechanism is expected to dominate and is explored in **Chapter 2** as a possible route of DNA alkylation.

A.



B.



Scheme 1-3: (A) General mechanism for hydrolysis of *N*-nitrosamides. (B) Thermal decomposition of *N*-nitrosamides by a [1,3] sigmatropic rearrangement resulting in an N_2 -separated ion pair.

As briefly mentioned in **Section 1.1.3**, the generally stable *N*-nitrosamines can be transformed into carcinogenic species through metabolism (**Fig. 1-3A**). α -Hydroxylation

by cytochrome P450s produces a highly unstable α -hydroxynitrosamine that spontaneously *N*-dealkylates to give an aldehyde and a diazohydroxide analogous to the type seen in *N*-nitrosamide hydrolysis. Under acidic conditions, the diazohydroxide loses water to form a diazonium ion that can either be hydrolyzed or bind to DNA or proteins in the form of adducts. As discussed in **Sections 1.1.4** and **1.1.5**, the accumulation of adducts results in mutations and changes to cellular function that can initiate cancer. Based on this scheme, one would expect that absence of α -C-H bonds would diminish the carcinogenic activity of *N*-nitrosamines. This is indeed true as α -deutero species^{101–103} and those containing full branched α -carbons⁷³ generally have diminished activity. *N*-nitrosoproline is an interesting case where not only does it have diminished α -C-H content, but also is negatively charged at physiological pH, likely preventing it from entering cells and evading the cytochrome P450 metabolism¹⁰⁴. This general P450-bioactivation scheme is imperative to the overall dissertation and is further studied for the tobacco-specific nitrosamines, NNK and NNN, in **Chapters 2-4**.

1.2.3 Exogenous and Endogenous Sources of *N*-Nitroso Compounds

Exposure to *N*-nitroso species can occur from a broad range of exogenous and endogenous sources. One major exogenous source is tobacco smoke. Druckrey and Preussmann were the first to hypothesize that amines could be nitrosated by the nitric oxides produced during tobacco combustion¹⁰⁵. This was of course found to be true as several *N*-nitrosamines are found in tobacco and tobacco smoke (**Section 1.4**). The first official confirmation of environmental *N*-nitrosamines came from work by Ender who found NDMA in nitrite-preserved herrings¹⁰⁶. This phenomenon of nitrite-induced *N*-nitrosamine production, while not too surprising based on chemistry established in the previous section, has become a reoccurring theme for exogenous exposure. Nitrite is now known to form *N*-nitrosamines at relatively low levels (< 100 $\mu\text{g}/\text{kg}$) in a variety of foods such cured meats, beer, bacon, dairy products, and cereal^{107,108}. Nitrite can also be implicated in industrial sources of *N*-nitrosamines after conversion to N_2O_3 or NO^+ . A prominent example is the near-ubiquitous presence of NDMA at leather tanning factories¹⁰⁹. Levels ranged from 19 – 47 $\mu\text{g}/\text{m}^3$ and were attributed to using

dimethylamine sulfate as a hair-removal agent. Under the high-pH of the process and the NO_x in forklift exhaust, dimethylamine is nitrosated to NDMA. Other occupations found to have *N*-nitrosamine contamination include rubber¹¹⁰ and metal-working plants¹¹¹. Pesticides¹¹², cosmetics¹¹³, and pharmaceuticals¹¹⁴ have also been found to contain *N*-nitrosamines. Routes of contamination for these products include undesired contact with nitrosating agents, use of an *N*-nitrosamine during chemical synthesis, and storage conditions.

In addition to exogenous sources, endogenous formation of *N*-nitroso compounds is another large source of exposure. The primary mechanism is believed to be nitrosation of amines and amides consumed in the diet. The stomach is one of the most important sites as the acidic and aqueous conditions readily convert NO_2^- to N_2O_3 and NO^+ ¹¹⁵. Additionally, the salt content of the stomach helps catalyze nitrosation through transient formation of nitrosyl halides¹¹⁶. It should also be noted that dietary compounds such as α -tocopherol, ascorbic acid, and tea extracts inhibit endogenous nitrosation^{117,118}, making it difficult to predict the extent of nitrosation in an individual. One method of measuring this is by administering L-proline¹¹⁹. When ingested, L-proline is nitrosated and quantitatively excreted in the urine as non-carcinogenic, *N*-nitrosoproline. Use of this technique identified that nitrosation must also be occurring outside of the stomach. Possible extragastric mechanisms include reduction of nitrate to nitrite by bacteria¹²⁰, synthesis of nitrate by macrophages^{121,122}, and production of nitric oxide by endothelial cells¹²³, neurons¹²⁴, and bacteria¹²⁵. One example of non-gastric nitrosation is production of NNN in the oral cavity of e-cigarette users¹²⁶. NNN is not a component of e-liquids; however, normicotine is, indicating that endogenous nitrosation by any of the discussed mechanisms may be occurring. Based on all these reports of exogenous and endogenous *N*-nitrosamine sources, amines and amides of all types are being recognized as potentially less inert than once believed.

1.3 Metabolism of *N*-Nitrosamines by Cytochrome P450s

1.3.1 Structure and Properties of Cytochrome P450

Cytochrome P450s are transmembrane, heme-containing monooxygenase enzymes that coordinate molecular oxygen to perform a variety of oxidative chemistry. These enzymes received their name due to the characteristic UV absorption band at 450 nm upon exposure to carbon monoxide¹²⁷⁻¹³⁰. P450s can be further characterized and named by their sequence homology. For example, P450 1A1 denotes this enzyme is of family 1, subfamily A, and is the first enzyme of its type to be characterized. P450 2A6 and 2A13 are most important for this dissertation and will be discussed in **Section 1.3.4**. This type of analysis has identified a total of 57 putative human P450 genes based on their ability to bind heme.

Although this is a relatively small family of enzymes, P450s metabolize ~75% of all xenobiotics¹³¹. P450s also metabolize many endogenous substrates such as steroids, fatty acids, and vitamins. Within the cell, P450s are anchored to the membrane of the endoplasmic reticulum and the inner mitochondrial membrane. The opening to the active site is near the membrane interface and might explain why steroids, fatty acids, and other hydrophobic molecules are preferred substrates. The most important component of the active site is the cysteine-coordinated heme containing Fe(III), whose redox potential is tightly regulated through a hydrogen bond network^{132,133}. Additionally, the active site is organized to facilitate proper electron, oxygen, proton, and water transport^{134,135}. Within the body, P450s are mainly found in the liver; however, they are also widely distributed to extrahepatic tissues including, but not limited, the lungs, kidney, oral cavity, nasal mucosa, and bladder¹³⁶. Not surprisingly, the tissue distribution of P450s localizes the site of action of certain xenobiotics requiring bioactivation and is a major hypothesis for what defines the organotropy of *N*-nitrosamines such as NNK¹³⁷. Another important feature of P450s is their inducibility by substrates¹³⁸. This allows for P450 expression to be upregulated when most needed and ensure xenobiotics are dealt with accordingly.

1.3.2 General Catalytic Cycle of Cytochrome P450s

The catalytic cycle for cytochrome P450s has been well characterized¹³⁹ and is shown in **Fig 1-6**.

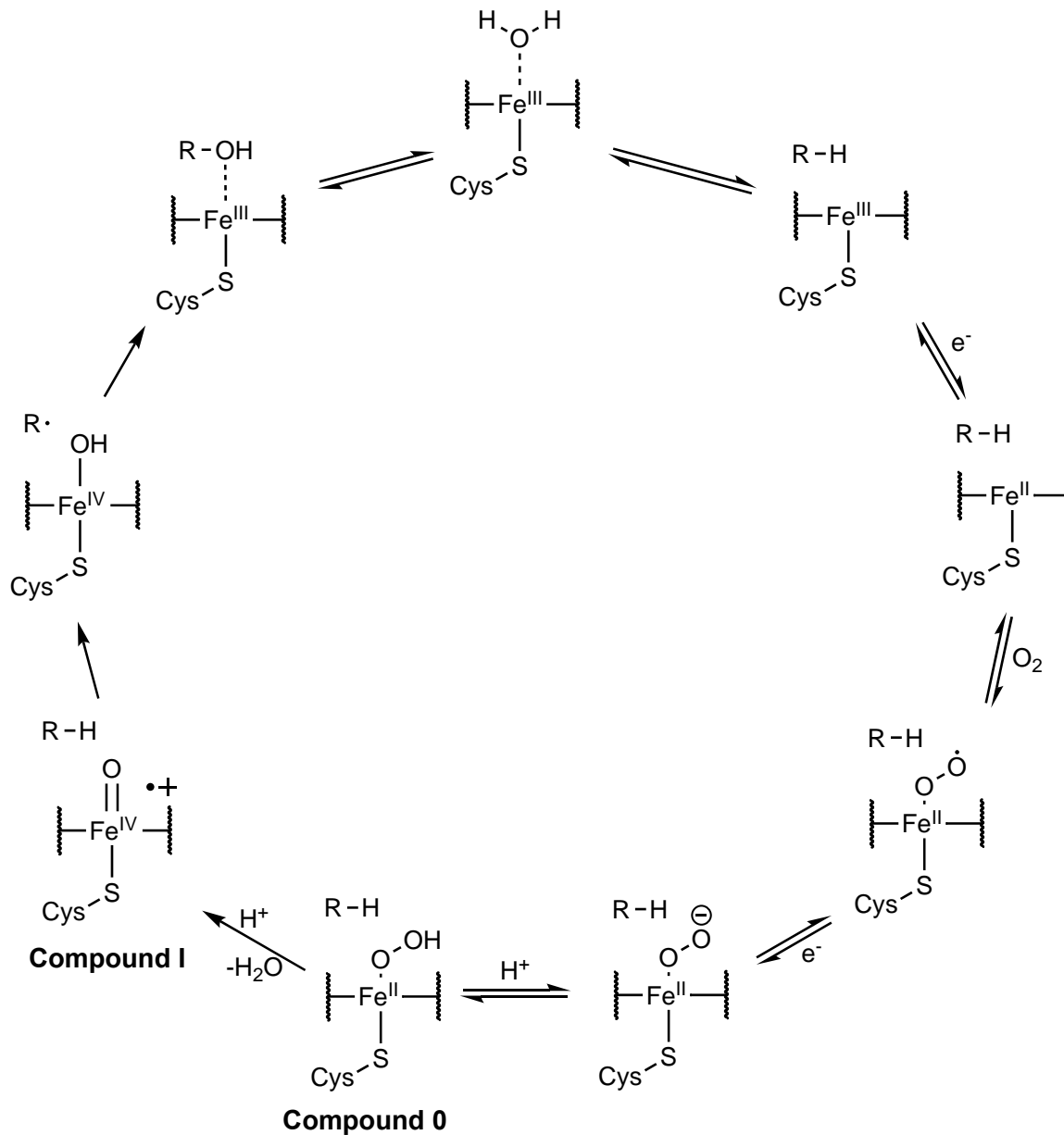


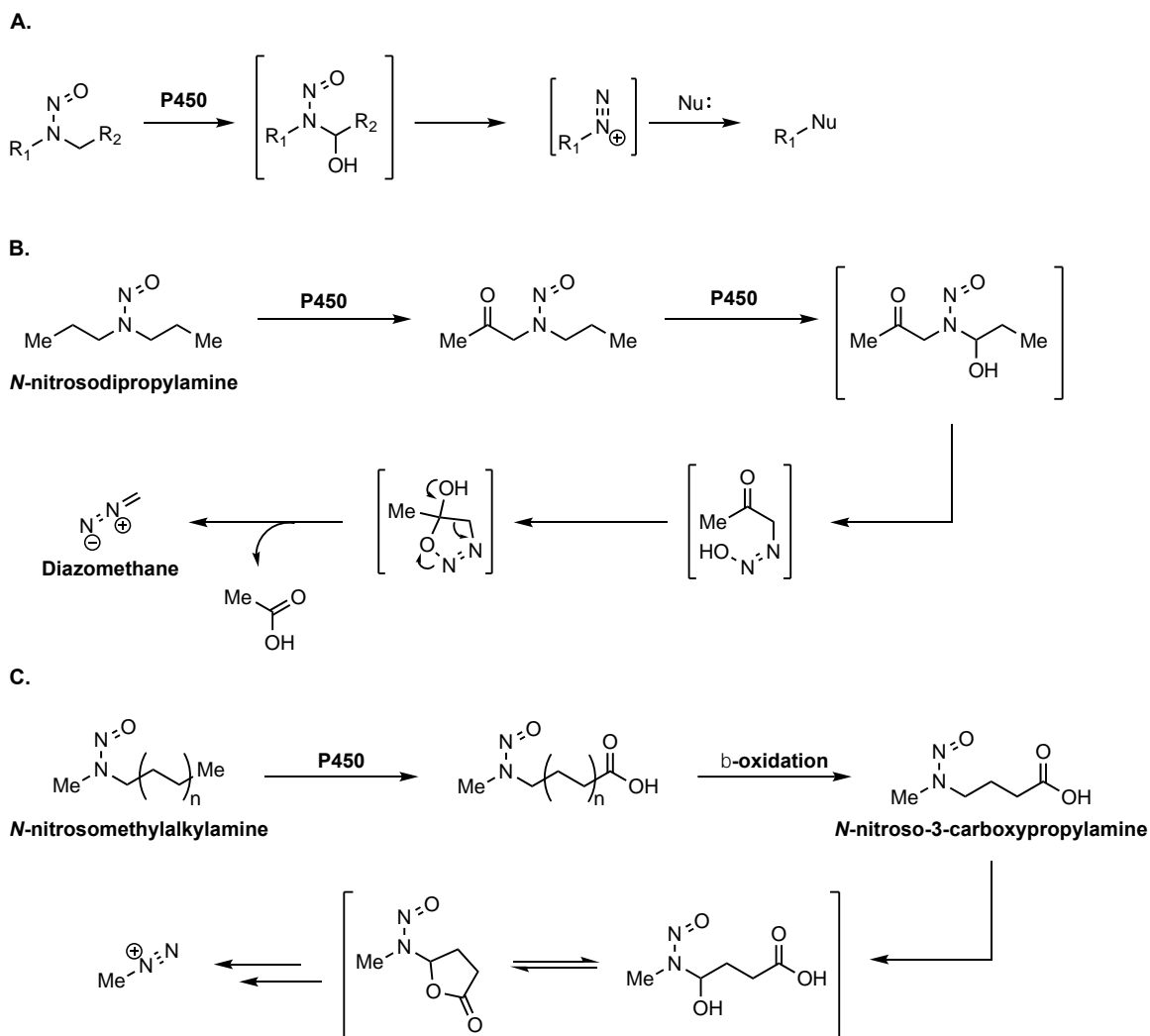
Figure 1-6: The general catalytic cycle of cytochrome P450 oxidation. This representation is based on a previous reviews^{136,139,140}

The cycle begins with displacement of the heme-coordinated H₂O by substrate. This induces a structural shift into a closed conformation that traps the substrate in the active

site and theoretically keeps the enzyme from undergoing futile cycles¹⁴⁰. Water displacement also converts the Fe(III) center into a pentacoordinated state with high reduction potential¹⁴¹. These events together allow NADPH-cytochrome P450 oxidoreductase (POR) to reduce the Fe(III) to Fe(II). POR is unique in that it accepts two electron reductants (NADPH) but only delivers electrons to one electron acceptors (heme). This is accomplished by a “1-3-2-1” redox cycle utilizing FAD and FMN cofactors¹⁴². After reduction to Fe(II), molecular oxygen enters and coordinates to heme to form a ferrous-oxy radical. One more electron is transferred to the complex from POR to form Compound 0. After two proton transfer steps and loss of water, we arrive at Compound I. Most literature indicates that Compound I conducts most of the known P450 reactivity but certain reports may indicate Compound 0 activity^{143,144}. Compound I can be formally described as an Fe(V) complex but is more accurately described as a Fe(IV)oxo radical cation with charge distributed over the porphoryin ring. This high valency and reduction potential is ultimately the driving force in the observed P450 chemistry. The Fe(IV)-oxo can now abstract hydrogens from carbons to produce an Fe(IV)-OH species and a carbon radical. The carbon radical then receives the hydroxide radical from the Fe-complex through an “oxygen-rebound” mechanism^{145,146} and regenerates the original Fe(III) center. To close the cycle, the substrate leaves the active site and is replaced by H₂O; however, recent studies suggest that the product can be retained in the active site and undergo another round of oxidation³⁷. This phenomenon will be studied in the context of NNK and NNN in **Chapter 2**.

1.3.3 α , β , and ω -Oxidation of *N*-Nitrosamines

The most important P450-mediated reaction for this thesis is C-H hydroxylation. For *N*-nitrosamines, this type of reactivity is observed most commonly at α -, β -, and ω -carbons relative to the *N*-nitroso group. α -Hydroxylation is particularly important as it initiates the carcinogenic mechanism of *N*-nitrosamines as discussed in **Sections 1.1.3** and **1.2.2 (Scheme 1-4A)**.



Scheme 1-4: Mechanisms of (A) α -hydroxylation, (B) β -oxidation and decomposition of *N*-nitrosodipropylamine, and (C) tandem ω -oxidation-Knoepf-type β -oxidation of even-chained *N*-nitrosomethylalkylamines to *N*-nitroso-3-carboxypropylamine. n = any even number

The outcomes of β -oxidation can be more complex. In **Section 1.2.2**, it was briefly mentioned that β -oxidized nitrosamines can be unstable and undergo retroaldol cleavage. Rates for decomposition typically increase with the stability of the carbonyl product formed⁷³. Another outcome of β -oxidation is the dual alkylating activity of *N*-nitrosodipropylamine¹⁴⁷. Based on the canonical α -hydroxylation mechanism, one would only expect propylating activity, but methylation is also observed. This surprising behavior is explained mechanistically in **Scheme 1-4B**. After two sequential β -oxidations, the β -oxo-nitrosamine is α -hydroxylated, which *N*-dealkylates, undergoes a

5-exo-trig cyclization to form a tetrahedral intermediate, and finally collapses to produce acetic acid and diazomethane. This phenomenon has also been observed with other β -oxidized species^{148,149}. β -Oxidation can also lead to alkylating agents via sulfation of β -hydroxynitrosamines¹⁵⁰. In opposition to these reports, β -oxidation can also be inert as seen with NNN¹⁵¹.

ω -Oxidation has been shown to give tissue specificity to certain *N*-nitrosamines, like unsymmetrical, even-chained methylalkylnitrosamines (**Section 1.2.1**). In this case, ω -oxidation to an acid occurs (**Scheme 1-4C**). These types of molecules are then intercepted by Knoop-type β -oxidation enzymes normally participating in fatty acid catabolism¹⁵², ultimately shortening the *N*-nitrosamines to *N*-nitrosomethyl-3-carboxypropylamine, a known bladder carcinogen¹⁴⁹. The carboxylate is hypothesized to keep the molecule outside of the cell and direct it to the bladder where it ultimately exhibits carcinogenic behavior. α -Hydroxylation of the 3-carboxypropyl chain produces a species that is stabilized by equilibrating with a lactone structure¹⁵³ (**Scheme 1-4C**). Together, it is apparent that all three oxidation modes described can act separately or together to diversify the carcinogenic activity of seemingly simple *N*-nitrosamines.

1.3.4 P450 2A6 and 2A13

Cytochrome P450 2A6 is of great importance to this thesis because nicotine and NNN are major substrates. P450 2A6 is primarily expressed in the liver, but also found in the trachea, lung, nasal-pharyngeal mucosa¹⁵⁴, and esophageal mucosa¹⁵⁵, which is especially important for NNN (**Section 1.4.2**). Levels seem to be variable and have been measured to be ~4 – 21% of all P450s found in liver microsomes, rivaling the levels of P450 3A4^{156,157}. A crystal structure of P450 2A6 has been published and shows similar structure to P450 2A13 and 2E1, except for its relatively small and rigid active site^{158,159}.

In addition to NNN and nicotine, coumarin is the most characteristic substrate and has been used to understand mechanistic details of P450 2A6. Prior to establishing total 3'-hydroxycotinine/cotinine as a biomarker for P450 2A6 activity³⁹, coumarin 7-hydroxylation was a common *in vivo* human phenotypic assay¹⁶⁰. Other substrates for P450 2A6 include tegafur (a 5-fluorouracil prodrug)¹⁶¹, pilocarpaine¹⁶², bilirubin¹⁶³, and

NNK¹³⁷. P450 2A6 also has a few known inhibitors including 8-methoxypsoralen and menthofuran. Nicotine has also been shown to be converted into a P450 2A6 inhibitor through its own oxidation¹⁶⁴; however, the inhibitory metabolite has yet to be identified. Several groups have started drug discovery programs towards novel P450 2A6 inhibitors in hopes of reducing NNN and NNK bioactivation. A few inhibitors and docking studies have been reported with only limited success thus far¹⁶⁵⁻¹⁶⁷.

P450 2A6 is highly polymorphic. To date, 86 allelic variants have been found and all range in their activity¹³⁶. For example, *CYP2A6*2*¹⁶⁸ has lowered and non-native catalytic activity due to a L160H mutation while *CYP2A6*12*¹⁶⁸ is a splice variant that has lost all activity. *CYP2A6*4*, a complete gene deletion, is also of interest due to its bias towards certain ethnicities¹⁶⁹. These polymorphisms are ultimately important because they have been extensively linked to smoking behavior. Lowered P450 2A6 activity is not only correlated with reduced smoking behavior,¹⁷⁰ nicotine metabolism¹⁷¹, and lower tobacco-specific carcinogen burden¹⁷², but also reduced risk of lung cancer onset^{40,173,174}. These correlations will become important when considering biomarkers of NNN bioactivation in **Chapter 4**.

P450 2A13 resembles P450 2A6 in many ways¹³⁶. P450 2A13 has 94% sequence homology and has a similar, albeit slightly larger active site. Additionally, P450 2A13 is known to metabolize NNK¹³⁷, NNN, nicotine, cotinine¹⁷⁵, the nicotinium Δ^5 -iminium ion³⁸, and coumarin¹⁷⁶. P450 2A13 is also capable of metabolizing aflatoxin B₁¹⁷⁷, 4-aminobiphenyl¹⁷⁸, and phenacetin¹⁷⁹ due to its large active site. P450 2A13 has been found in the trachea, lungs, and nasal mucosa at the mRNA level; however, P450 2A13 is almost undetectable in the liver, while P450 2A6 is primarily found there¹⁵⁴. The association of P450 2A13 to the respiratory system, specifically the lungs, is one hypothesis for the tissue specificity of NNK and is supported by DNA adduct data found in **Chapter 3**. P450 2A13 is also polymorphic, but less so than P450 2A6 with only 21 variants having been reported. In analogy to P450 2A6, many have reduced activity¹⁸⁰ and correlate to risk for lung cancer¹⁸¹. For that reason, many inhibitors have been tested such as 2-phenethyl isothiocyanate and shown to have modest effects¹⁸², however, selectivity is a persistent issue¹⁸³.

1.4 Tobacco-Specific Nitrosamines

1.4.1 Overview

As discussed in **Section 1.2.1**, the early studies by Magee and Barnes^{71,72} sparked a movement to determine the generality and potency of *N*-nitrosamines as carcinogens. In 1962, it occurred to Druckrey and Preussmann that *N*-nitrosamines may naturally occur in tobacco¹⁰⁵. By this point, much was known about methods of *N*-nitrosation (**Section 1.2.2**) and thus it was plausible that tobacco alkaloids such as nicotine, nornicotine, anabasine, and anatabine could be nitrosated during tobacco curing or pyrolysis. This led to the panel of putative, and eventually confirmed, class of compounds called “tobacco-specific nitrosamines” (TSNAs, **Fig. 1-7**)¹⁸⁴.

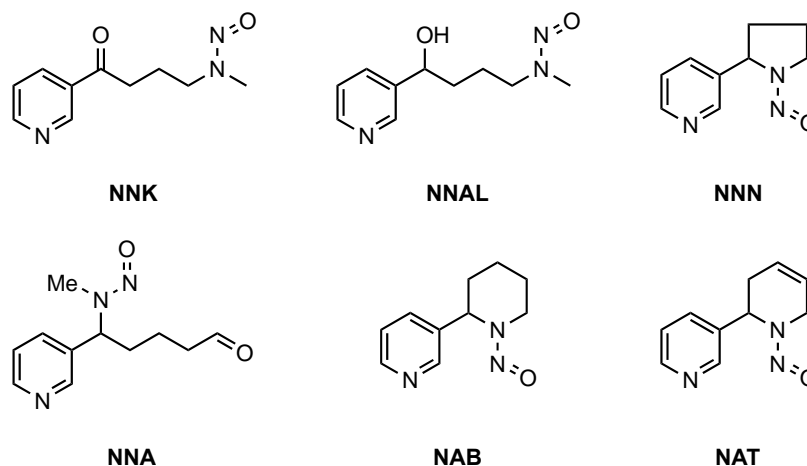


Figure 1-7: Chemical structures of known TSNAs.

Important among these was *N*'-nitrosornicotine (NNN), a compound previously shown to cause pulmonary tumors in mice¹⁸⁵. This compound evaded detection in tobacco until 1974, where Hoffmann and Hecht measured NNN in both unburned tobacco and tobacco smoke at unprecedented levels ranging between 1.9 – 88.6 ppm; *N*-nitrosamines were commonly < 0.1 ppm¹⁸⁶. Detection of NNN and knowledge of established mechanisms for tertiary amine nitrosation⁸³ led to the hypothesis that two more nicotine-derived *N*-nitrosamines are present in tobacco: 4-(methylnitrosamino)-1-(3-pyridyl)-1-butanone and 4-(methylnitrosamino)-4-(3-pyridyl)butanal, which were given the abbreviations NNK (nicotine-derived nitrosaminoketone) and NNA (nicotine-

derived nitrosaminoaldehyde), respectively, to reflect their association with NNN (**Fig. 1-7**). Indeed, both of these compounds form from the reaction of nicotine and sodium nitrite⁸⁵, but only NNK was found in tobacco⁸⁴. Follow up bioactivity assays on NNK and NNA demonstrated that NNK is a potent lung carcinogen and NNA is inactive¹⁸⁷. The activity of NNK was remarkable because it defied common organotropy for unsymmetrical nitrosamines (**Section 1.2.1**) and was exceedingly carcinogenic compared to NNN. Other TSNA's such as *N'*-nitrosoanatabine (NAT)¹⁸⁸ and *N'*-nitrosoanabasine (NAB)¹⁸⁹ have also been found in tobacco but are weakly or non-carcinogenic. For that reason, the majority of research, including this dissertation, has focused on the metabolism, DNA adducts, and carcinogenicity of NNN and NNK¹⁹⁰. In the next sections, each of these three subjects will be briefly reviewed for each compound. For a complete review of NNN and NNK, a number of seminal reviews are recommended¹⁹⁰⁻¹⁹³.

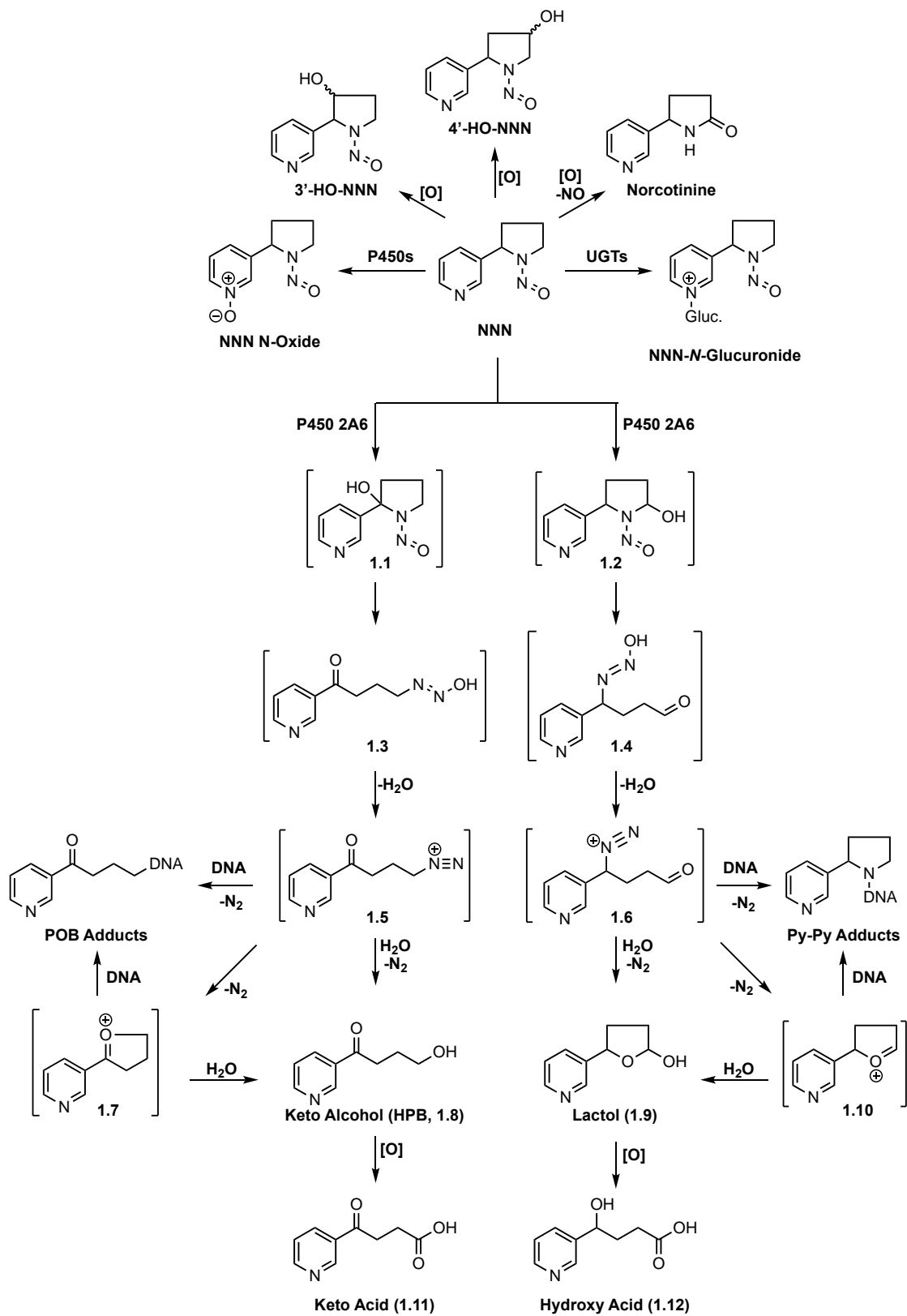
1.4.2 NNN

1.4.2.1 Metabolism

NNN is well metabolized through bioactivation and detoxification processes (**Scheme 1-5**) and <1% is excreted unmodified in the urine¹⁸⁸. The major detoxification routes for NNN include *N*-oxidation, β -hydroxylation, denitrosation-oxidation, and *N*-glucuronidation, which will become relevant in **Chapter 4**. *N*-Oxidation of the pyridine ring is a minor pathway in rat and hamster liver (3-11% of dose), and is not observed in either monkey or human liver^{194,195}. β -Oxidation is an extremely minor route and has only been reported in one study¹⁵¹. Conversely, formation of norcotinine through a tandem denitrosation-oxidation process is observed in several cases. Three mechanisms have been proposed¹⁹⁶. The first is simply denitrosation to nornicotine that is sequentially or processively oxidized to norcotinine. The second mechanism is the reverse where NNN is oxidized to *N*-nitrosanorcotinine and immediately denitrosated. The last mechanism invokes 5'-radical formation that releases nitric oxide; the resulting *iso*-myosmine is then oxidized to norcotinine. Regardless of mechanism, norcotinine is relatively minor in rat

urine¹⁹⁵. However, norcotinine, in combination with its *N*-oxide, were ~30% of all NNN metabolites in monkey urine¹⁹⁷. Additionally, norcotinine was further metabolized to 3'-hydroxynorcotinine in monkeys and has potential as a human biomarker for NNN^{197,198}. Lastly, *N*-glucuronidation of NNN is very minor, but is used to compute Total NNN, the only established biomarker for NNN exposure^{199,200}.

As expected for all *N*-nitrosamines, the major bioactivation route for NNN is α -hydroxylation by P450 2A6 (**Scheme 1-5**)¹⁰³. P450 3A4 and 1A2 also perform this transformation but with reduced activity^{201,202}. Oxidation can occur either at the 2'- or 5'-position. 2'-HydroxyNNN (**1.1**) undergoes spontaneous ring opening to diazohydroxide **1.3**. As discussed in **Section 1.3.3**, this species decomposes to a diazonium ion that can either hydrolyze to keto alcohol **1.8** or alkylate DNA to produce pyridyloxobutyl (POB) DNA adducts. There is also evidence that diazonium ion **1.5** cyclizes to oxonium ion **1.7** before hydrolysis or adduct formation²⁰³. 5'-Hydroxylation follows a similar pathway to produce diazonium ion **1.6**, which has been shown to hydrolyze to lactol **1.9** or form pyridine-pyrrolidine (Py-Py) DNA adducts. Similar to 2'-metabolism, it is possible oxonium **1.10** forms prior to hydrolysis or adduct formation. Both **1.8** and **1.9** can be further oxidized *in vivo* to keto acid **1.11** or hydroxy acid **1.12**. Measurement of these of these acids has been achieved in rats²⁰⁴ and monkeys¹⁹⁷, but as evaded measurement in humans due to the interference of nicotine. An approach to overcome this hurdle and use **1.12** as a human biomarker is the focus of **Chapter 4**.



Scheme 1-5: Overall metabolism of NNN

The preference between 2'- and 5'-hydroxylation depends on the tissue, species, and chirality of NNN. In rats, 2'-hydroxylation is a major route of metabolism in the esophagus and nasal mucosa while 5'-hydroxylation dominates in the liver¹⁹⁶. Because the esophagus and nasal mucosa are major sites of NNN carcinogenicity, DNA adducts resulting from 2'-hydroxylation could be important. On the other hand, extensive 5'-hydroxylation is seen in target tissues of Syrian golden hamsters, namely the trachea²⁰⁵. Similarly, 5'-hydroxylation was found to be a major pathway in A/J mouse lungs and 18-day-old minipigs^{206,207}. Monkeys also indicate preference for 5'-hydroxylation as hydroxy acid **1.12** was ~44% of the recovered dose¹⁹⁷; however, it is possible that most keto acid **1.11** (2.7% of recovered dose) is reduced to hydroxy acid **1.12** before urinary excretion. For humans, 5'-hydroxylation is presumably major based on studies with human liver microsomes, isolated P450s, and *ex vivo* esophagus tissue^{194,208}. Work in **Chapter 4** adds to this data through measurement of hydroxy acid **1.12** in the urine of smokeless tobacco users. This picture of metabolism is even more complex when considering NNN enantiomers with respect to the 2'-center. As an example, the ratio of 2'- to 5'-hydroxylation of (*S*)-NNN in the rat esophagus is 6-8:1 as determined by keto acid **1.11** and keto alcohol **1.8** excretion. In contrast, (*R*)-NNN undergoes almost equal levels of 2'- and 5'-hydroxylation¹⁹⁶. The enantiomeric differences in metabolism become even more apparent when studied at the DNA adduct level.

1.4.2.2 Known Adducts

Until recently, the only NNN-derived DNA adducts measured in animals were four POB adducts: 7-POB-dGuo, *O*²-POB-Thd, *O*²-POB-dCyd, and *O*⁶-POB-dGuo (Fig. 1-8).

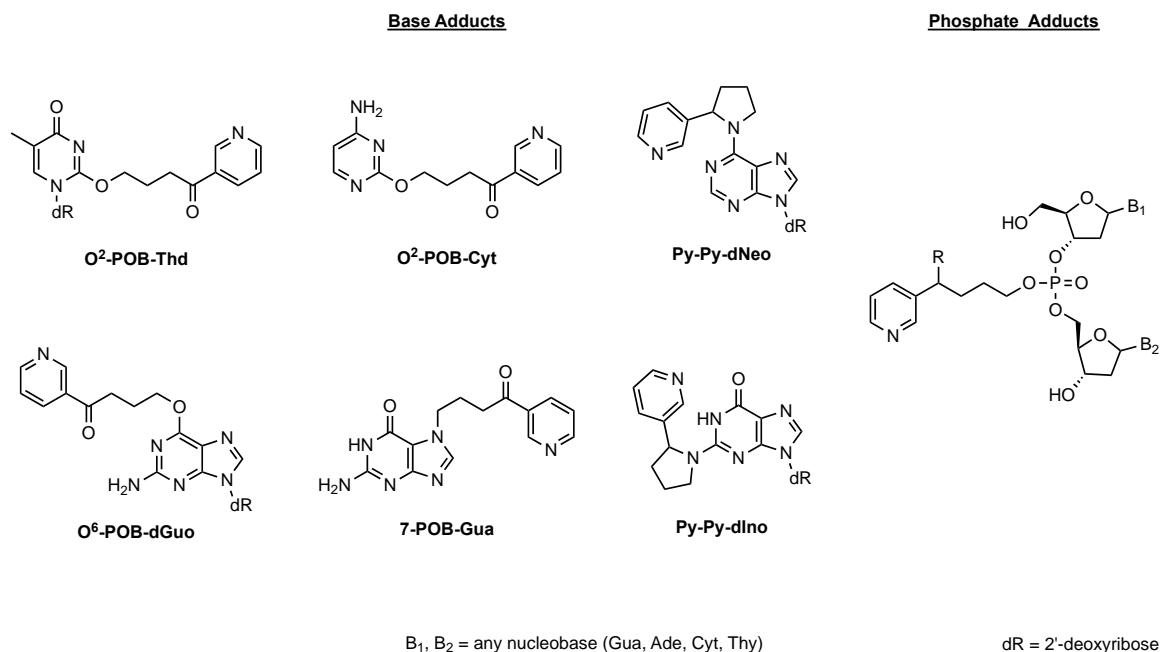


Figure 1-8: Chemical structures of NNN-derived adducts measured *in vivo*

Because 7-POB-dGuo and *O*²-POB-dCyd have destabilized glycosidic bonds, these adducts are measured as 7-POB-Gua and *O*²-POB-Cyt after neutral thermal hydrolysis. All but *O*⁶-POB-dGuo were found in a 20-week study involving rats chronically treated with 10 ppm (*S*)- or (*R*)-NNN²⁰⁹. 7-POB-Gua was most abundant in the majority of tissues, followed by *O*²-POB-Thd and *O*²-POB-Cyt. In agreement with metabolite levels discussed in the previous section, (*S*)-NNN produced more adducts overall than (*R*)-NNN in the esophagus, liver, and oral cavity; the levels were reversed for the lung and nasal mucosa. A follow-up study, in which rats were treated analogously for 70 weeks, was conducted and similar enantioselectivity was seen except nasal respiratory mucosa, but not nasal olfactory mucosa, had more (*S*)-NNN-adducts²¹⁰.

More recently, 5'-hydroxylation was evaluated in rat and human hepatocytes, human liver S9 fraction, and F-344 rats²⁰⁸. Py-Py-dIno was found as the most predominant 5'-adduct in the esophagus, liver, lung, oral cavity, and nasal cavity. Py-Py-

dNeo, a dAdo-derived adduct, was also detected but at much lower levels in the lungs and nasal cavity; the adduct was not observed in the liver, esophagus, or oral cavity. Py-Py-dIno was also observed in human liver S9 fraction and human hepatocytes, indicating this adduct might be major in humans exposed to NNN; however, efforts to confirm this have not yet been successful. In this study, considerable diastereoselectivity was seen for (*S*)- and (*R*)-NNN and the resulting Py-Py-dIno diastereomers but is out of scope for discussion here.

One other type of NNN-derived adducts worth noting are DNA-phosphate adducts. Originally discovered in the context of NNK⁵⁰, many B₁(POB)pB₂ adducts are known and also form from chronic NNN treatment (**Fig. 1-8**)²¹¹. All 32 possible POB-phosphotriesters were observed in rat esophageal and nasal mucosa. When taken together, phosphate adducts are less abundant than all POB-/Py-Py-base adducts in the oral cavity, nasal mucosa, and liver; the esophagus was the opposite and could indicate these adducts are important for carcinogenicity in this tissue. The enantiomers of NNN are also discriminated for these adducts. (*S*)-NNN forms more phosphate adducts in the oral cavity, esophagus, and rat liver, which mirrors the distribution of NNN-derived base adducts. Trends for each set of dinucleotides were also observed but are complex and outside the scope of this dissertation.

1.4.2.3 Known Carcinogenicity

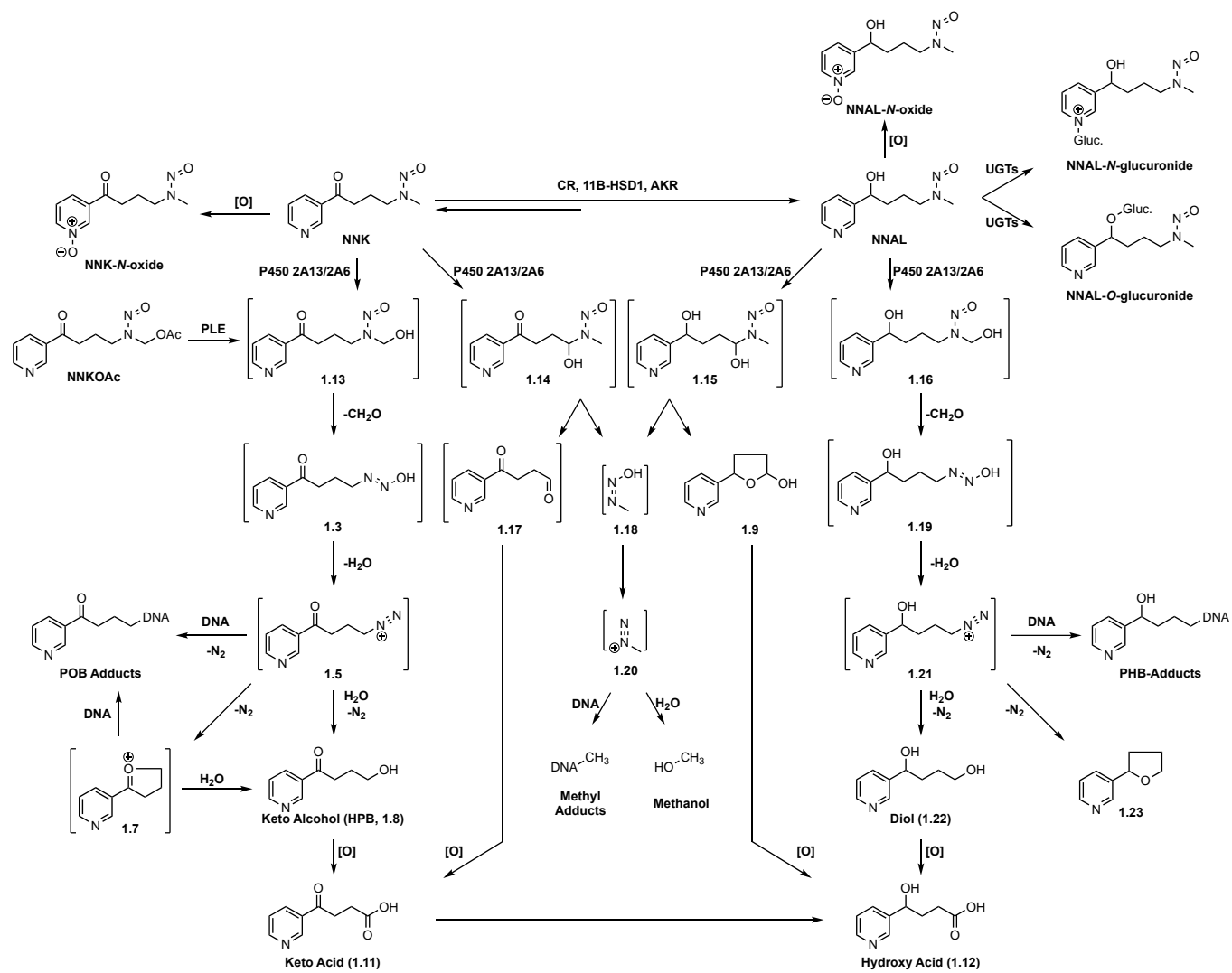
NNN has been shown to cause tumors in a variety of tissues and animals. In rats, NNN mainly causes esophageal and nasal tumors^{212,213}. As previously described, these tissues are also major sites of NNN metabolism and POB adduct formation, which helps link these lesions to carcinogenicity. A recent study evaluating (*S*)- and (*R*)-NNN separately showed (*S*)-NNN to cause >200 tumors amongst 20 rats treated chronically for 70 week at 14 ppm in the drinking water²¹⁴. In addition to the esophagus, ~40-50% of tumors were found within the oral cavity. (*R*)-NNN surprisingly showed very little carcinogenicity, but seemed to synergize with (*S*)-NNN as a racemic mixture. It was hypothesized that DNA adduct levels would synergize as well, however, little to no synergy was seen other than for *O*⁶-POB-dGuo²¹⁵. In mice, NNN causes lung tumors

when given i.p.^{84,185}; topical application showed no dose-dependent effects²¹⁶. Hamsters and mink were similar in that trachea and nasal cavity tumors are observed²¹⁷⁻²¹⁹. All this data together with the levels of human exposure and concordance with target tissues of tobacco-related cancers implicates NNN as a human carcinogen for esophageal and oral cancers and is recognized as a Group 1 carcinogen by the International Agency for Research on Cancer when in combination with NNK⁹. Given this proclamation, it may be surprising that, prior to this dissertation, no specific NNN bioactivation metabolites or DNA adducts have been measured in humans. Thus, the study conducted in **Chapter 4** is a major step forward in our understanding of human NNN carcinogenesis in that we successfully measure NNN bioactivation in humans for the first time.

1.4.3 NNK

1.4.3.1 Metabolism

The metabolism of NNK is shown in **Scheme 1-6**. Similar to NNN, NNK undergoes pyridine *N*-oxidation and denitrosation as minor *in vitro* detoxification mechanisms, but not β -oxidation; however, γ -oxidation has recently been described²²⁰. Interestingly, only *N*-oxidation has been observed *in vivo*.



Scheme 1-6: Metabolism of NNK and NNAL *in vivo*

The key metabolic difference between NNK and NNN metabolism is reduction of NNK to NNAL (nicotine-derived nitrosaminoalcohol) by cytosolic carbonyl reductase (CR), 11- β -hydroxysteroid dehydrogenase (11 β -HSD1) and aldo-keto reductases (AKR)^{26,221,222}. NNAL is a significant metabolite in rat and human liver, human lung, and rat and human pancreas tissue^{190,223}. While NNAL itself is not a detoxification product, *N*- or *O*-NNAL-glucuronide is a significant detoxification product *in vivo* and used as a urinary biomarker, along with unmodified NNAL, for NNK exposure¹⁷⁴. This widely applied biomarker is referred to as Total NNAL and is now prospectively linked to lung cancer risk^{172,173}. Along with *N*-oxidation, NNAL can also be enzymatically converted back to NNK in an enantioselective process. The ketone in NNK is enantiotopic and gives (*S*)- and (*R*)-enantiomers after enzymatic reduction. AKR1C1, 1C2, and 1C4 produce >90% (*S*)-NNAL which is an agreement with the enantioselectivity of rat and human liver, placenta, and lung tissues²²². Conversely, (*R*)-NNAL is 35% and 70% of total NNAL from purified 11 β -HSD1 and human microsome reduction, respectively²⁶. While the full complexity of NNAL enantioselectivity is outside the scope of this thesis, it should be noted that (*S*)- and (*R*)-NNAL appear to form different types and levels of DNA adducts *in vivo*, which is a theme supported in **Chapter 3**.

NNK and NNAL are both extensively α -hydroxylated *in vitro* and *in vivo*. In the case of NNK, α -hydroxylation can occur at the α -methyl and α -methylene position. While a variety of P450s are known to perform this reaction, P450 2A6 and 2A13 are believed to be most important due to their tissue expression and productive catalytic activity (**Section 1.3.4**)¹³⁷. Hydroxylation of the α -methyl position creates unstable α -hydroxynitrosamine **1.13** that decomposes by expected mechanisms (**Section 1.1.3 & 1.3.3**) to the same diazonium ion, or oxonium ion, seen from 2'-hydroxylation of NNN. Consequentially, α -methyl-hydroxylation produces a series of POB-DNA adducts. Likewise, hydrolysis products of NNK are keto alcohol **1.8** and keto acid **1.11**. α -Methylene hydroxylation produces α -hydroxynitrosamine **1.14** that releases methyldiazohydroxide **1.18**, a potent methylating agent. The keto aldehyde (**1.17**) released is a major product from *in vitro* P450 assays, but is commonly not observed in

the urine of animals and humans¹⁹⁰. Instead, it is believed that keto aldehyde is further oxidized to keto acid **1.11**.

NNAL also undergoes α -hydroxylation at both the α -methyl or α -methylene position. The α -hydroxynitrosamine species (**1.15** & **1.16**) proceed through identical decomposition pathways as NNK to produce pyridylhydroxybutyl (PHB) DNA adducts and methyl adducts (**Scheme. 1-6**). Both hydrolysis products, lactol **1.9** and diol **1.22**, are observed *in vitro* but are further oxidized *in vivo* to hydroxy acid **1.12** and excreted in the urine of animals and humans.

Interestingly, both NNN and NNK produce the same metabolic activation biomarkers. Deuterated versions of keto acid and hydroxy acid were recently measured in the urine of smokers using [pyridine-D₄]NNK cigarettes, establishing α -hydroxylation of NNK as a major route of human metabolism²²⁴. The analogous study with [pyridine-D₄]NNN in smokeless tobacco is the focus of **Chapter 4**.

1.4.3.2 Known Adducts

NNK produces the same four POB adducts seen with NNN (**Fig 1-9**). When NNKOAc, a precursor to α -methyl-hydroxyNNK, is incubated with calf thymus DNA and porcine liver esterase (PLE), the relative abundance of DNA adducts is 7-POB-Gua > O⁶-POB-dGuo > O²-POB-Thd > O²-POB-Cyt²²⁵. In a 20-week rat study, these relative levels changed to O²-POB-Thd > 7-POB-Gua > O²-POB-Cyt > O⁶-POB-dGuo for nearly every time point in the liver, lung, pancreas, nasal and oral mucosas^{210,226}. A follow up 70-week rat study showed the same trend except O²-POB-Cyt was not observed²⁰, possibly due to its instability *in vivo* and during sample work-up. Attempts to stabilize this adduct through bisulfite-mediated deamination were mostly unsuccessful, but did reveal two new Cyt-adducts *in vitro*: N⁴-POB-dCyd and N³-POB-dCyd²²⁷. The change in relative adduct levels between *in vitro* and *in vivo* implicate a role for DNA repair of 7-POB-dGuo and O⁶-POB-dGuo by spontaneous depurination and subsequent BER⁵³ or direct repair by AGT²²⁸, respectively. In comparison, O²-POB-Thd appears to persist and possibly avoid repair; however, NER does seem to be involved in its repair¹⁹³. In both

studies, adduct levels were most abundant in the lung, matching the established carcinogenicity of NNK and NNAL.

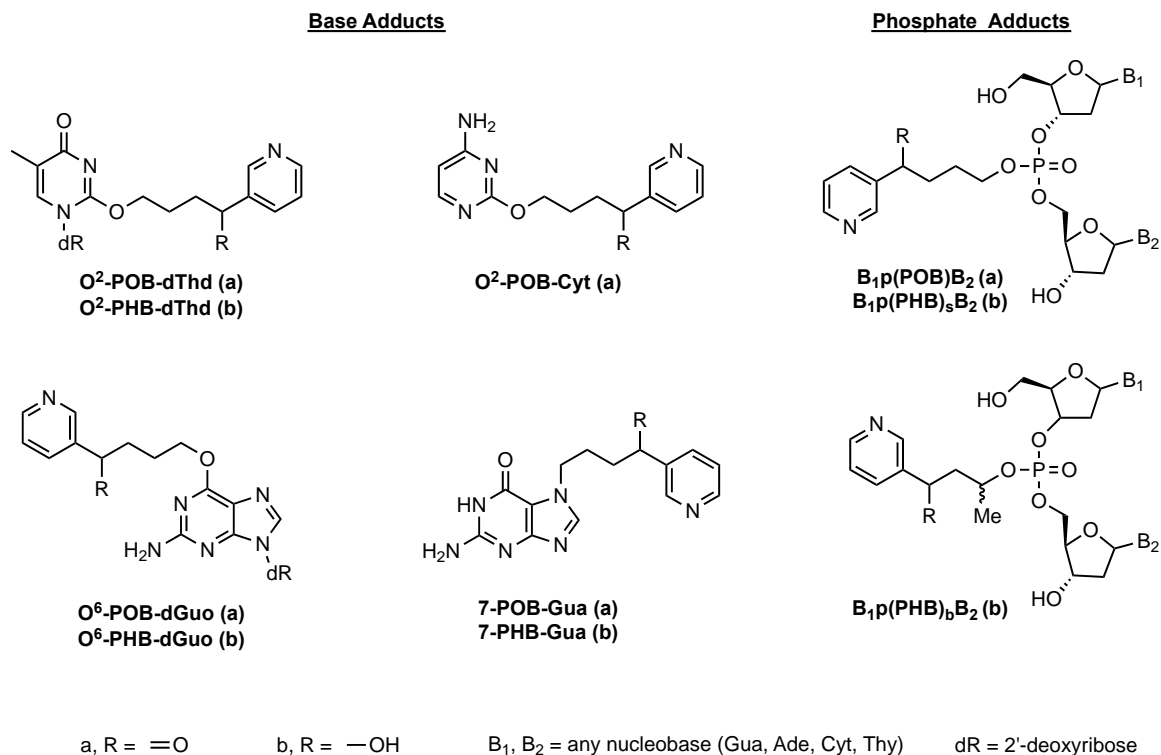


Figure 1-9: Chemical structures of POB- and PHB-adducts found in NNK- and NNAL-treated rats.

NNAL produces adducts with identical alkylation sites except with PHB instead of POB. NNAL is more complicated at the enantiomer level since (*S*)-NNAL appears to favor POB adduct formation while (*R*)-NNAL almost exclusively forms PHB adducts²²⁹. The prevailing hypothesis is (*S*)-NNAL is rapidly oxidized back to NNK at its site of action before exerting its alkylating effects. Notably missing from this panel of DNA adducts are 2'-deoxyadenosine adducts; **Chapter 3** fills this gap by identifying the structures and abundance of NNK- and NNAL-derived dAdo adducts *in vitro* and in rat liver and lung tissue.

As briefly mentioned in the context of NNN, NNK was recently shown to produce a variety of POB-phosphate adducts. Similar to NNN, POB-phosphate adducts are minor when compared to all NNK-derived base adducts. For example, the total POB phosphate adduct content is 5% of all possible POB DNA adducts *in vitro* and 5-9% *in vivo*⁵⁰. PHB phosphate adducts resulting from NNK and NNAL enantiomers have also been

investigated and have a shockingly high abundance. To date, >100 distinct PHB-phosphotriesters have been detected and measured in rat tissues. For NNK-treated rats, B₁p(PHB)B₂ adducts are between 34 – 55% of all adducts in the liver and lungs⁵¹. The high abundance observed is consistent with NNAL being the primary metabolite of NNK *in vivo*. Consistently, B₁p(PHB)B₂ adducts are 30 – 51% of all adducts for rats chronically treated with either NNAL enantiomer²³⁰. While the biological effects of these adducts are not fully elucidated, their overall abundance indicates they could serve a critical role in carcinogenesis.

NNK and NNAL are potent methylating agents via α -methylene hydroxylation. While many DNA methyl adducts are possible, the two primarily studied in the context of NNK and NNAL are *O*⁶-Me-dGuo and 7-Me-dGuo, which are both commonly measured as *O*⁶-Me-Gua and 7-Me-Gua *in vivo*. In the same 20-week rat study mentioned above, *O*⁶-Me-Gua was measured as a relatively major adduct in rat liver and lungs during the first 5 weeks of treatment but decreased afterward. This behavior was seen again in the follow-up 70 week study, but was a comparatively minor adduct throughout the study. *O*⁶-Me-dGuo is believed to be the most mutagenic methyl adduct and potentially the most mutagenic NNK- and NNAL-derived adduct²³¹. It is known that NNK produces this adduct within codon 12 of KRas, which induces GC to AT mutations, conferring constitutive activity to the protein^{232,233}. The potency of this adduct is enhanced by *O*⁶-POB-dGuo potentially due to it acting as a decoy substrate for AGT, thus allowing *O*⁶-Me-dGuo to persist^{234,235}. 7-Me-dGuo, on the other hand, is clearly more abundant in rat liver and lung tissue but has little to no effects on DNA replication⁴⁷. It is likely that 7-Me-dGuo, similar to 7-POB-dGuo, produces an AP site that is rapidly repaired by BER.

1.4.3.3 Known Carcinogenicity

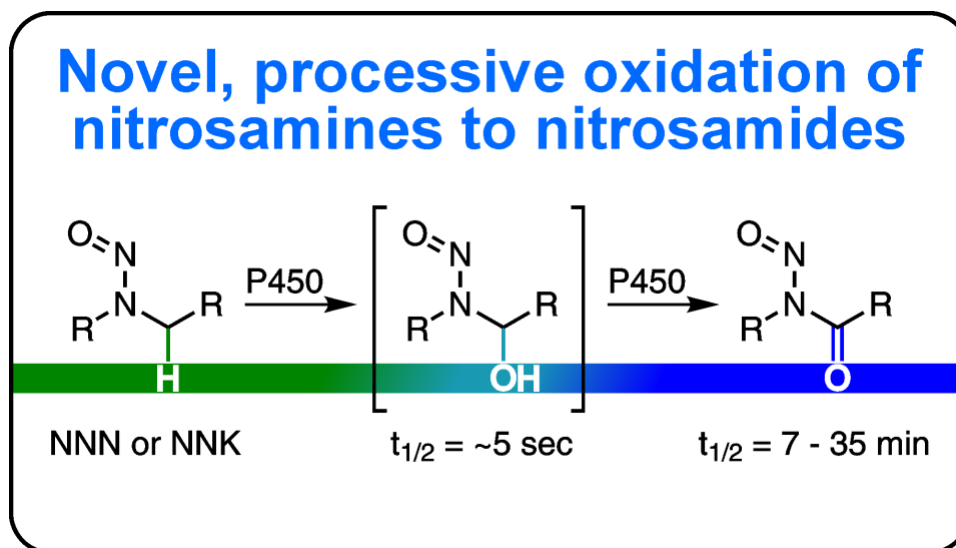
The major target tissue for NNK and NNAL is the lungs. Lung tumors have been induced in rats, mice, and hamsters regardless of the route of administration¹⁹⁰. For example, tumors formed in F-344 rats when administered NNK through the drinking water, oral swab, gavage, and subcutaneous injection^{20,236-238}. This indicates that local

application is not important and that carcinogenicity relies more on systemic distribution of NNK to the site of bioactivation. The potencies of NNK and NNAL were well demonstrated in the 70-week rat study described in the previous section²⁰. All rats chronically treated with 5 ppm NNK, (*S*)-NNAL, or (*R*)-NNAL presented lung tumors at necropsy while no tumors were found in any control rat. The NNK-treated rats had statistically more carcinomas than (*R*)-NNAL-treated rats, but were statistically similar with the (*S*)-NNAL-treated rats. Additionally, almost all rats contained adenomas and adenocarcinomas and a few showed metastases to the pancreas, an organ also found to contain POB- and PHB-adducts. As pointed out in the previous section, the lung-specificity of NNK and NNAL correlates with DNA adduct formation. This correlation was particularly strong in A/J mice where *O*⁶-Me-Gua levels directly correlated with tumor incidence²³¹. Other tissues targets of NNK and NNAL include rat nasal cavity and hamster trachea, but generally require higher doses and subcutaneous injection¹⁹⁰.

As previously stated in **Section 1.4.2.3**, NNK and NNN have been evaluated as Group 1 carcinogens by IARC and NNK is heavily implicated in tobacco-related lung cancer. The rationale for this decision stems from the animal work described here along with epidemiology linking NNK exposure to cancer risk. To summarize, NNK is found in both unburned tobacco and tobacco smoke, is productively activated by lung-specific P450 2A13, forms POB-, PHB-, and methyl-DNA adducts in the lungs of animals, initiates lung tumors in animals treated at the dose of a chronic smoker, and introduces mutations in *KRAS* that can initiate cancer. Together we build a strong case for human carcinogenicity, especially since recent data supports NNK bioactivation as a major metabolic pathway in humans²²⁴.

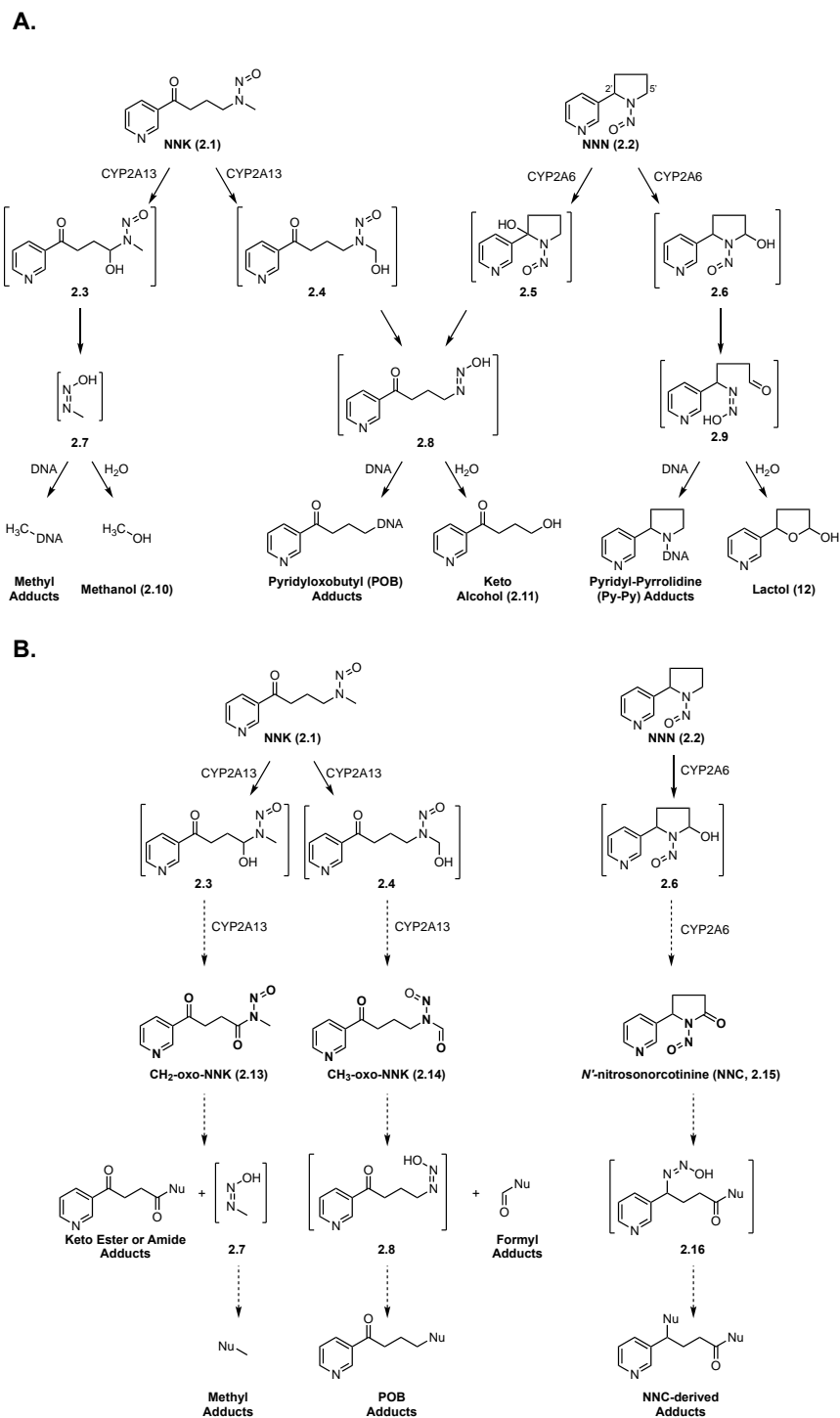
Chapter 2 *N*-Nitrosamides are Minor Oxidation Products in *N*-Nitrosamine Metabolism

The following chapter describes work that was previously published in *Chemical Research in Toxicology* (DOI: 10.1021/acs.chemrestox.6b00384) and is adapted with permission from the American Chemical Society²³⁹. The study was primarily performed by Erik S. Carlson and was co-authored by Pramod Upadhyaya and Stephen S. Hecht. This study was supported by the U.S. National Cancer Institute through grant CA-81301. The authors thank Bob Carlson for editorial assistance, Dr. Peter Villalta and Xun Ming for mass spectrometry assistance in the Analytical Biochemistry Shared Resource (partially supported by National Cancer Institute grant CA-77598), and Dr. Linda Von Weymarn and the laboratory of Dr. Sharon Murphy for allowing use of their facilities and providing enzymes for the cytochrome P450 incubations. We also thank Dr. Adam T. Zarth and Dr. Anna K. Michel for their valuable discussions and input.



2.1 Introduction

As discussed in **Section 1.1**, tobacco use remains a public health concern as it causes ~30% of all cancer deaths nationwide²⁴⁰. NNK (**2.1**) and NNN (**2.2**) are thought to play a critical role in this process (**Section 1.4**) and require metabolic activation to α -hydroxynitrosamines by cytochrome P450s to exert their carcinogenicity (**Scheme 2-1A**)^{190,191,241}. Prior work indicates α -hydroxynitrosamines have half-lives of ~5 sec^{242,243} before decomposing to diazonium ions that either hydrolyze to urinary products **2.10** – **2.12** or react with DNA and proteins to form adducts¹⁹⁰ (**Scheme 2-1A**). If left unrepaired, DNA adducts can cause mutations in critical oncogenes such as K-ras, initiating tumor development. Methyl adducts such as *O*⁶-methylguanine (*O*⁶-meGua) are especially tumorigenic in animal models.²³¹ For NNN, α -hydroxylation at the 2' or 5' position by P450 2A6 initiates a similar cascade leading to a variety of DNA adducts and urinary products (**Scheme 2-1A**). Both NNK- and NNN-derived DNA adducts have been identified and quantified in several animal models and show promise as biomarkers for carcinogen activation in humans.^{20,208,244–246}



Scheme 2-1: (A) Established *in vivo* metabolism of NNK (**2.1**) and NNN (**2.2**) by P450 2A13- or P450 2A6-mediated oxidation, respectively. Oxidation results in unstable α -hydroxynitrosamines (**2.3** – **2.6**) which spontaneously decompose to diazohydroxides (**2.7** – **2.9**). These either hydrolyze to products excreted in the urine (**2.10** – **2.12**) or react with DNA to form adducts. (B) Proposed P450-mediated oxidation of NNK (**2.1**) and NNN (**2.2**) to *N*-nitrosamides (**2.13** – **2.15**) through retention of the α -hydroxynitrosamines **2.3**, **2.4**, and **2.6** within the P450 active site.

While the α -hydroxynitrosamine hypothesis accounts for many of the metabolic products and DNA adducts produced in the metabolism of NNK, NNN, and other carcinogenic nitrosamines (**Section 1.2.1**), there are also inconsistencies with this hypothesis.^{247,248} Important among these is the short lifetime of α -hydroxynitrosamines, which raises questions about their ability to alkylate nuclear DNA after having been formed in the endoplasmic reticulum. A few studies have shown these intermediates exist long enough for *O*-glucuronidation, but measured levels were minor (<1% of the excreted dose)²⁴⁹. In addition, it is unclear if this pathway mediates detoxification or intracellular transportation to the nucleus^{249–251}. Elespuru et al and Guttenplan have explored the hypothesis that the α -hydroxynitrosamines are further oxidized to *N*-nitrosamides, which are also direct DNA alkylating agents, but this alternate hypothesis lacks compelling supportive data^{247,248}. In the study reported here, we explore this hypothesis with respect to NNK and NNN. We hypothesize that the α -hydroxynitrosamines could be retained in the active site of P450 2A13 or P450 2A6 and further oxidized to the corresponding *N*-nitrosamides: 4-(methylnitrosamino)-1-(3-pyridyl)-1,4-butanedione (CH₂-oxo-NNK, **2.13**), 4-(nitrosoformamido)-1-(3-pyridyl)-1-butanone (CH₃-oxo-NNK, **2.14**) from NNK and *N'*-nitrosanorcotinine (NNC, **2.15**) from NNN.

There is precedent for retention of substrates in P450s leading to processive oxidation. Metabolism of nicotine by P450 2A6 proceeds through a retained iminium ion or hemiaminal intermediate before releasing cotinine as the major metabolite.³⁸ The Guengerich group has shown that P450 2E1 oxidizes ethanol directly to acetic acid with limited substrate dissociation.²⁵² Likewise, they showed that formaldehyde and acetaldehyde formed in the metabolism of dimethylnitrosamine and diethylnitrosamine by P450 2A6 are directly oxidized to formic acid and acetic acid, respectively, without release of the intermediate aldehydes.²⁵³ They later proposed an alternate route for acid formation via an *N*-nitrosamide intermediate; however, it was undetectable under their conditions.²⁵⁴

N-Nitrosamides are recognized as direct-acting carcinogens with common half-lives being on the scale of minutes.⁹⁴ Extensive research shows that their stability and reactivity is dependent on temperature, steric and electronic factors, and solvent

composition.^{95,97,98,255,256} In nucleophilic environments,²⁵⁷ the major products are the corresponding carboxylic acid derivatives and the diazonium species discussed earlier (**Scheme 2-1B** & **Section 1.2**). Thus, if released into a cell, *N*-nitrosamides should have not only better stability for traversing the hydrolytic environment of the cytosol, but also the ability to alkylate DNA. If *N*-nitrosamines are oxidized to *N*-nitrosamides, this could lead to the identification of new classes of DNA adducts and a better understanding of the mechanisms of *N*-nitrosamine carcinogenesis.

In this study, we examine the hypothesis that NNK and NNN are metabolized to their corresponding *N*-nitrosamides. We synthesized these three *N*-nitrosamides and evaluated their half-lives and major degradation products *in vitro*. We describe our finding that CH₂-oxo-NNK and NNC are minor metabolites of NNK and NNN in *in vitro* assays with human cytochrome P450s. Further evaluation of CH₂-oxo-NNK demonstrated that it methylates dGuo in DNA and is thus potentially mutagenic. Together, this work provides the first account of an *N*-nitrosamine being converted metabolically to an *N*-nitrosamide and furthers our understanding of the metabolism of NNK and NNN.

2.2 Experimental Procedures

CAUTION: *NNN and NNK are carcinogenic in animal models and are IARC Group 1 carcinogens. All nitrosamides are presumed to be carcinogens based on their structure and reactivity. Handle these in a well-ventilated fume hood with personal protective equipment and extreme care.*

2.2.1 Chemicals and Enzymes

NNK, NNN, 4-oxo-4-(3-pyridyl)-butanol (keto alcohol, **2.11**), 5-(3-pyridyl)-2-hydroxytetrahydrofuran (lactol, **2.12**), *O*⁶-methylguanine (*O*⁶meGua), and [CD_3]*O*⁶meGua were synthesized as previously described.^{258–261} 5-(3-Pyridyl)-2-pyrrolidinone (norcotinine, **2.28**) was obtained from AKos GmbH (Steinen, Germany). P450 2A6 Baculosomes, regeneration system and reaction buffer were available as a Vivid CYP450 Screening Kit from Life Technologies (Carlsbad, CA). Purified P450 2A13 and P450 reductase were a generous gift from Dr. Sharon Murphy (University of Minnesota). All other chemicals and solvents used were obtained from either Sigma Aldrich (Milwaukee, WI) or Thermo Scientific (Waltham, MA) in reagent grade and used without further purification.

2.2.2 General Synthetic Procedures

NMR spectra were recorded on a Bruker 500 MHz spectrometer. Chemical shifts are reported as parts per million (ppm). Residual solvent peaks were used as an internal reference for ¹H-NMR (7.26 ppm CDCl₃; 2.50 ppm D₆-DMSO) and ¹³C-NMR (77.2 ppm CDCl₃; 39.5 ppm D₆-DMSO). Peak splitting used the following abbreviations: s = singlet, d = doublet, t = triplet, q = quartet, dd = doublet of doublets, dt = doublet of triplets, ddd = doublet of doublet of doublets, bs = broad singlet, and m = multiplet. High resolution mass spectrometry (HRMS) for selected compounds was performed on an LTQ Orbitrap Velos (Thermo Scientific, Carlsbad, CA) and reported as *m/z*. Thin-layer chromatography (TLC) utilized Polygram pre-coated silica gel TLC plate (40 x 80 mm, 0.2 mm thick) with 254 nm fluorescent indicator. TLC plates were visualized with

permanganate stain when necessary, otherwise UV lamp irradiation sufficed. Flash chromatography was performed on SiliCycle 60 (70-150) mesh silica gel. Reactions were performed under an atmosphere of N₂ unless specified otherwise.

2.2.3 Synthesis of Chemical Standards

Methyl 4-oxo-4-(3-pyridyl)-1-butanoate (2.18):

Sodium cyanide (0.104 g, 2.12 mmol) was suspended in anhydrous *N,N*-dimethylformamide (DMF, 10 mL) and brought to 35 °C. 3-Pyridinecarboxaldehyde (2.27 g, 21.2 mmol, 2 mL) was added dropwise to the suspension. After 10 min of stirring, the resulting red solution was treated dropwise with methyl acrylate (1.90 g, 22.1 mmol, 2 mL). Over 4 h, the solution became increasingly yellow and slightly viscous. The reaction was quenched with acetic acid (100 µL). The resulting yellow solution was diluted in CH₂Cl₂ and washed with H₂O and brine. The organic layer was dried over MgSO₄, filtered, and concentrated *in vacuo* to a crude, yellow solid. Purification by column chromatography (50 to 100% EtOAc in hexanes) yielded pure product as a white, crystalline solid (3.02 g, 73.8%).

¹H-NMR (500 MHz; CDCl₃): δ 9.21 (dd, *J* = 2.2, 0.8 Hz, 1H, 2-Py), 8.79 (dd, *J* = 4.8, 1.7 Hz, 1H, 6-Py), 8.25 (ddd, *J* = 8.0, 2.2, 1.8 Hz, 1H, 4-Py), 7.43 (ddd, *J* = 8.0, 4.8, 0.9 Hz, 1H, 5-Py), 3.72 (s, 3H, CH₃), 3.33 (t, *J* = 6.5 Hz, 2H, COCH₂CH₂), 2.80 (t, *J* = 6.5 Hz, 2H, COCH₂CH₂); ¹³C-NMR (126 MHz; CDCl₃): δ 197.1 (CO), 173.2 (CO₂CH₃), 153.8 (2-Py), 149.8 (5-Py), 135.5 (4-Py), 131.9 (3-Py), 123.8 (5-Py), 52.1 (CH₃), 33.8 (COCH₂CH₂CO₂), 27.9 (COCH₂CH₂CO₂) ppm.

4-Oxo-4-(3-pyridyl)-butanoic acid (2.19):

Compound **2.18** (393 mg, 2.03 mmol) was dissolved in 1N NaOH (4 mL) and stirred for 3 h at room temperature. The solution went from colorless to yellow. The pH was adjusted to ~5-6 with an equal volume of 1N HCl and a precipitate formed. The solid was filtered and dried under vacuum to give a white, crystalline solid (251 mg, 69%).

¹H-NMR (500 MHz; DMSO-*d*₆): δ 12.18 (s, 1H, COOH), 9.14 (d, *J* = 2.1 Hz, 1H, 2-Py), 8.80 (dd, *J* = 4.8, 1.6 Hz, 1H, 6-Py), 8.31 (dd, *J* = 8.0, 1.8 Hz, 1H, 4-Py), 7.57 (dd, *J* = 8.0, 4.8 Hz, 1H, 5-Py), 3.30 (t, *J* = 6.3 Hz, 2H, COCH₂), 2.60 (t, *J* = 6.3 Hz, 2H, CH₂COOH). ¹³C-NMR (126 MHz; DMSO): δ 198.1 (CO), 173.7 (COOH), 153.5 (2-Py), 149.1 (6-Py), 135.4 (4-Py), 131.7 (3-Py), 123.9 (5-Py), 33.4 (COCH₂), 27.7 (CH₂COOH) ppm.

Methyl 4-oxo-4-(3-pyridyl)-butanamide (2.20a):

A solution of **2.19** (43.57 mg, 0.243 mmol), methylamine hydrochloride (25.41 mg, 0.376 mmol), and *N*-hydroxysuccinimide (NHS, 45.2mg, 0.393 mmol) in anhydrous dimethylsulfoxide (DMSO, 3 mL) was treated with *N,N*-diisopropylethylamine (DIPEA, 75.7 mg, 0.586 mmol, 102 μL) and 1-ethyl-3-(3-dimethylaminopropyl)carbodiimide (EDAC, 196 mg, 1.03 mmol). The reaction was stirred for 22 h at room temperature before diluting with EtOAc. The mixture was washed with H₂O and brine, dried over MgSO₄, filtered, and concentrated *in vacuo* to yield a crude, pink oil. Purification by column chromatography (5:100 MeOH/CH₂Cl₂) yielded pure product as an off-white solid (32.9 mg, 70%).

¹H-NMR (500 MHz; DMSO-*d*₆): δ 9.13 (d, *J* = 1.2 Hz, 1H, 2-Py), 8.79 (dd, *J* = 4.7, 1.3 Hz, 1H, 6-Py), 8.30 (d, *J* = 7.9 Hz, 1H, 4-Py), 7.84 (s, 1H, NH), 7.57 (dd, *J* = 7.9, 4.7 Hz, 1H, 5-Py), 3.27 (t, *J* = 6.6 Hz, 2H, COCH₂), 2.57 (d, *J* = 4.6 Hz, 3H, CH₂CONH), 2.48 (t, *J* = 6.6 Hz, 2H, NHCH₃). ¹³C NMR (126 MHz; DMSO): δ 198.6 (CO), 171.3 (CONH), 153.3 (6-Py), 149.1 (2-Py), 135.4 (4-Py), 131.8 (3-Py), 123.9 (5-Py), 33.7 (COCH₂), 29.0 (CH₂CONH), 25.5 (NHCH₃) ppm.

4-(Methylnitrosamino)-1-(3-pyridyl)-1-butanedione (CH₂-oxo-NNK, 2.13):

A solution of **2.20a** (31.4mg, 0.163 mmol) in a 5:1 mixture of acetic anhydride and acetic acid (6 mL) was brought to 0 °C. To this was added NaNO₂ (30.7 mg, 0.445 mmol) all at once. After 4 h, the mixture was poured onto ice-cold H₂O. The aqueous mixture was extracted with CH₂Cl₂. The pooled organics were dried over MgSO₄, filtered, and concentrated *in vacuo* to yield a crude yellow oil. Purification by column

chromatography on silica gel (100% EtOAc) yielded pure product as a bright, yellow oil (28.8 mg, 65%).

$^1\text{H-NMR}$ (500 MHz; CDCl_3): δ 9.27 (s, 1H, 2-Py), 8.83 (d, $J = 4.1$ Hz, 1H, 6-Py), 8.31 (d, $J = 7.9$ Hz, 1H, 4-Py), 7.48 (dd, $J = 7.8, 4.9$ Hz, 1H, 5-Py), 3.67 (t, $J = 6.0$ Hz, 2H, COCH_2), 3.55 (t, $J = 6.0$ Hz, 2H, CH_2CON), 3.14 (s, 3H, CH_3). $^{13}\text{C NMR}$ (126 MHz; CDCl_3): δ 196.7 (CO), 175.9 (CONNO), 153.5 (6-Py), 149.4 (2-Py), 135.6 (4-Py), 131.9 (3-Py), 123.8 (5-Py), 33.0 (CH_2CONNO), 28.7 (COCH_2), 25.9 (NCH_3) ppm. HRMS Calc: 222.08732, Found: 222.08719

CH_2 -oxo-NNK from 5'-Hydroxycotinine:

5'-Hydroxycotinine (54.23 mg, 0.282 mmol) in CH_2Cl_2 (25 mL) was brought to 0 °C and treated with *p*-toluenesulfonic acid (111 mg, 0.584 mmol). After 5 min of stirring, NaNO_2 (151.2 mg, 2.2 mmol) was added. Stirring was continued for 3 h before pouring onto ice-cold H_2O . The organic layer was separated and the aqueous extracted with CH_2Cl_2 . The pooled organics were dried over MgSO_4 , filtered, and concentrated *in vacuo* to give a crude orange oil. The product was purified by HPLC using a 150 x 4.6 mm, 5 μm , Kinetix HILIC column (Phenomenex) with 1:1 hexanes/ CHCl_3 and isopropanol as mobile phases. The gradient was 5% to 20% isopropanol over 10 min at 1 mL/min. The product eluted at ~4 min. The purified product was a bright, yellow oil (4.98 mg, 8%).

***N'*-Nitrosonorcotinine (NNC, 2.15):**

A solution of norcotinine (31.4 mg, 0.163 mmol) in a 5:1 mixture of acetic anhydride and acetic acid (6 mL) was brought to 0 °C. To this was added NaNO_2 (30.7 mg, 0.445 mmol) all at once. After 4 h, the mixture was poured onto ice-cold H_2O . The aqueous mixture was extracted with CH_2Cl_2 . The pooled organics were dried over MgSO_4 , filtered, and concentrated *in vacuo* to yield a crude yellow oil. Purification by column chromatography (100% EtOAc) yielded pure product as a bright, yellow oil (92%).

$^1\text{H-NMR}$ (500 MHz; CDCl_3): δ 8.56 (d, $J = 4.3$ Hz, 1H, 6-Py), 8.46 (d, $J = 1.8$ Hz, 1H, 2-Py), 7.36 (d, $J = 8.0$ Hz, 1H, 4-Py), 7.30-7.28 (m, 1H, 5-Py), 5.29 (dd, $J = 9.1,$

3.1 Hz, 1H, NCH), 2.97 (dt, $J = 18.6, 9.4$ Hz, 1H, COCH₂), 2.87 (ddd, $J = 18.5, 9.4, 4.0$ Hz, 1H, COCH₂'), 2.66 (dq, $J = 13.4, 9.4$ Hz, 1H, CHCH₂), 2.15-2.09 (m, 2H, CHCH₂') ppm; ¹³C-NMR (126 MHz; CDCl₃): δ 172.7 (CO), 149.4 (6-Py), 147.1 (2-Py), 134.1 (3-Py), 132.7 (4-Py), 123.8 (5-Py), 55.7 (NCH), 26.2 (COCH₂), 22.2 (CHCH₂) ppm. HRMS Calc: 192.07675, Found: 192.07670

2-(3-Pyridyl)-1,3-dithiane (2.21):

A solution of 3-pyridylcarboxaldehyde (114 mg, 1.06 mmol, 100 μ L) and 1,3-propanedithiol (162 mg, 1.50 mmol, 150 μ L) in anhydrous tetrahydrofuran (THF, 5 mL) was treated with BF₃•Et₂O (173 mg, 1.22 mmol 300 μ L) dropwise at room temperature. The mixture was then heated to reflux at 80 °C and stirred for 24 h before quenching with sat'd NaHCO₃ solution. The aqueous phase was extracted several times with CH₂Cl₂. The pooled organic layers were washed with brine, dried over MgSO₄, filtered, and evaporated *in vacuo* to give crude yellow crystals. Purification by column chromatography (hexanes/EtOAc 1:1) yielded the product as a fine, white powder (199.4 mg, >95%).

¹H-NMR (500 MHz; CDCl₃): δ 8.72 (d, $J = 2.0$ Hz, 1H, 2-Py), 8.57 (dd, $J = 4.9, 1.5$ Hz, 1H, 6-Py), 7.85 (dt, $J = 7.9, 2.0$ Hz, 1H, 4-Py), 7.31 (dd, $J = 7.9, 4.9$ Hz, 1H, 5-Py), 5.21 (s, 1H, S₂CH), 3.10 (ddd, $J = 14.6, 12.3, 2.4$ Hz, 2H, SCH₂CH₂-ax), 2.96 (dt, $J = 14.0, 3.8$ Hz, 2H, SCH₂CH₂-eq), 2.22 (dtt, $J = 14.2, 4.6, 2.4$ Hz, 1H, SCH₂CH₂-ax), 2.02-1.93 (m, 1H, SCH₂CH₂-eq) ppm; ¹³C NMR (126 MHz; CDCl₃): δ 150.1 6-Py, 149.5 (2-Py), 135.7 (4-Py), 135.4 (3-Py), 124.0 (5-Py), 48.8 (S₂CH), 32.3 (SCH₂CH₂), 25.2 (SCH₂CH₂) ppm.

tert-Butyl 3-(2-(3-pyridyl)-1,3-dithianyl)-1-propylcarbamate (2.22):

A solution of **2.21** (222 mg, 1.13 mmol) and tetramethylethylenediamine (TMEDA, 131.8 mg, 1.13 mmol, 170 μ L) in anhydrous THF (6 mL) was cooled to -78 °C and treated with *n*-BuLi in hexanes dropwise (1.28 mmol, 800 μ L). The resulting dark red solution was stirred at -78 °C for 30 min before dropwise addition of **2.27** in THF (360 mg, 1.26 mmol, 3 mL). The mixture was stirred at -78 °C for 2 h before allowing the bath

to come to room temperature. After 14 h of stirring, the reaction was quenched with H₂O. The aqueous phase was extracted several times with EtOAc. The pooled organics were dried over MgSO₄, filtered, and concentrated *in vacuo* to give a crude, yellow oil. Purification by column chromatography (hexanes/EtOAc 1:1) yielded the product as yellow crystals (290 mg, 72.5%).

¹H-NMR (500 MHz; CDCl₃): δ 9.13 (d, *J* = 2.1 Hz, 1H, 2-Py), 8.52 (dd, *J* = 4.7, 1.6 Hz, 1H, 6-Py), 8.20 (ddd, *J* = 8.1, 2.4, 1.6 Hz, 1H, 4-Py), 7.32 (ddd, *J* = 8.1, 4.7, 0.6 Hz, 1H, 5-Py), 4.41 (bs, 1H, NH), 3.03-3.00 (m, 2H, NHCH₂), 2.72-2.61 (m, 4H, SCH₂CH₂), 2.03-2.00 (m, 2H, CCH₂), 1.99-1.91 (m, 2H, SCH₂CH₂), 1.48-1.42 (m, 2H, CH₂CH₂CH₂), 1.40 (s, 9H, C(CH₃)₃) ppm; ¹³C NMR (126 MHz; CDCl₃): δ 155.9 (NHCO), 150.8 (2-Py), 148.4 (6-Py), 137.6 (3-Py), 136.8 (4-Py), 123.4 (5-Py), 79.4 (C(CH₃)₃), 56.5 (SCS), 42.5 (CCH₂), 40.4 (NHCH₂), 28.5 (CH₃), 27.6 (SCH₂CH₂), 25.1 (SCH₂CH₂), 24.7 (CH₂CH₂CH₂) ppm.

3-(2-(3-Pyridyl)-1,3-dithianyl)-1-propylformamide (2.23):

A solution of **2.22** (87.6 mg, 0.247 mmol) in CH₂Cl₂ (3 mL) was treated with trifluoroacetic acid (TFA, 1.49 g, 13.1 mmol, 1 mL), which resulted in gas evolution. After 3 h, the solvent was evaporated *in vacuo* to remove excess TFA. The resulting oil was reconstituted in CH₂Cl₂ and washed with sat'd. NaHCO₃ solution and brine. The organic layer was dried over MgSO₄, filtered, and concentrated *in vacuo* to give a yellow oil. This was dissolved in MeOH (5 mL) and treated with triethylamine (29.04 mg, 0.288 mmol, 40 μL) and methyl formate (95.7 mg, 1.60 mmol, 110 μL). The flask was sealed and heated to 55 °C with stirring. After 4 h, the mixture was concentrated *in vacuo* to yield a yellow oil. ¹H-NMR indicated the product was a 9:1 mixture of *cis*- and *trans*-formamide isomers. Purity was sufficient to carry forward without column purification.

¹H-NMR (500 MHz; CDCl₃): δ 9.09 (d, *J* = 2.5 Hz, *trans*-2-Py), 9.08 (d, *J* = 2.1 Hz, 1H, *cis*-2-Py), 8.49 (dd, *J* = 4.8, 1.6 Hz, *trans*-6-Py), 8.48 (dd, *J* = 4.7, 1.5 Hz, 1H, *cis*-6-Py), 8.19-8.16 (m, 1H, 4-Py), 8.07 (d, *J* = 1.1 Hz, 1H, *cis*-NHCHO), 7.92 (d, *J* = 11.9 Hz, *trans*-NHCHO), 7.32-7.29 (m, 1H, 5-Py), 5.94 (s, 1H, *cis*-NHCHO), 5.84 (s, *trans*-NHCHO), 3.18 (q, *J* = 6.7 Hz, 2H, *cis*-CH₂NH), 3.10 (q, *J* = 6.8 Hz, *trans*-

CH_2NH), 2.63 (m, 4H, SCH_2), 2.02-1.99 (m, 2H, CCH_2), 1.98-1.85 (m, 2H, SCH_2CH_2), 1.52-1.46 (m, 2H, CH_2CH_2NH). ^{13}C -NMR (126 MHz; $CDCl_3$): δ 164.4 (*trans*-CHO), 161.2 (*cis*-CHO), 150.5 (2-Py), 148.37 (*trans*-6-Py), 148.25 (*cis*-6-Py), 137.45 (*cis*-3-Py), 137.35 (*trans*-3-Py), 136.73 (*cis*-4-Py), 136.67 (*trans*-4-Py), 123.33 (*trans*-5-Py), 123.29 (*cis*-5-Py), 56.28 (*cis*-SCS), 56.17 (*trans*-SCS), 42.3 (*cis*- CCH_2), 42.0 (*trans*- CCH_2), 41.4 (*trans*- $NHCH_2$), 37.6 (*cis*- $NHCH_2$), 27.5 (SCH_2), 25.7 (*trans*- $CH_2CH_2CH_2$), 24.85 (*cis*- SCH_2CH_2), 24.79 (*trans*- SCH_2CH_2), 24.1 (*cis*- $CH_2CH_2CH_2$) ppm.

4-(Formamido)-1-(3-pyridyl)-1-butanone (2.24):

N-Chlorosuccinimide (NCS, 101.8 mg, 0.762 mmol) and $AgNO_3$ (168.5 mg, 0.992 mmol) were suspended in 1:1 MeCN/ H_2O (1 mL) and cooled to 0 °C. To this was added a solution of **2.23** in MeCN (0.247 mmol, 1.5 mL), which resulted in immediate precipitate formation. After 30 min, the reaction was quenched with sat. Na_2SO_3 , sat'd $NaHCO_3$, and brine solutions in succession (1 mL each). The mixture was filtered and extracted with CH_2Cl_2 . The pooled organics were dried over $MgSO_4$, filtered, and concentrated *in vacuo* to give a crude solid. Purification by column chromatography on silica gel (6% MeOH in $CHCl_3$) yielded pure product as a white solid (20.5 mg, 43% over three steps).

1H -NMR (500 MHz; $CDCl_3$): δ 9.15 (dd, $J = 2.2, 0.7$ Hz, 1H, 2-Py), 8.78 (dd, $J = 5.5, 1.7$ Hz, 1H, *trans*-6-Py), 8.77 (dd, $J = 4.8, 1.7$ Hz, 1H, *cis*-6-Py), 8.22 (dt, $J = 8.0, 2.1$ Hz, 1H, *trans*-4-Py), 8.21 (dt, $J = 8.0, 2.0$ Hz, 1H, *cis*-4-Py), 8.18 (s, 1H, *cis*-CHO), 8.06 (d, $J = 11.9$ Hz, *trans*-CHO), 7.42 (m, 1H, 5-Py), 5.96 (s, 1H, $NHCHO$), 3.41 (q, $J = 6.6$ Hz, 2H, *cis*- CH_2NH), 3.36 (q, $J = 6.8$ Hz, *trans*- CH_2NH), 3.08 (t, $J = 6.9$ Hz, 2H, *cis*- $COCH_2$), 3.07 (t, $J = 6.8$ Hz, *trans*- $COCH_2$), 2.01 (quintet, $J = 6.9$ Hz, 2H, *cis*- $CH_2CH_2CH_2$), 2.01 (quintet, $J = 6.9$ Hz, *trans*- $CH_2CH_2CH_2$); ^{13}C -NMR (126 MHz; $CDCl_3$): δ 198.6 (CO), 161.5 (CHO), 153.8 (6-Py), 149.7 (2-Py), 135.5 (4-Py), 132.0 (3-Py), 123.8 (5-Py), 37.8 (CH_2NH), 36.3 ($COCH_2$), 23.5 ($CH_2CH_2CH_2$) ppm.

***tert*-Butyl 3-hydroxypropyl-1-carbamate (2.26):**

A solution of 3-amino-1-propanol (4.94 g, 65.8 mmol, **2.25**) and triethylamine (7.26 g, 71.7 mmol, 10 mL) in CH₂Cl₂ (175 mL) was treated with Boc anhydride (16.15 g, 74.0 mmol, 17 mL) dropwise, which resulted in vigorous gas evolution. Once bubbling ceased, the reaction was quenched with sat'd NH₄Cl. The organic layer was collected and the aqueous layer was further extracted with CH₂Cl₂. The pooled organics were washed with brine, dried over MgSO₄, filtered, and concentrated *in vacuo*. NMR indicated the product was sufficiently pure to be brought directly to the next step.

¹H-NMR (500 MHz; CDCl₃): δ 4.84 (bs, 1H, OH), 3.67 (q, *J* = 5.5 Hz, 2H, HOCH₂), 3.30 (d, *J* = 5.7 Hz, 2H, CH₂NH), 3.07 (bs, 1H, NH), 1.68 (quintet, *J* = 5.7 Hz, 2H, CH₂CH₂CH₂), 1.46 (s, 9H, t-Bu) ppm. ¹³C NMR (126 MHz; CDCl₃): δ 157.2 (CONH₂), 79.6 (C(CH₃)₃), 59.2 (HOCH₂), 36.9 (CH₂NH), 32.9 (CH₂CH₂CH₂), 28.4 (t-Bu) ppm.

***tert*-Butyl 3-iodopropyl-1-carbamate (2.27):**

Imidazole (Im., 5.42 g, 79.7 mmol) and triphenylphosphine (20.72 g, 79.0 mmol) were dissolved in CH₂Cl₂ (250 mL) and brought to 0 °C. To this was added I₂ (20.50 g, 80.8 mmol) scoopwise, resulting in a dark orange solution. After 20 min of stirring, **2.26** in CH₂Cl₂ (11.5 g, 65.7 mmol, 50 mL) was added and the solution was allowed to come to room temperature. After 22 h of stirring, the mixture was filtered over Celite and washed with 5% Na₂S₂O₃. The organics were dried over MgSO₄, filtered, and concentrated *in vacuo* to give a yellow solid. Purification by column chromatography (hexanes/EtOAc 4:1) gave pure product as a light yellow solid (83.2% over 2 steps).

¹H-NMR (500 MHz; CDCl₃): δ 4.63 (bs, 1H, NH), 3.19 (m, 4H, NHCH₂/ICH₂), 2.00 (quintet, *J* = 6.6 Hz, 2H, CH₂CH₂CH₂), 1.44 (s, 9H, t-Bu) ppm. ¹³C NMR (126 MHz; CDCl₃): δ 155.9 (CONH), 79.4 (C(CH₃)₃), 41.0 (CH₂NH), 33.4 (CH₂), 28.4 (C(CH₃)₃), 3.1 (ICH₂) ppm.

4-(Nitrosoformamido)-1-(3-pyridyl)-1-butanone (CH₃-oxo-NNK, 2.14)

A solution of **2.24** (31.4mg, 0.163 mmol) in a 5:1 mixture of acetic anhydride and acetic acid (6 mL) was brought to 0 °C. To this was added NaNO₂ (30.7mg, 0.445 mmol) all at once. After 4 h, the mixture was poured onto ice-cold H₂O. The aqueous mixture was extracted with CH₂Cl₂. The pooled organics were dried over MgSO₄, filtered, and concentrated *in vacuo* to yield a crude yellow oil. Purification by column chromatography (100% EtOAc) yielded pure product as a bright, yellow oil (28.8mg, 80%).

¹H-NMR (500 MHz; CDCl₃): δ 10.00 (s, 1H, CHO), 9.13 (d, *J* = 1.1 Hz, 1H, 2-Py), 8.80 (dd, *J* = 4.8, 1.1 Hz, 1H, 6-Py), 8.24 (dd, *J* = 8.0, 1.6 Hz, 1H, 4-Py), 7.47 (dd, *J* = 8.0, 4.9 Hz, 1H, 5-Py), 4.11 (q, *J* = 7.1 Hz, 1H, NCH₂), 2.92 (t, *J* = 6.9 Hz, 2H, COCH₂), 1.91 (quintet, *J* = 6.9 Hz, 2H, CH₂CH₂CH₂) ppm. ¹³C NMR (126 MHz; CDCl₃): δ 196.8 (CO), 168.5 (CHO), 153.1 (6-Py), 149.0 (2-Py), 136.0 (4-Py), 132.2 (3-Py), 124.1 (5-Py), 37.6 (NCH₂), 35.8 (COCH₂), 20.9 (CH₂CH₂CH₂) ppm; HRMS Calc: 222.08732, Found: 222.08719

2.2.4 Determination of t_{1/2} of *N*-Nitrosamides

HPLC-UV analysis was performed using a 250 x 4.6 mm Gemini-NX C18 column (Phenomenex, Torrance, CA) with the following solvent gradients for the analyses indicated below: (1) isocratic for 5 min at 4% B followed sequentially by a linear gradient to 12% B over 15 min, a 10 min hold, a linear gradient to 30% B over 10 min, and a final linear gradient to 40% B over 2 min; (2) isocratic for 5 min at 12% B followed sequentially by a linear gradient to 30% B over 10 min, a linear gradient to 40% B over 15 min, and a final linear gradient to 70% B over 2 min. In both systems, solvent A was 15 mM NH₄OAc and solvent B was methanol.

For t_{1/2} determination, an aliquot of NNC (180 nmol) in CH₂Cl₂ was dried and reconstituted in 30 μL of 0.5X P450 2A6 Reaction Buffer (Life Technologies) and incubated for 0 to 30 min at 37 °C. After the desired incubation time, 5 μL of sample was analyzed by HPLC using gradient 1. A₂₅₄ was monitored and the peaks for NNC and its decomposition products were integrated. NNC eluted at 36.0 min. Peak area for NNC

was fit to a single-order exponential plot while using the 0 min incubation peak area as a normalizing factor. The analysis was similarly performed for CH₂-oxo-NNK and CH₃-oxo-NNK, except HPLC gradient 2 was used. CH₂-oxo-NNK and CH₃-oxo-NNK eluted at 33.0 and 29.5 min, respectively. Decomposition products were identified by retention time comparisons and co-injection with synthetic standards.

2.2.5 *In vitro* Detection of CH₂-oxo-NNK using P450 2A13

Incubations with P450 2A13 were performed as previously reported.²⁶² Briefly, purified P450 2A13 and cytochrome P450 reductase were reconstituted with dilauroylphosphatidylcholine (DLPC, Sigma Aldrich) for 45 min on ice before diluting with Tris buffer to give a final concentration of 1 μM P450 2A13, 2 μM P450 reductase, 0.1 μg/μL DLPC, and 50 mM Tris, pH = 7.4. To initiate the reaction, an aliquot of this (containing 5 pmol P450) was added to a Tris-buffered solution of NNK (4 μM) and NADPH (0.2 mM). Final reaction volumes were always 100 μL. The mixture was brought to 37 °C for 1–60 min before quenching with 10 μL of both Ba(OH)₂ and ZnSO₄. After centrifuging the sample at 8000 g for 4 min, the supernatant was collected and 2 μL were immediately analyzed by liquid chromatography-positive nanoelectrospray-ionization high-resolution tandem mass spectrometry (LC-NSI⁺-HRMS/MS) with an LTQ Orbitrap Velos (Thermo Scientific, Carlsbad, CA). LC employed a hand-packed, Luna C18 (5 μm), 100 mm x 75 μm, 15 μm orifice capillary column with a multi-step gradient. Initially, 5% B at 1 μL/min from 0–5 min was used to load the sample. Afterwards, the flow rate was dropped to 0.3 μL/min and a linear gradient was started from 5% to 20% B over 4 min, followed by a ramp to 55% B over 10 min, and re-equilibration, where solvent A was 5 mM NH₄OAc and solvent B was acetonitrile. CH₂-oxo-NNK and CH₃-oxo-NNK were monitored by both full scan and MS² fragmentation. Full scan was performed at a resolution of 60,000 and the accurate parent mass of both nitrosamides ($m/z = 222.0872$) was extracted at a mass tolerance of 5 ppm. For MS² fragmentation, parent ions were isolated (2.0 amu isolation width) and fragmented by collision-induced dissociation (CID) with a collision energy of 25 eV, resolution of 15,000, and scan time of 30 ms. Accurate product ion masses from characteristic

transitions for CH₂-oxo-NNK (m/z 222 \rightarrow m/z 180.0654, -H₃CNNO +OH), CH₃-oxo-NNK (m/z 222 \rightarrow m/z 106.0285), NNK (m/z 208 \rightarrow m/z 178.1100), and keto alcohol **2.11** (m/z 166 \rightarrow m/z 148.0756) were extracted at a mass tolerance of 5 ppm.

2.2.6 *In vitro* Detection of NNC using P450 2A6

Incubations with P450 2A6 were performed as described by the manufacturer with modifications.²⁶³ After thawing the P450 2A6 Baculosomes and Vivid-NADPH-Regeneration System (Life Technologies) on ice, aliquots were combined and diluted 1:10 and 1:50, respectively, with 0.5X Vivid Reaction Buffer (Life Technologies). For each incubation, an aliquot of the combined-enzyme system (containing 5 pmol P450) was added to a 0.5X Reaction-Buffered solution of NNN (4 μ M) and this new mixture was pre-incubated for 2 min at 37 °C. To initiate the reaction, an aliquot of NADP⁺ (containing 3 nmol) was added. Final reaction volumes were 100 μ L. The incubation and work-up were as described earlier for NNK-P450 2A13 incubations. NNC detection was performed by adapting the NNK-P450 2A13 LC-NSI⁺-HRMS/MS method described above to the accurate parent mass of NNC (m/z 192.0767) in full scan. Likewise, the MS² analysis was used to monitor for the accurate product ion masses from characteristic transitions of NNC (m/z 192 \rightarrow m/z 134.04739, 162.0787), NNN (m/z 178 \rightarrow m/z 148.0994), and lactol **2.12** (m/z 166 \rightarrow m/z 148.0757).

2.2.7 *In vitro* Methylation of dGuo by CH₂-oxo-NNK

A solution of CH₂-oxo-NNK in CH₂Cl₂ was dried under a stream of N₂ and reconstituted in a phosphate-buffered solution of dGuo (4.34 mM dGuo, 25 mM NaHPO₄, pH = 7.4) so that the molar ratio of CH₂-oxo-NNK to dGuo was 1:1. This was brought to 37 °C and incubated for 18 h. To assess methylation, 200 fmol of [CD₃]O⁶meGua was added as internal standard. Samples were brought up to 1 mL with 0.1N HCl and incubated at 90 °C for 30 min. After cooling on ice, the samples were neutralized with 1.0N NaOH and purified by solid-phase extraction (Strata-X polymeric reversed phase, 30 mg, Phenomenex, Torrance, CA). Before sample addition, the

cartridge was activated using 1 mL each of MeOH and H₂O. After sample addition, the cartridge was washed with 1 mL of both H₂O and 10% MeOH. The sample was eluted and collected with 1 mL of MeOH. The collected fraction was evaporated to dryness in a Speedvac. The residue was reconstituted in 30 μ L of H₂O and analyzed by LC-MS/MS.²²⁶

We used a well-established liquid chromatography-positive electrospray ionization-tandem mass spectrometry (LC-ESI⁺-MS/MS) method. A 0.5 x 150 mm Zorbax SB-C18, 5 μ m column (Agilent, Santa Clara, CA) was eluted with a multi-step gradient and flow rate of 10 μ L/min. After a linear gradient from 5% to 10% B over 10 min, the eluent was brought to 40% B over 5 min, followed by a wash at 90% B and re-equilibration, where solvent A was 15mM NH₄OAc and solvent B was methanol. MS was performed on a TSQ Vantage triple quadrupole mass analyzer (Thermo Scientific). The SRM transitions were m/z 166.1 \rightarrow m/z 149.1 and m/z 166.1 \rightarrow m/z 124.1 for ⁶OmeGua and m/z 169.1 \rightarrow m/z 152.1 for [CD₃]⁶OmeGua using a collision energy of 30 eV and a 0.2 amu scan width.

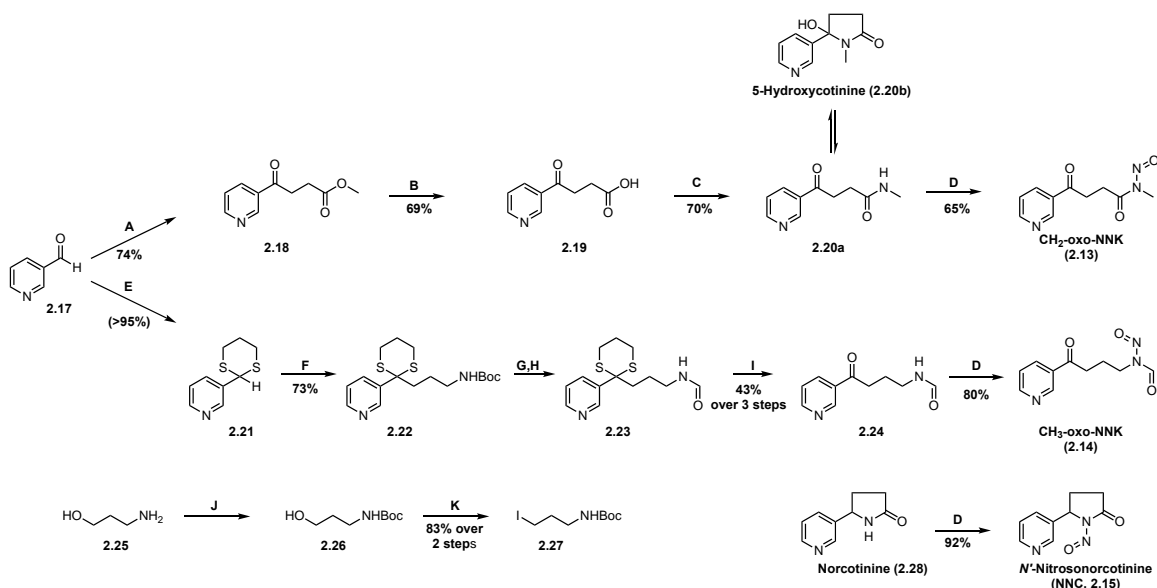
2.2.8 *In vitro* Methylation of Calf Thymus DNA by CH₂-oxo-NNK

A solution of CH₂-oxo-NNK was dried under a stream of N₂ and reconstituted in a phosphate-buffered solution of calf thymus DNA so that the ratio was 3 nmol CH₂-oxo-NNK :1 μ g DNA. This was brought to 37 °C and incubated for 18 h. The aqueous sample was extracted twice with equal volumes of CHCl₃:isoamyl alcohol (24:1). The DNA was precipitated by addition of an equal volume of isopropanol and gentle shaking. Isolated DNA was washed with 500 μ L of 70% EtOH and 100% EtOH, and dried under N₂. To assess methylation, isolated DNA was dissolved in 100 μ L of sodium phosphate buffer (25 mM, pH = 7.4) and 200 fmol of [CD₃]⁶OmeGua was added as internal standard. The samples were then processed and analyzed as described above for dGuo methylation.

2.3 Results

2.3.1 Synthesis of *N*-Nitrosamides

Retrosynthetic analysis identified 3-pyridinecarboxaldehyde (**2.17**) as a common precursor for both NNK-derived nitrosamides (**Scheme 2-2**).



Scheme 2-2: Synthesis of Nitrosamides (A) Methyl Acrylate, NaCN, DMF, 40 °C, 4h; (B) NaOH, H₂O, RT, 3h; (C) EDAC, NHS, MeNH₂•HCl, DMSO, RT, 22h; (D) NaNO₂, Ac₂O:HOAc, 0 °C, 4h; (E) HS(CH₂)₃SH, BF₃•OEt₂, THF, 80 °C, 24h; (F) (i) *n*-BuLi, TMEDA, THF, -78 °C, 1h; (ii) 27, THF, -78 °C to RT, 16h; (G) 25% TFA, CH₂Cl₂, RT, 3h; (H) HCO₂Me, Et₃N, MeOH, 55 °C, 4h; (I) AgNO₃, NCS, MeCN:H₂O (1:1), 0 °C, 30 min; (J) Boc₂O, Et₃N, CH₂Cl₂, RT, 30 min; (K) I₂, PPh₃, Im., CH₂Cl₂, 0 °C-RT, 22h

The synthesis of CH₂-oxo-NNK started with the formation of keto acid **2.19** by first coupling aldehyde **2.17** with methyl acrylate under Stetter conditions²⁶⁴, followed by basic hydrolysis. This method is a convenient alternative to more commonly used routes to this compound^{265,266}. Keto acid **2.19** was coupled to methylamine using 1-ethyl-3-(3-dimethylaminopropyl)carbodiimide (EDAC) and *N*-hydroxysuccinimide (NHS) in dimethylsulfoxide (DMSO), resulting in the open-chain and lactam conformers of **2.20** in a 2:1 ratio, respectively. Nitrosation of the open-chain conformer produced CH₂-oxo-NNK (**2.13**) as a single rotamer²⁶⁷. Nitrosation of the lactam conformer also produced CH₂-oxo-NNK; however, new conditions using a strong acid catalyst were required. These conditions also degraded the product which limited the isolatable yield (<10%).

Ultimately, only the open-chain route was synthetically useful for CH₂-oxo-NNK production.

Synthesis of CH₃-oxo-NNK (**Scheme 2-2**) started with protection of **2.17** with 1,3-propanedithiol in nearly quantitative yield to give **2.21**. This was coupled to **2.27** by classic umpolung chemistry²⁶⁸ to give **2.22** in excellent yield. Compound **2.27** was prepared in two steps from **2.25** on a multi-gram scale by first Boc-protecting the amine and then converting the alcohol to an iodide using a modified Appel reaction.²⁶⁹ After Boc removal from **2.22** and *N*-formylation to achieve **2.23**, the dithiane group was oxidatively removed²⁷⁰ to produce **2.24** in 43% yield over 3 steps. To complete the synthesis, **2.24** was nitrosated to give CH₃-oxo-NNK (**2.14**) in excellent yield.

NNC (**2.15**) was prepared by nitrosation of norcotinine (**2.28**) in 92% yield. The three nitrosamides were stored in CH₂Cl₂ at 4 °C. They were stable for at least three months under these conditions. Attempts to store these compounds neat or in H₂O-miscible solvents (MeOH, MeCN, acetone, etc.) resulted in decomposition.

2.3.2 Stability of *N*-Nitrosamides

The stabilities of the *N*-nitrosamides were determined in buffers to be used in our P450 assays at pH 7.4 and 37 °C. Reactions were followed by HPLC and major products were identified (**Figure 2-1**).

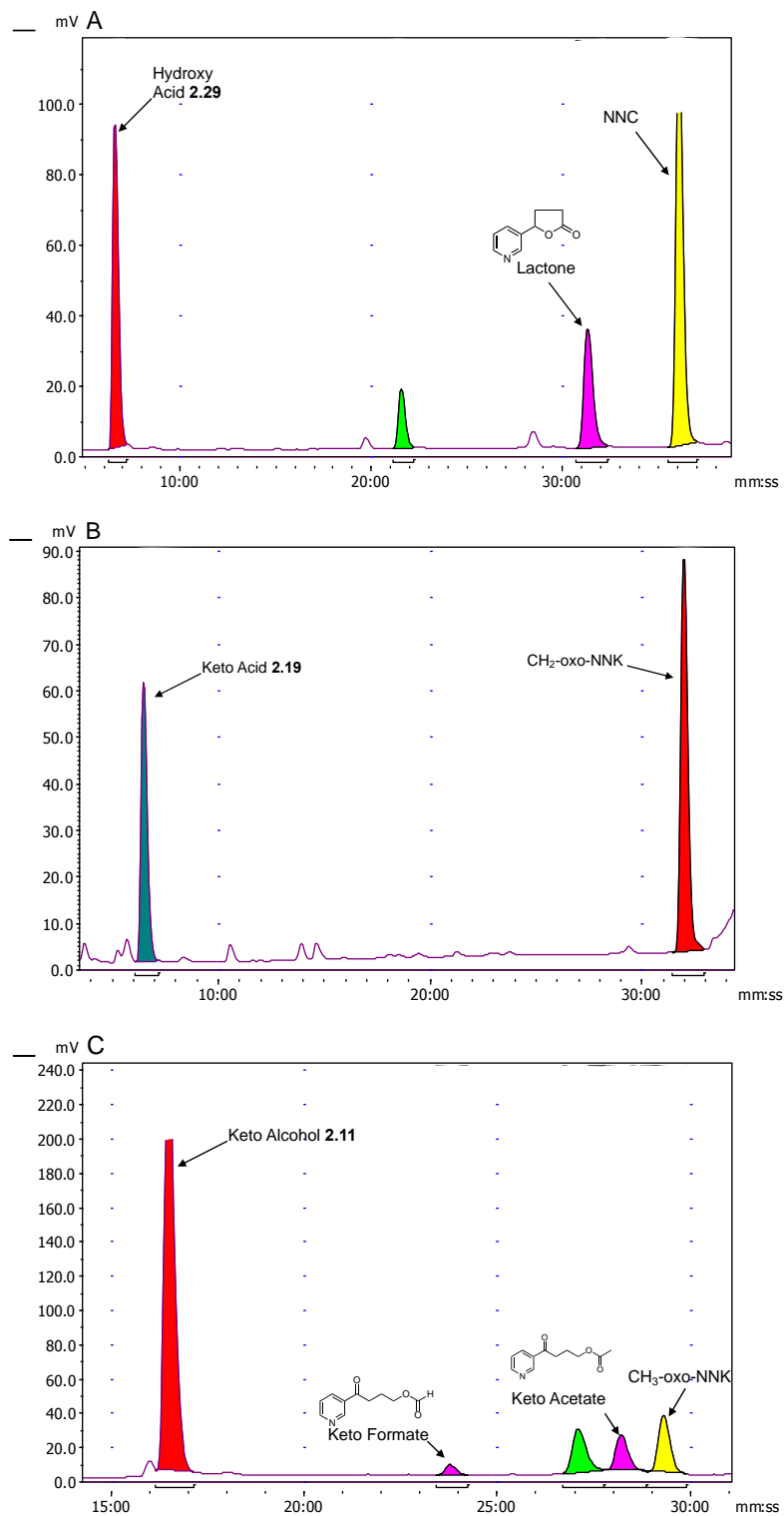


Figure 2-1: HPLC-UV chromatograms of the decay of (A) NNC, (B) CH₂-oxo-NNK, and (C) CH₃-oxo-NNK in assay buffer at 37 °C. Chromatograms are the 15-min, 25-min, and 10-min time point for NNC, CH₂-oxo-NNK, and CH₃-oxo-NNK, respectively. All decomposition products are noted if their identity was supported by a synthetic standard.

Decay curves for each nitrosamide are shown in **Figure 2-2**. The half-lives of CH₂-oxo-NNK and CH₃-oxo-NNK were 35.5 min and 6.7 min, respectively. The half-life of NNC under these conditions was 12.3 min.

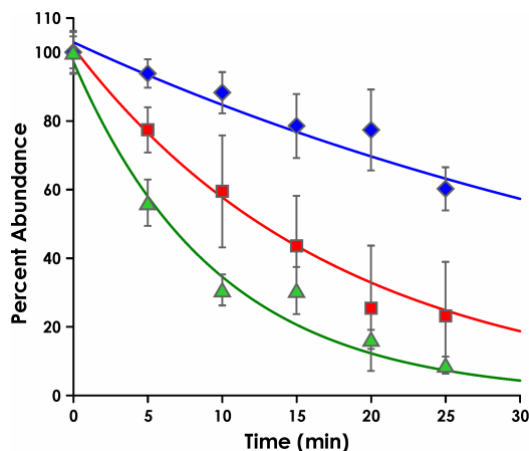
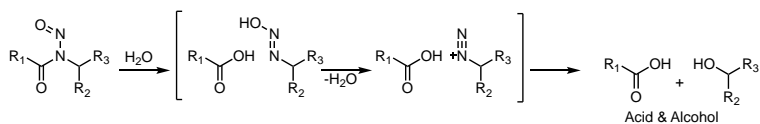


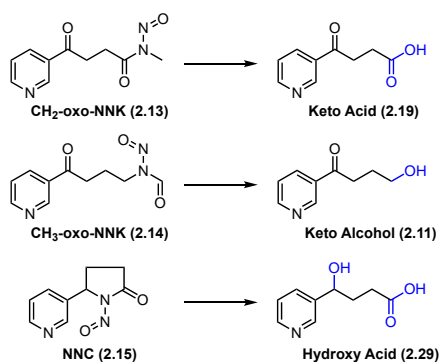
Figure 2-2: Stability of CH₂-oxo-NNK (blue diamonds), CH₃-oxo-NNK (green triangles), and NNC (red squares) in reaction buffer at 37 °C. The half-lives were determined to be 35.5, 6.7, and 12.3 min, respectively, by HPLC-UV. Nitrosamide peak areas were normalized to the 0-min peak area and fit to a first-order exponential. Relative amounts of each nitrosamide were determined at each time point in triplicate with error bars denoting the standard deviation.

The major product in each case was that expected by nitrosamide hydrolysis, namely keto acid **2.19** from CH₂-oxo-NNK, keto alcohol **2.11** from CH₃-oxo-NNK, and hydroxy acid **2.29** from NNC (**Scheme 2-3**).

A.



B.



Scheme 2-3: (A) Mechanism of hydrolysis of nitrosamides. Hydrolysis results in a carboxylic acid and an alcohol via a transient diazohydroxide that decomposes to a diazonium ion. (B) The hypothesized decomposition products of CH₂-oxo-NNK, CH₃-oxo-NNK, and NNC in assay buffer (pH = 7.4) at 37 °C.

2.3.3 *In vitro* Cytochrome P450-catalyzed Metabolism of NNK to CH₂-oxo-NNK

With synthetic *N*-nitrosamide standards in hand and an understanding of their stability, we designed an assay to detect their formation by P450-mediated metabolism. P450 2A13 is the most efficient enzyme for α -hydroxylation of NNK and was chosen for this part of the study¹³⁷. The NNK concentration was set at 4 μ M, the K_m for production of hydroxylated products. Samples were analyzed immediately after work-up to minimize nitrosamide decomposition. We used an LTQ High-Resolution Orbitrap Velos MS system to enhance sensitivity and minimize background noise. We monitored for the accurate masses of the most abundant product ions of CH₂-oxo-NNK and CH₃-oxo-NNK resulting from MS² fragmentation, and extracted their accurate parent masses in full scan mode. Similar monitoring was performed for NNK and keto alcohol **2.11** to ensure catalytic turnover as **2.11** is the most abundant product from α -methyl hydroxylation.^{137,190}

When NNK was incubated with the relevant enzymes and cofactors, we detected a peak that matched the accurate parent ion mass, accurate product ion mass resulting from MS² of [M+H]⁺ = 222, and the retention time of synthetic CH₂-oxo-NNK (**Figure 2-3**). This peak was detectable as early as the 1-min time point, reached its maximum concentration at 5 min, tapered off by 10–30 min, and was nearly undetectable by 60 min (**Figure 2-3C-F**). We did not detect CH₃-oxo-NNK at any time point.

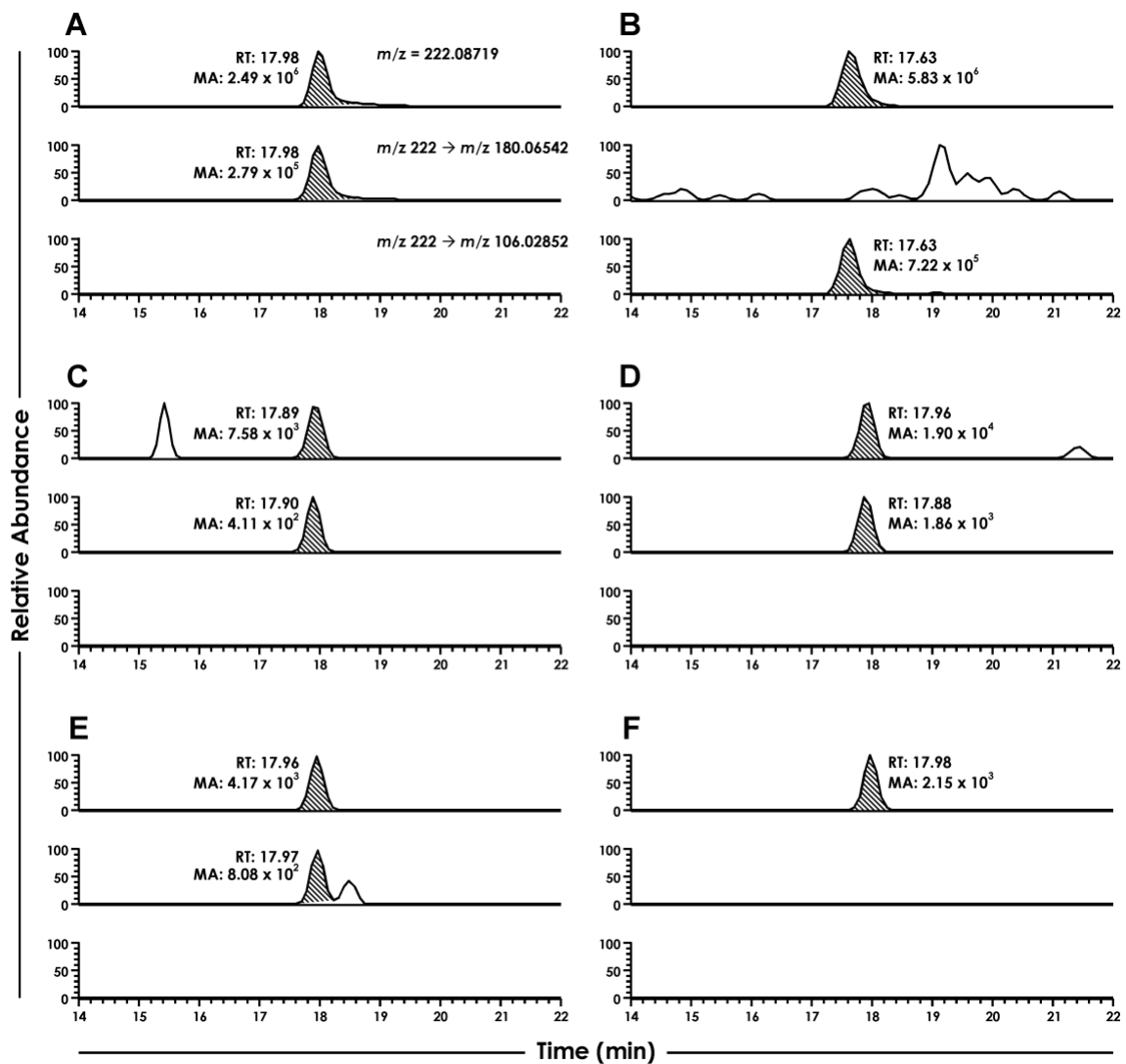


Figure 2-3: LC-NSI-HRMS chromatograms resulting from the NNK-P450 2A13 incubations. For all sections, the top chromatogram is the accurate parent mass extracted from full scan for CH₂-oxo-NNK and CH₃-oxo-NNK. The middle and bottom chromatogram is the accurate product ion masses extracted from MS² fragmentation for CH₂-oxo-NNK and CH₃-oxo-NNK, respectively. Sections are as follows: (A) CH₂-oxo-NNK standard, (B) CH₃-oxo-NNK standard, and NNK-P450 2A13 incubations containing all relevant enzymes and cofactors with incubation times of (C) 1 min, (D) 5 min, (E) 10 min, and (F) 60 min. RT = Retention Time; MA = Mass Area

The signal for NNK decreased 8-fold while the signal for keto alcohol **2.11** simultaneously increased 4-fold over the 60-min period (data not shown). This indicates that NNK metabolism was rapid over the assay time period. CH₂-oxo-NNK was a minor metabolite as its signal was >4000-fold less than that of keto alcohol **2.11**. No

metabolites were observed in control incubations lacking enzyme or cofactors (data not shown).

When identical incubations containing CH₂-oxo-NNK (10 nM) were performed, the peak area was 10-fold higher than in unspiked samples, indicating that CH₂-oxo-NNK was recoverable under our conditions. Based on this, we estimate that CH₂-oxo-NNK was produced at concentrations less than 1 nM in our incubations.

2.3.4 *In vitro* Cytochrome P450-catalyzed Metabolism of NNN to NNC

The NNN incubations were performed in essentially the same way as those with NNK except that P450 2A6 was used instead of P450 2A13 as it is the most efficient enzyme for NNN metabolism.²⁰¹ Catalytic turnover was assessed by measuring lactol **2.12**, because it is the major product from 5'-hydroxylation of NNN (**Scheme 2-1A**).²⁷¹ We detected NNC as early as the 1-min time point (**Figure 2-4**). The peak matched the synthetic standard with respect to the accurate parent ion mass in full scan, the accurate mass of the most abundant product ions in the MS² of [M + H]⁺ = 192, and retention time.

The NNC signal was maximal at 5 min and was approximately 1000-fold lower in intensity than that of lactol **2.12** (**Scheme 2-1A**). The concentration of NNC at the 5-min time point was estimated to be ~10 nM.

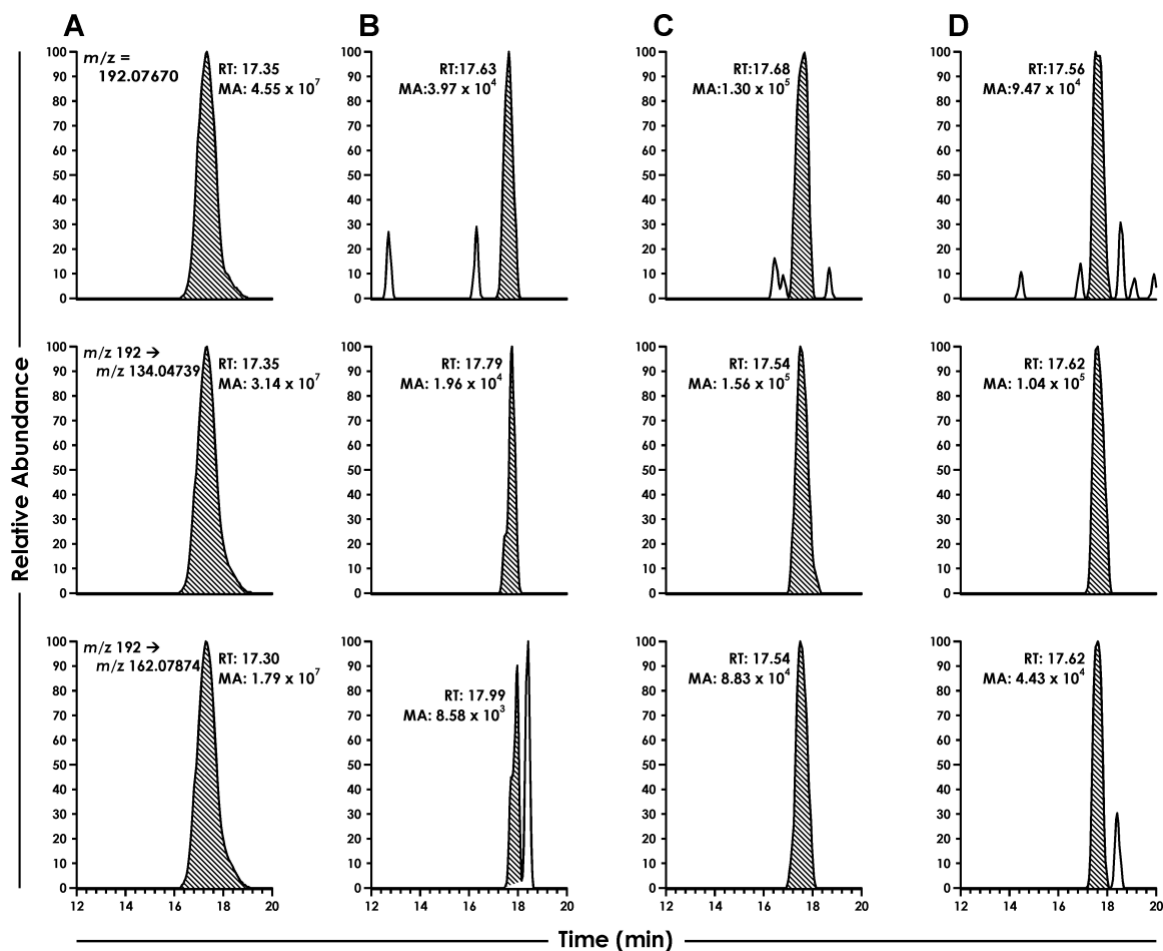


Figure 2-4: LC-NSI⁺-HRMS chromatograms resulting from the NNN-P450 2A6 incubations. For all sections, the top chromatogram is the accurate parent mass extracted from full scan for NNC. The middle and bottom chromatograms are two accurate product ion masses extracted from MS² fragmentation for NNC. Sections are as follows: (A) NNC standard, and NNC-P450 2A6 incubations containing all relevant enzymes and cofactors with incubation times of (B) 1 min, (C) 5 min, and (D) 10 min. RT = retention time; MA = Mass Area.

2.3.5 *In vitro* Methylation of dGuo and DNA by CH₂-oxo-NNK

We tested the ability of CH₂-oxo-NNK to methylate DNA by incubating it with a molar equivalent of dGuo and calf thymus DNA in phosphate buffer for 18 h. Levels of O⁶-meGua were 61.7 and 802 μmol/mg Gua for the dGuo and DNA reactions, respectively, as determined by LC-MS/MS analysis (**Figures 2-5**). Formation of 7-meGua was also noted, but not quantified.

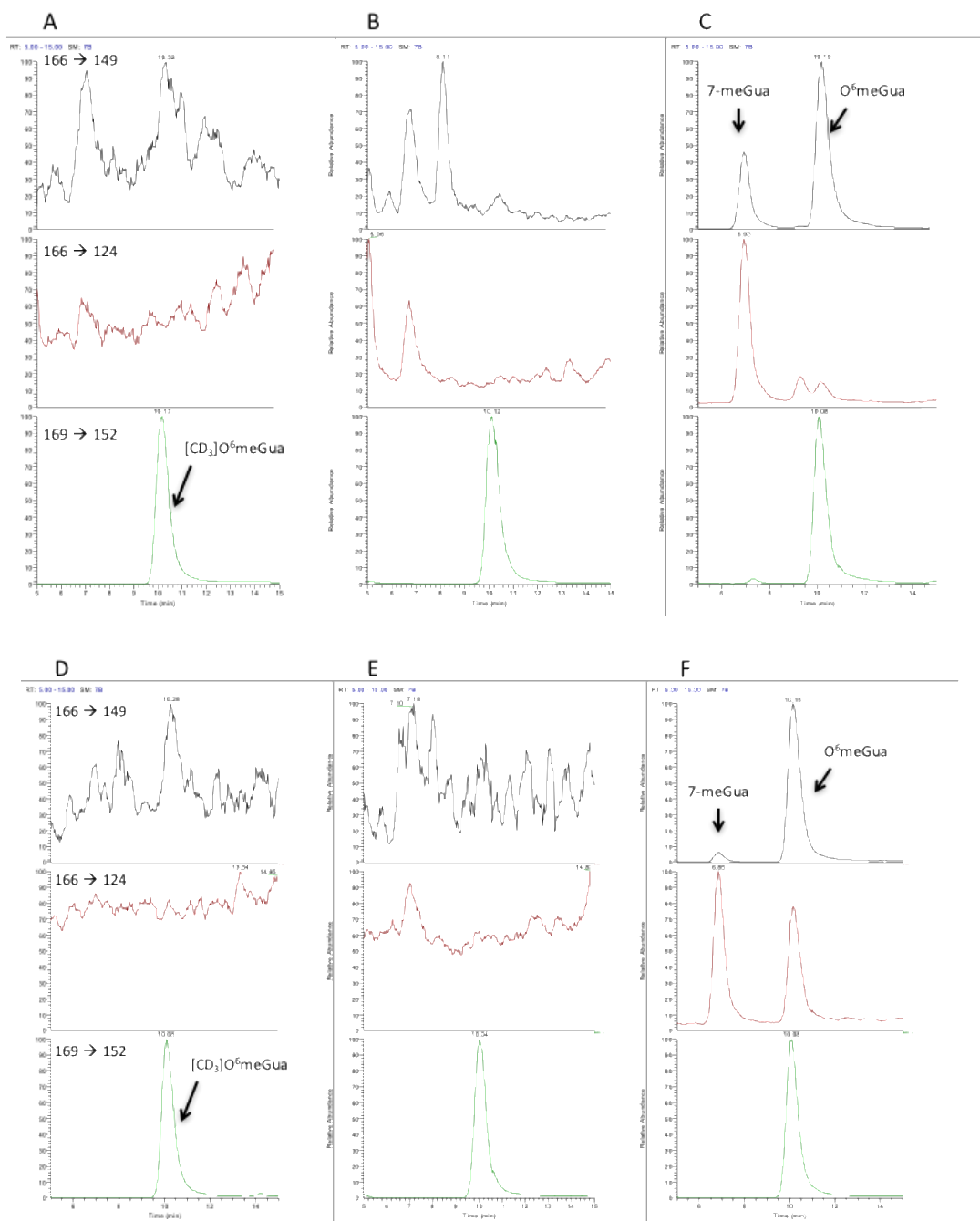


Figure 2-5: LC-MS/MS chromatograms resulting from in vitro methylation of dGuo and DNA by CH₂-oxo-NNK. For all sections, the top and middle chromatogram are the characteristic SRM transition for 7-meGua (eluting first) and O⁶-meGua (eluting second). The bottom chromatogram showcases the SRM transition for the internal standard, [D₃]-O⁶-meGua. Chromatograms are as follows: CH₂-oxo-NNK:dGuo type reactions containing (A) no CH₂-oxo-NNK or dGuo, (B) only dGuo, (C) CH₂-oxo-NNK with dGuo; CH₂-oxo-NNK-DNA type reactions containing (D) no CH₂-oxo-NNK or DNA, (E) calf thymus DNA, (F) CH₂-oxo-NNK with calf thymus DNA.

2.4 Discussion

This study presents the first account of *N*-nitrosamines being directly converted to *N*-nitrosamides by P450 catalysis. This breaks new ground in our knowledge of nitrosamine metabolism and provides an impetus to determine if this phenomenon applies to all nitrosamines. Specifically, we found that CH₂-oxo-NNK and NNC are novel metabolites of P450-mediated oxidation of NNK and NNN, respectively. We did not observe formation of CH₃-oxo-NNK, perhaps due to its short half-life (6.7 min). These novel metabolites also provide a potentially new mechanism for NNK- and NNN-DNA adduct formation (**Scheme 2-1B**). It has long been known that the α -hydroxynitrosamine intermediates **2.3–2.6** (**Scheme 2-1A**) alkylate DNA, but their short lifetimes raise questions regarding their ability to traverse the hydrolytic cytosol. The detected nitrosamides had half-lives of 12–35 min, 100-fold more than those of the α -hydroxynitrosamines.^{242,243} Additionally, we showed that CH₂-oxo-NNK methylates both dGuo and calf thymus DNA (**Figure 2-5**). Thus, in the case of NNK, it is plausible that CH₂-oxo-NNK could be partially responsible for the methyl adducts previously thought to be formed purely by α -hydroxynitrosamine **2.3**.

However, we note that both CH₂-oxo-NNK and NNC are quite minor metabolites of NNK and NNN. It was estimated that CH₂-oxo-NNK and NNC form at concentrations of ~1 nM and 10 nM, respectively, while keto alcohol **2.11** and lactol **2.12**, the hydrolysis products of α -hydroxyNNK and α -hydroxyNNN, form at levels ~4000-fold higher. Because P450 2A13 and P450 2A6 are the most efficient enzymes for NNK and NNN oxidation and the formation of their known products keto alcohol **2.11** and lactol **2.12** (**Scheme 2-1A**) was rapid, it is unlikely that the low levels of CH₂-oxo-NNK and NNC result from low catalytic turnover. Likewise, the positive controls indicate that analyte recovery was achievable under our incubation conditions. We noted that formation of both CH₂-oxo-NNK and NNC started at 1 min, peaked at 5 min, and that both were nearly undetectable by 30 min. This may indicate that as metabolism proceeds, newly formed side products and P450-related reactive-oxygen species are eliminating the nitrosamides via secondary reactions at a rate faster than nitrosamide formation.

We were not able to quantify nitrosamide formation in these reactions. We initially attempted quantification by HPLC-radioflow techniques, but this approach was not sensitive enough (LOD = 400 fmol on column, data not shown). After nitrosamide detection was achieved by LC-NSI⁺-HRMS, we attempted to trap these products with *N*- α -acetyl-lysine and *N*- α -acetyl-cysteine. Though trapping was achieved with synthetic standards, this method was unsuccessful in our assay due to low trapping efficiency and low sample recovery after solid phase extraction (SPE), which resulted in no analyte detection even with accurate mass detection (data not shown). Therefore, we settled on estimating formation levels by comparing peak areas to those of spiked positive controls.

Despite being minor metabolites, the long half-lives and strong DNA-binding properties of the nitrosamides suggest potential biological relevance. However, determining whether it is more important to be low-forming and stable versus high-forming and unstable would require further study. Additionally, though CH₂-oxo-NNK and NNC are formed to low extents, the nitrosamide pathway may be more efficient for other nitrosamines. For example, studies by Chowdhury et al noted considerable, processive conversion of dimethylnitrosamine and diethylnitrosamine to acid byproducts by P450 2A6.²⁵³ It was hypothesized that the α -hydroxynitrosamine intermediate decomposed within the active site and the resulting aldehyde was then oxidized to the acid. The nitrosamide hypothesis was also tested, but detection was unsuccessful. Given our results, it is plausible that nitrosamides were readily produced, but instability limited their detection.

Our synthesis of each nitrosamide proceeded essentially as expected, except for a few key findings. First, our method for keto acid **2.19** (**Scheme 2-2**), though not entirely novel,²⁷² is considerably more convenient than previously reported routes.^{265,266} The two-step process involves milder conditions, gives reproducible yields, and simpler product purification; the latter step provides >99% pure product after only filtration. Next, the conversion of keto acid **2.19** to keto amide **2.20** (**Scheme 2-2**) was noteworthy because a previous study²⁷³ reported compound **2.20** to be in a ring-chain equilibrium heavily favoring the lactam (~6:1). In our hands, the compounds were readily separable on silica gel and showed no isomerization while stored neat at 2–8 °C. They were clearly distinct

by NMR (**Figure 2-6**). The open-chain product had two clean triplets integrating to 2H each while these signals collapsed into non-distinct multiplets integrating to 4H in the ring product. Additionally, the methyl resonance in the lactam is a singlet as opposed to a doublet in the open-chain product. In support of the results reported by Nguyen et al,²⁷³ when we performed this reaction in solvents other than DMSO, the lactam 5'-hydroxycotinine (**2.20b**, **Scheme 2-2**), predominated. Similarly, **2.20b** was the major product when harsher amide coupling conditions were used, such as *in situ* acid chloride formation by oxalyl chloride or AlMe₃-mediated amide formation^{274,275} from **2.18**. It is apparent that DMSO and mild coupling conditions favor the open chain conformer.

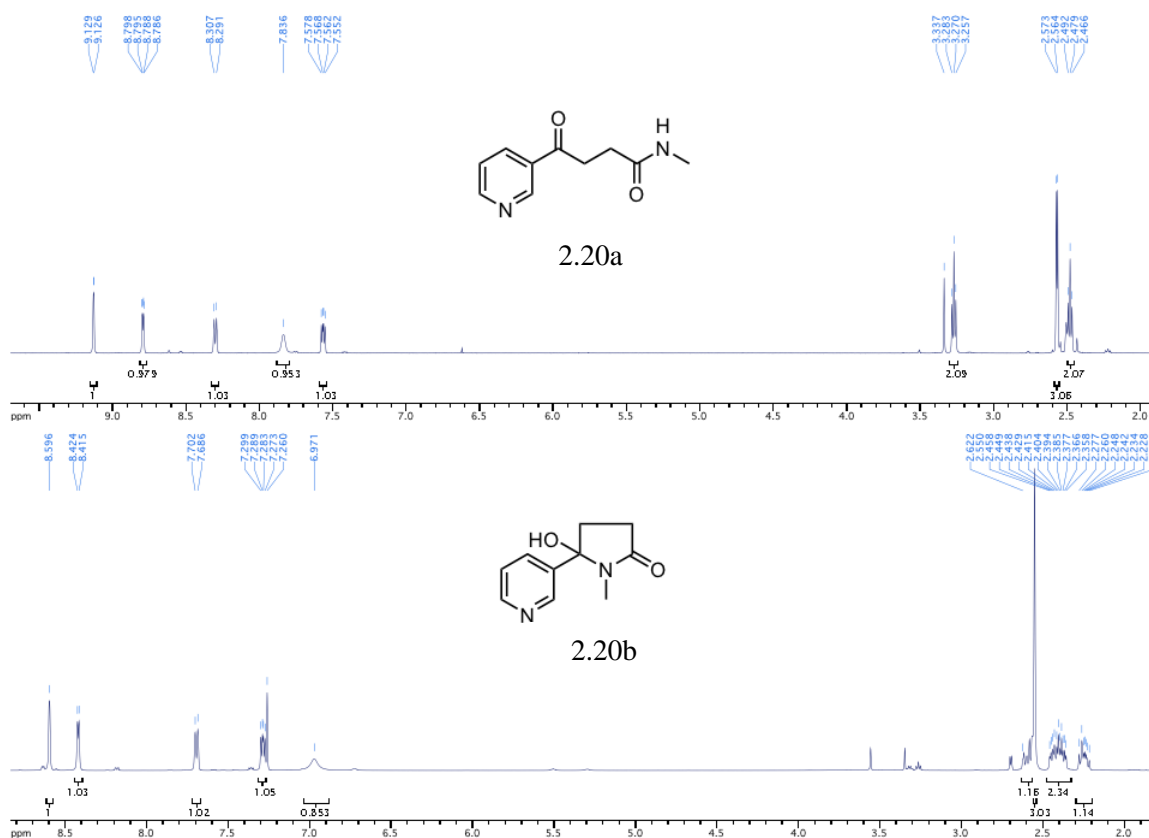


Figure 2-6: ¹H-NMR spectra for compound **2.20a** and **2.20b**. The top spectra is of the open-chain conformer, while the bottom spectra is of the lactam conformer

Our nitrosamides were each isolated exclusively as one rotamer. This is in contrast to nitrosamines that are commonly mixtures of both (*E*)- and (*Z*)-isomers. Past studies indicate that the (*E*)-conformer is electronically favored for most *N*-

nitrosamides.⁹⁴ Furthermore, rotation to the (*Z*)-conformer is commonly believed to be the rate-limiting step for *N*-nitrosamide decomposition by a pericyclic process⁹⁴ and thus, may not be isolatable.

The order of compound stability was CH₂-oxo-NNK > NNC > CH₃-oxo-NNK. This ranking fits with known factors contributing to nitrosamide decomposition.^{94,255,267} In hydrolytic environments,²⁵⁷ nitrosamides with bulkier groups adjacent to the carbonyl group are more stable. This suggests that CH₃-oxo-NNK should be the least stable, consistent with our observations. Likewise, bulky groups adjacent to the nitrogen decrease stability. This is consistent with CH₂-oxo-NNK being most stable and NNC being relatively less stable. The decomposition products suggest that the mechanism is primarily hydrolysis. The products shown in **Scheme 2-3B** were all either the major or only identified product. However, for NNC and CH₃-oxo-NNK, we did identify a lactone and ester as minor products, respectively (**Figure 2-1**). These presumably result from the extensively studied 1,3-sigmatropic rearrangement mechanism.⁹⁷ Though this rearrangement is highly favored when nitrosamides are heated in organic solvents, aqueous conditions seem to favor hydrolysis and are most relevant to the *in vivo* situation.

With data supporting the formation of CH₂-oxo-NNK, we were interested in testing one of its possible modes of DNA damage: methylation. Methylation was expected since keto acid is the major product of CH₂-oxo-NNK hydrolysis (**Scheme 2-3**). This implies that methane diazohydroxide, a known methylating agent, is also released. Our results clearly demonstrated the formation of O⁶meGua in these reactions, indicating that CH₂-oxo-NNK methylates DNA. In addition to the methyl DNA adducts readily formed by CH₂-oxo-NNK, both CH₂-oxo-NNK and NNC could potentially generate a set of novel DNA adducts (**Scheme 2-1B**). Further studies are needed to establish the structures, level, and importance of possible adducts derived from the nitrosamide pathway.

In summary, we hypothesized that NNK and NNN are metabolized by P450 2A13 and P450 2A6, respectively, to their corresponding nitrosamides *in vitro*. We tested this by synthesizing CH₂-oxo-NNK, CH₃-oxo-NNK, and NNC and evaluating their stability

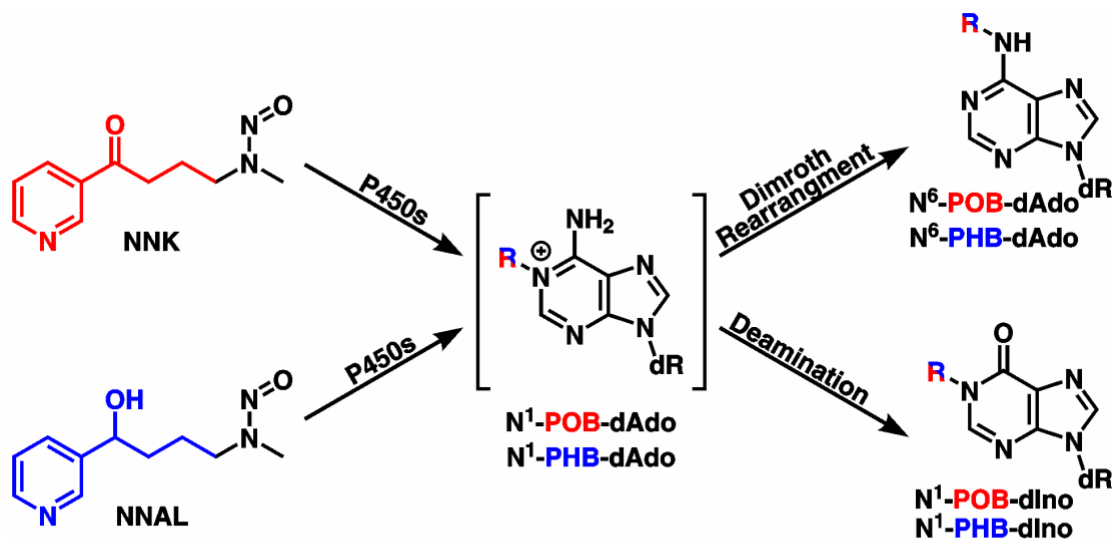
at pH = 7.4 and 37 °C. They were quite stable relative to the corresponding α -hydroxynitrosamines. We then showed that CH₂-oxo-NNK and NNC are novel, though minor, metabolites of NNK and NNN, respectively, in an *in vitro* P450 model. With the knowledge that CH₂-oxo-NNK has a relatively long half-life and methylates DNA, it could potentially play a role in the mechanism of carcinogenesis by NNK. More broadly, this is the first direct evidence for the conversion of *N*-nitrosamines to *N*-nitrosamides by P450 catalysis and provides rationale for further studies to determine whether this is a general transformation in *N*-nitrosamine metabolism.

2.5 Conclusion

NNK and NNN were shown to be converted to the minor metabolites CH₂-oxo-NNK and NNC through processive P450 oxidation *in vitro*. To our knowledge, this is the first direct evidence of a nitrosamine being metabolized to a nitrosamide, a phenomenon that could be general for all nitrosamines. The resulting nitrosamides were generally more stable than the corresponding α -hydroxynitrosamines, indicating the small amount of nitrosamides formed could still be biologically relevant if able to productively reach the nucleus. CH₂-oxo-NNK was found to be a potent DNA methylating agent, but future studies are required to elucidate the full biological significance of the newly discovered compounds.

Chapter 3 Formation and Quantitation of 2'-Deoxyadenosine Adducts resulting from NNK Bioactivation *in vitro* and *in vivo*

The following chapter describes work that was previously published in *Chemical Research in Toxicology* (DOI: 10.1021/acs.chemrestox.8b00056) and is adapted with permission from the American Chemical Society²⁷⁶. The study was primarily performed by Erik S. Carlson and was co-authored by Pramod Upadhyaya, Peter W. Villalta, Bin Ma, and Stephen S. Hecht. This study was supported by the U.S. National Cancer Institute through grant CA-81301. The authors thank Bob Carlson for editorial assistance, Xun Ming and Makenzie Pillsbury for mass spectrometry assistance in the Analytical Biochemistry Shared Resource (partially supported by National Cancer Institute grant CA-77598). We also thank Dr. Adam T. Zarth for valuable discussions and NMR assistance.

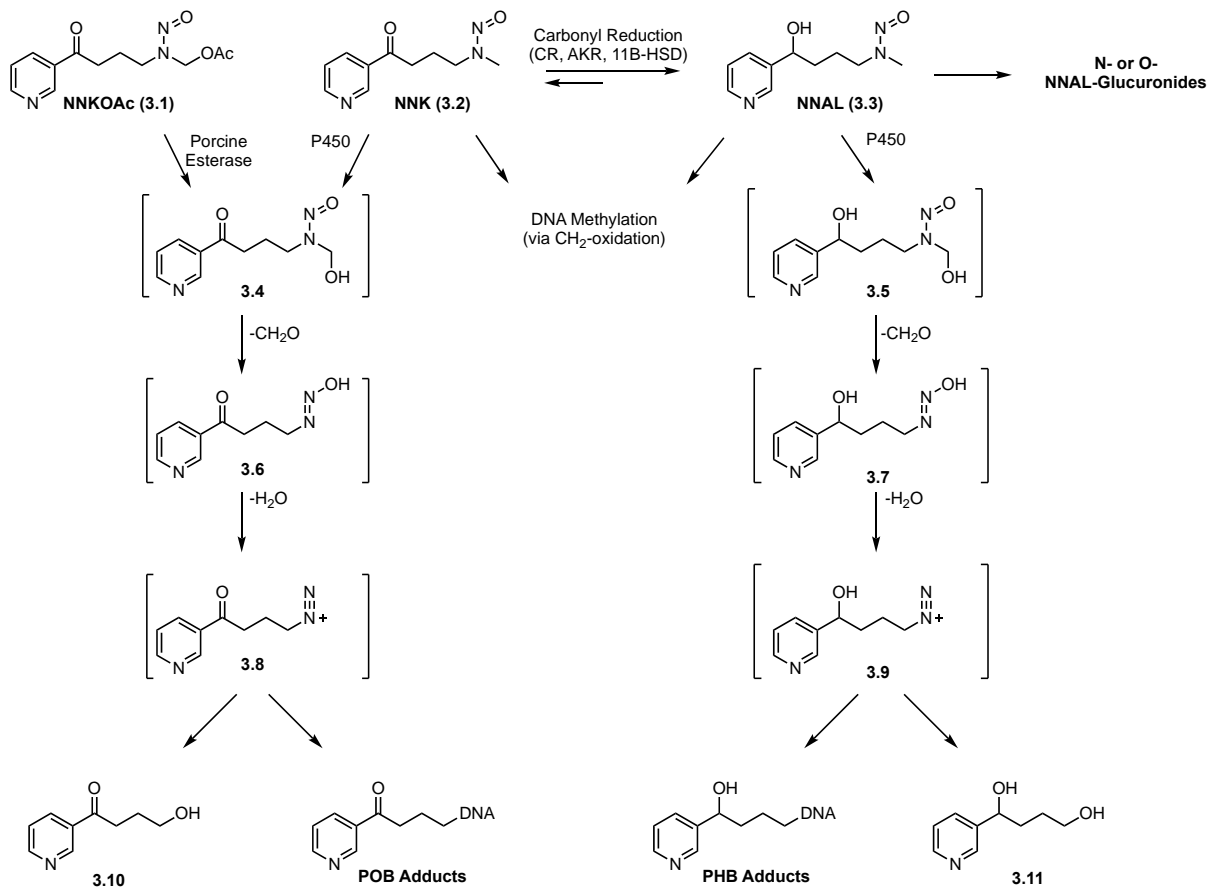


- Novel 2'-deoxyadenosine adducts from NNK and NNAL
- Evidence of formation *in vitro* and *in vivo*

3.1 Introduction

Understanding the mechanisms of tobacco-induced carcinogenesis can potentially lead to new approaches to cancer prevention by identifying cigarette smokers particularly susceptible to lung cancer and other tobacco-related cancers. In this chapter, we will focus solely on the carcinogenic mechanisms of NNK (3.2). As previously mentioned (Section 1.4), NNK is found solely in tobacco products and readily causes adenocarcinoma of the lung in rats, mice, hamsters, and ferrets regardless of the route of administration and at relatively low doses.¹⁹⁰ Additionally, epidemiological studies have correlated NNK metabolites in smokers' urine to future lung cancer onset.¹⁷²⁻¹⁷⁴

A brief overview of NNK metabolism leading to DNA adduct formation is presented in Scheme 3-1.

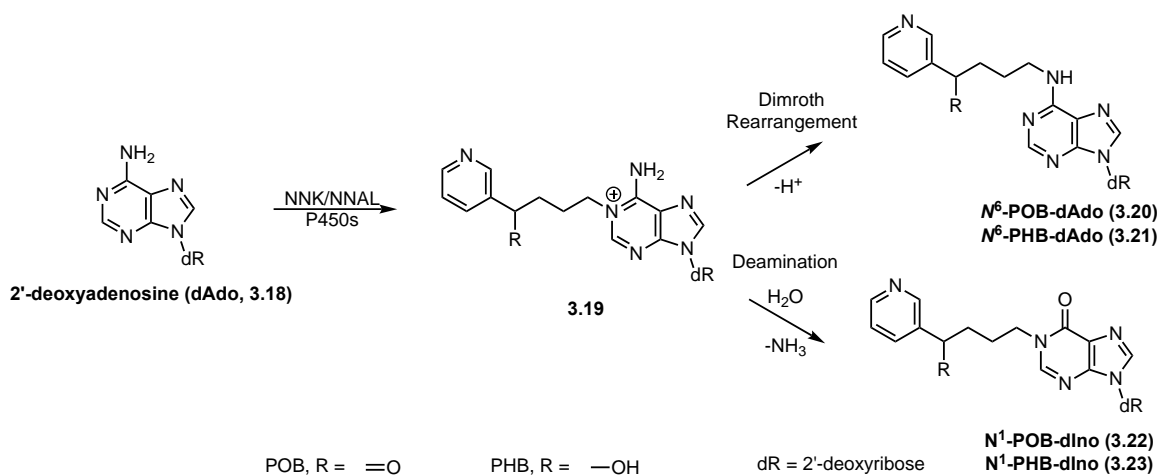


Scheme 3-1: Overview of NNK (3.2) and NNAL (3.3) metabolism and DNA adduct formation in vivo. NNK is in enzymatic equilibrium with NNAL, which is commonly glucuronidated. Both NNK and NNAL can alternatively be oxidized to α -hydroxynitrosamines 3.4 or 3.5. These further decompose to diazonium ions 3.8 or 3.9 and ultimately hydrolyze to 3.10 or 3.11, or form DNA adducts.

NNK is converted in humans to both enantiomers of the carcinogenic metabolite 4-(methylnitrosamino)-1-(3-pyridyl)-1-butanol (NNAL, **3.3**) by enzymatic carbonyl reduction.^{26,190} Studies suggest that this process may be partially reversible as (*S*)-NNAL can be enzymatically oxidized to NNK *in vivo* while (*R*)-NNAL commonly remains reduced.²¹⁰ Both enantiomers are *O*- or *N*-glucuronidated and excreted in the urine.²⁴⁹ These and unmodified NNAL serve as useful biomarkers and were the basis of the epidemiology studies noted above.^{172–174}

Both NNK and NNAL are metabolized by P450s, activating them to DNA-alkylating agents¹⁹⁰. These mechanisms were fully elaborated in Section 1.4, but will be briefly summarized here. Initial hydroxylation of the terminal methyl group of NNK or NNAL by either P450 2A6 or P450 2A13¹³⁷ produces the unstable α -hydroxy species **3.4** or **3.5**. In the previous chapter, we found that a small fraction of these may be converted to nitrosamides,²³⁹ but most will rapidly decompose to diazonium ions **3.8** and **3.9**, which hydrolyze to form metabolites **3.10** and **3.11**, which are excreted in the urine after further enzymatic processing. However, **3.8** and **3.9** can also react with DNA to form pyridyloxobutyl- (POB) or pyridylhydroxybutyl- (PHB) DNA adducts, respectively (Section 1.4.2.2 & 1.4.3.2.). The POB-DNA adducts can also be formed *in vitro* from NNKOAc, a precursor to **3.4** that does not require P450 metabolism. Analogously, the α -methylene group can be hydroxylated to ultimately form methyl DNA adducts. DNA adducts left unrepaired can cause mutations and initiate tumor development.^{190,277} To date, only four POB- and three PHB- base adducts have been detected and quantified in animal models (**Figure 1-10**).^{20,209,210,229} In addition to these base adducts, a large family of DNA phosphate adducts have recently been uncovered and quantified *in vivo*.^{50,51}

Notably missing from this panel of adducts are those formed with 2'-deoxyadenosine (dAdo). Therefore, the goal of this study was to determine the structure and levels of dAdo-derived POB- and PHB-adducts in NNK- and NNAL-treated rats. We hypothesized that initial alkylation of dAdo would occur at the *N*¹-position (**Scheme 3-2**).



Scheme 3-2: Proposed mechanism for dAdo adduct formation. After initial N^1 -alkylation, the resulting cationic intermediate either undergoes Dimroth rearrangement or deamination to yield N^6 -dAdo (**3.20-3.21**) or N^1 -dIno (**3.22-3.23**) DNA adducts, respectively.

This results in an unstable cationic intermediate (**3.19**), which can deprotonate and undergo spontaneous Dimroth rearrangement to give N^6 -dAdo adducts **3.20** and **3.21**.²⁷⁸⁻²⁸⁰ Alternatively, deamination via an addition-elimination mechanism can occur yielding N^1 -dIno adducts **3.22** and **3.23**.²⁸⁰⁻²⁸³ In support of this general mechanism, N^6 -dAdo and N^1 -dIno type adducts have been found after *in vitro* treatment of DNA with styrene oxide and butadiene monoxide.^{284,285} Along with these adduct types, previous studies have identified N^3 - and N^7 -dAdo adducts, but these are known to be unstable and generate abasic sites,^{286,287} thus were not considered in this study. N^1 -dIno adducts are thought to be potentially important as they can cause A:G mutations through Hoogsteen base pairing,²⁸⁸ while N^6 -dAdo adducts may interfere with base pairing due to their steric bulk. Regardless of their potential mutagenicity, these adducts also may serve as DNA damage biomarkers.¹⁹² Therefore, to meet the goals of this study, we synthesized standards for all four proposed dAdo-derived adducts, detected POB adduct formation *in vitro*, and quantified dAdo adduct formation in the livers and lungs of rats treated chronically with NNK and NNAL.

3.2 Experimental Procedures

CAUTION: *NNK and NNAL are carcinogenic in animal models. NNKOAc, an activated form of NNK, is mutagenic and is presumed to be carcinogenic. Handle these compounds in a well-ventilated fume hood while wearing proper personal protective equipment.*

3.2.1 Chemicals and Enzymes

NNK and NNKOAc were purchased from Toronto Research Chemicals. (*S*)-NNAL, (*R*)-NNAL, *N*⁶-PHB-dAdo, 2-(3-pyridyl)-1,3-dithiane, *tert*-butyl 3-(2-(3-pyridyl)-1,3-dithianyl)-1-propylcarbamate, and [pyridine-D₄]*tert*-butyl 3-(2-(3-pyridyl)-1,3-dithianyl)-1-propylcarbamate were synthesized as previously described.^{239,289,290} [¹⁵N₅]2'-deoxyadenosine (>99% ¹⁵N₅ incorporation) was obtained from Cambridge Isotope Laboratories (Tewksbury, MA). 6-Chloropurine-2'-deoxyriboside was obtained from Carbosynth (Compton, United Kingdom). Reagents for DNA isolation were purchased from Qiagen (Hilden, Germany). Calf thymus DNA, phosphodiesterase II, and micrococcal nuclease were obtained from Worthington Biochemical Co. (Lakewood, NJ). Alkaline phosphatase was procured from Roche Diagnostics GmbH (Mannheim, Germany). Porcine liver esterase and all other chemicals and solvents were obtained from either Sigma Aldrich (Milwaukee, WI) or Thermo Scientific (Waltham, MA) in reagent grade or higher and used without further purification.

3.2.2 General Synthetic Procedures

NMR spectra were recorded on a Bruker 500 MHz spectrometer. Chemical shifts are reported as parts per million (ppm). Residual solvent peaks were used as an internal reference for ¹H-NMR (7.26 ppm CDCl₃; 2.50 ppm D₆-DMSO) and ¹³C-NMR (77.2 ppm CDCl₃; 39.5 ppm D₆-DMSO). Peak splitting was abbreviated as follows: s = singlet, d = doublet, t = triplet, q = quartet, dd = doublet of doublets, dt = doublet of triplets, ddd = doublet of doublet of doublets, bs = broad singlet, and m = multiplet. High resolution mass spectrometry (HRMS) of selected compounds was performed on an LTQ Orbitrap Velos (Thermo Scientific, Waltham, MA) and reported as *m/z*. Thin-layer

chromatography (TLC) utilized Polygram pre-coated silica gel TLC plate (40 x 80 mm, 0.2 mm thick) with 254 nm fluorescent indicator. TLC plates were visualized with permanganate stain when necessary, otherwise UV lamp irradiation sufficed. Flash chromatography was performed on SiliCycle 60 (70-150) mesh silica gel. Reactions were performed with oven-dried glassware and under an atmosphere of N₂ unless specified otherwise.

3.2.3 Synthesis of Chemical Standards

[¹⁵N₅]6-*N*-(4-(3-pyridyl)-4-hydroxy-1-butyl)-2'-deoxyadenosine ([¹⁵N₅]N⁶-PHB-dAdo, **3.21**):

This was prepared as previously described²⁹⁰ for N⁶-PHB-dAdo except using [¹⁵N₅]2'-deoxyadenosine as starting material.

¹H-NMR (500 MHz; DMSO-*d*₆): δ 8.51 (d, *J* = 10.4 Hz, 1H, 2-Pyr), 8.42 (d, *J* = 4.7 Hz, 1H, 6-Pyr), 8.33-8.29 (m, 1H, C8), 8.18 (s, 1H, C2), 7.87 (bs, 1H, NH), 7.71-7.69 (m, 1H, 4-Pyr), 7.32 (dd, *J* = 7.8, 4.8 Hz, 1H, 5-Pyr), 6.34 (t, *J* = 7.0 Hz, 1H, C1'), 5.31 (m, 2H, 3'-OH/CHOH), 5.24 (s, 1H, 5'-OH), 4.62 (m, 1H, CH), 4.41-4.40 (m, 1H, C3'), 3.88 (d, *J* = 2.2 Hz, 1H, C4'), 3.62 (m, 1H, C5'), 3.50 (m, 3H, C5'/NHCH₂), 2.72 (dt, *J* = 12.0, 5.5 Hz, 1H, C2'), 2.25 (dd, *J* = 12.4, 4.4 Hz, 1H, C2'), 1.69-1.54 (m, 4H, CH₂CH₂). ¹³C-NMR: (126 MHz; DMSO-*d*₆): δ 152.6 (C2), 148.4 (6-Pyr), 148.1 (2-Pyr), 139.5 (C8), 133.9 (4-Pyr), 123.5 (5-Pyr), 88.5 (C4'), 84.3 (C1'), 71.4 (C3'), 70.4 (CH), 62.4 (C5'), 39.9 (C2'), 39.8 (NCH₂), 36.8 (CHCH₂), 25.9 (NCH₂CH₂). 3-Pyr, C4, C5, and C6 not observed. HRMS: calc'd: 406.17835; found: 406.17756

3-(2-(3-Pyridyl)-1,3-dithianyl)-1-propylamine (**3.26**):

A solution of **3.25** (87.6 mg, 0.247 mmol) in CH₂Cl₂ (3 mL) was treated with trifluoroacetic acid (TFA, 1.49 g, 13.1 mmol, 1 mL) and stirred at room temperature. After 3h, the solution was concentrated by rotary evaporation to remove excess TFA. The resulting oil was dissolved in CH₂Cl₂ and washed with sat'd NaHCO₃ solution and brine. The organic layer was then dried over MgSO₄, filtered, and concentrated *in vacuo* to give

a yellow oil. Purification by column chromatography (CH₂Cl₂/MeOH/Et₃N 85:15:1) yielded the product as a light, yellow oil (41.4 mg, 66%).

¹H-NMR (500 MHz; CDCl₃): δ 9.11 (d, *J* = 1.8 Hz, 1H), 8.49-8.48 (m, 1H), 8.21 (d, *J* = 8.1 Hz, 1H), 7.31 (dd, *J* = 8.0, 4.8 Hz, 1H), 2.72-2.64 (m, 6H), 2.10-2.06 (m, 2H), 1.95 (dd, *J* = 8.9, 4.7 Hz, 2H), 1.53-1.49 (m, 2H). ¹³C-NMR (126 MHz; CDCl₃): δ 150.5, 148.1, 137.6, 136.9, 123.3, 56.3, 42.1, 41.2, 27.5, 26.2, 24.9

6-*N*-(4-(3-pyridyl)-4-oxo-1-butyl)-2'-deoxyadenosine (*N*⁶-POB-dAdo, 3.20):

A solution of **3.26** (6.35 mg, 0.0250 mmol), 6-chloropurine-9-2'-deoxyriboside (10.4 mg, 0.0384 mmol), and iPr₂EtN (7.42 mg, 0.0574 mmol, 10 μL) in DMSO (300 μL) was heated to 60 °C for 16 h. The compound was crudely isolated by solid-phase extraction using a Strata-X 33 μm polymeric reversed phase cartridge (30 mg/mL; Phenomenex, Torrance, CA). The cartridge was preconditioned with 1 mL of MeOH, followed by 1 mL of H₂O. After sample addition, the cartridge was washed with 2 mL of H₂O, 1 mL of 5% (v/v), 10%, and 50% MeOH, and eluted with 1 mL of 80% MeOH. The eluent was evaporated to dryness in a Speedvac.

The isolated product was dissolved in 4:1 MeCN/H₂O (1 mL) and added to a suspension of *N*-chlorosuccinimide (NCS, 11.9 mg, 0.0891 mmol) and AgNO₃ (20.2 mg, 0.1188) in 4:1 MeCN/H₂O (1 mL) at 0 °C. The reaction was stirred at 0 °C for 30 min before quenching with sat'd Na₂SO₃, sat'd NaHCO₃, and brine solutions in succession (1 mL each). The product was isolated by HPLC using a 250 mm x 10 mm, 5 μm, Luna C-18 column (Phenomenex) with H₂O and MeCN as mobile phases. The gradient was 30% to 45% MeCN over 5 min at 3 mL/min. The product eluted at 4.1 min. The product was a light yellow solid (2.37 mg, 24% over two steps).

¹H-NMR (500 MHz; DMSO-*d*₆): δ 9.09 (d, *J* = 1.1 Hz, 1H, 2-Pyr), 8.77 (dd, *J* = 4.7, 0.8 Hz, 1H, 6-Pyr), 8.32 (s, 1H, C-8), 8.25 (d, *J* = 8.0 Hz, 1H, 4-Pyr), 8.12 (s, 1H, C-2), 7.94-7.93 (bs, 1H, NH), 7.54 (dd, *J* = 7.9, 4.8 Hz, 1H, 5-Pyr), 6.34 (t, *J* = 7.0 Hz, 1H, C1'), 5.30 (d, *J* = 3.9 Hz, 1H, 3'-OH), 5.22 (t, *J* = 5.7 Hz, 1H, 5'-OH), 4.41-4.40 (m, 1H, C3'), 3.88 (d, *J* = 2.5 Hz, 1H, C4'), 3.64-3.50 (m, 4H, C5'+ NHCH₂), 3.15 (t, *J* = 6.9 Hz, 2H, COCH₂), 2.74-2.69 (m, 1H, C2'), 2.27-2.23 (m, 1H, C2'), 1.96 (quintet, *J* = 6.8 Hz,

2H, COCH₂CH₂). ¹³C-NMR (126 MHz; DMSO-*d*₆): δ 199.5 (CO), 155.1 (C6), 153.7 (6-Pyr), 152.7 (C2), 149.6 (2-Pyr), 148.5 (C4), 139.8 (C8), 135.7 (4-Pyr), 132.4 (3-Pyr), 124.3 (5-Pyr), 120.1 (C5), 88.5 (C4'), 84.4 (C1'), 71.4 (C3'), 62.4 (C5'), 39.9 (C2'), 39.3 (NHCH₂), 36.0 (COCH₂), 21.6 (COCH₂CH₂). HRMS: calc'd: 399.17753; found: 399.17742

[Pyridine-D₄]3-(2-(3-Pyridyl)-1,3-dithianyl)-1-propylamine:

This compound was prepared analogously to **3.26** except [pyridine-D₄]**3.25** (>98% D₄-incorporation) was used as starting material. The product was a light-yellow oil (7.67 mg, 35%).

¹H-NMR (500 MHz; CDCl₃): δ 2.71-2.64 (m, 4H), 2.61 (t, *J* = 7.0 Hz, 2H), 2.05 (dt, *J* = 7.9, 4.2 Hz, 2H), 1.98-1.93 (m, 2H), 1.47-1.41 (m, 2H). ¹³C-NMR (126 MHz; CDCl₃): δ 56.5, 42.5, 41.8, 27.52, 27.42, 25.0

[Pyridine-D₄]6-*N*-(4-(3-pyridyl)-4-oxo-1-butyl)2'-deoxyadenosine ([pyridine-D₄]*N*⁶-POB-dAdo):

This compound was prepared analogously to *N*⁶-POB-dAdo except [pyridine-D₄]**3.26** (7.67mg, 0.0297 mmol) was used as the starting material. The isolated product was a light yellow solid (2.08 mg, 18% over two steps).

¹H-NMR (500 MHz; DMSO-*d*₆): δ 8.32 (s, 1H, C8), 8.11 (s, 1H, C2), 7.94 (bs, 1H, NH), 6.33 (dd, *J* = 7.7, 6.2 Hz, 1H, C1'), 5.33 (d, *J* = 0.3 Hz, 1H, 3'-OH), 5.24 (m, 1H, 5'-OH), 4.41-4.40 (m, 1H, C3'), 3.88 (q, *J* = 3.4 Hz, 1H, C4'), 3.62-3.50 (m, 4H, C5'/COCH₂), 3.15 (dd, *J* = 10.6, 5.9 Hz, 2H, NHCH₂), 2.71-2.69 (m, 1H, C2'), 2.25 (ddd, *J* = 13.1, 6.1, 2.8 Hz, 1H, C2'), 1.96 (t, *J* = 6.9 Hz, 2H, CH₂). ¹³C-NMR (126 MHz; DMSO-*d*₆): δ 199.6 (CO), 155.1 (C6), 152.7 (C2), 147.0 (C4), 139.7 (C8), 132.3 (3-Pyr), 120.4 (C5), 88.5 (C4'), 84.4 (C1'), 71.4 (C3'), 62.3 (C5'), 39.6 (C2'), 39.2 (NHCH₂), 36.1 (COCH₂), 23.8 (COCH₂CH₂). HRMS: calc'd: 403.20264; found: 403.20173

3',5'-bis-O-(tert-butyldimethylsilyl)-2'-deoxyinosine (3.29):

2'-Deoxyinosine (463 mg, 1.84 mmol) and imidazole (554.5 mg, 8.14 mmol) were suspended in anhydrous pyridine (5 mL) and treated with *tert*-butyldimethylsilyl chloride (TBS-Cl, 585 mg, 3.88 mmol). The mixture was stirred at room temperature. After 4 h, the mixture became completely homogenous, and the reaction was quenched with H₂O (10 mL). The solution was extracted twice with CH₂Cl₂ (15 mL). The pooled organics were dried over MgSO₄, filtered, and concentrated. The resulting product was evaporated from toluene (5 mL) multiple times to remove residual pyridine. NMR indicated that purity was sufficient to carry forward without further purification.

¹H-NMR (500 MHz; CDCl₃): δ 12.61 (s, 1H), 8.19 (s, 1H), 8.08 (s, 1H), 6.40 (t, *J* = 6.4 Hz, 1H), 4.60 (dt, *J* = 5.6, 3.6 Hz, 1H), 4.01 (q, *J* = 3.5 Hz, 1H), 3.85-3.75 (m, 2H), 2.58-2.42 (m, 2H), 0.90 (d, *J* = 2.6 Hz, 18H), 0.10-0.08 (m, 12H). ¹³C NMR (126 MHz; CDCl₃): δ 158.7, 148.3, 144.6, 138.4, 125.0, 88.0, 84.5, 71.7, 62.7, 41.6, 26.0, 25.7, 18.4, 18.0, -4.67, -5.40.

1-N-(2,4-dinitrophenyl)-3',5'-bis-O-(tert-butyldimethylsilyl)-2'-deoxyinosine (3.30):

A mixture of **3.29** (1384 mg, 2.14 mmol), K₂CO₃ (608.6 mg, 4.40 mmol), and 1-chloro-2,4-dinitrobenzene (499.5 mg, 2.22 mmol) in DMF (10 mL) was heated to 80 °C for 2.5 h. The bright red solution turned orange during the reaction. After 2.5 h, the reaction mixture was cooled to room temperature and diluted with EtOAc (10 mL). The mixture was filtered over Celite and concentrated to a thick, red oil. Purification by column chromatography (EtOAc/hexanes 1:2 →1:1) yielded pure product as a yellow solid (1.26 g, 91% over 2 steps).

¹H-NMR (500 MHz; CDCl₃): δ 9.05 (d, *J* = 1.2 Hz, 1H), 8.68-8.66 (m, 1H), 8.21 (d, *J* = 10.3 Hz, 1H), 8.00 (s, 1H), 7.72-7.68 (m, 1H), 6.47-6.41 (m, 1H), 4.64-4.61 (m, 1H), 4.06-4.04 (m, 1H), 3.89-3.79 (m, 2H), 2.60-2.45 (m, 2H), 0.93 (s, 18H), 0.13-0.11 (m, 12H). ¹³C-NMR (126 MHz; CDCl₃): δ 155.2, 148.2, 147.1, 146.50, 146.48, 144.72, 144.61, 139.2, 138.9, 135.9, 131.96, 131.83, 128.75, 128.70, 124.37, 124.17, 121.43, 121.38, 88.32, 88.18, 84.64, 84.44, 71.87, 71.71, 62.77, 62.63, 42.1, 41.8, 26.0, 25.7, 18.4, 18.0, -4.63, -4.66, -5.37, -5.48

1-*N*-(3-hydroxypropyl)-3',5'-bis-*O*-(*tert*-butyldimethylsilyl)-2'-deoxyinosine (3.31):

A solution of **3.30** (701.2 mg, 1.08 mmol) was dissolved in DMF (10 mL) and treated with 3-amino-1-propanol (810.2 mg, 10.8 mmol, 820 μ L). The yellow solution immediately became red. The solution was brought to 80 °C for 2 h, then back to room temperature. It was concentrated to a dark red oil. Purification by column chromatography (EtOAc/hexanes 2:1 \rightarrow 1:0) yielded pure product as a yellow oil that solidified upon refrigeration (522.9 mg, 90%).

$^1\text{H-NMR}$ (500 MHz; CDCl_3): δ 8.08 (s, 1H), 8.03 (s, 1H), 6.35 (t, $J = 6.4$ Hz, 1H), 4.58 (dt, $J = 5.7, 3.1$ Hz, 1H), 4.24 (t, $J = 6.4$ Hz, 2H), 3.99 (d, $J = 3.4$ Hz, 1H), 3.82-3.73 (m, 2H), 3.59 (t, $J = 5.5$ Hz, 2H), 2.52 (dt, $J = 13.0, 6.4$ Hz, 1H), 2.40 (ddd, $J = 13.0, 5.9, 4.0$ Hz, 1H), 1.97 (quintet, $J = 5.9$ Hz, 2H), 0.89 (d, $J = 3.9$ Hz, 18H), 0.09-0.06 (m, 12H). $^{13}\text{C-NMR}$ (126 MHz; CDCl_3): δ 157.4, 147.29, 147.18, 138.5, 124.6, 88.0, 84.2, 71.8, 62.7, 57.9, 43.1, 41.5, 32.6, 25.9, 18.4, 18.0, -4.7, -5.4

1-*N*-(3-iodopropyl)-3',5'-bis-*O*-(*tert*-butyldimethylsilyl)-2'-deoxyinosine (3.32):

Imidazole (69.0 mg, 1.01 mmol) and triphenylphosphine (222.7 mg, 0.849 mmol) were dissolved in CH_2Cl_2 (7 mL) and brought to 0 °C. To this was added I_2 (218.8 mg, 0.862 mmol). After 15 min, the color of the mixture changed from yellow to dark orange. A CH_2Cl_2 -diluted solution of **3.31** (415.9 mg, 0.772 mmol, 7 mL) was then added. After 10 min, the reaction was warmed to room temperature and stirred for 2 h. Then the mixture was filtered over Celite and washed with sat'd $\text{Na}_2\text{S}_2\text{O}_3$ solution. The organic layer was separated and further washed with brine, dried over MgSO_4 , filtered, and concentrated to a yellow solid. Purification by column chromatography (EtOAc/hexanes 3:1) yielded pure product as a yellow oil (461.4 mg, 95%).

$^1\text{H-NMR}$ (500 MHz; CDCl_3): δ 8.26 (s, 1H), 8.08 (s, 1H), 6.39 (t, $J = 6.4$ Hz, 1H), 4.60 (dt, $J = 5.9, 3.2$ Hz, 1H), 4.19 (t, $J = 6.6$ Hz, 2H), 4.03 (q, $J = 3.5$ Hz, 1H), 3.85-3.76 (m, 2H), 3.17 (t, $J = 6.4$ Hz, 2H), 2.59-2.43 (m, 2H), 2.33 (quintet, $J = 6.5$ Hz, 2H), 0.91 (d, $J = 4.7$ Hz, 18H), 0.11-0.08 (m, 12H). $^{13}\text{C-NMR}$ (126 MHz; CDCl_3): δ 155.5, 147.5,

146.9, 138.3, 123.8, 88.3, 84.7, 71.8, 62.7, 47.5, 41.6, 31.9, 26.0, 25.7, 18.4, 18.0, 2.3, -4.65, -4.78, -5.35, -5.45.

1-*N*-(3-(2-(3-Pyridyl)-1,3-dithianyl)propyl)-3',5'-bis-*O*-(*tert*-butyldimethylsilyl)-2'-deoxyinosine (3.34):

A solution of **3.33**²³⁹ (78.1 mg, 0.396 mmol) and tetramethylethylenediamine (TMEDA, 46.5 mg, 0.400 mmol, 60 μ L) in anhydrous THF (4 mL) was cooled to -78 °C and treated with *n*-BuLi in hexanes dropwise (0.480 mmol, 300 μ L). The resulting red solution was stirred for 10 min. A THF-diluted solution of **3.32** (228.5 mg, 0.352 mmol, 3 mL) was then added dropwise. The mixture was stirred for 4 h and the color slowly transitioned from red to yellow. The reaction was quenched with H₂O (5 mL) and warmed to room temperature. The mixture was diluted with EtOAc and washed with brine. The aqueous phase was extracted twice with EtOAc. The pooled organics were dried over MgSO₄, filtered, and concentrated to an orange oil. Purification by column chromatography (100% EtOAc) yielded the product as a yellow solid (179.4 mg, 71%).

¹H-NMR (500 MHz; CDCl₃): δ 9.12 (d, *J* = 1.9 Hz, 1H), 8.53 (d, *J* = 3.9 Hz, 1H), 8.30 (m, 1H), 8.05 (s, 1H), 7.85 (s, 1H), 7.42 (dd, *J* = 8.0, 4.9 Hz, 1H), 6.38-6.33 (m, 1H), 4.59-4.55 (m, 1H), 4.27 (s, 1H), 3.97 (m, 4H), 3.82-3.59 (m, 2H), 2.77-2.49 (m, 6H), 2.06 (dd, *J* = 9.8, 6.4 Hz, 2H), 1.98-1.76 (m, 4H), 0.78 (s, 18H), 0.07 (m, 12H). ¹³C-NMR (126 MHz; CDCl₃): δ 156.5, 149.0, 147.2, 146.86, 146.69, 139.5, 138.6, 138.3, 124.9, 89.9, 84.8, 73.2, 63.5, 56.1, 46.2, 41.9, 41.7, 27.6, 26.1, 24.7, 18.6, 18.1, -4.53, -4.67, -5.35, -5.39

1-*N*-(4-oxo-4-(3-pyridyl)-butyl)-2'-deoxyinosine (*N*¹-POB-dIno, 3.22):

N-Chlorosuccinimide (NCS, 11.5 mg, 0.0861) and AgNO₃ (15.5 mg, 0.0912) were suspended in 1:1 MeCN/H₂O (400 μ L) and cooled to 0 °C. To this was added a solution of **3.34** in MeCN (11.1 mg, 0.0155 mmol, 600 μ L). The reaction mixture was stirred at 0 °C for 30 min before quenching with sat'd Na₂SO₃, sat'd NaHCO₃, and brine solutions in succession (1 mL each). The mixture was diluted with CH₂Cl₂ (5 mL) and filtered. The organic layer was collected and the aqueous phase further extracted once

with CH₂Cl₂. The pooled organics were dried over MgSO₄, filtered, and concentrated to a yellow oil. The crude product was then transferred and concentrated into a 2-mL polypropylene tube and reconstituted in THF (200 μL). To this was added 5 μL of a K₂HPO₄-buffered solution of tetra-*n*-butylammonium fluoride (TBAF, 3.4M, 25mM 2:1 K₂PO₄, pH 7.1/THF). The solution immediately turned orange and was shaken for 24 h. The solvent was evaporated to give an orange solid, which was reconstituted in H₂O (2 mL) and purified by HPLC using a 250 mm x 10 mm, 5 μm, Luna C-18 column (Phenomenex) with H₂O and MeCN as mobile phases. The gradient was 30% to 45% MeCN over 5 min at 3 mL/min. The product eluted at 10.7 min. The product was a white solid (2.37 mg, 24% over two steps).

¹H-NMR (500 MHz; DMSO-*d*₆): δ 9.09 (d, *J* = 1.7 Hz, 1H, 2-Pyr), 8.78 (dd, *J* = 4.8, 1.6 Hz, 1H, 6-Pyr), 8.42 (s, 1H, C2), 8.31 (s, 1H, C8), 8.25 (dt, *J* = 8.0, 1.9 Hz, 1H, 4-Pyr), 7.56 (dd, *J* = 7.9, 4.8 Hz, 1H, 5-Pyr), 6.30 (t, *J* = 6.9 Hz, 1H, C1'), 5.32 (d, *J* = 3.7 Hz, 1H, 3'-OH), 4.97 (t, *J* = 5.5 Hz, 1H, 5'-OH), 4.39-4.37 (m, 1H, C3'), 4.09 (t, *J* = 7.0 Hz, 2H, NCH₂), 3.86 (q, *J* = 3.7 Hz, 1H, C4'), 3.61-3.49 (m, 2H, C5'), 3.16 (t, *J* = 7.0 Hz, 2H, COCH₂), 2.62 (ddd, *J* = 13.3, 7.2, 6.1 Hz, 1H, C2'), 2.31-2.27 (m, 1H, C2'), 2.05 (t, *J* = 7.0 Hz, 2H, COCH₂CH₂). ¹³C-NMR (126 MHz; DMSO-*d*₆): δ 198.6 (CO), 156.1 (C6), 153.3 (6-Pyr), 149.1 (2-Pyr), 148.4 (C2), 147.1 (C4), 139.3 (C8), 135.3 (4-Pyr), 131.8 (3-Pyr), 123.8 (5-Pyr), 123.4 (C5), 88.6 (C4'), 83.6 (C1'), 70.6 (C3'), 61.5 (C5'), 45.2 (NCH₂), 40.4 (C2'), 35.2 (COCH₂), 23.5 (COCH₂CH₂). HRMS: calc'd: 400.16155; found: 400.16162

1-*N*-(4-hydroxy-4-(3-pyridyl)-butyl)-3',5'-bis-*O*-(*tert*-butyldimethylsilyl)-2'-deoxyinosine (3.35):

N-Chlorosuccinimide (NCS, 12.9 mg, 0.0966) and AgNO₃ (20.6 mg, 0.121) were suspended in 1:1 MeCN/H₂O (200 μL) and cooled to 0 °C. To this was added a solution of **3.34** in 1:1 MeCN:H₂O (15.6 mg, 0.0217 mmol, 800 μL). The reaction mixture was stirred at 0 °C for 30 min before quenching with sat'd Na₂SO₃, sat'd NaHCO₃, and brine solutions in succession (1 mL each). The mixture was diluted with CH₂Cl₂ (5 mL) and filtered. The organic layer was collected and the aqueous phase extracted once with

CH₂Cl₂. The pooled organics were dried over MgSO₄, filtered, and concentrated to a yellow oil. The crude product was then dissolved in MeOH (800 μL) and treated with NaBH₄ (7.0 mg, 0.185 mmol) at room temperature. After 1 h, the reaction mixture was quenched with sat'd NH₄Cl, diluted with CH₂Cl₂ and washed with sat'd NaHCO₃. The aqueous phase was further extracted three times with CH₂Cl₂. The pooled organics were dried over MgSO₄, filtered, and concentrated to a white solid (6.15 mg). The crude material was carried forward without further purification.

1-N-(4-hydroxy-4-(3-pyridyl)-butyl)-2'-deoxyinosine (N¹-PHB-dIno, 3.23):

A solution of **3.35** (3.4 mg, 0.00540 mmol) in THF (450 μL) was treated with TBAF in THF (0.0150 mmol, 15 μL) at room temperature. After 1 h, the reaction mixture was diluted with H₂O and filtered through a 4 mm Acrodisc syringe filter (Sigma Aldrich). The resulting solution was purified by HPLC using a 250 mm x 10 mm, 5 μm, Luna C-18 column (Phenomenex) with H₂O and MeCN as mobile phases. The gradient was 30% to 45% MeCN over 5 min at 3 mL/min. The product eluted at 7.1 min. The product was a white solid (1.61 mg, 34% over 3 steps).

¹H-NMR (500 MHz; DMSO-*d*₆): δ 8.51-8.51 (m, 1H, 2-Pyr), 8.43 (dd, *J* = 4.7, 1.5 Hz, 1H, 6-Pyr), 8.40 (s, 1H, C2), 8.33 (s, 1H, C8), 7.70 (dd, *J* = 7.8, 1.6 Hz, 1H, 4-Pyr), 7.33 (dd, *J* = 7.7, 4.7 Hz, 1H, 5-Pyr), 6.29 (dd, *J* = 7.7, 2.8 Hz, 1H, C1'), 5.43 (m, 2H, 3'-OH/5'-OH), 4.85 (s, 1H, OH), 4.63-4.61 (m, 1H, CH), 4.32-4.29 (m, 1H, C3'), 4.14-4.11 (m, 1H, C4'), 4.03-4.00 (m, 2H, NCH₂), 3.48-3.41 (m, 2H, C5'), 2.76-2.70 (m, 1H, C2'), 2.33-2.29 (m, 1H, C2'), 1.79-1.56 (m, 4H, CH₂CH₂). ¹³C-NMR (126 MHz; DMSO-*d*₆): δ 156.4 (C6), 148.8 (C2), 148.5 (6-Pyr), 148.0 (2-Pyr), 146.8 (C4), 139.8 (C8), 136.5 (3-Pyr), 133.8 (4-Pyr), 125.5 (C5), 123.7 (5-Pyr), 89.5 (C4'), 84.1 (C1'), 71.0 (C3'), 70.2 (CH), 62.0 (C5'), 46.1 (NCH₂), 36.3 (CHCH₂), 26.1 (CHCH₂CH₂). HRMS: calc'd: 402.17720; found: 402.17661

3.2.4 *In vitro* Detection of POB-DNA Adducts using NNKOAc

Calf thymus DNA (0.99 mg) was dissolved in 1.0 mL of 25 mM phosphate buffer, pH 7.4. To this was added porcine liver esterase (1.33 mg, 24U) and NNKOAc (1

mg, 3.7 μmol in 20 μL of MeOH) and the mixture was placed in a 37 $^{\circ}\text{C}$ water bath with shaking for 24 h. Then, the solution was diluted with 1 mL of H₂O and extracted twice with 2 mL of CHCl₃/isoamyl alcohol (24:1). The DNA was precipitated by addition of 0.4 mL of 5M NaCl and 2 mL of ice-cold isopropyl alcohol. The DNA was further washed with 1 mL of 70% EtOH, followed by 1 mL of 100% EtOH and dried under a stream of N₂. DNA was stored at -20 $^{\circ}\text{C}$.

Isolated DNA was dissolved in 0.5 mL of 10 mM sodium succinate, 5 mM CaCl₂ buffer and incubated at 37 $^{\circ}\text{C}$ with micrococcal nuclease (30 U) and phosphodiesterase II (0.5 U) for 5 h, followed by 37 $^{\circ}\text{C}$ incubation with alkaline phosphatase (150 U) for 16 h. [Pyridine-D₄]*N*⁶-POB-dA (100 fmol) was added as an internal standard. Samples were placed in 0.45 μm Nylon SpinX centrifugal tube filters and centrifuged at 12,000 g for 10 min. A 20 μL aliquot was removed from each sample and diluted as necessary for dGuo quantitation by HPLC.^{20,225} The remaining sample was purified by solid-phase extraction using a Strata-X 33 μm polymeric reversed phase cartridge (30 mg/mL; Phenomenex, Torrance, CA). The cartridge was preconditioned with 1 mL of MeOH, followed by 1 mL of H₂O. After sample addition, the cartridge was washed with 2 mL of H₂O and 1 mL of 10% (v/v) MeOH, and eluted with 1 mL of 100% MeOH. The eluent was evaporated to dryness in a Speedvac. The residue was dissolved in 25 μL of H₂O and analyzed by liquid chromatography-positive electrospray ionization-tandem mass spectrometry (LC-ESI⁺-MS/MS).

A previously reported LC-ESI⁺-MS/MS method was performed with modifications.²⁰ Briefly, a 0.5 \times 150 mm Zorbax SB-C18, 5 μm column (Agilent, Santa Clara, CA) was eluted with a multi-step gradient and flow rate of 10 $\mu\text{L}/\text{min}$. After a 5-min hold at 5% B, the eluent was brought to 65% B over 25 min, followed by a wash at 85% B and re-equilibration, where solvent A was 15 mM NH₄OAc and solvent B was methanol. MS was performed on a TSQ Vantage triple quadrupole mass analyzer (Thermo Scientific). The selected reaction monitoring (SRM) transitions were m/z 400.1 \rightarrow m/z 284.1 for *N*¹-POB-dIno, m/z 399.1 \rightarrow m/z 265.1 for *N*⁶-POB-dAdo, and m/z 403.1 \rightarrow m/z 269.1 for [pyridine-D₄]*N*⁶-POB-dAdo using collision energies of 10, 20, and 20 eV, respectively, and a 0.4 amu scan width for all transitions.

3.2.5 *In vivo* Detection and Quantitation of POB- and PHB-DNA Adducts in Rat Liver and Lung Tissues

The lung and liver tissues were obtained from a previous study in which male F-344 rats were treated with 5 ppm of NNK, (*S*)-NNAL, or (*R*)-NNAL in drinking water for 50 weeks.^{20,225} Control rats were given unmodified tap water. DNA was isolated from these tissues (n = 3) using a modified Qiagen protocol that has been applied in previous studies.^{225,229,291} Isolated DNA was stored at -20 °C until further analysis.

Isolated DNA samples were hydrolyzed and spiked with [pyridine-D₄]*N*⁶-POB-dAdo and [¹⁵N₅]*N*⁶-PHB-dAdo as described above for our *in vitro* experiment, then analyzed for adducts as described previously.^{20,226,229,291} LC-ESI⁺-MS/MS conditions were the same as described above for our *in vitro* experiment except SRM transitions were added for *N*⁶-PHB-dAdo (*m/z* 401.1 → *m/z* 132.1), *N*¹-PHB-dIno (*m/z* 402.1 → *m/z* 286.1), and [¹⁵N₅]*N*⁶-PHB-dAdo (*m/z* 406.1 → *m/z* 132.1) at collision energies of 26, 10, 26 eV, respectively. Corresponding fragmentation patterns are shown in Figure 3-1.

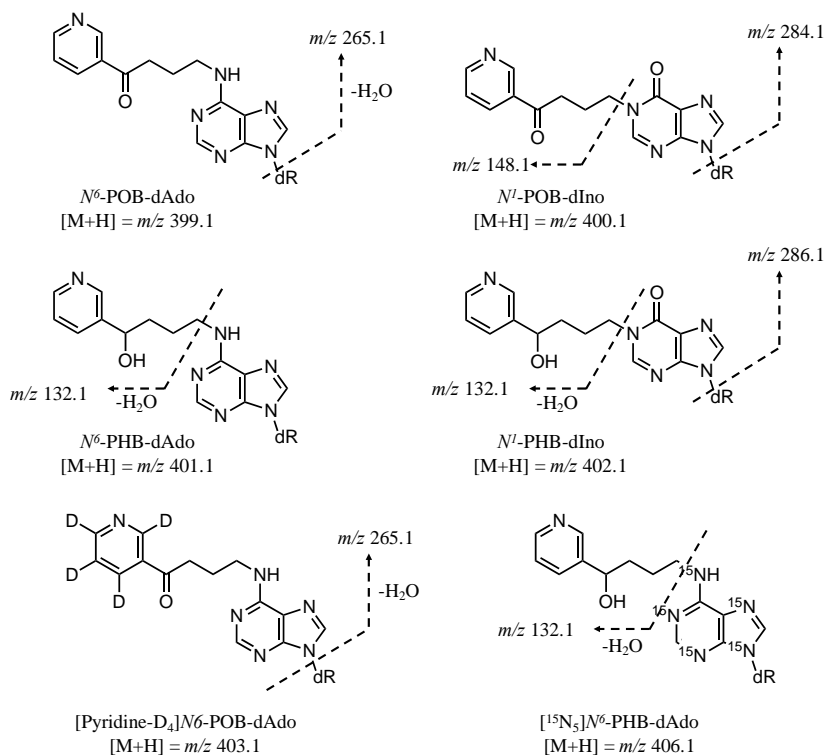


Figure 3-1: Structures and fragmentation patterns for the monitored *N*⁶-dAdo and *N*¹-dIno adducts. dR: 2'-deoxyribose

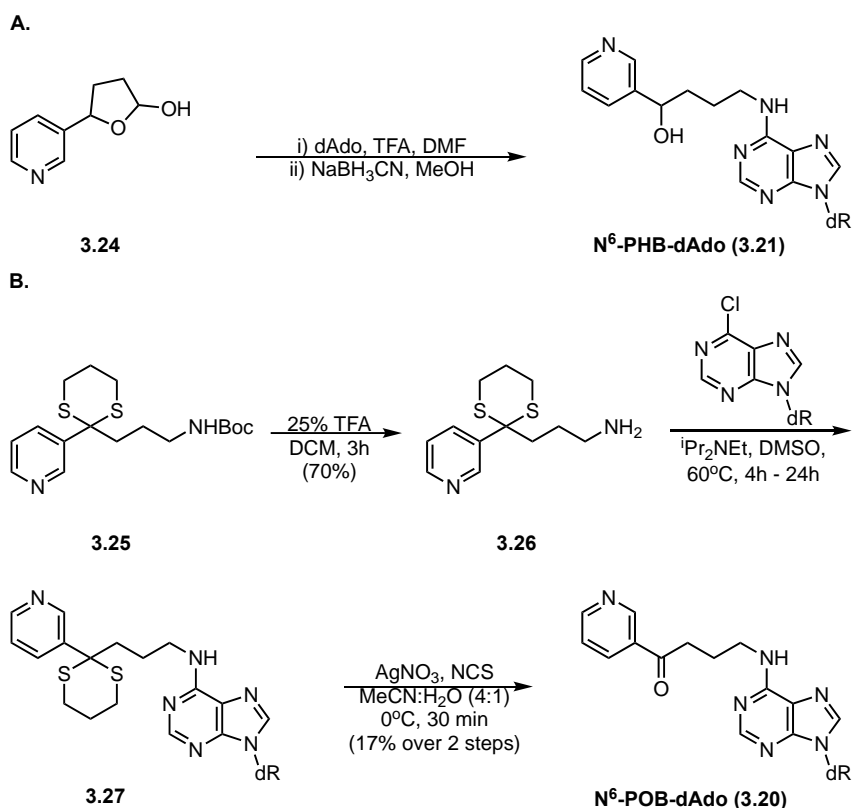
Samples were further analyzed by an optimized liquid chromatography-positive nanoelectrospray ionization-high resolution tandem mass spectrometry (LC-NSI⁺-HRMS/MS) method. A New Objective (Woburn, MA) emitter (75 μm ID, 10 μm orifice) was hand-packed with Luna (Phenomenex) C18, 5 μm stationary phase to create a 200 mm capillary column and a multistep gradient was used for chromatographic separation. With 5 mM NH₄OAc and MeCN as solvents A and B, respectively, the sample was loaded onto the column by running 2% B at 1 $\mu\text{L}/\text{min}$ for 5 min. Then the flow rate was decreased to 0.3 $\mu\text{L}/\text{min}$ over 1 min, the injection valve was removed from the flow path, and a linear gradient was started that ramped from 2% B to 40% B over 20 min. This was followed by an increase to 98% B over 1 min, in which the column was washed for 2 min at 1 $\mu\text{L}/\text{min}$ before a 5 min re-equilibration at 2% B. All dAdo and dIno adducts were monitored by MS² fragmentation on an Orbitrap Fusion Tribrid mass spectrometer (Thermo Scientific, Waltham, MA). The spray voltage was 2.2 kV, the capillary temperature was 300 °C, and the S-Lens RF level was 60%. Each parent ion was isolated (1.5 amu isolation width) and fragmented by higher-energy collision dissociation (HCD) at a normalized energy of 22% with a resolution of 60,000 and mass range of m/z 100 – 425. Accurate product ion masses from characteristic transitions for *N*¹-POB-dIno (m/z 400 \rightarrow 284.1140, 148.0757), *N*¹-PHB-dIno (m/z 402 \rightarrow 286.1296, 268.1191), *N*⁶-POB-dAdo (m/z 399 \rightarrow 283.1300, 265.1194), *N*⁶-PHB-dAdo (m/z 401 \rightarrow 287.1550, 269.1445), [D₄]*N*⁶-POB-dAdo (m/z 403 \rightarrow 285.1456, 267.1350), and [¹⁵N₅]*N*⁶-PHB-dAdo (m/z 406 \rightarrow 290.1307, 272.1202) were extracted at a mass tolerance of 5 ppm.

Quantitation of other DNA base adducts (**3.12**, **3.14**, and **3.15**) for comparison was performed as previously described using similar DNA isolation and LC-ESI⁺-MS/MS or LC-NSI⁺-HRMS/MS techniques.^{20,50,230}

3.3 Results

3.3.1 Synthesis of DNA Adduct Standards

*N*⁶-PHB-dAdo was previously synthesized by a 2-step procedure²⁹⁰ (**Scheme 3-3A**) which was applied to produce a ¹⁵N₅-labelled standard starting from [¹⁵N₅]2'-deoxyadenosine.



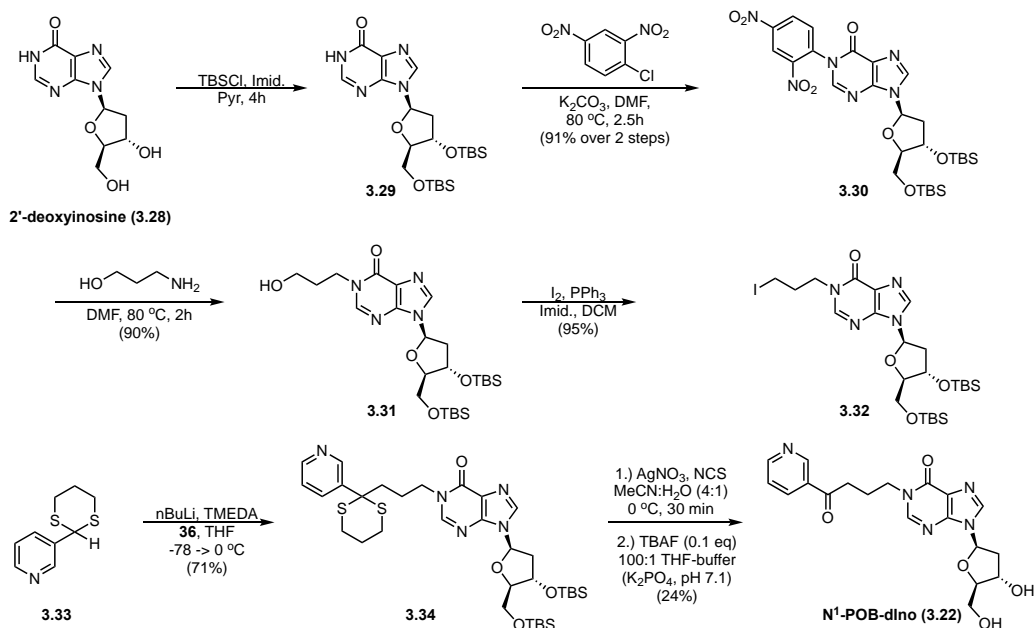
Scheme 3-3: Synthetic route for *N*⁶-PHB-dAdo and *N*⁶-POB-dAdo. dAdo = 2'-deoxyadenosine, TFA = trifluoroacetic acid, NCS = *N*-chlorosuccinimide

Initial attempts to oxidize *N*⁶-PHB-dAdo to *N*⁶-POB-dAdo were unsuccessful. Therefore, we devised a new route that utilized previously prepared compound **3.25** as starting material²³⁹ (**Scheme 3-3B**). After Boc deprotection by TFA, primary amine **3.26** was coupled to 6-chloropurine-2'-deoxyribose. The synthesis was completed by a final oxidative dithiane deprotection²⁷⁰ and HPLC purification resulting in a 17% overall yield. A [pyridine-D₄]-labeled standard was synthesized analogously using [pyridine-D₄]**3.25**,

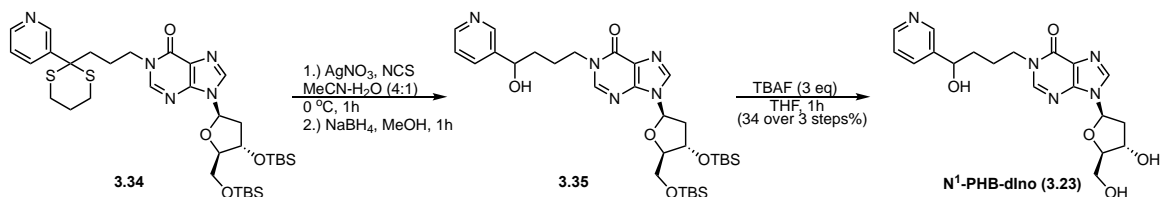
which was prepared in 2 steps²³⁹ from commercially available [pyridine-D₄]3-pyridylcarboxaldehyde.

The synthesis of *N*¹-POB-dIno (**3.22**, Scheme 3-4A) began with protection of both hydroxyl groups of 2'-deoxyinosine with *tert*-butyldimethylsilyl chloride and *N*¹-arylation with 1-chloro-2,4-dinitrobenzene to produce **3.30** as a 1:1 mixture of atropisomers in excellent yield. Compound **3.30** was heated with 3-amino-1-propanol to give **3.31** in good to excellent yield through a transamidation-like mechanism.²⁹² This was converted into iodide **3.32**²⁶⁹ and further coupled to dithiane **3.34** under Seebach's conditions²⁶⁸ with good yields for both steps. Lastly, the keto and hydroxyl groups were deprotected by *N*-chlorosuccinimide oxidation and a pH-neutral, catalytic TBAF procedure,²⁹³ respectively, to produce *N*¹-POB-dIno (**3.22**) in modest yield over these two steps.

A.



B.



Scheme 3-4: Synthetic Scheme for (A) *N*¹-POB-dIno and (B) *N*¹-PHB-dIno. TBSCl = *tert*-butyldimethylsilyl chloride, Imid = imidazole, Pyr = pyridine, DMF = *N,N*-dimethylformamide, DCM = dichloromethane, TMEDA = *N,N,N,N*-tetramethylethylenediamine, TBAF = tetra-*n*-butylammonium fluoride.

N^1 -PHB-dIno (**3.23**, **Scheme 3-4B**) was obtained by reducing the ketone after deprotection of **3.34** and removing the TBS groups with an unbuffered TBAF solution with moderate yield. All final DNA adduct structures were confirmed by one- and two-dimensional NMR experiments (^1H , ^{13}C , HSQC, HMBC) and high-resolution mass spectrometry.

3.3.2 *In vitro* Detection of 2'-Deoxyadenosine-derived POB Adducts

Mixtures of calf thymus DNA, NNKOAc, and porcine liver esterase were incubated at 37 °C and pH 7.4 for 24 h. After DNA hydrolysis and enrichment, samples were analyzed by LC-ESI⁺-MS/MS using [pyridine-D₄] N^6 -POB-dAdo as an internal standard. As shown in **Figure 3-2**, peaks corresponding to both N^6 -POB-dAdo and N^1 -POB-dIno were observed. Based on relative quantitation, N^1 -POB-dIno was 25 times more abundant than N^6 -POB-dAdo. These peaks were not detected in control incubations that either contained esterase alone or lacked NNKOAc. This indicates that both deamination and Dimroth rearrangement occur under these conditions and implicates the N^1 -position as the initial site of alkylation.

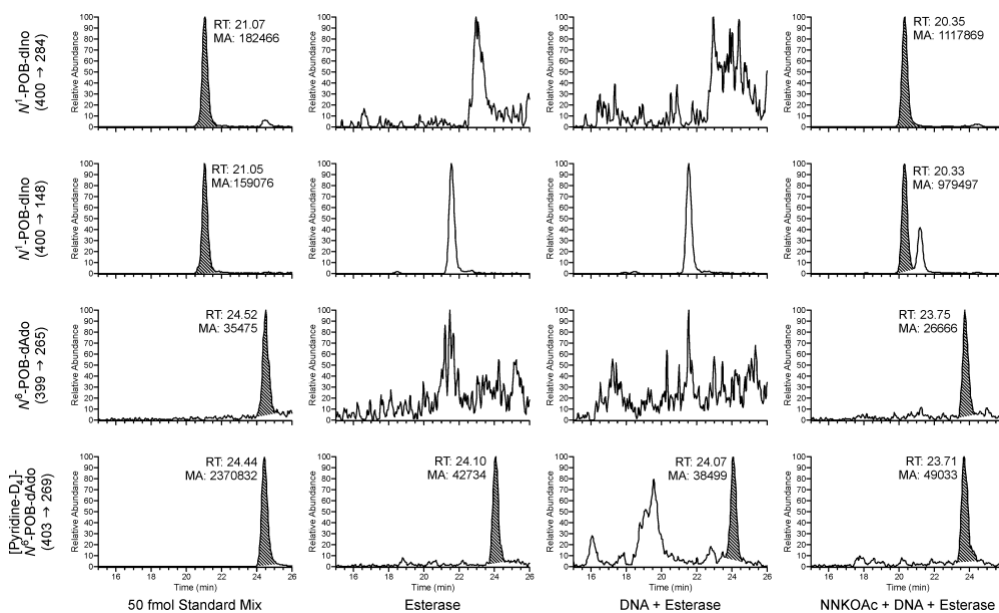


Figure 3-2: Representative LC-ESI⁺-MS/MS chromatograms for *in vitro* formation of N^6 -POB-dAdo and N^1 -POB-dIno. In each case, the top two channels are monitoring separate transitions for the N^1 -POB-dIno adducts (m/z 400 → m/z 284, 148). The bottom two channels are monitoring the N^6 -POB-dAdo adduct (m/z 399 → m/z 265) and its isotopically-labeled internal standard (m/z 403 → m/z 269).

3.3.3 *In vivo* Detection and Quantification of 2'-dAdo Adducts

DNA was extracted from the livers and lungs of rats chronically treated with 5 ppm NNK, (*S*)-NNAL, or (*R*)-NNAL in the drinking water for 50 weeks.²⁰ Hydrolysis and analysis by LC-ESI⁺-MS/MS of these samples were performed as in our *in vitro* experiment. Representative chromatograms for lung samples are shown in **Figure 3-3**.

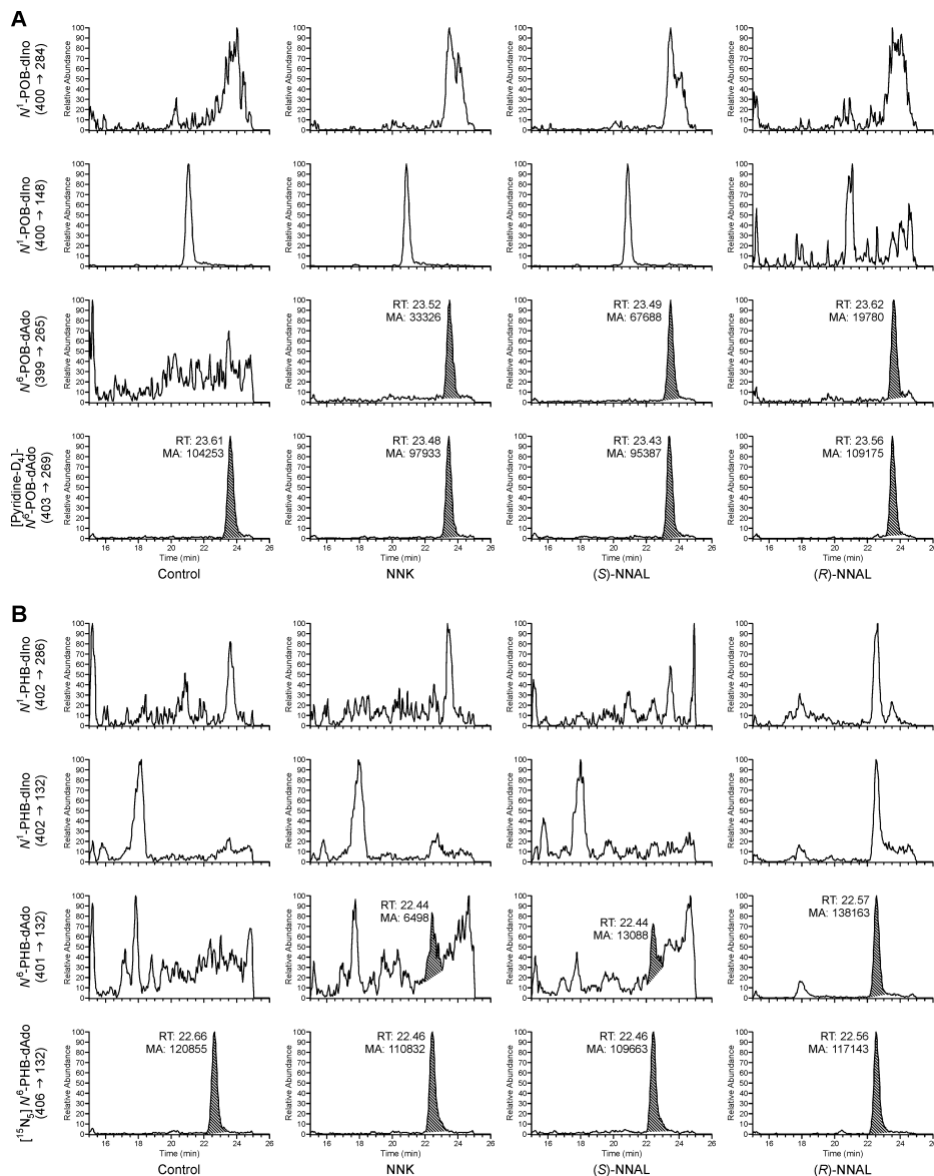


Figure 3-3: Representative chromatograms obtained from the LC-ESI⁺-MS/MS analyses of (A) POB- and (B) PHB-DNA adducts in the lungs of rats chronically treated with 5 ppm NNK for 50 weeks. In each case, the top two channels are monitoring separate transitions for the N^1 -dIno adducts (POB: m/z 400 \rightarrow m/z 284, 148; PHB: m/z 402 \rightarrow m/z 286, 132). The bottom two channels are monitoring the N^6 -dAdo adducts (POB: m/z 399 \rightarrow m/z 265; PHB: m/z 401 \rightarrow m/z 132) and its isotopically-labeled internal standard (POB: m/z 403 \rightarrow m/z 269; PHB: m/z 406 \rightarrow m/z 132).

N^6 -POB-dAdo and N^6 -PHB-dAdo were detected, while both N^1 -POB-dIno and N^1 -PHB-dIno remained unobserved. Though a characteristic peak at 20.9 min, possibly corresponding to N^1 -POB-dIno, was found in the m/z 400 \rightarrow m/z 148 SRM channel, the corresponding peak in the m/z 400 \rightarrow m/z 284 SRM channel was not observed. The 20.9 min peak was detected in all control samples indicating this signal is ubiquitous to the sample matrix. This same trend was also seen for N^1 -PHB-dIno.

In the liver, levels of N^6 -POB-dAdo were higher in the NNK and (S)-NNAL treatment groups (27-32 fmol/mg DNA or 9-10.7 adducts/ 10^9 nts) as compared to the (R)-NNAL group (4 fmol/mg DNA or 1.3 adduct/ 10^9 nts). The trend was reversed for N^6 -PHB-dAdo in that levels were lower in the NNK and (S)-NNAL treatment groups (4-6 fmol/mg DNA or 1-2 adducts/ 10^9 nts) than in the (R)-NNAL group (21-25 fmol/mg DNA or 7-8.3 adducts/ 10^9 nts) (**Figure 3-4**).

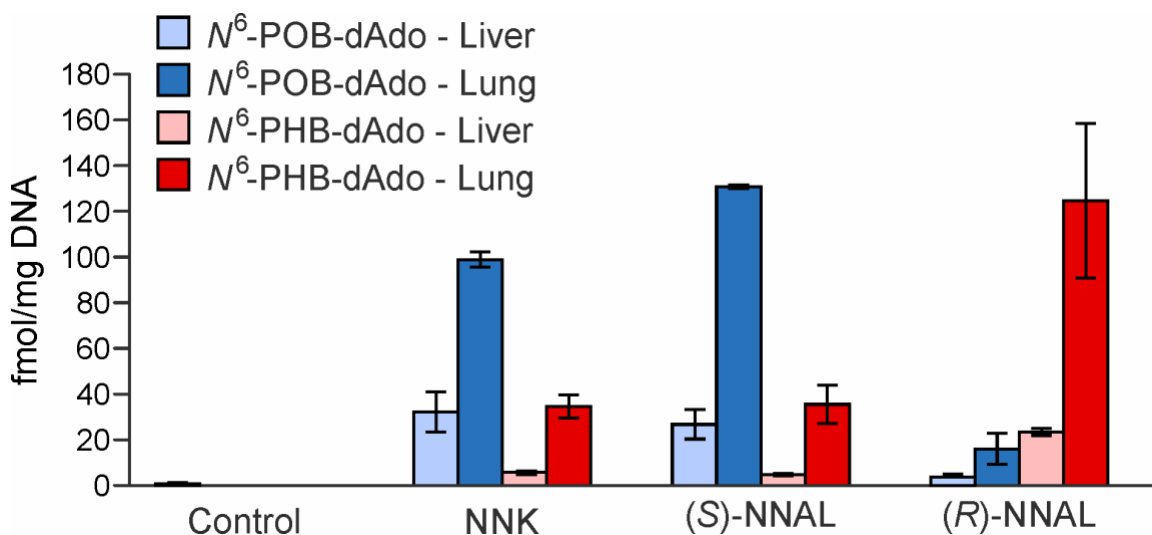


Figure 3-4: Levels of N^6 -POB-dAdo and N^6 -PHB-dAdo in the liver and lung DNA of rats treated with NNK-, (S)-NNAL, and (R)-NNAL at a dose of 5 ppm in their drinking water for 50 weeks. Values are the average of three replicates and error bars denote their standard deviation. POB- and PHB-adducts are represented in blue and red, respectively. Liver and lung tissue are differentiated by light and dark hues, respectively.

Analysis of rat lung DNA revealed the same trend, however, at higher overall levels. N^6 -POB-dAdo was relatively abundant in the NNK and (S)-NNAL groups at 99 fmol/mg DNA (33 adducts/ 10^9 nts) and 130 fmol/mg DNA (43.3 adducts/ 10^9 nts), respectively, while N^6 -PHB-dAdo was relatively high in the (R)-NNAL group at 125 fmol/mg DNA (41.7 adducts/ 10^9 nts). Similar to the liver, N^6 -POB-dAdo was a minor

product after (*R*)-NNAL treatment (16 fmol/mg DNA or 5.3 adducts/10⁹ nts) and *N*⁶-PHB-dAdo was less abundant in both NNK and (*S*)-NNAL treatment groups (35 fmol/mg DNA or 11.7 adducts/10⁹ nts). Control rats given unmodified tap water showed no adduct formation. To evaluate if the lack of dIno adducts was due to insufficient sensitivity, these samples were reanalyzed by a LC-NSI⁺-HRMS/MS method utilizing accurate mass detection. After extensive method optimization, the dIno adducts were still undetectable, while dAdo adducts were easily observed (**Figure 3-5**).

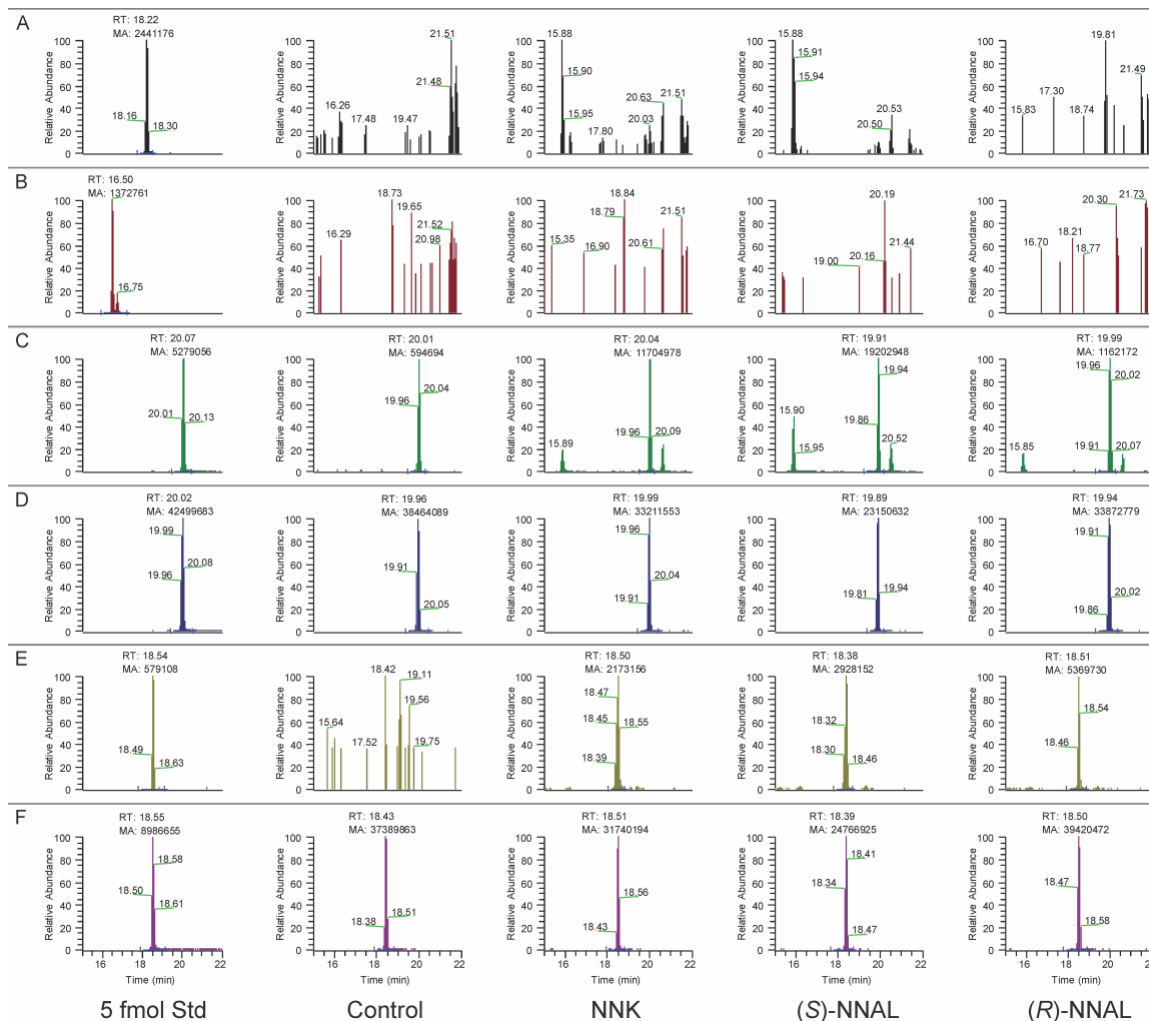


Figure 3-5: Representative chromatograms obtained from the LC-NSI⁺-HRMS/MS analyses of POB- and PHB-DNA adducts in the lungs of rats chronically treated with 5 ppm NNK, (*S*)-NNAL, or (*R*)-NNAL for 50 weeks. Each channel is monitoring the two most abundant product ions from MS²-fragmentation of a particular DNA adduct. Adduct identity and product ions are the following: (A) *N*¹-POB-dIno (400 → 283.1300, 265.1194), (B) *N*¹-PHB-dIno (402 → 286.1296, 268.1191), (C) *N*⁶-POB-dAdo (399 → 283.1300, 265.1194), (D) [D₄]*N*⁶-POB-dAdo (403 → 285.1456, 267.1350), (E) *N*⁶-PHB-dAdo (401 → 287.1550, 269.1445), (F) [¹⁵N₅]*N*⁶-PHB-dAdo (406 → 290.1307, 272.1202).

3.4 Discussion

We describe the first characterization of dAdo base adducts formed in the metabolism of NNK by α -hydroxylation. Synthesis of the standards N^6 -POB-dAdo, N^6 -PHB-dAdo, N^1 -POB-dIno, and N^1 -PHB-dIno as well as stable isotope-labelled analogues allowed us to interrogate their presence and abundance *in vitro* and *in vivo*. Detection of both N^6 -dAdo and N^1 -dIno type adducts *in vitro*, from reactions of NNKOAc with calf thymus DNA, supports our hypothesized mechanism of formation involving either a spontaneous Dimroth rearrangement or deamination, respectively. Likewise, quantitation of the N^6 -dAdo adducts in liver and lung DNA of NNK and NNAL-treated rats supports the occurrence of this mechanism *in vivo*.

Levels of the dAdo adducts in liver and lung of rats treated chronically with NNK or enantiomers of NNAL in their drinking water for 50 weeks are compared to those of some other characterized NNK-DNA adducts⁵⁰ in **Table 3-1**. dAdo adduct levels were relatively low in both tissues, exceeding only those of O^6 -POB-dGuo when measurable. Levels were otherwise considerably lower than the 7-Gua and O^2 -Thd POB- and PHB-DNA adducts. Levels of the dAdo adducts were higher in lung than in liver of the NNK treated rats, consistent with the comparative tissue levels of the other DNA adducts.²⁰ This reflects extensive metabolic activation of NNK and NNAL in rat lung upon treatment with relatively low doses of these carcinogens. Consistent with previous studies, levels of N^6 -POB-dAdo were higher in rats treated with NNK or (*S*)-NNAL than those found in rats treated with (*R*)-NNAL. In comparison, N^6 -PHB-dAdo amounts were highest in lung and liver DNA of (*R*)-NNAL-treated rats. These consistent findings presumably result from the facile conversion of (*S*)-NNAL to NNK *in vivo* and slow conversion of (*R*)-NNAL to NNK as compared to direct metabolic activation by P450s.²¹⁰

In contrast to the results of our *in vitro* studies, in which NNKOAc was reacted with calf thymus DNA, we found no evidence for the presence of either N^1 -dIno adduct in lung and liver DNA of rats treated with NNK or enantiomers of NNAL. This was in spite of the use of a highly sensitive and specific LC-NSI⁺-HRMS/MS method. The accurate mass detection feature of this method, when coupled with nano-spray ionization, guarantees both high specificity and sensitivity in detection of analytes. Even after

rigorous application of this method, the dIno adducts remained undetected, perhaps due to their efficient repair *in vivo*. Since other N^1 -dIno adducts form Hoogsteen base pairs and partially flip outside the DNA helix, it is possible that our POB- and PHB- N^1 -dIno adducts are prime targets for base excision repair or other DNA repair mechanisms.^{193,288,294}

In our preliminary studies of the reaction of NNKOAc with calf thymus DNA, we observed an HPLC peak which decreased relatively rapidly with time, as peaks corresponding to N^6 -POB-dAdo and N^1 -POB-dIno increased (data not shown). We presume that this peak was N^1 -POB-dAdo. Ultimately, the concentration of N^1 -POB-dIno was about 25 times greater than that of N^6 -POB-dAdo in these *in vitro* reactions. This preference is consistent with previous studies where deamination dominated under neutral pH and when the N^1 -alkyl group possessed a nucleophilic oxygen group.²⁸⁰⁻²⁸³ In the case of styrene oxide, the latent alcohol was shown to facilitate the addition-elimination mechanism of deamination,²⁸¹ however, it is unclear how these results translate to the POB- and PHB-adducts. While Dimroth rearrangement is the most plausible explanation for the presence of N^6 -POB-dAdo and N^6 -PHB-dAdo, direct N^6 -alkylation cannot be excluded as there is some evidence for this in reactions of acrolein²⁹⁵ and 1,2,3,4-diepoxybutane²⁹⁶ with DNA.

Synthesis of the adduct standards proceeded as expected with the exception of two major findings. First, the transformation of **3.30** (Scheme 3-4) to N^1 -alkyl structures showed a dependence on steric features. It was our original plan to directly produce **3.34** by using **3.26** (Scheme 3-3 & 3-4) as the nucleophile, but this reaction gave little to no yield. We believe that steric repulsion between the dithiane and TBS-groups blocked the amino group from engaging the C2-position of the nucleoside. Therefore, we simplified the attacking group to 3-amino-1-propanol and obtained good yields of **3.31**, which was further elaborated to the final product. Next, we found TBS-deprotection of **3.34** to be very sensitive to pH. After dithiane removal, unbuffered TBAF removed not only the TBS groups, but also the entire POB moiety, perhaps due to the basicity of fluoride. We surmise that N^1 -POB cleavage occurred via an enolate-ring closure that released dIno and presumably a cyclopropyl byproduct.²⁰³ When recently developed conditions using

catalytic fluoride and neutral pH buffer were applied,²⁹³ selective TBS cleavage was observed. In agreement with the enolate-ring closure hypothesis, unbuffered TBAF could be used to deprotect compound **3.35** with no cleavage of the PHB group.

Table 3-1: Levels of DNA adducts in lung and liver DNA from rats chronically treated with NNK, (*S*)-NNAL, or (*R*)-NNAL (5 ppm in their drinking water) for 50 weeks. Values are the average of three replicates and their standard deviations.

Tissue	Treatment	N⁶-POB-dAdo (fmol/mg DNA)	O⁶-POB-dGuo (fmol/mg DNA)	7-POB-Gua (fmol/mg DNA)	O²-POB-Thd (fmol/mg DNA)	O²-POB-Cyt (fmol/mg DNA)
Liver	NNK	32 ± 9	< LOQ ^a	257 ± 32 ^a	1531 ± 161 ^a	< LOQ
	(<i>S</i>)-NNAL	27 ± 6	< LOQ	356 ± 18	1680 ± 100	< LOQ
	(<i>R</i>)-NNAL	4 ± 1	< LOQ	28 ± 5	130 ± 27	< LOQ
Lung ^b	NNK	99 ± 3	9 ± 2	688 ± 65	4409 ± 320	< LOQ
	(<i>S</i>)-NNAL	130 ± 1	10 ± 5	568 ± 68	3951 ± 328	< LOQ
	(<i>R</i>)-NNAL	16 ± 7	< LOQ	136 ± 10	584 ± 45	< LOQ
		N⁶-PHB-dAdo (fmol/mg DNA)	O⁶-PHB-dGuo (fmol/mg DNA)	7-PHB-Gua (fmol/mg DNA)	O²-PHB-Thd (fmol/mg DNA)	
Liver	NNK	6 ± 1	< LOQ	295 ± 42	658 ± 107	
	(<i>S</i>)-NNAL	5 ± 1	< LOQ	133 ± 15	422 ± 36	
	(<i>R</i>)-NNAL	24 ± 2	< LOQ	436 ± 23	2995 ± 121	
Lung ^b	NNK	35 ± 5	< LOQ	129 ± 34	1259 ± 66	
	(<i>S</i>)-NNAL	36 ± 8	< LOQ	100 ± 25	1152 ± 41	
	(<i>R</i>)-NNAL	125 ± 34	< LOQ	379 ± 19	6291 ± 885	

Though adduct levels were relatively low *in vivo*, they may play a biological role. As discussed earlier, *O*⁶-POB-dGuo is found at very low or undetectable levels *in vivo* (**Table 3-1**); however, this adduct is thought to contribute to tumorigenesis as it is strongly mutagenic in a variety of cell models.¹⁹³ Though efficient repair tempers this mutagenicity *in vivo*, it may increase the persistence of other adducts such as *O*⁶-Me-dGuo, since previous work identified GC to AT transitions as a major NNK-induced mutation.²³² The same study also found moderate levels of AT to GC mutations, perhaps due to the persistence of *N*⁶-dAdo adducts. This is reasonable as the bulky *N*⁶-linkage could block base pairing with Thd. In studies with 1,3-butadiene, particular *N*⁶-dAdo adducts were bypassed by several DNA polymerases and in some cases caused mutations *in vitro*.²⁹⁷ However, in a follow-up study,²⁹⁸ the same adducts were found to be far less mutagenic, possibly due to base-excision repair. In studies with polycyclic aromatic hydrocarbons (PAHs), *N*⁶-dAdo adducts were highly mutagenic, and sometimes tumorigenic, depending on the PAH structure and location on the DNA strand.^{299,300} When adducts significantly distorted the DNA helix, cells were found to halt during DNA replication, possibly alluding to DNA polymerases stalling near the adduct site.²⁹⁹ Together, these findings seem to indicate that effective *N*⁶-dAdo adducts require steric balance; adducts should be large enough to disrupt base pairing, but small enough to evade detection by cellular machinery. It is currently unknown how POB- and PHB-adducts fit into this context and thus requires future study. Along with possible biological effects, *N*⁶-POB-dAdo and *N*⁶-PHB-dAdo have potential as biomarkers. These products directly link to the DNA damaging properties of NNK and NNAL and could be used to study differences between demographic groups.¹⁹² With analytical power continuing to increase, measurement of low levels of DNA adducts in humans is starting to become an achievable feat.³⁰¹

In summary, this work has identified and quantified the first dAdo-derived DNA adducts of NNK and its enantiomers NNAL formed *in vitro* and *in vivo*. We found general support for our proposed adduct formation mechanism by quantifying both *N*¹-POB-dIno and *N*⁶-POB-dAdo *in vitro*. Though *N*¹-dIno type adducts were the major ones formed *in vitro*, they were undetectable *in vivo*. *N*⁶-dAdo adduct levels were relatively

modest *in vivo* when compared to most DNA adducts of NNK and NNAL previously detected. This research allows and encourages future studies on the biological properties of these adducts and their potential utility as specific DNA damage biomarkers.

3.5 Conclusion

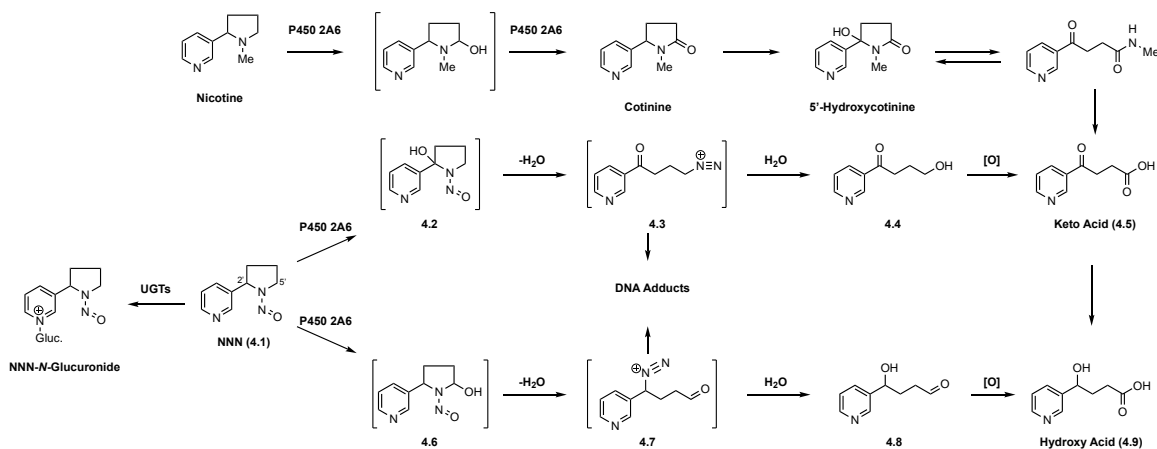
This study identified that NNK and NNAL form two stable dAdo-derived adduct types: N^6 -dAdo and N^1 -dIno. This implicates that dAdo is initially alkylated at the N^1 -position and then undergoes either Dimroth rearrangement or deamination to stabilize its structure. When evaluated *in vitro*, N^6 -POB-dAdo and N^1 -POB-dIno were found with the latter being most abundant. To our surprise, only N^6 -POB-dAdo and N^6 -PHB-dAdo could be measured in NNK- or NNAL-treated rats, implying that the N^1 -dIno adducts are extensively repaired *in vivo*. The two N^6 -dAdo adducts had relatively modest levels and followed the expected tissue and enantiomer trends seen for NNK, (*S*)-NNAL, and (*R*)-NNAL. In the future, the biological consequences of these adducts will be evaluated in hopes of understanding their role in tobacco carcinogenicity.

Chapter 4 Measurement of *N'*-Nitrosornicotine Bioactivation in Humans Using Deuterium-Labeled Analogs

The following chapter describes work that is currently in progress and working towards publication. The study was primarily performed by Erik S. Carlson, whom conducted this research in collaboration with Andrew Goode, Vadim Gurvich, Hanna Vanderloo, Joshua Ikuemonisan, Irina Stepanov, Dorothy Hatsukami, Stephen S. Hecht. This study was supported by the U.S. National Cancer Institute through grant CA-81301. We thank Anshu Jain and Dr. Jing Yang for providing useful advice on performing the hydroxy acid and NNN assays, respectively; Dr. Peter Villalta, Xun Ming, Makenzie Pillsbury, and Yingchun Zhao for assistance in the Analytical Biochemistry Shared Resource (partially supported by National Cancer Institute grant CA-77598); and the Tobacco Research Programs staff for recruiting subjects and collecting the primary samples. The authors also thank Bob Carlson for editorial assistance.

4.1 Introduction

Consistent with all *N'*-nitrosamines (**Section 1.2**), NNN requires metabolism to elicit its carcinogenic effects. The mechanistic details of NNN metabolism were discussed in **Section 1.4.2**. and are reviewed again here. Upon absorption and distribution to various target tissues, NNN is bioactivated through α -hydroxylation by cytochrome P450 2A6 (**Scheme 4-1**). If α -hydroxylation occurs at the 2'-position, species **4.2** is produced which spontaneously ring opens and loses water to deliver diazonium **4.3**. This compound is an excellent electrophile and can either hydrolyze to **4.4** or, if in the presence of DNA, alkylate a nucleobase or the phosphate backbone to form a POB DNA adduct. Likewise, if α -hydroxylation occurs at the 5'-position, a similar cascade of ring opening, water loss, and hydrolysis produces **4.8**; alkylation of DNA produces Py-Py adducts where Py-Py-dIno is the major product observed *in vivo*²⁰⁸. NNN can also be metabolized through non-carcinogenic pathways such as *N*-glucuronidation, tandem denitrosation-oxidation, and *N*-oxidation (**Section 1.4.2**).

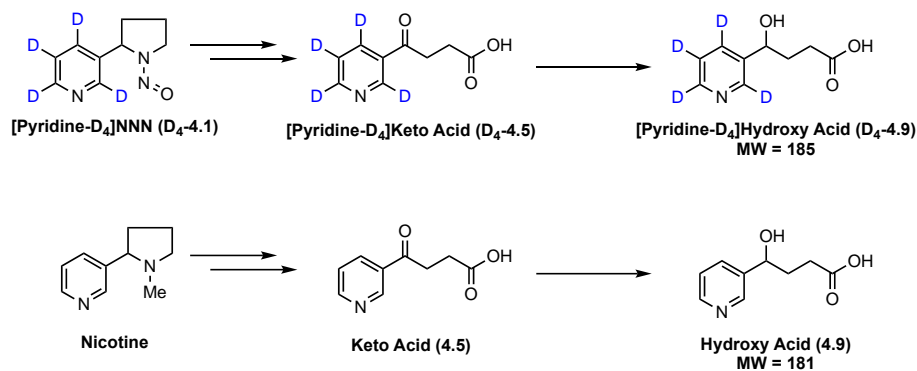


Scheme 4-1: Convergent metabolism of NNN and nicotine *in vivo*

To date, the only human biomarker for NNN is the combination of NNN-glucuronide and unmodified NNN, referred to as total NNN³⁰². However, this accounts for ~1% of the overall dose²⁰⁰ and only truly measures NNN exposure. We hypothesize that individuals who productively activate NNN are at a higher risk for cancer, and thus we would like to develop a biomarker specific to NNN bioactivation. The most direct approach would be measuring known DNA adducts, but past attempts to quantify DNA

adducts in humans have been exceedingly difficult analytical challenges³⁰¹. Instead, measurement of the hydrolysis byproducts **4.4** and **4.8** could be a viable alternative. In rats and patas monkeys, these compounds are excreted in the urine after further oxidation to keto acid **4.5** and hydroxy acid **4.9**, respectively. However, this strategy has been thwarted in humans because nicotine, which is >10,000 fold more abundant in tobacco products, is also metabolized to these compounds through minor pathways^{303–305}. For this reason, it is unclear what fraction of keto acid **4.5** and hydroxy acid **4.9** in the urine is NNN-derived. A past attempt to circumvent this issue was measuring (*S*)-hydroxy acid, since rats almost exclusively metabolize nicotine to (*R*)-hydroxy acid **4.5** and metabolize NNN to a racemic hydroxy acid **4.9**²⁰⁴. Unfortunately, this approach failed in humans because nicotine and NNN were metabolized to identical levels of (*S*)-hydroxy acid **4.9**³⁰⁶.

In this study, we envisioned overcoming the issue of nicotine interference by enriching Swedish Snus, which contains low levels of NNN (0.98 µg/g tobacco)³⁰⁷, with [pyridine-D₄]NNN. Because of this labeling, all [pyridine-D₄]NNN metabolites are distinct from nicotine-derived products by LC-ESI⁺-MS/MS (**Scheme 4-2**). This approach was successfully used in a related study assessing NNK metabolism in cigarette smokers and thus gave us confidence in applying this to NNN²²⁴. To execute this approach, we developed a spray-based method for enriching smokeless tobacco with [pyridine-D₄]NNN and recruited 10 subjects to use the product for 3 days, where individual 24-hour urine samples were collected. After extensive sample work up, urinary levels of [pyridine-D₄]hydroxy acid, [pyridine-D₄]keto acid, and total [pyridine-D₄]NNN were determined. When normalized by total [pyridine-D₄]NNN, this study showed that [pyridine-D₄]hydroxy acid **4.9** is a major metabolite of NNN, providing the first direct evidence of human NNN bioactivation.



Scheme 4-2: Metabolism of [pyridine-D₄]NNN and nicotine. Due to the deuterium-labeling, metabolites are distinguishable by LC-MS analysis.

4.2 Experimental Procedures

Caution: *NNN and [pyridine-D₄]NNN are carcinogenic in animal models and evaluated as Group 1 carcinogens by IARC. These compounds should only be handled in a well-ventilated fume hood while wear proper personal protective equipment.*

4.2.1 Chemicals and Enzymes

[Pyridine-D₄]NNN and [pyridine-D₄]keto acid were purchased from Toronto Research Chemicals (Toronto, ON) and [pyridine-D₄]hydroxy acid, [¹³C₆]4.9, [pyridine-D₄]methyl 4-hexanoyl-4-(3-pyridyl)butanoate and [¹³C₆]methyl 4-hexanoyl-4-(3-pyridyl)butanoate were all synthesized as previously described²²⁴. [¹³C₆]NNN was purchased from Cambridge Isotope Laboratories (Andover, MA). Recombinant β-glucuronidase from *E. coli* was purchased from Sigma Aldrich (St. Louis, MO). Phosphate-buffered saline (PBS) was purchased from Invitrogen (Grand Island, NY). All other chemicals, reagents, and consumable glassware were obtained from Sigma Aldrich or Fisher Scientific (Waltham, MA).

4.2.2 Rat Study

Approval for this study was gained by the University of Minnesota Institutional Animal Care and Use Committee. Three male F-344 rats (Charles River Laboratories) were housed individually in metabolism cages designed to collect urine and feces (20 – 24 °C, 12 h light/dark cycle). After 1 week of acclimation, the rats were administered 1

mL of [pyridine-D₄]NNN solution (1 μM, 1X PBS) by gavage. Rats were put back into their cages and urine was collected for 24 hours. After a week to re-establish baseline urine, rats were similarly treated with 1 mL of NNN solution (1 μM, 1X PBS) and had their urine collected for 24 hours. Each urine sample was assayed and analyzed for [pyridine-D₄]hydroxy acid or hydroxy acid as described in the corresponding section below.

4.2.3 Production of [Pyridine-D₄]NNN-enriched Chewing Tobacco

Prior to clinical study use, the commercially-obtained [pyridine-D₄]NNN was purified under GMP conditions at the FDA-registered Institute of Therapeutics Discovery & Development at the University of Minnesota. Briefly, [pyridine-D₄]NNN was applied to a 2.5-gram RediSep Rf silica gel cartridge (Teledyne, Lincoln, NE) and eluted with 100% EtOAc. Five mL fractions were collected and those containing product were combined and evaporated *in vacuo*. Purity was determined to be 98-102% by HPLC-UV (254 nm) and ¹H-NMR.

In the same facility and under analogous conditions, the purified [pyridine-D₄]NNN was then applied to General Swedish Snus (Swedish Match, Stockholm, Sweden) by a spraying method. Briefly, an aqueous solution of [pyridine-D₄]NNN (4.0 μg/mL) was poured into a 250 mL flask-type sprayer (Sigma Aldrich) equipped with an air compressor (TCP Global) and a HEPA filter (Sigma Aldrich). The [pyridine-D₄]NNN solution was then sprayed at a measured flow rate over a thinly-laid bed of tobacco for the necessary time to enrich the product by 2.0 μg/g wet tobacco. The flow rate was determined by spraying the solution into an empty Erlenmeyer flask for 1 min and measuring the increase in weight; 5 replicates were averaged to obtain the flow rate. Spray time was then calculated based on the accurate solution concentration and flow rate of the apparatus. Once the tobacco was sprayed, the product was thoroughly mixed and packaged into tobacco tins designated for clinical use. To ensure sufficient product enrichment and uniformity, five 30 mg samples were taken for [pyridine-D₄]NNN quantitation by LC-ESI⁺-MS/MS^{307,308}.

4.2.4 Subject Recruitment and Urine Collection

Subjects were recruited by the University of Minnesota Tobacco Research Program after study and urine collection approval by the University of Minnesota Institutional Review Board and the U.S. Food and Drug Administration. Criteria for selection included being older than 18, using smokeless tobacco regularly for at least 1 year, and having appropriate physical and mental health. Recruited subjects were given enough tobacco for 1 tin per day and asked to solely use our product while enrolled in the study. Similar to an analogous study with [pyridine-D₄]NNK²²⁴, subjects were asked to collect their 24-hour urine after a 7-day acclimation period. This sample was brought back the next day to the Tobacco Research Programs clinic at the University of Minnesota. This was repeated for 2 additional days, giving us three 24-hour urine samples per subject. All subject urine was stored at -20 °C.

4.2.5 Analysis of [Pyridine-D₄]hydroxy Acid in Tobacco Users' Urine

Urinary levels of [pyridine-D₄]hydroxy acid (D₄-4.9) were determined as previously described²²⁴. Briefly, 1 – 3 mL of each urine sample was spiked with [¹³C₆]hydroxy acid (5 pg) and treated with excess NaBH₄ under basic conditions. After 2 h, samples were neutralized with 1N HCl and reduced to ~1 mL. These samples were applied to 3 mL pre-conditioned, 200 mg Strata-X cartridges (Phenomenex - Torrance, CA) and eluted with H₂O. The aqueous samples were evaporated to dryness and reconstituted in 3% (v/v) H₂SO₄ in MeOH. Samples were incubated for 2 h at room temperature before neutralization with aqueous NaHCO₃. These samples were then applied to 5 mL, unbuffered ChemElut cartridges (Agilent Technologies – Santa Clara, CA) and extracted with CH₂Cl₂. The organic extracts were reduced to ~0.5 – 1.0 mL by SpeedVac and added to activated BondElut silica cartridges (Agilent Technologies). The cartridges were washed with CH₂Cl₂ and 1:1 CH₂Cl₂/EtOAc before elution with 100% EtOAc. The eluents were evaporated to dryness by SpeedVac and immediately derivatized with hexanoic anhydride. After incubation at 70 °C for 20 min, samples were diluted with 9:1 hexanes/EtOAc and extracted twice with 1N HCl. Aqueous extracts were applied to 60 mg Oasis MCX cartridges (Waters – Milford, MA), rigorously washed with

1N HCl, 4:6 1N HCl/MeOH, and 80:15:4 H₂O/MeOH/NH₄OH, and finally eluted with 30:60:5 H₂O/MeOH/NH₄OH. Eluents were dried by Speedvac, reconstituted in MeCN, and filtered through Spin-X centrifuge tubes before evaporation into 300 μ L LC autosampler vials (Agilent Technologies). Samples were reconstituted in 25 μ L of 5 mM NH₄OAc and analyzed by liquid chromatography-positive electrospray ionization-tandem mass spectrometry (LC-ESI⁺-MS/MS). Prior to analysis, samples were stored frozen at -20 °C.

A previously described LC-ESI⁺-MS/MS analysis was performed with modifications. LC was performed identically except with a 0.5 x 150 mm Zorbax SB-C18 5 μ m column (Agilent Technologies) and 5 mM NH₄OAc and MeCN as mobile phases. MS was performed on a TSQ Quantiva triple quadrupole mass analyzer (Thermo Scientific) with identical selected reaction monitoring (SRM) transitions. The Q1 and Q3 resolutions were set to 0.4 and 0.7 amu, respectively. The collision gas was 1.0 mTorr, the spray voltage was 3500 V, and the ion transfer tube temperature was 250 °C. Lastly, the collision energy was 18 eV for m/z 298 \rightarrow m/z 182 and m/z 300 \rightarrow m/z 184, and 35 eV for m/z 298 \rightarrow m/z 122 and m/z 300 \rightarrow m/z 124.

To measure the urinary level of [pyridine-D₄]keto acid, the same sample work-up protocol was followed except without using NaBH₄. Accordingly, the urinary level of [pyridine-D₄]keto acid was calculated as the difference between [pyridine-D₄]hydroxy acid levels measured in the NaBH₄-containing and NaBH₄-lacking protocols.

4.2.6 Analysis of [Pyridine-D₄]NNN in Tobacco Users' Urine

Urinary levels of [pyridine-D₄]NNN were determined as previously described²²⁴ but with modification. Briefly, 3 mL of subject urine was spiked with [¹³C₆]NNN (5 pg) and incubated with β -glucuronidase (Sigma Aldrich) overnight. The next morning, samples were adjusted to pH 5 with 1M NaOAc buffer and applied to 5 mL Isolute cartridges (Biotage – Charlotte, NC). Cartridges were eluted with CH₂Cl₂ and evaporated to dryness by SpeedVac. Samples were reconstituted with 1 mL 1N HCl and applied to 60 mg Oasis MCX cartridges (Waters). These were extensively washed with 1N HCl, MeOH, and 90:5:5 H₂O/MeOH/NH₄OH before eluting with 35:60:5

H₂O/MeOH/NH₄OH. The eluents were then dried by SpeedVac and reconstituted in 1 mL of CH₂Cl₂. The samples were applied to BondElut cartridges (Agilent Technologies), washed with CH₂Cl₂ and 1:1 CH₂Cl₂/EtOAc, and eluted with 100% EtOAc. Samples were evaporated to dryness, reconstituted in MeOH, and dried down in 300 µL LC vials. Samples were reconstituted in 25 µL of 5 mM NH₄OAc immediately before LC-ESI⁺-MS/MS analysis or stored frozen at -20 °C.

LC was performed with the same column described for [pyridine-D₄]hydroxy acid analysis at 40 °C and a flow rate of 10 µL/min. Using a binary solvent system of 5 mM NH₄OAc and MeOH, the column was eluted with a linear ramp of 30% MeOH to 40% MeOH over 10 min. The column was then brought to 90% MeOH over 1 min, held at 90% MeOH for 1 min, and brought back to 30% MeOH over 1 min. The column was re-equilibrated for 5 min before each injection. MS was performed on a Quantiva triple quadrupole mass analyzer (Thermo Scientific). SRM transitions were m/z 182 → m/z 124 and m/z 182 → m/z 152 for [pyridine-D₄]NNN and m/z 184 → m/z 126 and m/z 184 → m/z 154 for ¹³C₆-NNN. The Q1 and Q3 resolutions were set to 0.4 and 0.7 amu, respectively. The collision gas was 1.0 mTorr, the spray voltage was 3000 V, and the ion transfer tube temperature was 270 °C. Lastly, the collision energy was 11 eV for m/z 182/184 → m/z 152/154 and 21 eV for m/z 182/184 → m/z 124/126.

4.2.7 Cotinine and 3'-Hydroxycotinine

Urinary levels of total cotinine and total 3'-hydroxycotinine (where “total” refers to the sum of the metabolite and its glucuronide) were measured as previously described³⁹. Briefly, 10 µl of urine was diluted with 100 mM NH₄OAc and spiked with [methyl-D₃]cotinine and [methyl-D₃]3'-hydroxycotinine (1 ng each). Each sample was incubated with β-glucuronidase (Sigma Aldrich) overnight and then applied to a pre-conditioned 2 mg Oasis MCX 96-well plate. Each loaded well was washed with 0.5% HCO₂H and MeOH in succession. The analytes were eluted with 2% NH₄OH/MeOH into a clean 96-well plate and evaporated to dryness after acidification. Samples were

reconstituted with 25 μ L of 100 mM $\text{NH}_4\text{OAc}:\text{MeOH}$ just before LC-ESI⁺-MS/MS analysis. Otherwise, samples were stored at -20 °C until analysis.

4.3 Results

4.3.1 Rat Study

To confirm that [pyridine-D₄]NNN does not possess a metabolic isotope effect, we compared urinary total hydroxy acid, the combination of [pyridine-D₄]keto acid and [pyridine-D₄]keto acid, between three rats administered 1 nmol of [pyridine-D₄]NNN or NNN by gavage. Urine was collected from each rat separately and assayed for both [pyridine-D₄]hydroxy acid or hydroxy acid. The average urinary concentrations for each metabolite are shown in **Figure 4-1**. Baseline urine contained no [pyridine-D₄]hydroxy acid and only minor levels hydroxy acid. In comparison, urinary concentrations for [pyridine-D₄]hydroxy acid and hydroxy acid were significantly higher after treatment with the corresponding NNN derivative. Importantly, there was no statistical difference between the levels, indicating that hydroxy acid excretion is not affected by deuterium-labelling.

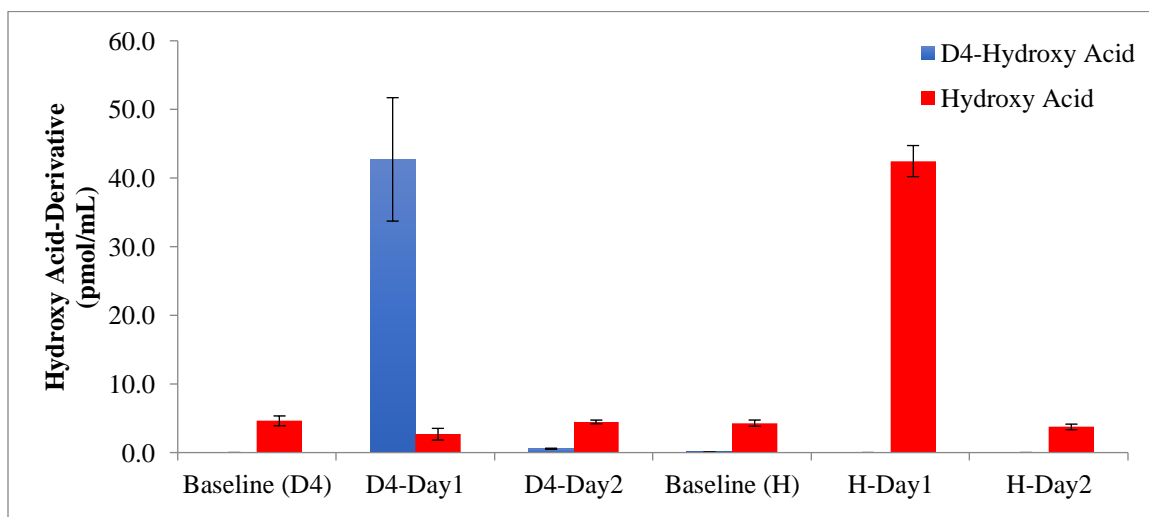


Figure 4-1: Total hydroxy acid levels in the urine of rats treated with 1 nmol of NNN or [pyridine-D₄]NNN. Blue and red bars indicate [pyridine-D₄]hydroxy acid and hydroxy acid concentration, respectively. Values are the average of three replicates and error bars denote their standard deviation.

4.3.2 Tobacco Enrichment and Production

[Pyridine-D₄]NNN was purified to 98 – 102% under GMP conditions and sprayed onto loose Swedish Snus as an aqueous solution. Each lot of tobacco was thoroughly mixed and analyzed for accuracy and uniformity. As shown in **Table 4-1**, the average

enrichment value of [pyridine-D₄]NNN was 0.1927 ± 0.0303 $\mu\text{g/g}$ tobacco, which is in very close agreement to our desired value of 0.2 $\mu\text{g/g}$. Additionally, each lot was uniform as indicated by the relative standard deviations never exceeding 10%. Together, this indicates our spraying method produces smokeless tobacco that is accurately and uniformly enriched with [pyridine-D₄]NNN.

Table 4-1: Accuracy and uniformity of [pyridine-D₄]NNN-enriched tobacco

	Avg. [pyridine-D ₄]NNN ($\mu\text{g/g}$ tobacco)	St. Dev	% CV	% Expected
Lot 001	0.2162	0.00613	2.84	108
Lot 002	0.1585	0.00952	6.01	79.3
Lot 003	0.2033	0.01778	8.75	102
Average	0.1927	0.03025	15.7	96.3

4.3.3 Urinary Analysis of [Pyridine-D₄]hydroxy Acid and [Pyridine-D₄]keto Acid

24-hour urine samples were collected and analyzed from 10 subjects whom were given 1 tin (~30 g) of [pyridine-D₄]NNN-enriched tobacco per day for a 3-day period. As seen in **Figure 4-2**, [pyridine-D₄]hydroxy acid was seen in all subjects' urine except for one, who used less than 5 g of product per day. Similarly, [pyridine-D₄]hydroxy acid was not detected in negative control urine. Representative chromatograms of assayed urine samples are shown in **Figure 4-3**. Daily tobacco use was recorded for each subject and found to directly correlate with their daily [pyridine-D₄]hydroxy acid excretion ($R^2 = 0.817$, **Fig. 4-4**).

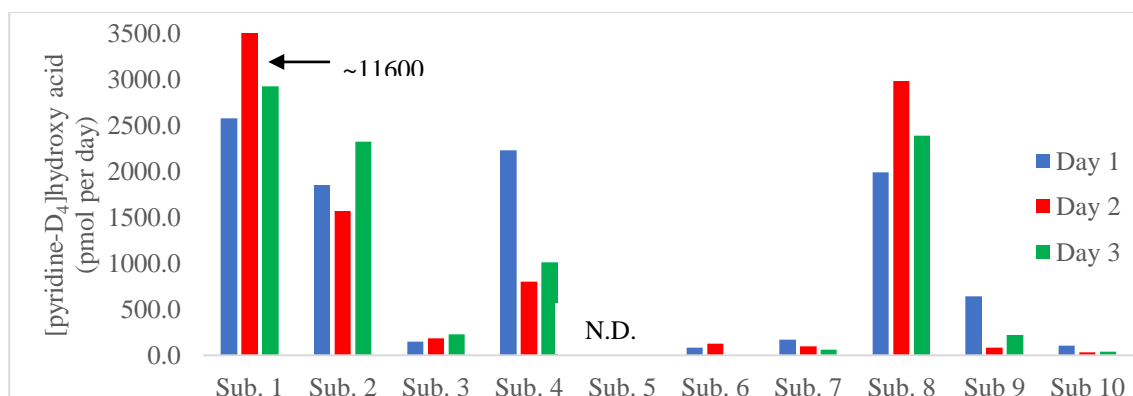


Figure 4-2: Urinary levels of total hydroxy acid for each subject. Blue, red, and green bars denote Day 1, Day 2, and Day 3 urine collections. N.D. – Not detectable

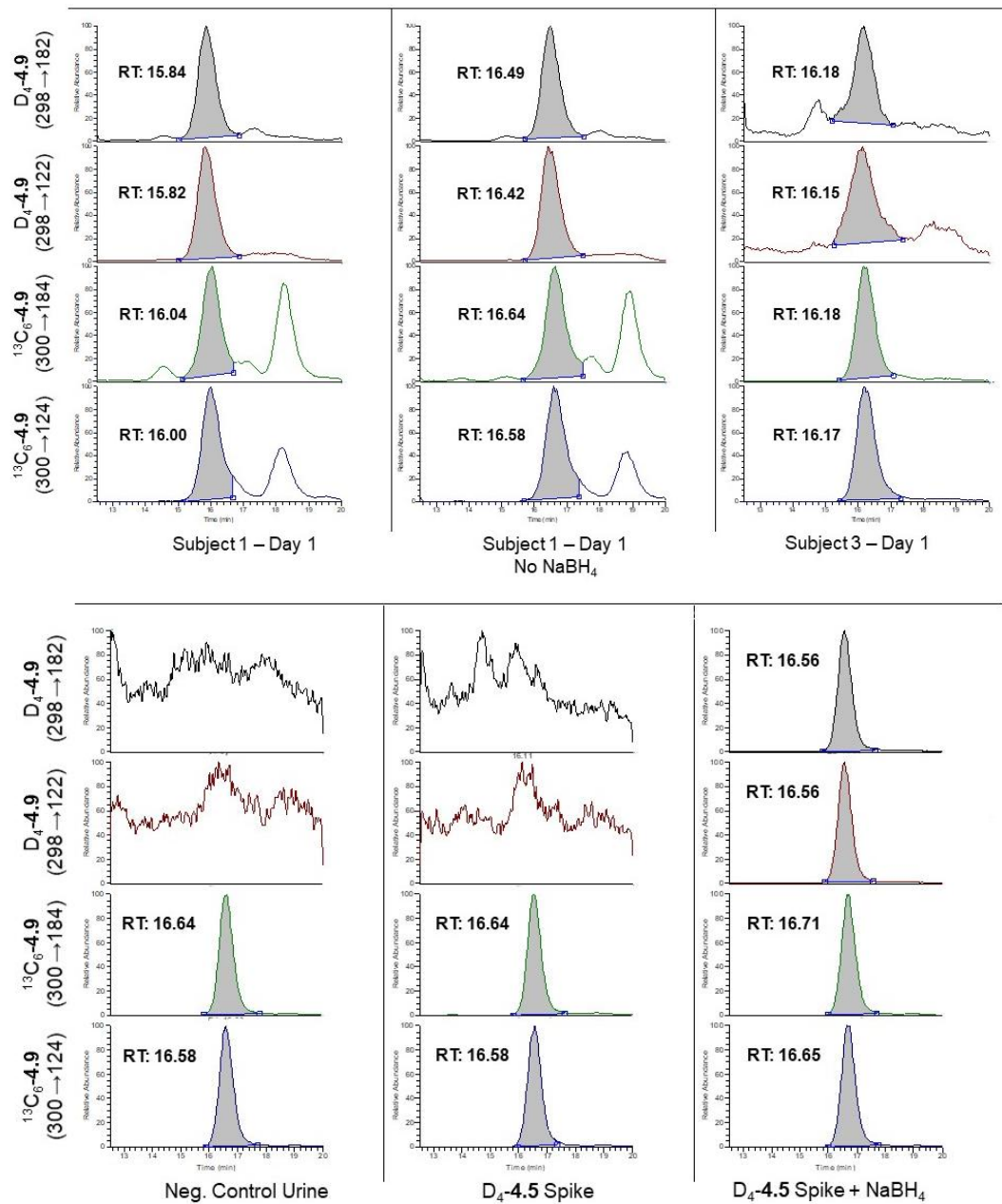


Figure 4-3: Representative LC-ESI⁺-MS/MS chromatograms for total hydroxy acid. In each case, the top two channels are monitoring separate transitions for derivatized [pyridine-D₄]hydroxy acid **4.9** (m/z 298 → m/z 182, 148). The bottom two channels are monitoring derivatized ¹³C₆-**4.9** (m/z 300 → m/z 184, 124).

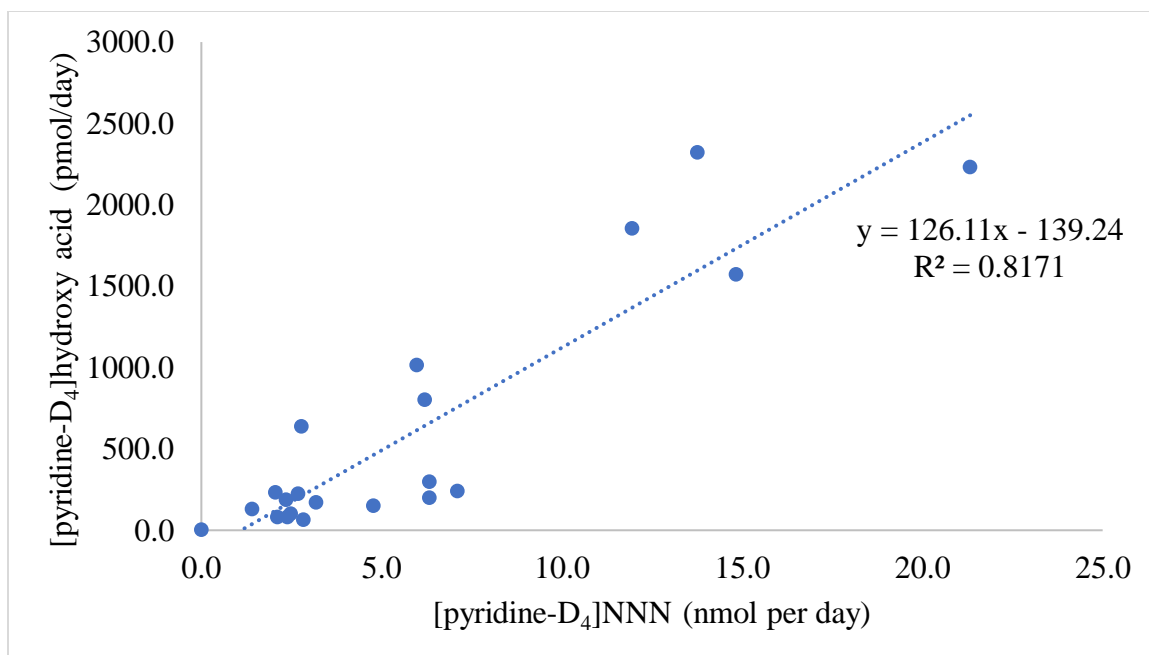


Figure 4-4: Urinary total hydroxy acid plotted against estimated [pyridine-D₄]NNN dose.

To measure [pyridine-D₄]keto acid, we omitted NaBH₄ from the total hydroxy acid assay; all other steps and procedures were analogous to before. The difference in [pyridine-D₄]hydroxy acid levels measured with and without NaBH₄ theoretically equates to [pyridine-D₄]keto acid levels because NaBH₄ reduction normally converts all [pyridine-D₄]keto acid to [pyridine-D₄]hydroxy acid during the assay. Surprisingly, samples with and without reduction were shown to be nearly identical (**Fig 4-5**). Importantly, [pyridine-D₄]keto acid is only quantified with this assay when NaBH₄ is used (**Fig. 4-3**), indicating no artefactual reduction is occurring during the assay. For this reason, we assume that little to no [pyridine-D₄]keto acid is present in any subject's urine.

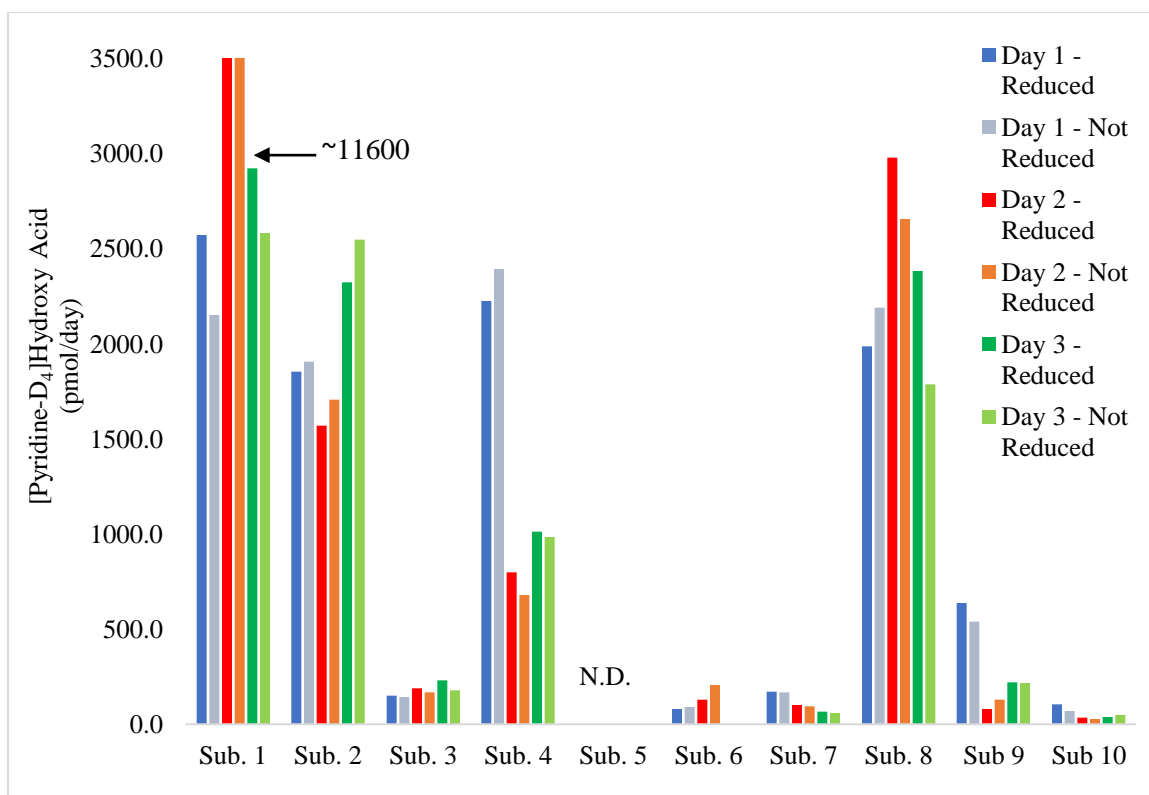


Figure 4-5: Comparison of Total Hydroxy Acid levels with and without NaBH₄ reduction during the assay.

4.3.4 Urinary Analysis of Total [Pyridine-D₄]NNN

Total [pyridine-D₄]NNN, the sum of [pyridine-D₄]NNN-*N*-glucuronide and unmetabolized [pyridine-D₄]NNN, was measured in the same urine samples described for total hydroxy acid analysis. Representative chromatograms for total [pyridine-D₄]NNN analysis are shown in **Fig. 4-6**. In agreement with past reports, total [pyridine-D₄]NNN levels were very low overall and generally did not exceed 90 pmol/day (**Fig. 4-7**). [pyridine-D₄]NNN was found in all subjects except subject 5 who used < 5 g of the product. Likewise, [pyridine-D₄]NNN was not observed in negative control urine (**Fig. 4-6**). In contrast to [pyridine-D₄]hydroxy acid, daily total [pyridine-D₄]NNN levels did not correlate to daily tobacco use (data not shown).

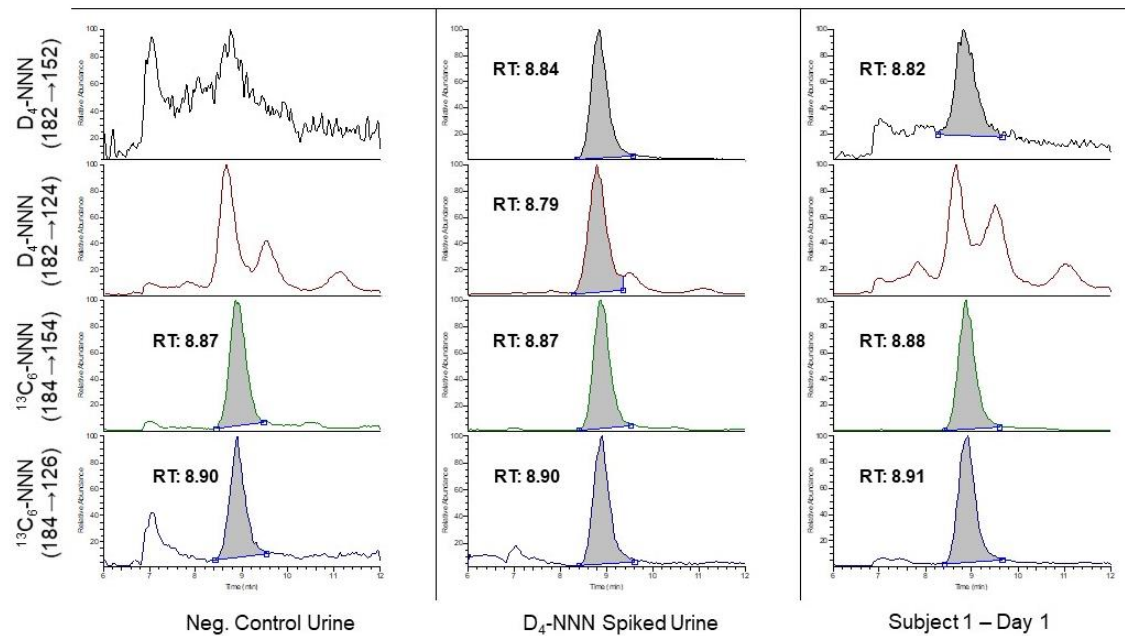


Figure 4-6: Representative LC-ESI⁺-MS/MS chromatograms for total [pyridine-D₄]NNN. In each case, the top two channels are monitoring separate transitions for [pyridine-D₄]NNN (m/z 182 → m/z 152, 124). The bottom two channels are monitoring [¹³C₆]NNN (m/z 184 → m/z 154, 126).

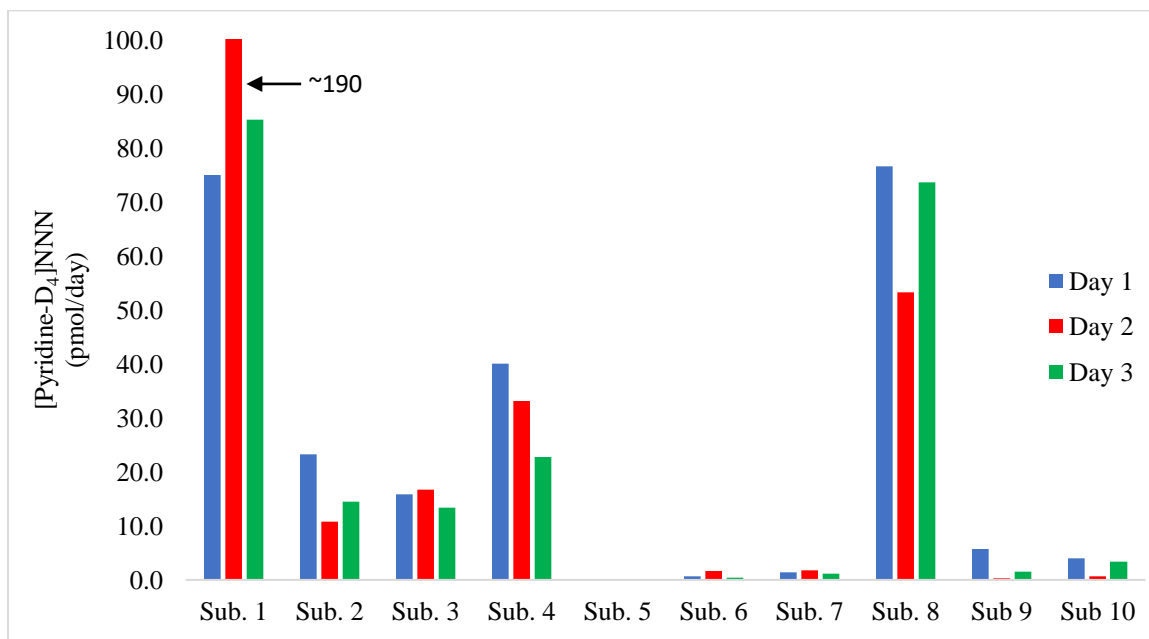


Figure 4-7: Urinary levels of total [pyridine-D₄]NNN in each subject. Blue, red, and green bars denote Day 1, Day 2, and Day 3 urine collections. N.D. – Not detectable

4.3.5 Comparison of “Metabolic Activation Ratio” to “Nicotine Metabolite Ratio”

To compare metabolic activation between subjects, we computed the average ratio of total hydroxy acid to total [pyridine-D₄]NNN over their 3-day study period. In this study, we refer to this value as Metabolic Activation Ratio (MAR). This ratio is informative because total [pyridine-D₄]NNN is an established biomarker for exposure and normalizes total hydroxy acid levels for 24-hour urine volume and [pyridine-D₄]NNN dose. MAR values for all subjects in ascending order are shown in **Fig. 4-8**. While the denoted groups were not statistically significant different ($p > 0.05$), this ratio begins to show a trend of low, medium, and high activators (**Fig. 4-8**). To further evaluate this ratio to metabolic activation proficiency, we measured the Nicotine Metabolite Ratio (total 3'-hydroxycotinine/cotinine), an established biomarker for P450 2A6 activity, for each subject³⁹. When plotted against MAR (**Fig. 4-9**), we observe a strong, positive correlation, potentially indicating that P450 2A6 activity is associated with metabolic activation of NNN.

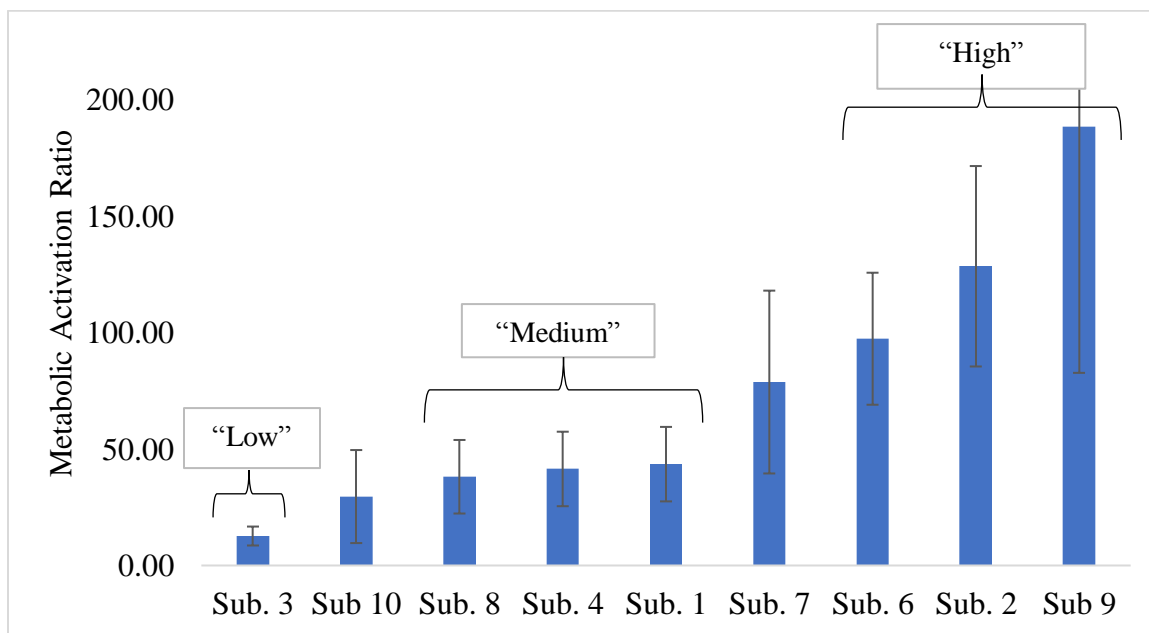


Figure 4-8: Metabolic Activation Ratio (total hydroxy acid/ total [pyridine-D₄]NNN) for each subject arranged in ascending order. Based on error bars, three potential activation groups are denoted: low, medium, and high.

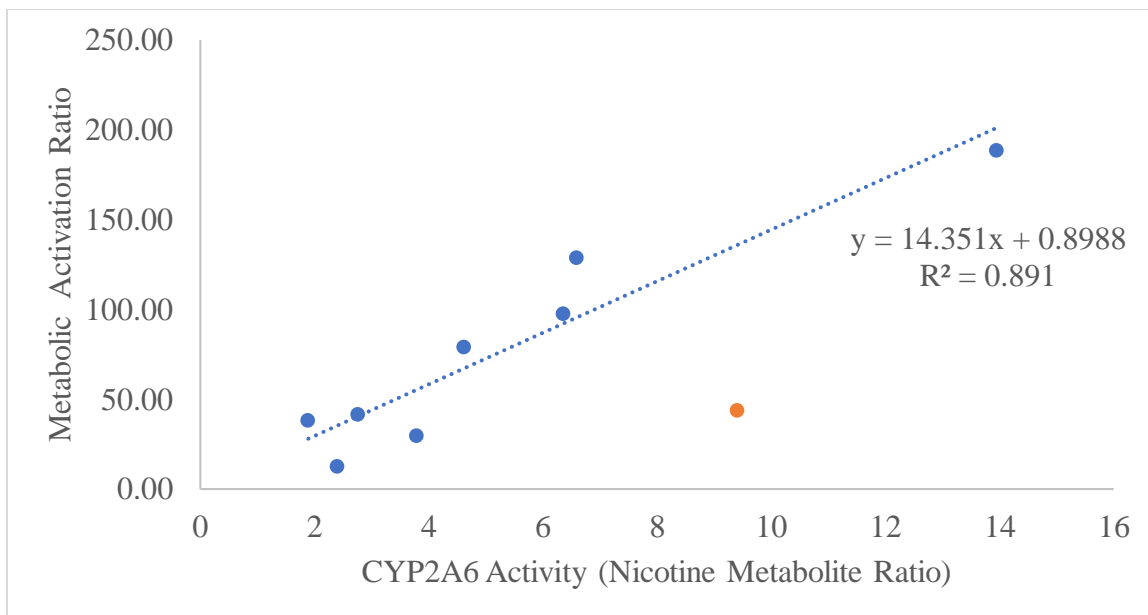


Figure 4-9: Metabolic Activation Ratio plotted against Nicotine Metabolite Ratio, a phenotypic marker for P450 2A6 activity. The red data point is Subject 1 whom had abnormally high Day 2-[pyridine-D₄]hydroxy acid excretion.

4.4 Discussion

In this study, we report the first direct evidence of NNN bioactivation in humans through use of tobacco enriched with [pyridine-D₄]NNN. Past studies have gathered indirect evidence such as HPB-releasing adducts from both hemoglobin³⁰⁹ and oral cells^{192,245}, but neither of these are specific to NNN since they also result from NNK metabolism and potentially unknown sources. As mentioned previously, efforts to measure activation metabolites, keto acid **4.5** and hydroxy acid **4.9**, suffer the same problem, and are also overwhelmed by nicotine metabolism. The use of [pyridine-D₄]NNN circumvented these issues as all metabolites will be 4 mass units higher, allowing selective analysis by LC-ESI⁺-MS/MS.

The measured [pyridine-D₄]hydroxy acid levels varied significantly among subjects. For example, Subjects 1, 2, and 8 had generally higher [pyridine-D₄]hydroxy acid excretion (~1500 – 11,600 pmol/day) than Subjects 3, 6, 7, 9, and 10 (~65 – 640 pmol/day). Levels for each subject also varied over the 3-day period. The most obvious example is Subject 1 who had intraday levels varying from ~2500 – 11,600 pmol/day. These inter-individual and intraday differences could be related to how subjects use the product. In our study, these variations were partially explained by overall tobacco usage. **Figure 4-4** shows a strong, positive correlation between daily [pyridine-D₄]hydroxy acid excretion and the theoretical [pyridine-D₄]NNN dose ingested. Another explanation for the variation is the time and frequency of tobacco use, however, this was outside the scope of this study. Ideally, subjects would use the product uniformly throughout the day. Deviations from this could result in abnormally high [pyridine-D₄]hydroxy acid excretion that is not representative of daily use. Subject 1– Day 2 is a possible example of this may behavior.

In a related study with [pyridine-D₄]NNK-enriched cigarettes (0.225 µg/g tobacco), smokers had urinary [pyridine-D₄]hydroxy acid concentrations of 130 fmol/mL²²⁴. If we assume an average 24-h urine volume of 1400 mL³¹⁰, subjects excreted ~182 pmol/day. This is completely in line with the data found in this study and is even on the lower end of values observed for [pyridine-D₄]NNN; however, this finding could be reflecting the differences in carcinogen uptake from cigarettes and smokeless tobacco

rather than differences in NNK and NNN metabolism. In accordance with the current study, subjects in the [pyridine-D₄]NNK study showed a range of urinary [pyridine-D₄]hydroxy acid concentrations, which implicates inter-individual differences in metabolism.

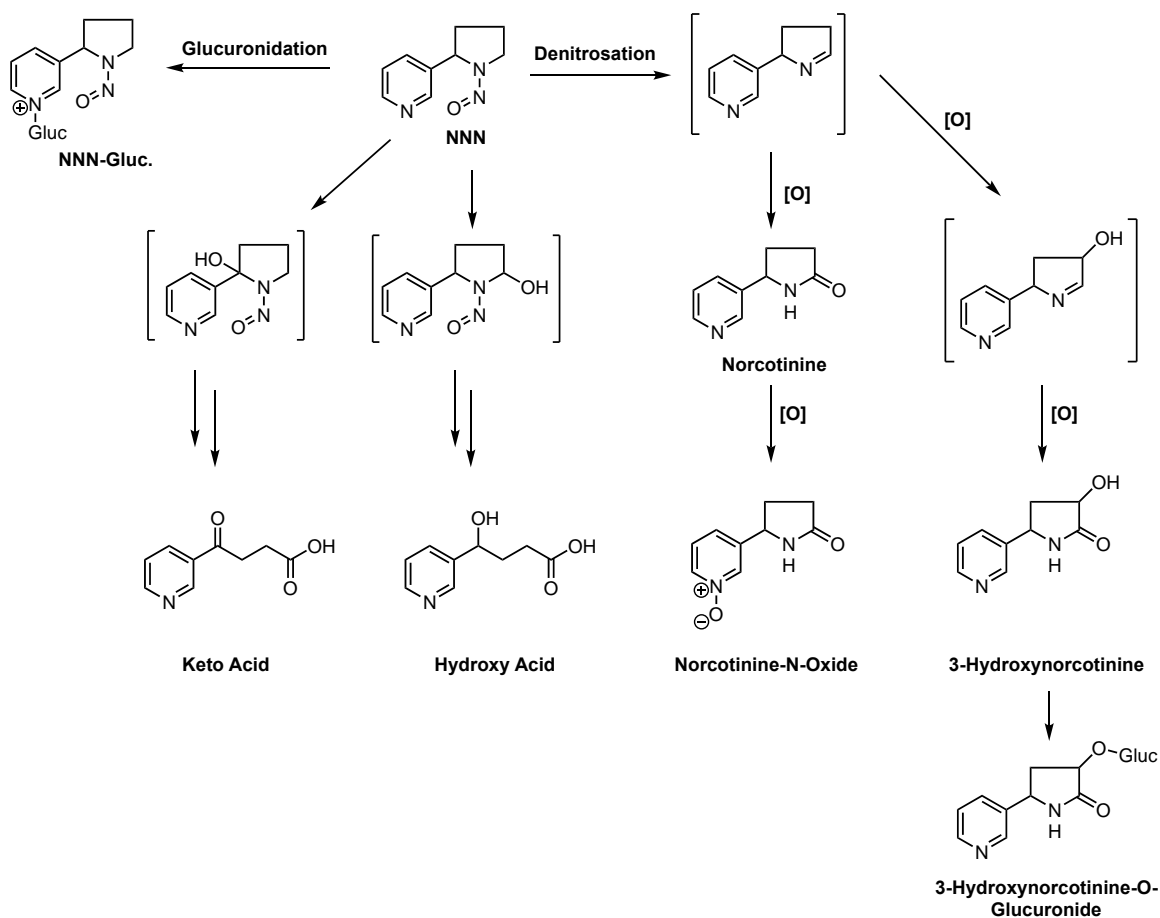
Our study indicates that [pyridine-D₄]keto acid excretion in humans is extremely minor. Levels of urinary [pyridine-D₄]hydroxy acid excretion with and without NaBH₄ reduction were very similar for each subject and each day of collection (**Figure 4-5**). While each sample has only a single analysis, we expect the reduced- and non-reduced samples to not be statistically similar after repeated assays. Currently, our data does not explain the reason for low to non-existent [pyridine-D₄]keto acid level, but two hypotheses are likely. The first is humans preferentially perform 5'-hydroxylation relative to 2'-hydroxylation. This is supported by work conducted by Zarth et al which found Py-Py-dIno, a 5'-specific adduct, to be the major adduct produced in human liver S9 fraction and human liver microsomes²⁰⁸. The other hypothesis is that almost all [pyridine-D₄]keto acid is reduced to [pyridine-D₄]hydroxy acid *in vivo*. This also seems likely because ~85% of keto acid **4.5** resulting from nicotine metabolism was reduced to [pyridine-D₄]hydroxy acid³⁰⁶. Future work is necessary to fully test these hypotheses.

In agreement with past studies, total [pyridine-D₄]NNN was an extremely minor component of urinary metabolites²⁰⁰. The highest levels of [pyridine-D₄]NNN were seen in subjects 1, 4, and 8, who also had high levels of hydroxy acid excretion, and ranged from ~23 – 187 pmol/day. The lowest levels of NNN were found in subjects 6, 7, 9, and 10 (0.42 – 5.7 pmol/day). Likewise, these subjects had comparatively low hydroxy acid excretion, however, this behavior was not always seen. Interestingly, daily [pyridine-D₄]NNN levels did not correlate to daily tobacco use. While this rejects the notion that total [pyridine-D₄]NNN is a good biomarker for tobacco use, total NNN was correlated with risk for esophageal cancer¹⁹⁹ and is inevitably a biomarker its own exposure. For these reasons, we felt it was a suitable measure for normalizing total hydroxy acid. In future studies, it will be worthwhile to explore if using other biomarkers of exposure, such as Total Nicotine Equivalents³⁶, changes the overall bioactivation trends.

Figure 4-8 displays Metabolic Activation Ratio (MAR, total hydroxy acid/ total [pyridine-D₄]NNN) for each subject. A major finding is subjects with high total hydroxy acid levels do not necessarily have high MAR. For example, subjects 1 and 11 have low MAR values (43.5 ± 15.9 and 38.1 ± 15.8) while possessing the highest total hydroxy acid values. In contrast, subject 13 has the highest average MAR value (188.6 ± 105.8) and relatively low total hydroxy acid excretion. It was also noted that almost no MAR values had statistical significance between each other; however, the data does show a trend for three groups of relative activation. Subjects 2, 6, and 9 are tentatively “high activators”, Subjects 1, 4, and 8 are tentatively “medium activators”, and Subject 3 is tentatively a “low activator”. Subjects 7 and 10 appear to be between these groups. The only subjects with statistically significant MAR values, as determined by Student’s t-test, are Subjects 2 and 3 ($p = 0.0373$), indicating that Subject 2 α -hydroxylates NNN to a higher extent than Subject 3, the “low activator”. Additionally, the MAR value of Subject 2 was nearly statistically different than Subject 8 ($p = 0.052$), Subject 1 ($p = 0.068$), and Subject 10 ($p = 0.071$), whom are all tentatively “medium” activators. Together, this suggests a trend towards different activation groups that may gain true statistical significance as more subjects complete the study.

Potentially the most important finding from this study is that MAR is directly correlated to Nicotine Metabolite Ratio, a biomarker for P450 2A6 activity (**Fig. 4-9**). This finding supports the hypothesis that high metabolic activation of NNN is due to increased P450 activity. Additionally, it may indicate that Nicotine Metabolite Ratio, a biomarker measurable without using specialized tobacco, could be a surrogate for NNN bioactivation. Likewise, MAR could potentially be a biomarker for cancer risk because Nicotine Metabolite Ratio was recently linked to prospective lung cancer risk in a large epidemiology study⁴⁰. Either way, the strong association between NNN bioactivation and P450 2A6 activity is an important link for the general scheme of tobacco carcinogenesis. Because P450 2A6 activity is also linked to changes in tobacco use behavior, future work is necessary to fully establish how P450 2A6 activity relates to NNN bioactivation and individual cancer risk.

Another major goal of the overall study is understanding the overall pattern of human NNN metabolism in relation to monkeys and rats. With regards to α -hydroxylation, rats and monkeys excreted 31.8 and 43.8% of their NNN dose as hydroxy acid **4.9**, respectively^{197,204}. In rats, only 1.1% of keto acid administered was converted to hydroxy acid **4.9**, indicating almost all of the hydroxy acid observed is through 5'-hydroxylation²⁰⁴. In monkeys, it is not known how much keto acid is reduced to hydroxy acid, but overall keto acid is only 2.7% of the recovered dose. This indicates that in monkeys either 2'-hydroxylation is a minor pathway or keto acid reduction is a major pathway, which is what we hypothesize for subjects in the current study. It is hard to estimate the dose of [pyridine-D₄]NNN for each subject in this study due to presumed differences in individual tobacco use; however, if we assume 35% of NNN is extracted from tobacco and absorbed by the user³¹¹, [pyridine-D₄]hydroxy acid is ~3 – 47% of the dose. Using the same assumptions, total [pyridine-D₄]NNN is 0.01 – 2% of the dose.



Scheme 4-3: Known metabolism of NNN in patas monkeys.

In addition to activation metabolites, patas monkeys excrete a variety of putative detoxification metabolites such as norcotinine and 3'-hydroxynorcotinine (**Scheme 4-3**). 3'-Hydroxynorcotinine is of particular interest because it is not known to be a nicotine metabolite³⁶. However, a recent report measured this analyte in the urine of both smokers and nicotine patch users, suggesting that 3'-hydroxynorcotinine is a metabolite of nicotine and NNN¹⁹⁸. Current efforts in our lab seek to reanalyze urine from this study to specifically determine the contribution of NNN to the observed 3'-hydroxynorcotinine levels. Ultimately, we hope to use this unique [pyridine-D₄]NNN methodology to fully characterize the metabolic profile of NNN in humans and establish novel biomarkers, or biomarker ratios, for metabolic activation and detoxification and apply them to identifying individuals at high risk for tobacco-related cancer.

4.5 Conclusion

This study established α -hydroxylation as a significant route of human NNN metabolism for the first time. While the overall dose percent is difficult to predict, hydroxy acid was > 12-fold higher than total [pyridine-D₄]NNN, which is usually less than ~1% of the total dose. The ratio of total hydroxy acid to total [pyridine-D₄]NNN has been defined as the Metabolic Activation Ratio (MAR) and was found to vary amongst individuals and showed a trend towards three separate groups of activators. Additionally, the Metabolic Activation Ratio strongly correlated to a phenotypic biomarker for P450 2A6 activity, linking our bioactivation marker to a distinct enzyme with carcinogenic implications. As this study continues and gains more subjects, we hope to more confidently establish this link, stratify subjects into activation groups, and potentially develop this ratio into a biomarker of tobacco-related cancer risk.

Bibliography

- (1) Ravenholt, R. T. (1990) Tobacco's Global Death March. *Popul. Dev. Rev.* 16, 213–240.
- (2) Brandt, A. (2007) *The Cigarette Century: The Rise, Fall, and Deadly Persistence of the Product that Defined America*. Basic Books, New York.
- (3) United States Public Health Service. Office of the Surgeon General, U. S. (1979) *Smoking and Health. A Report of the Surgeon General*. Washington D.C.
- (4) Office on Smoking and Health, United States Department of Health and Human Services, Center for Disease Control and Prevention, National Center for Chronic Disease Prevention and Health Promotion, U. S. (2014) *The Health Consequences of Smoking—50 Years of Progress A Report of the Surgeon General*. Atlanta.
- (5) United States Public Health Service. Office of the Surgeon General, U. S. (1964) *United States Surgeon General Report 1964. Smoking and Health: Report of the Advisory Committee To The Surgeon General of the Public Health Service*. United States Public Health Service. Office of the Surgeon General., Washington D.C., 20402.
- (6) Department of Health and Human Services, Centers for Disease Control and Prevention, Division of Health Interview Statistics, U. S. (2016) *National Health Interview Survey*. Hyattsville, MD.
- (7) Tomar, S., Renner, C. C., Granero, R., Bastos de Andrade, A. C., and Oliveira da Silva, A. L. (2014) Smokeless Tobacco Use in the Region of the Americas, in *Smokeless Tobacco and Public Health: A Global Perspective*, pp 271–299. U.S. Department of Health and Human Services, Centers for Disease Control and Prevention and National Institutes of Health, National Cancer Institute, Bethesda, MD.
- (8) Kumar, A., Bhartiya, D., Mehrotra, R., Sharma, S., Sinha, D. N., Gupta, P. C., Agarwal, N., Singh, H., and Parascandola, M. (2017) *The Poorest of Poor Suffer the*

Greatest Burden From Smokeless Tobacco Use: A Study From 140 Countries. *Nicotine Tob. Res.* 20, 1529–1532.

(9) International Agency for Research on Cancer. (2007) Monographs on the Evaluation of Carcinogenic Risks to Humans - Volume 89. *Smokeless Tob. Some Tobacco-specific N-Nitrosamines*. Lyon.

(10) Jacobs, E. J., Newton, C. C., Carter, B. D., Feskanich, D., Freedman, N. D., Prentice, R. L., and Flanders, W. D. (2015) What proportion of cancer deaths in the contemporary United States is attributable to cigarette smoking? *Ann. Epidemiol.* 25, 179–182.

(11) Islami, F., Goding Sauer, A., Miller, K. D., Siegel, R. L., Fedewa, S. A., Jacobs, E. J., McCullough, M. L., Patel, A. V., Ma, J., Soerjomataram, I., Flanders, W. D., Brawley, O. W., Gapstur, S. M., and Jemal, A. (2018) Proportion and number of cancer cases and deaths attributable to potentially modifiable risk factors in the United States. *CA. Cancer J. Clin.* 68, 31–54.

(12) United States Food and Drug Administration, U. S. (2012) Harmful and potentially harmful constituents in tobacco products and tobacco smoke: Established List.

(13) Taghavi, S., Khashyarmanesh, Z., Moalemzadeh-Haghighi, H., Nassirli, H., Eshraghi, P., Jalali, N., and Hassanzadeh-Khayyat, M. (2012) Nicotine content of domestic cigarettes, imported cigarettes and pipe tobacco in iran. *Addict. Heal.* 4, 28–35.

(14) U.S. Department of Health and Human Services. (2010) How Tobacco Smoke Causes Disease: The Biology and Behavioral Basis for Smoking-Attributable Disease: a report of the Surgeon General. *Surg. Gen. Rep.*

(15) Gray, R., Rajan, A. S., Radcliffe, K. A., Yakehiro, M., and Dani, J. A. (1996) Hippocampal synaptic transmission enhanced by low concentrations of nicotine. *Nature* 383, 713–716.

(16) Schilström, B., Svensson, H. M., Svensson, T. H., and Nomikos, G. G. (1998)

Nicotine and food induced dopamine release in the nucleus accumbens of the rat putative role of $\alpha 7$ nicotinic receptors in the ventral tegmental area. *Neuroscience* 85, 1005–1009.

(17) Mansvelder, H. D., and McGehee, D. S. (2000) Long-term potentiation of excitatory inputs to brain reward areas by nicotine. *Neuron* 27, 349–357.

(18) Grady, S. R., Meinerz, N. M., Cao, J., Reynolds, A. M., Picciotto, M. R., Changeux, J. P., Michael McIntosh, J., Marks, M. J., and Collins, A. C. (2001) Nicotinic agonists stimulate acetylcholine release from mouse interpeduncular nucleus: A function mediated by a different nAChR than dopamine release from striatum. *J. Neurochem.* 76, 258–268.

(19) Grenhoff, J., Aston-Jones, G., and Svensson, T. H. (1986) Nicotinic effects on the firing pattern of midbrain dopamine neurons. *Acta Physiol. Scand.* 128, 351–358.

(20) Balbo, S., Johnson, C. S., Kovi, R. C., James-Yi, S. A., O’Sullivan, M. G., Wang, M., Le, C. T., Khariwala, S. S., Upadhyaya, P., and Hecht, S. S. (2014) Carcinogenicity and DNA adduct formation of 4-(methylnitrosamino)-1-(3-pyridyl)-1-butanone and enantiomers of its metabolite 4-(methylnitrosamino)-1-(3-pyridyl)-1-butanol in F-344 rats. *Carcinogenesis* 35, 2798–2806.

(21) Boyland, E., and Chasseaud, L. F. (1969, January 1) The role of glutathione and glutathione s-transferases in mercapturic acid biosynthesis. *Adv. Enzymol. Relat. Areas Mol. Biol.*

(22) Spanogiannopoulos, P., Bess, E. N., Carmody, R. N., and Turnbaugh, P. J. (2016) The microbial pharmacists within us: A metagenomic view of xenobiotic metabolism. *Nat. Rev. Microbiol.* 14, 273–287.

(23) Koppel, N., Rekdal, V. M., and Balskus, E. P. (2017) Chemical transformation of xenobiotics by the human gut microbiota. *Science* (80-.). 356, 1246–1257.

(24) Guengerich, F. P. (2001) Common and uncommon cytochrome P450 reactions related to metabolism and chemical toxicity. *Chem. Res. Toxicol.* 14, 611–650.

- (25) Edenberg, H. J., and Bosron, W. F. (2017) Alcohol Dehydrogenases, in *Comprehensive Toxicology: Third Edition*.
- (26) Finckh, C., Atalla, A., Nagel, G., Stinner, B., and Maser, E. (2001) Expression and NNK reducing activities of carbonyl reductase and 11beta-hydroxysteroid dehydrogenase type 1 in human lung. *Chem. Biol. Interact.* 130–132, 761–773.
- (27) Satoh, T., and Hosokawa, M. (2002) The mammalian carboxylesterases: from molecules to functions. *Annu. Rev. Pharmacol. Toxicol.* 38, 257–288.
- (28) Jancova, P., Anzenbacher, P., and Anzenbacherova, E. (2010) Phase II drug metabolizing enzymes. *Biomed. Pap.* 154, 103–116.
- (29) Negishi, M., Pedersen, L. G., Petrotchenko, E., Shevtsov, S., Gorokhov, A., Kakuta, Y., and Pedersen, L. C. (2001) Structure and function of sulfotransferases. *Arch. Biochem. Biophys.* 390, 149–157.
- (30) Hein, D. W., Doll, M. A., Rustan, T. D., Gray, K., Feng, Y., Ferguson, R. J., and Grant, D. M. (1993) Metabolic activation and deactivation of arylamine carcinogens by recombinant human NAT1 and polymorphic NAT2 acetyltransferases. *Carcinogenesis* 14, 1633–1638.
- (31) Wang, L., and Weinshilboum, R. (2006) Thiopurine S-methyltransferase pharmacogenetics: Insights, challenges and future directions. *Oncogene* 25, 1629–1638.
- (32) Cummins, I., Dixon, D. P., Freitag-Pohl, S., Skipsey, M., and Edwards, R. (2011) Multiple roles for plant glutathione transferases in xenobiotic detoxification. *Drug Metab. Rev.* 43, 266–80.
- (33) Rowland, A., Miners, J. O., and Mackenzie, P. I. (2013) The UDP-glucuronosyltransferases: Their role in drug metabolism and detoxification. *Int. J. Biochem. Cell Biol.* 45, 1121–1132.
- (34) Ohno, S., and Nakajin, S. (2009) Determination of mRNA expression of human

UDP-glucuronosyltransferases and application for localization in various human tissues by real-time reverse transcriptase-polymerase chain reaction. *Drug Metab. Dispos.* 37, 32–40.

(35) Mulhall, A., de Louvois, J., and Hurley, R. (1983) Chloramphenicol toxicity in neonates: its incidence and prevention. *Br. Med. J. (Clin. Res. Ed)*. 287, 1424–1427.

(36) Hukkanen, J. (2005) Metabolism and Disposition Kinetics of Nicotine. *Pharmacol. Rev.* 57, 79–115.

(37) Guengerich, F. P., Sohl, C. D., and Chowdhury, G. (2011) Multi-step oxidations catalyzed by cytochrome P450 enzymes: Processive vs. distributive kinetics and the issue of carbonyl oxidation in chemical mechanisms. *Arch. Biochem. Biophys.* 507, 126–134.

(38) von Weymarn, L. B., Retzlaff, C., and Murphy, S. E. (2012) CYP2A6- and CYP2A13-catalyzed metabolism of the nicotine Delta5'(1')iminium ion. *J Pharmacol Exp Ther* 343, 307–315.

(39) Tanner, J. A., Novalen, M., Jatlow, P., Huestis, M. A., Murphy, S. E., Kaprio, J., Kankaanpää, A., Galanti, L., Stefan, C., George, T. P., Benowitz, N. L., Lerman, C., and Tyndale, R. F. (2015) Nicotine metabolite ratio (3-Hydroxycotinine/Cotinine) in plasma and urine by different analytical methods and laboratories: Implications for clinical implementation. *Cancer Epidemiol. Biomarkers Prev.* 24, 1239–1246.

(40) Park, S. L., Murphy, S. E., Wilkens, L. R., Stram, D. O., Hecht, S. S., and Le Marchand, L. (2017) Association of CYP2A6 activity with lung cancer incidence in smokers. *PLoS One* 12, 1–10.

(41) Bauer, E., Guo, Z., Ueng, Y.-F., Bell, L. C., Zeldin, D., and Guengerich, F. P. (1995) Oxidation of Benzo[a]pyrene by Recombinant Human Cytochrome P450 Enzymes. *Chem. Res. Toxicol.* 8, 136–142.

(42) Turesky, R. J., and Le Marchand, L. (2011) Metabolism and Biomarkers of

Heterocyclic Aromatic Amines in Molecular Epidemiology Studies: Lessons Learned from Aromatic Amines. *Chem. Res. Toxicol.* 24, 1169–1214.

(43) Sinha, R. P., and Häder, D. P. (2002) UV-induced DNA damage and repair: A review. *Photochem. Photobiol. Sci.* 1, 225–236.

(44) Rastogi, R. P., Richa, Kumar, A., Tyagi, M. B., and Sinha, R. P. (2010) Molecular mechanisms of ultraviolet radiation-induced DNA damage and repair. *J. Nucleic Acids* 2010, 592980.

(45) Klaunig, J. E., Kamendulis, L. M., and Hocevar, B. A. (2010) Oxidative stress and oxidative damage in carcinogenesis. *Toxicol. Pathol.* 38, 96–109.

(46) Cooke, M. S., Evans, M. D., Dizdaroglu, M., and Lunec, J. (2003) Oxidative DNA damage: mechanisms, mutation, and disease. *FASEB J.* 17, 1195–1214.

(47) Fu, D., Calvo, J. A., and Samson, L. D. (2012) Balancing repair and tolerance of DNA damage caused by alkylating agents. *Nat. Rev. Cancer* 12, 104–120.

(48) Noll, D. M., McGregor Mason, T., and Miller, P. S. (2006) Formation and repair of interstrand cross-links in DNA. *Chem. Rev.* 106, 277–301.

(49) Stingele, J., and Jentsch, S. (2015) DNA-protein crosslink repair. *Nat. Rev. Mol. Cell Biol.* 16, 455–460.

(50) Ma, B., Villalta, P. W., Zarth, A. T., Kotandeniya, D., Upadhyaya, P., Stepanov, I., and Hecht, S. S. (2015) Comprehensive high-resolution mass spectrometric analysis of DNA phosphate adducts formed by the tobacco-specific lung carcinogen 4-(methylnitrosamino)-1-(3-pyridyl)-1-butanone. *Chem. Res. Toxicol.* 28, 2151–2159.

(51) Ma, B., Zarth, A. T., Carlson, E. S., Villalta, P. W., Upadhyaya, P., Stepanov, I., and Hecht, S. S. (2018) Identification of more than one hundred structurally unique DNA-phosphate adducts formed during rat lung carcinogenesis by the tobacco-specific nitrosamine 4-(methylnitrosamino)-1-(3-pyridyl)-1-butanone. *Carcinogenesis* 39, 232–

241.

(52) Wu, J., Wang, P., and Wang, Y. (2018) Cytotoxic and mutagenic properties of alkyl phosphotriester lesions in *Escherichia coli* cells. *Nucleic Acids Res.* *46*, 4013–4021.

(53) Garrett, E. R., and Mehta, P. (1972) Solvolysis of adenine nucleosides. I. Effects of sugars and adenine substituents on acid solvolyses. *J. Am. Chem. Soc.* *2219*, 8532–8541.

(54) Lindahl, T., and Andersson, A. (1972) Rate of chain breakage at apurinic sites in double-stranded deoxyribonucleic acid. *Biochemistry* *11*, 3618–3623.

(55) Dutta, S., Chowdhury, G., and Gates, K. S. (2007) Interstrand Cross-Links Generated by Abasic Sites in Duplex DNA. *J. Am. Chem. Soc.* *129*, 1852–1853.

(56) Kim, Y.-J., and Wilson, D. M. (2012) Overview of Base Excision Repair Biochemistry. *Curr. Mol. Pharmacol.* *5*, 3–13.

(57) Slupphaug, G., Mol, C. D., Kavli, B., Arvai, A. S., Krokan, H. E., and Tainer, J. A. (1996) A nucleotide-flipping mechanism from the structure of human uracil–DNA glycosylase bound to DNA. *Nature* *384*, 87–92.

(58) Lau, A. Y., Schärer, O. D., Samson, L., Verdine, G. L., and Ellenberger, T. (1998) Crystal structure of a human alkylbase-DNA repair enzyme complexed to DNA: Mechanisms for nucleotide flipping and base excision. *Cell* *95*, 249–258.

(59) Mullins, E. A., Shi, R., Parsons, Z. D., Yuen, P. K., David, S. S., Igarashi, Y., and Eichman, B. F. (2015) The DNA glycosylase AlkD uses a non-base-flipping mechanism to excise bulky lesions. *Nature* *527*, 1–5.

(60) Frosina, G., Fortini, P., Rossi, O., Carrozzino, F., Raspaglio, G., Cox, L. S., Lane, D. P., Abbondandolo, A., and Dogliotti, E. (1996) Two Pathways for Base Excision Repair in Mammalian Cells. *J. Biol. Chem.* *271*, 9573–9578.

(61) O'Connor, T. R., and Laval, J. (1989) Physical association of the 2,6-diamino-4-

hydroxy-5N-formamidopyrimidine-DNA glycosylase of *Escherichia coli* and an activity nicking DNA at apurinic/apyrimidinic sites. *Proc. Natl. Acad. Sci.* 86, 5222–5226.

(62) Boyce, R. P., and Howard-Flanders, P. (1964) Release of ultraviolet light-induced thymine dimers from DNA in *E. coli* K-12. *Proc. Natl. Acad. Sci.* 51, 293–300.

(63) Schärer, O. D. (2013) Nucleotide excision repair in eukaryotes. *Cold Spring Harb. Perspect. Biol.* 5, a012609.

(64) Pegg, A. E. (2011) Multifaceted roles of alkyltransferase and related proteins in DNA repair, DNA damage, resistance to chemotherapy, and research tools. *Chem. Res. Toxicol.* 24, 618–639.

(65) Daniels, D. S., Woo, T. T., Luu, K. X., Noll, D. M., Clarke, N. D., Pegg, A. E., and Tainer, J. A. (2004) DNA binding and nucleotide flipping by the human DNA repair protein AGT. *Nat. Struct. Mol. Biol.* 11, 714.

(66) Falnes, P. Ø., Johansen, R. F., and Seeberg, E. (2002) AlkB-mediated oxidative demethylation reverses DNA damage in *Escherichia coli*. *Nature* 419, 178–182.

(67) Zaidi, N. H., Pretlow, T. P., O’riordan, M. A., Dumenco, L. L., Allay, E., and Gerson, S. L. (1995) Transgenic expression of human mgmt protects against azoxymethane-induced aberrant crypt foci and g to a mutations in the k-ras oncogene of mouse colon. *Carcinogenesis* 16, 451–456.

(68) Kitange, G. J., Carlson, B. L., Schroeder, M. A., Grogan, P. T., Lamont, J. D., Decker, P. A., Wu, W., James, C. D., and Sarkaria, J. N. (2009) Induction of MGMT expression is associated with temozolomide resistance in glioblastoma xenografts. *Neuro. Oncol.* 11, 281–291.

(69) Fedeles, B. I., Singh, V., Delaney, J. C., Li, D., and Essigmann, J. M. (2015) The AlkB family of Fe(II)/ α -ketoglutarate-dependent dioxygenases: Repairing nucleic acid alkylation damage and beyond. *J. Biol. Chem.* 290, 20734–20742.

- (70) Zdzalik, D., Domańska, A., Prorok, P., Kosicki, K., van den Born, E., Falnes, P. Ø., Rizzo, C. J., Guengerich, F. P., and Tudek, B. (2015) Differential repair of etheno-DNA adducts by bacterial and human AlkB proteins. *DNA Repair (Amst)*. 30, 1–10.
- (71) Barnes, J. M., and Magee, P. N. (1954) Some toxic properties of dimethylnitrosamine. *Br. J. Ind. Med.* 11, 167–74.
- (72) Magee, P. N., and Barnes, J. M. (1956) The production of malignant primary hepatic tumours in the rat by feeding dimethylnitrosamine. *Br. J. Cancer* 10, 114–122.
- (73) Preussmann, R., Stewart, B. W. (1984) N-Nitroso Carcinogens, in *Chemical Carcinogens* (Searle, C. E., Ed.) 2nd ed., pp 643–828. American Chemical Society, Washington D.C.
- (74) Greenblatt, M., and Lijinsky, W. (1972) Failure to induce tumors in swiss mice after concurrent administration of amino acids and sodium nitrite. *J. Natl. Cancer Inst.* 48, 1389–1392.
- (75) Schoental, R. (1960) Carcinogenic action of diazomethane and of nitroso-N-methyl urethane. *Nature* 188, 420–421.
- (76) Schoental, R. (1966) Carcinogenic activity of N-methyl-N-nitroso-N'-nitroguanidine. *Nature* 209, 726–727.
- (77) IARC. (1972) Some inorganic substances, chlorinated hydrocarbons, aromatic amines, N-nitroso compounds, and natural products. *IARC Monogr. Eval. Carcinog. Risks to Humans* 1, 1–184.
- (78) IARC. (1978) Some N-Nitroso Compounds. *IARC Monogr. Eval. Carcinog. Risks to Humans* 1–350.
- (79) Birney, D. M. (2004) Nitrosation of amides involves a pseudopericyclic 1,3-sigmatropic rearrangement. *Org. Lett.* 6, 851–854.

- (80) Leach, S. A., Thompson, M., and Hill, M. (1987) Bacterially catalysed N-nitrosation reactions and their relative importance in the human stomach. *Carcinogenesis* 8, 1907–1912.
- (81) Calmels, S., Ohshima, H., Vincent, P., Gounot, A. M., and Bartsch, H. (1985) Screening of microorganisms for nitrosation catalysis at pH 7 and kinetic studies on nitrosamine formation from secondary amines by *E. coli* strains. *Carcinogenesis* 6, 911–915.
- (82) Ng, T. L., Rohac, R., Mitchell, A. J., Boal, A. K., and Balskus, E. P. (2019) An N-nitrosating metalloenzyme constructs the pharmacophore of streptozotocin. *Nature* 566, 94–99.
- (83) Smith, P. A. S., and Loepky, R. N. (1967) Nitrosative Cleavage of Tertiary Amines. *J. Am. Chem. Soc.* 89, 1147–1157.
- (84) Hecht, S. S., Chen, C. B., Hirota, N., Ornaf, R. M., Tso, T. C., and Hoffmann, D. (1978) Tobacco-specific nitrosamines: formation from nicotine in vitro and during tobacco curing and carcinogenicity in strain A mice. *J. Natl. Cancer Inst.* 60, 819–824.
- (85) Hecht, S. S., Chen, C. B., Ornaf, R. M., Jacobs, E., Adams, J. D., and Hoffmann, D. (1978) Reaction of nicotine and sodium nitrite: Formation of nitrosamines and fragmentation of the pyrrolidine ring. *J. Org. Chem.* 43, 72–76.
- (86) Fridman, A. L., Mukhametshin, F. M., and Novikov, S. S. (1971) Advances in the chemistry of Aliphatic-N-nitrosamines. *Russ. Chem. Rev.* 40, 34–50.
- (87) Klement, U., and Schmidpeter, A. (1968) Structure of dimethylnitrosaminecopper(II) chloride. *Angew. Chemie Int. Ed. English* 7, 470.
- (88) Seebach, D., and Enders, D. (1972) C-C-Bond formation in the α -position to nitrogen in secondary amines. Lithiodimethylnitrosamine. *Angew. Chemie Int. Ed. English* 11, 301–302.

- (89) Seebach, D., and Enders, D. (1975) Umpolung of amine reactivity. Nucleophilic α -(secondary amino)-alkylation via metalated nitrosamines. *Angew. Chemie Int. Ed. English* 14, 15–32.
- (90) Fischer, E. (1875) Ueber die hydrazinverbindungen der fettreihe. *Chem. Ber.* 8, 1587–1590.
- (91) Hanna, C., and Schueler, F. W. (1952) The reaction of disubstituted nitrosamines with lithium aluminum hydride. *J. Am. Chem. Soc.* 74, 3693–3694.
- (92) Paal, C., and Yao, W.-N. (1930) Über die katalytische Reduktion einiger Nitrosamine. *Berichte der Dtsch. Chem. Gesellschaft (A B Ser.)* 63, 57–66.
- (93) Emmons, W. D. (1954) Peroxytrifluoroacetic acid. I. The oxidation of nitrosamines to nitramines. *J. Am. Chem. Soc.* 76, 3468–3470.
- (94) Chow, Y. L. (1979) Chemistry of N-nitrosamides and related N-nitrosamino acids, in *N-Nitrosamines*, pp 13–37. American Chemical Society, Washington D.C.
- (95) White, E. H. (1955) The chemistry of the N-alkyl-N-nitrosoamides. II. A new method for the deamination of aliphatic amines. *J. Am. Chem. Soc.* 77, 6011–6014.
- (96) White, E. H. (1955) The chemistry of the N-alkyl-N-nitrosoamides. III. Mechanism of the nitrogen elimination reaction. *J. Am. Chem. Soc.* 77, 6014–6022.
- (97) White, E. H., Field, K. W., Hendrickson, W. H., Dzadzic, P., Roswell, D. F., Paik, S., and Mullen, P. W. (1992) Inert-molecule-separated ion pairs. Stereochemical, IR, and product studies. *J. Am. Chem. Soc.* 114, 8023–8031.
- (98) Darbeau, R. W., White, E. H., Song, F., Darbeau, N. R., and Chou, J. (1999) A study of essentially free carbocations derived via diazonium and oxo diazonium ions in the liquid phase. *J. Org. Chem.* 64, 5966–5978.
- (99) White, E. H., Darbeau, R. W., Chen, Y., Chen, S., and Chen, D. (2002) A new look

at the Friedel–Crafts alkylation reaction. *J. Org. Chem.* 61, 7986–7987.

(100) Darbeau, R. W., and White, E. H. (2002) The direct alkylation of π -rich, acid-sensitive heterocyclic compounds via essentially free carbocations. *J. Org. Chem.* 62, 8091–8094.

(101) Elespuru, R. K. (1978) Deuterium isotope effects in mutagenesis by nitroso compounds. *Mutat. Res. Mutagen. Relat. Subj.* 54, 265–270.

(102) Charnley, G., and Archer, M. C. (1977) Deuterium isotope effect in the activation of nitrosomorpholine into a bacterial mutagen. *Mutat. Res.* 46, 265–268.

(103) Hecht, S. S., and Young, R. (1981) Metabolic α -hydroxylation of N-nitrosomorpholine and 3,3,5,5-tetradeutero-N-nitrosomorpholine in the F344 rat. *Cancer Res.* 41, 5039–5043.

(104) Chu, C., and Magee, P. N. (1981) Metabolic fate of nitrosoproline in the rat. *Cancer Res.* 41, 3653–3657.

(105) Druckrey, H., and Preussmann, R. (1962) Zur Entstehung carcinogener Nitrosamine am Beispiel des Tabakrauchs. *Naturwissenschaften* 49, 498.

(106) Ender, F., Havre, G., Helgebostad, A., Koppang, N., Madsen, R., and Ceh, L. (1964) Isolation and identification of a hepatotoxic factor in herring meal produced from sodium nitrite preserved herring. *Naturwissenschaften* 51, 637–638.

(107) Hotchkiss, J. H. (1989) Preformed N-nitroso compounds in foods and beverages. *Cancer Surv.* 8, 295–321.

(108) Hotchkiss, J. H., Helsler, M. A., Maragos, C. M., and Weng, Y. M. (1992) Nitrate, nitrite, and N-nitroso compounds - food safety and biological implications. *ACS Symp. Ser.* 484, 400–418.

(109) Rounbehler, D., Krull, I., Goff, E., Mills, K., Morrison, J., Edwards, G., Fine, D.,

- Fajen, J., Carson, G., and Reinhold, V. (1979) Exposure to N-nitrosodimethylamine in a leather tannery. *Food Cosmet. Toxicol.* 17, 487–491.
- (110) Fajen, J. M., Carson, G. A., Rounbehler, D. P., Fan, T. Y., Vita, R., Goff, U. E., Wolf, M. H., Edwards, G. S., Fine, D. H., Reinhold, V., and Biemann, K. (1979) N-nitrosamines in the rubber and tire industry. *Science* (80-). 205, 1262–1264.
- (111) Fan, T., Morrison, J., Rounbehler, D., Ross, R., Fine, D., Miles, W., and Sen, N. (1977) N-Nitrosodiethanolamine in synthetic cutting fluids: a part-per-hundred impurity. *Science* (80-). 197, 70–71.
- (112) Bontoyan, W., Law, M., and Wright, D. (1979) Nitrosamines in agricultural and home-use pesticides. *J. Agric. Food Chem.* 27, 631–635.
- (113) Spiegelhalder, B., and Preussmann, R. (1984) Contamination of toiletries and cosmetic products with volatile and nonvolatile N-nitroso carcinogens. *J. Cancer Res. Clin. Oncol.* 108, 160–163.
- (114) Eisenbrand, G., Spiegelhalder, B., Kann, J., Klein, R., and Preussmann, R. (1979) Carcinogenic N-nitrosodimethylamine as a contaminant in drugs containing 4-dimethylamino--2,3-dimethyl-1-phenyl-3-pyrazolin-5-one (amidopyrine, aminophenazone). *Arzneimittelforsch. (Drug Res.)* 29, 267–269.
- (115) Sander, J., and Burkle, G. (1969) Induction of malignant tumors in rats by simultaneous feeding of nitrite and secondary amines. *Z. Krebsforsch.* 73, 54–66.
- (116) Fan, T., and Tannenbaum, S. (1973) Factors influencing the rate of formation of nitrosomorpholine from morpholine and nitrite: acceleration by thiocyanate and other anions. *J. Agric. Food Chem.* 21, 237–240.
- (117) Tanaka, K., Hayatsu, T., Negishi, T., and Hayatsu, H. (1998) Inhibition of N-nitrosation of secondary amines in vitro by tea extracts and catechins. *Mutat. Res. - Genet. Toxicol. Environ. Mutagen.* 412, 91–98.

- (118) Lathia, D., and Blum, A. (1989) Role of vitamin E as nitrite scavenger and N-nitrosamine inhibitor: a review. *Int. J. Vitam. Nutr. Res.* 59, 430–438.
- (119) Ohshima, H., and Bartsch, H. (1981) Quantitative estimation of endogeneous nitrosation in humans by monitoring N-nitrosoproline excretion in the urine. *Cancer Res.* 41, 3658–3666.
- (120) Lundberg, J. O., Weitzberg, E., Cole, J. A., and Benjamin, N. (2004) Nitrate, bacteria and human health. *Nat. Rev. Microbiol.* 2, 593–602.
- (121) Miwa, M., Stuehr, D., Marletta, M., Wishnok, J., and Tannenbaum, S. (1987) Nitrosation of amines by stimulated macrophages. *Carcinogenesis* 8, 955–958.
- (122) Marletta, M. A., Yoon, P. S., Iyengar, R., Leaf, C. D., and Wishnok, J. S. (1988) Macrophage oxidation of L-arginine to nitrite and nitrate: nitric oxide is an intermediate. *Biochemistry* 27, 8706–8711.
- (123) Palmer, R. M. J., Ashton, D. S., and Moncada, S. (1988) Vascular endothelial cells synthesize nitric oxide from L-arginine. *Nature* 333, 664–666.
- (124) Garthwaite, J., Charles, S. L., and Chess-Williams, R. (1988) Endothelium-derived relaxing factor release on activation of NMDA receptors suggests role as intercellular messenger in the brain. *Nature* 336, 385–388.
- (125) Ji, X., and Hollocher, T. (1988) Mechanism for nitrosation of 2,3-diaminonaphthalene by *Escherichia coli*. Enzymatic production of nitric oxide followed by oxygen-dependent chemical nitrosation. *Appl. Environ. Microbiol.* 54, 1791–1794.
- (126) Bustamante, G., Ma, B., Yakovlev, G., Yershova, K., Le, C., Jensen, J., Hatsukami, D. K., and Stepanov, I. (2018) Presence of the carcinogen N'-nitrosornicotine in saliva of E-cigarette users. *Chem. Res. Toxicol.* 31, 731–738.
- (127) Garfinkel, D. (1958) Studies on pig liver microsomes. I. Enzymic and pigment composition of different microsomal fractions. *Arch. Biochem. Biophys.* 77, 493–509.

- (128) Klingenberg, M. (1958) Pigments of rat liver microsomes. *Arch. Biochem. Biophys.* 75, 376–386.
- (129) Omura, T., Sato, R. (1964) The carbon monoxide-binding pigment of liver microsomes. *J Biol Chem* 239, 2370–2378.
- (130) Omura, T., and Sato, R. (1962) A new cytochrome in liver microsomes. *J. Biol. Chem.* 237, 1375–1376.
- (131) Williams, J. A., Hyland, R., Jones, B. C., Smith, D. A., Hurst, S., Goosen, T. C., Peterkin, V., Koup, J. R., and Ball, S. E. (2004) Drug-drug interactions for UDP-glucuronosyltransferase substrates: A pharmacokinetic explanation for typically observed low exposure (AUCI/AUC) ratios. *Drug Metab. Dispos.* 32, 1201–1208.
- (132) Ueyama, N., Terakawa, T., Nakata, M., and Nakamura, A. (1983) Positive shift of redox potential of [Fe₄S₄(Z-cys-Gly-Ala-OMe)₄]²⁻ in dichloromethane. *J. Am. Chem. Soc.* 105, 7098–7102.
- (133) Ueyama, N., Nishikawa, N., Yamada, Y., Okamura, T., and Nakamura, A. (1996) Cytochrome P-450 model (porphinato)(thiolato)iron(III) complexes with single and double NH···S hydrogen bonds at the thiolate site. *J. Am. Chem. Soc.* 118, 12826–12827.
- (134) Nagano, S., Cupp-Vickery, J. R., and Poulos, T. L. (2005) Crystal structures of the ferrous dioxygen complex of wild-type cytochrome P450eryF and its mutants, A245S and A245T: Investigation of the proton transfer system in P450eryF. *J. Biol. Chem.* 280, 22102–22107.
- (135) Denisov, I. G., Makris, T. M., Sligar, S. G., and Schlichting, I. (2005) Structure and chemistry of cytochrome P450. *Chem. Rev.* 105, 2253–2278.
- (136) de Montellano, P. R. O. (2015) Cytochrome P450: Structure, mechanism, and biochemistry, fourth edition. *Cytochrome P450 Struct. Mech. Biochem. Fourth Ed.*
- (137) Jalas, J. R., Murphy, S. E., and Hecht, S. S. (2005) Cytochrome P450 enzymes as

catalysts of metabolism of 4-(methylnitrosamino)-1-(3-pyridyl)-1-butanone (NNK), a tobacco-specific carcinogen. *Chem. Res. Toxicol.* *18*, 95–110.

(138) Nebert, D. W., and Gelboin, H. V. (1968) Substrate-inducible microsomal aryl hydroxylase in mammalian cell culture: I. Assay and properties of induced enzyme. *J. Biol. Chem.* *243*, 6242–6249.

(139) Guengerich, F. P. (2018) Mechanisms of cytochrome P450-catalyzed oxidations. *ACS Catal.* *8*, 10964–10976.

(140) Dubey, K. D., and Shaik, S. (2019) Cytochrome P450 - The wonderful nanomachine revealed through dynamic simulations of the catalytic cycle. *Acc. Chem. Res.* *52*, 389–399.

(141) Sligar, S. G., and Gunsalus, I. C. (1976) A thermodynamic model of regulation: modulation of redox equilibria in camphor monooxygenase. *Proc. Natl. Acad. Sci.* *73*, 1078 LP-1082.

(142) Oprian, D. D., and Coon, M. J. (1982) Oxidation-reduction states of FMN and FAD in NADPH-cytochrome P-450 reductase during reduction by NADPH. *J. Biol. Chem.* *257*, 8935–8944.

(143) Varfaj, F., Zulkifli, S. N. A., Park, H.-G., Challinor, V. L., De Voss, J. J., and Ortiz de Montellano, P. R. (2014) Carbon-carbon bond cleavage in activation of the prodrug Nabumetone. *Drug Metab. Dispos.* *42*, 828 LP-838.

(144) Shyadehi, A. Z., Lamb, D. C., Kelly, S. L., Kelly, D. E., Schunck, W.-H., Wright, J. N., Corina, D., and Akhtar, M. (1996) The mechanism of the acyl-carbon bond cleavage reaction catalyzed by recombinant sterol 14 α -demethylase of *Candida albicans* (other names are: lanosterol 14 α -demethylase, P-45014DM, and CYP51). *J. Biol. Chem.* *271*, 12445–12450.

(145) Rittle, J., and Green, M. T. (2010) Cytochrome P450 Compound I: Capture,

characterization, and C-H bond activation kinetics. *Science* (80-.). 330, 933–937.

(146) Groves, J. T., McClusky, G. A., White, R. E., and Coon, M. J. (1978) Aliphatic hydroxylation by highly purified liver microsomal cytochrome P-450. Evidence for a carbon radical intermediate. *Biochem. Biophys. Res. Commun.* 81, 154–160.

(147) Krüger, F. W. (1971) Metabolismus von nitrosaminen in vivo. *Zeitschrift für Krebsforsch. und Klin. Onkol.* 76, 145–154.

(148) Lijinsky, W. (1985) The metabolism and cellular interactions of some aliphatic nitrogenous carcinogens. *Cancer Lett.* 26, 33–42.

(149) Okada, M., Suzuki, E. M., and Mochizuki, M. (1976) Possible important role of urinary N-methyl-N(3-carboxypropyl)nitrosamine in the induction of bladder tumors in rats by N-methyl-N-dodecyl nitrosamine. *Gann* 67, 771–772.

(150) J Michejda, C., R Koepke, S., B Kroeger-Koepke, M., and Bosan, W. (1987) Recent findings on the metabolism of beta-hydroxyalkylnitrosamines. *IARC Sci. Publ.*

(151) Hecht, S. S., Chen, C. hong B., and Hoffmann, D. (1980) Metabolic β -hydroxylation and N-oxidation of N'-nitrosornicotine. *J. Med. Chem.* 23, 1175–1178.

(152) Knoop, F. (1904) Der Abbau aromatischer Fettsäuren im Tierkörper. Ernst Kuttruff, Freiburg, Germany.

(153) Mochizuki, M., Irving, C. C., Anjo, T., Wakabayashi, Y., Suzuki, E., and Okada, M. (1980) Synthesis and mutagenicity of 4-(N-butyl nitrosamino)-4-hydroxybutyric acid lactone, a possible activated metabolite of the proximate bladder carcinogen N-butyl-N-(3-carboxypropyl)nitrosamine. *Cancer Res.* 40, 162 LP-165.

(154) Ding, X., and Kaminsky, L. S. (2003) Human extrahepatic cytochromes P450: Function in xenobiotic metabolism and tissue-selective chemical toxicity in the respiratory and gastrointestinal tracts. *Annu. Rev. Pharmacol. Toxicol.* 43, 149–173.

- (155) Schirmer, C. C., Higa, C., Kruehl, C. D. P., Saito, E. H., Moraes, E. G., Filho, I. M., Pinto, L. F. R., Lang, M. A., Pinho, P. R. A., Gurski, R., Nunes, R. A., Albano, R. M., and Godoy, W. (2002) CYP2A6/2A7 and CYP2E1 expression in human oesophageal mucosa: regional and inter-individual variation in expression and relevance to nitrosamine metabolism. *Carcinogenesis* 23, 611–616.
- (156) Achour, B., Russell, M. R., Barber, J., and Rostami-Hodjegan, A. (2014) Simultaneous quantification of the abundance of several cytochrome P450 and uridine 5'-diphospho-glucuronosyltransferase enzymes in human liver microsomes using multiplexed targeted proteomics. *Drug Metab. Dispos.* 42, 500–510.
- (157) Shimada, T., Yamazaki, H., Mimura, M., Inui, Y., and Guengerich, F. P. (1994) Interindividual variations in human liver cytochrome P-450 enzymes involved in the oxidation of drugs, carcinogens and toxic chemicals: studies with liver microsomes of 30 Japanese and 30 Caucasians. *J. Pharmacol. Exp. Ther.* 270, 414 LP-423.
- (158) DeVore, N. M., Meneely, K. M., Bart, A. G., Stephens, E. S., Battaile, K. P., and Scott, E. E. (2012) Structural comparison of cytochromes P450 2A6, 2A13, and 2E1 with pilocarpine. *FEBS J.* 279, 1621–1631.
- (159) Yano, J. K., Hsu, M.-H., Griffin, K. J., Stout, C. D., and Johnson, E. F. (2005) Structures of human microsomal cytochrome P450 2A6 complexed with coumarin and methoxsalen. *Nat. Struct. Mol. Biol.* 12, 822.
- (160) Rautio, A., Kraul, H., Kojo, A., Salmela, E., and Pelkonen, O. (1992) Interindividual variability of coumarin 7-hydroxylation in healthy volunteer. *Pharmacogenetics* 2, 227–233.
- (161) Ikeda, K., Yoshisue, K., Matsushima, E., Nagayama, S., Kobayashi, K., Tyson, C. A., Chiba, K., and Kawaguchi, Y. (2000) Bioactivation of Tegafur to 5-fluorouracil is catalyzed by cytochrome P450 2A6 in human liver microsomes in vitro. *Clin. Cancer Res.* 6, 4409–4415.

- (162) Endo, T., Ban, M., Hirata, K., Yamamoto, A., Hara, Y., and Momose, Y. (2007) Involvement of CYP2A6 in the formation of a novel metabolite, 3-hydroxypilocarpine, from pilocarpine in human liver microsomes. *Drug Metab. Dispos.* 35, 476–483.
- (163) Abu-Bakar, A., Arthur, D. M., Wikman, A. S., Rahnasto, M., Juvonen, R. O., Vepsäläinen, J., Raunio, H., Ng, J. C., and Lang, M. A. (2012) Metabolism of bilirubin by human cytochrome P450 2A6. *Toxicol. Appl. Pharmacol.* 261, 50–58.
- (164) von Weymarn, L. B., Brown, K. M., and Murphy, S. E. (2006) Inactivation of CYP2A6 and CYP2A13 during nicotine metabolism. *J. Pharmacol. Exp. Ther.* 316, 295–303.
- (165) Luo, G., Lu, F., Jiang, L., Cai, Y., and Zhang, Y. (2015) Virtual screening of cytochrome P450 2A6 inhibitors from traditional chinese medicine using support vector machine and molecular docking, in *2015 8th International Conference on Biomedical Engineering and Informatics (BMEI)*, pp 505–509.
- (166) Chougnet, A., Woggon, W.-D., Locher, E., and Schilling, B. (2009) Synthesis and in vitro activity of heterocyclic inhibitors of CYP2A6 and CYP2A13, two cytochrome P450 enzymes present in the respiratory tract. *ChemBioChem* 10, 1562–1567.
- (167) Yano, J. K., Denton, T. T., Cerny, M. A., Zhang, X., Johnson, E. F., and Cashman, J. R. (2006) Synthetic inhibitors of cytochrome P-450 2A6: Inhibitory activity, difference spectra, mechanism of inhibition, and protein cocrystallization. *J. Med. Chem.* 49, 6987–7001.
- (168) Oscarson, M., McLellan, R. A., Asp, V., Ledesma, M., Ruiz, M. L. B., Sinues, B., Rautio, A., and Ingelman-Sundberg, M. (2002) Characterization of a novel CYP2A7/CYP2A6 hybrid allele (CYP2A6*12) that causes reduced CYP2A6 activity. *Hum. Mutat.* 20, 275–283.
- (169) Pang, C., Liu, J.-H., Xu, Y.-S., Chen, C., and Dai, P.-G. (2015) The allele frequency of CYP2A6*4 in four ethnic groups of China. *Exp. Mol. Pathol.* 98, 546–548.

- (170) Liu, T., David, S. P., Tyndale, R. F., Wang, H., Zhou, Q., Ding, P., He, Y.-H., Yu, X.-Q., Chen, W., Crump, C., Wen, X.-Z., and Chen, W.-Q. (2011) Associations of CYP2A6 genotype with smoking behaviors in southern China. *Addiction* 106, 985–994.
- (171) Yoshida, R., Nakajima, M., Watanabe, Y., Kwon, J.-T., and Yokoi, T. (2002) Genetic polymorphisms in human CYP2A6 gene causing impaired nicotine metabolism. *Br. J. Clin. Pharmacol.* 54, 511–517.
- (172) Yuan, J. M., Nelson, H. H., Carmella, S. G., Wang, R., Kuriger-Laber, J., Jin, A., Adams-Haduch, J., Hecht, S. S., Koh, W. P., and Murphy, S. E. (2017) CYP2A6 genetic polymorphisms and biomarkers of tobacco smoke constituents in relation to risk of lung cancer in the singapore chinese health study. *Carcinogenesis* 38, 411–418.
- (173) Yuan, J. M., Gao, Y. T., Murphy, S. E., Carmella, S. G., Wang, R., Zhong, Y., Moy, K. A., Davis, A. B., Tao, L., Chen, M., Han, S., Nelson, H. H., Yu, M. C., and Hecht, S. S. (2011) Urinary levels of cigarette smoke constituent metabolites are prospectively associated with lung cancer development in smokers. *Cancer Res.* 71, 6749–6757.
- (174) Yuan, J. M., Koh, W. P., Murphy, J. S. E., Fan, Y., Wang, R., Carmella, S. G., Han, S., Wickham, K., Gao, Y. T., Yu, M. C., and Hecht, S. S. (2009) Urinary levels of tobacco-specific nitrosamine metabolites in relation to lung cancer development in two prospective cohorts of cigarette smokers. *Cancer Res.* 69, 2990–2995.
- (175) Bao, Z., He, X.-Y., Ding, X., Prabhu, S., and Hong, J.-Y. (2005) Metabolism of nicotine and cotinine by human cytochrome P450 2A13. *Drug Metab. Dispos.* 33, 258 LP-261.
- (176) von Weymarn, L. B., and Murphy, S. E. (2003) CYP2A13-catalysed coumarin metabolism: comparison with CYP2A5 and CYP2A6. *Xenobiotica* 33, 73–81.
- (177) He, X.-Y., Tang, L., Wang, S.-L., Cai, Q.-S., Wang, J.-S., and Hong, J.-Y. (2006) Efficient activation of aflatoxin B1 by cytochrome P450 2A13, an enzyme predominantly

expressed in human respiratory tract. *Int. J. Cancer* 118, 2665–2671.

(178) Nakajima, M., Itoh, M., Sakai, H., Fukami, T., Katoh, M., Yamazaki, H., Kadlubar, F. F., Imaoka, S., Funae, Y., and Yokoi, T. (2006) CYP2A13 expressed in human bladder metabolically activates 4-aminobiphenyl. *Int. J. Cancer* 119, 2520–2526.

(179) Fukami, T., Nakajima, M., Sakai, H., Katoh, M., and Yokoi, T. (2007) CYP2A13 metabolizes the substrates of human CYP1A2, Phenacetin, and Theophylline. *Drug Metab. Dispos.* 35, 335–339.

(180) Zhang, X., Chen, Y., Liu, Y., Ren, X., Zhang, Q.-Y., Caggana, M., and Ding, X. (2003) Single nucleotide polymorphisms of the human CYP2A13 gene: Evidence for a null allele. *Drug Metab. Dispos.* 31, 1081–1085.

(181) Wang, H., Tan, W., Hao, B., Miao, X., Zhou, G., He, F., and Lin, D. (2003) Substantial reduction in risk of lung adenocarcinoma associated with genetic polymorphism in CYP2A13, the most active cytochrome P450 for the metabolic activation of tobacco-specific carcinogen NNK. *Cancer Res.* 63, 8057–8061.

(182) Yuan, J.-M., Stepanov, I., Murphy, S. E., Wang, R., Allen, S., Jensen, J., Strayer, L., Adams-Haduch, J., Upadhyaya, P., Le, C., Kurzer, M. S., Nelson, H. H., Yu, M. C., Hatsukami, D., and Hecht, S. S. (2016) Clinical trial of 2-phenethyl isothiocyanate as an inhibitor of metabolic activation of a tobacco-specific lung carcinogen in cigarette smokers. *Cancer Prev. Res.* 9, 396–405.

(183) Blake, L. C., Roy, A., Neul, D., Schoenen, F. J., Aubé, J., and Scott, E. E. (2013) Benzylmorpholine analogs as selective inhibitors of lung cytochrome P450 2A13 for the chemoprevention of lung cancer in tobacco users. *Pharm. Res.* 30, 2290–2302.

(184) Hoffmann, D., and Hecht, S. S. (1985) Nicotine-derived N-nitrosamines and tobacco-related cancer: Current status and future directions. *Cancer Res.* 45, 935–944.

(185) Boyland, E., Roe, F. J. C., and Gorrod, J. W. (1964) Induction of pulmonary

tumours in mice by nitrosornicotine, a possible constituent of tobacco smoke. *Nature* 202, 1126.

(186) Hoffmann, D., Hecht, S. S., Orna, R. M., and Wynder, E. L. (1974) N-Nitrosornicotine in tobacco. *Science* (80-). 186, 265–267.

(187) Hecht, S. S., Chen, C. B., Ohmori, T., and Hoffmann, D. (1980) Comparative carcinogenicity in F344 rats of the tobacco-specific nitrosamines, N'-nitrosornicotine and 4-(N-methyl-N-nitrosamino)-1-(3-pyridyl)1-butanone. *Cancer Res.* 40, 298–302.

(188) Hoffmann, D., Rivenson, A., Amin, S., and Hecht, S. S. (1984) Dose-response study of the carcinogenicity of tobacco-specific N-nitrosamines in F344 rats. *J. Cancer Res. Clin. Oncol.* 108, 81–86.

(189) Boyland, E., Roe, F. J. C., Gorrod, J. W., and Mitchley, B. C. V. (1964) The carcinogenicity of nitrosoanabasine, a possible constituent of tobacco smoke. *Br. J. Cancer* 18, 265–270.

(190) Hecht, S. S. (1998) Biochemistry, biology, and carcinogenicity of tobacco-specific N-nitrosamines. *Chem. Res. Toxicol.* 11, 559–603.

(191) Hecht, S. S. (1999) DNA adduct formation from tobacco-specific N-nitrosamines. *Mutat. Res. - Fundam. Mol. Mech. Mutagen.* 424, 127–142.

(192) Hecht, S. S. (2017) Oral cell DNA adducts as potential biomarkers for lung cancer susceptibility in cigarette smokers. *Chem. Res. Toxicol.* 30, 367–375.

(193) Peterson, L. A. (2017) Context matters: contribution of specific DNA adducts to the genotoxic properties of the tobacco-specific nitrosamine NNK. *Chem. Res. Toxicol.* 30, 420–433.

(194) Castonguay, A., Stoner, G. D., Schut, H. A., and Hecht, S. S. (1983) Metabolism of tobacco-specific N-nitrosamines by cultured human tissues. *Proc. Natl. Acad. Sci.* 80, 6694 LP-6697.

- (195) Chen, C. B., Lin, D., and Hecht, S. S. (1981) Comprehensive analysis of urinary metabolites of N'-nitroso-nornicotine. *Carcinogenesis* 2, 833–838.
- (196) McIntee, E. J., and Hecht, S. S. (2000) Metabolism of N'-nitrososnornicotine enantiomers by cultured rat esophagus and in vivo in Rats. *Chem. Res. Toxicol.* 13, 192–199.
- (197) Upadhyaya, P., Zimmerman, C. L., and Hecht, S. S. (2002) Metabolism and pharmacokinetics of N'-nitrososnornicotine in the patas monkey. *Drug Metab. Dispos.* 30, 1115–1122.
- (198) Upadhyaya, P., and Hecht, S. S. (2015) Quantitative analysis of 3'-hydroxynorcotinine in human urine. *Nicotine Tob. Res.* 17, 524–529.
- (199) Knezevich, A. D., Stepanov, I., Wang, R., Hecht, S. S., Yuan, J.-M., and Gao, Y.-T. (2011) Urinary levels of the tobacco-specific carcinogen N'-nitrososnornicotine and its glucuronide are strongly associated with esophageal cancer risk in smokers. *Carcinogenesis* 32, 1366–1371.
- (200) Kavvadias, D., Hagedorn, H.-W., Urban, M., Scherer, G., Roethig, H., Mendes, P., Muhammad, R., Serafin, R., Feng, S., Kapur, S., and Jin, Y. (2009) Quantitation of N'-nitrososnornicotine (NNN) in smokers' urine by liquid chromatography-tandem mass spectrometry. *J. Anal. Toxicol.* 33, 260–265.
- (201) Patten, C. J., Smith, T. J., Friesen, M. J., Tynes, R. E., Yang, C. S., and Murphy, S. E. (1997) Evidence for cytochrome P450 2A6 and 3A4 as major catalysts for N'-nitrososnornicotine α -hydroxylation by human liver microsomes. *Carcinogenesis* 18, 1623–1630.
- (202) Smith, T. J., Guo, Z., Guengerich, F. P., and Yang, C. S. (1996) Metabolism of 4-(methylnitrosamino)-1-(3-pyridyl)-1-butanone (NNK) by human cytochrome P450 1A2 and its inhibition by phenethyl isothiocyanate. *Carcinogenesis* 17, 809–813.

- (203) Spratt, T. E., Peterson, L. A., Confer, W. L., and Hecht, S. S. (1990) Solvolysis of model compounds for α -hydroxylation of N'-nitrosornicotine and 4-(methylnitrosamino)-1-(3-pyridyl)-1-butanone: evidence for a cyclic oxonium ion intermediate in the alkylation of nucleophiles. *Chem. Res. Toxicol.* 3, 350–356.
- (204) Trushin, N., and Hecht, S. S. (1999) Stereoselective metabolism of nicotine and tobacco-specific N-nitrosamines to 4-hydroxy-4-(3-pyridyl)butanoic acid in rats. *Chem. Res. Toxicol.* 12, 164–171.
- (205) Reiss, B., Lin, D., Williams, G. M., and Hecht, S. S. (1982) Metabolism of N'-nitrosornicotine by cultured rat esophagus. *Carcinogenesis* 3, 453–456.
- (206) Domellöf, L., Andersson, M., Tjälve, H., Trushin, N., Hecht, S. S., and Veals, S. (1987) Distribution and metabolism of N'-nitrosornicotine in the miniature pig. *Carcinogenesis* 8, 1741–1747.
- (207) Castonguay, A., Lin, D., Stoner, G. D., Radok, P., Furuya, K., Hecht, S. S., Schut, H. A. J., and Klaunig, J. E. (1983) Comparative carcinogenicity in A/J mice and metabolism by cultured mouse peripheral lung of N'-Nitrosornicotine, 4-(methylnitrosamino)-1-(3-pyridyl)-1-butanone, and their analogues. *Cancer Res.* 43, 1223–1229.
- (208) Zarth, A. T., Upadhyaya, P., Yang, J., and Hecht, S. S. (2016) DNA adduct formation from metabolic 5'-hydroxylation of the tobacco-specific carcinogen N'-nitrosornicotine in human enzyme systems and in rats. *Chem. Res. Toxicol.* 29, 380–389.
- (209) Lao, Y., Yu, N., Kassie, F., Villalta, P. W., and Hecht, S. S. (2007) Analysis of pyridyloxobutyl DNA adducts in F344 rats chronically treated with (R)- and (S)-N'-nitrosornicotine. *Chem. Res. Toxicol.* 20, 246–256.
- (210) Zhang, S., Wang, M., Villalta, P. W., Lindgren, B. R., Upadhyaya, P., Lao, Y., and Hecht, S. S. (2009) Analysis of pyridyloxobutyl and pyridylhydroxybutyl DNA adducts

in extrahepatic tissues of F344 rats treated chronically with 4-(methylnitrosamino)-1-(3-pyridyl)-1-butanone and enantiomers of 4-(methylnitrosamino)-1-(3-pyridyl)-1-butanol. *Chem. Res. Toxicol.* 22, 926–936.

(211) Li, Y., Ma, B., Cao, Q., Balbo, S., Zhao, L., Upadhyaya, P., and Hecht, S. S. (2019) Mass Spectrometric Quantitation of Pyridyloxobutyl DNA Phosphate Adducts in Rats Chronically Treated with N'-Nitrosornicotine. *Chem. Res. Toxicol.*

(212) Hoffmann, D., Raineri, R., Hecht, S. S., Maronpot, R., and Wynder, E. L. (1975) Effects of N'-nitrosornicotine and N'-nitrosoanabasine in rats. *J. Natl. Cancer Inst.* 55, 977–981.

(213) Singer, G. M., and Taylor, H. W. (1976) Carcinogenicity of N'-nitrosornicotine in Sprague-Dawley rats. *J. Natl. Cancer Inst.* 57, 1275–1276.

(214) Balbo, S., James-Yi, S., Johnson, C. S., O'Sullivan, M. G., Stepanov, I., Wang, M., Bandyopadhyay, D., Kassie, F., Carmella, S., Upadhyaya, P., and Hecht, S. S. (2013) (S)-N'-Nitrosornicotine, a constituent of smokeless tobacco, is a powerful oral cavity carcinogen in rats. *Carcinogenesis* 34, 2178–2183.

(215) Yang, J., Villalta, P. W., Upadhyaya, P., and Hecht, S. S. (2016) Analysis of O6-[4-(3-pyridyl)-4-oxobut-1-yl]-2'-deoxyguanosine and other DNA adducts in rats treated with enantiomeric or racemic N'-nitrosornicotine. *Chem. Res. Toxicol.* 29, 87–95.

(216) Deutsch-Wenzel, R. P., Brune, H., Grimmer, G., and Misfeld, J. (1985) Local application to mouse skin as a carcinogen specific test system for non-volatile nitroso compounds. *Cancer Lett.* 29, 85–92.

(217) Hecht, S. S., Young, R., and Maeura, Y. (1983) Comparative carcinogenicity in F344 rats and Syrian golden hamsters of N'-nitrosornicotine and N'-nitrosornicotine-1-N-oxide. *Cancer Lett.* 20, 333–340.

(218) Evensen, Ø., Koppang, N., Dahle, H. K., Rivenson, A., Hoffmann, D., and Reith,

- A. (1992) A study of tobacco carcinogenesis XLVIII. carcinogenicity of N'-nitrosornicotine in mink (*Mustela vison*). *Carcinogenesis* 13, 1957–1960.
- (219) Koppang, N., Rivenson, A., Dahle, H. K., and Hoffmann, D. (1997) A study of tobacco carcinogenesis, LIII: carcinogenicity of N'-nitrosornicotine (NNN) and 4-(methylnitrosamino)-1-(3-pyridyl)-1-butanone (NNK) in mink (*Mustela vison*). *Cancer Lett.* 111, 167–171.
- (220) Dator, R., von Weymarn, L. B., Villalta, P. W., Hooyman, C. J., Maertens, L. A., Upadhyaya, P., Murphy, S. E., and Balbo, S. (2018) In vivo stable-isotope labeling and mass-spectrometry-based metabolic profiling of a potent tobacco-specific carcinogen in rats. *Anal. Chem.* 90, 11863–11872.
- (221) Atalla, A., Breyer-Pfaff, U., and Maser, E. (2000) Purification and characterization of oxidoreductases-catalyzing carbonyl reduction of the tobacco-specific nitrosamine 4-methylnitrosamino-1-(3-pyridyl)-1-butanone (NNK) in human liver cytosol. *Xenobiotica* 30, 755–769.
- (222) Breyer-Pfaff, U., Martin, H.-J., Ernst, M., and Maser, E. (2004) Enantioselectivity of carbonyl reduction of 4-methylnitrosamino-1-(3-pyridyl)-1-butanone by tissue fractions from human and rat and by enzymes isolated from human liver. *Drug Metab. Dispos.* 32, 915–922.
- (223) Upadhyaya, P., Carmella, S. G., Guengerich, F. P., and Hecht, S. S. (2000) Formation and metabolism of 4-(methylnitrosamino)-1-(3-pyridyl)-1-butanol enantiomers in vitro in mouse, rat and human tissues. *Carcinogenesis* 21, 1233–1238.
- (224) Jing, M., Wang, Y., Upadhyaya, P., Jain, V., Yuan, J.-M., Hatsukami, D. K., Hecht, S. S., and Stepanov, I. (2014) Liquid chromatography–electrospray ionization–tandem mass spectrometry quantitation of urinary 4-hydroxy-4-(3-pyridyl) butanoic acid, a biomarker of 4-(methylnitrosamino)-1-(3-pyridyl)-1-butanone metabolic activation in smokers. *Chem. Res. Toxicol.* 27, 1547–1555.

- (225) Lao, Y., Villalta, P. W., Sturla, S. J., Wang, M., and Hecht, S. S. (2006) Quantitation of pyridyloxobutyl DNA adducts of tobacco-specific nitrosamines in rat tissue DNA by high-performance liquid chromatography- electrospray ionization-tandem mass spectrometry. *Chem. Res. Toxicol.* *19*, 674–682.
- (226) Upadhyaya, P., Lindgren, B. R., and Hecht, S. (2009) Comparative levels of O6-methylguanine, pyridyloxobutyl-, and pyridylhydroxybutyl-DNA adducts in lung and liver of rats treated chronically with the tobacco-specific carcinogen 4-(methylnitrosamino)-1-(3-pyridyl)-1-butanone. *Drug Metab. Dispos.* *37*, 1147–1151.
- (227) Michel, A. K., Zarth, A. T., Upadhyaya, P., and Hecht, S. S. (2017) Identification of 4-(3-pyridyl)-4-oxobutyl-2'-deoxycytidine adducts formed in the reaction of DNA with 4-(acetoxymethylnitrosamino)-1-(3-pyridyl)-1-butanone: A chemically activated form of tobacco-specific carcinogens. *ACS Omega* *2*, 1180–1190.
- (228) Wang, L., Spratt, T. E., Liu, X.-K., Hecht, S. S., Pegg, A. E., and Peterson, L. A. (1997) Pyridyloxobutyl Adduct O6-[4-oxo-4-(3-pyridyl)butyl]guanine Is present in 4-(acetoxymethylnitrosamino)-1-(3-pyridyl)-1-butanone-treated DNA and is a substrate for O6-alkylguanine-DNA alkyltransferase. *Chem. Res. Toxicol.* *10*, 562–567.
- (229) Upadhyaya, P., Kalscheuer, S., Hochalter, J. B., Villalta, P. W., and Hecht, S. S. (2008) Quantitation of pyridylhydroxybutyl-DNA adducts in liver and lung of F-344 rats treated with 4-(methylnitrosamino)-1-(3-pyridyl)-1-butanone and enantiomers of its metabolite 4-(methylnitrosamino)-1-(3-pyridyl)-1-butanol. *Chem. Res. Toxicol.* *21*, 1468–1476.
- (230) Ma, B., Zarth, A. T., Carlson, E. S., Villalta, P. W., Stepanov, I., and Hecht, S. S. (2017) Pyridylhydroxybutyl and pyridyloxobutyl DNA phosphate adduct formation in rats treated chronically with enantiomers of the tobacco-specific nitrosamine metabolite 4-(methylnitrosamino)-1-(3-pyridyl)-1-butanol. *Mutagenesis* *32*, 561–570.
- (231) Peterson, L. A., and Hecht, S. S. (1991) O6-methylguanine is a critical determinant of 4-(methylnitrosamino)-1-(3-pyridyl)-1-butanone tumorigenesis in A/J mouse lung.

Cancer Res. 51, 5557–5564.

(232) Belinsky, S. A., Devereux, T. R., Anderson, M. W., Maronpot, R. R., and Stoner, G. D. (1989) Relationship between the formation of promutagenic adducts and the activation of the k-ras protooncogene in lung tumors from A/J mice treated with nitrosamines. *Cancer Res.* 49, 5305–5311.

(233) Ronai, Z. A., Gradia, S., Peterson, L. A., and Hecht, S. S. (1993) G to A transitions and G to T transversions in codon 12 of the K-ras oncogene isolated from mouse lung tumors induced by 4-(methylnitrosamino)-1-(3-pyridyl)-1-butanone (NNK) and related DNA methylating and pyridyloxobutylating agents. *Carcinogenesis* 14, 2419–2422.

(234) Mijal, R. S., Loktionova, N. A., Vu, C. C., Pegg, A. E., and Peterson, L. A. (2005) O6-pyridyloxobutylguanine adducts contribute to the mutagenic properties of pyridyloxobutylating agents. *Chem. Res. Toxicol.* 18, 1619–1625.

(235) Peterson, L. A., Liu, X.-K., and Hecht, S. S. (1993) Pyridyloxobutyl DNA adducts inhibit the repair of O6-methylguanine. *Cancer Res.* 53, 2780–2785.

(236) Hecht, S. S., Chen, C. B., Ohmori, T., and Hoffmann, D. (1980) Comparative carcinogenicity in F344 rats of the tobacco-specific nitrosamines, N'-nitrosornicotine and 4-(N-Methyl-N-nitrosamino)-1-(3-pyridyl)-1-butanone. *Cancer Res.* 40, 298–302.

(237) Lijinsky, W., Saavedra, J., and M Kovatch, R. (1991) Carcinogenesis in rats by substituted dialkylnitrosamines given by gavage. *In Vivo*.

(238) Hecht, S. S., Rivenson, A., Braley, J., DiBello, J., Adams, J. D., and Hoffmann, D. (1986) Induction of oral cavity tumors in F344 rats by tobacco-specific nitrosamines and snuff. *Cancer Res.* 46, 4162–4166.

(239) Carlson, E. S., Upadhyaya, P., and Hecht, S. S. (2016) Evaluation of nitrosamide formation in the cytochrome P450-mediated metabolism of tobacco-specific nitrosamines. *Chem. Res. Toxicol.* 29, 2194–2205.

- (240) American Cancer Society. (2014) Cancer Facts & Figures 2014. *Cancer Facts Fig.* Atlanta.
- (241) Hecht, S. S., Castonguay, A., Chung, F. L., and Hoffmann, D. (1984) Carcinogenicity and metabolic activation of tobacco-specific nitrosamines: current status and future prospects. *IARC Sci. Publ.* 763–778.
- (242) Mesic, M., Revis, C., and Fishbein, J. (1996) Effects of structure on the reactivity of α -hydroxydialkylnitrosamines in aqueous solutions. *J. Am. Chem. Soc.* 118, 7412–7413.
- (243) Mochizuki, M., Anjo, T., and Okada, M. (1980) Isolation and characterization of N-alkyl-N-(hydroxymethyl)nitrosamines from N-alkyl-N-(hydroperoxymethyl)nitrosamines by deoxygenation. *Tetrahedron Lett.* 21, 3693–3696.
- (244) Hecht, S. S., Spratt, T. E., and Trushin, N. (1988) Evidence for 4-(3-pyridyl)-4-oxobutylation of DNA in F344 rats treated with the tobacco-specific nitrosamines 4-(methylnitrosamino)-1-(3-pyridyl)-1-butanone and N²-nitrosornicotine. *Carcinogenesis* 9, 161–165.
- (245) Stepanov, I., Muzic, J., Le, C. T., Sebero, E., Villalta, P., Ma, B., Jensen, J., Hatsukami, D., and Hecht, S. S. (2013) Analysis of 4-hydroxy-1-(3-pyridyl)-1-butanone (HPB)-releasing DNA adducts in human exfoliated oral mucosa cells by liquid chromatography-electrospray ionization-tandem mass spectrometry. *Chem. Res. Toxicol.* 26, 37–45.
- (246) Zhao, L., Balbo, S., Wang, M., Upadhyaya, P., Khariwala, S. S., Villalta, P. W., and Hecht, S. (2013) Quantification of pyridyloxobutyl-DNA adducts in tissues of rats treated chronically with (R)-or (S)-N²-nitrosornicotine (NNN) in a carcinogenicity study. *Chem. Res. Toxicol.* 26, 1526–1535.
- (247) Guttenplan, J. B. (1993) Effects of cytosol on mutagenesis induced by N-nitrosodimethylamine, N-nitrosomethylurea and α -acetoxy-N-nitrosodimethylamine in

different strains of Salmonella: evidence for different ultimate mutagens from N-nitrosodimethylamine. *Carcinogenesis* 14, 1013–1019.

(248) Elespuru, R. K., Saavedra, J. E., Kovatch, R. M., and Lijinsky, W. (1993) Examination of alpha-carbonyl derivatives of nitrosodimethylamine and ethylnitrosomethylamine as putative proximate carcinogens. *Carcinogenesis* 14, 1189–1193.

(249) Murphy, S. E., Spina, D. A., Nunes, M. G., and Pullo, D. A. (1995) Glucuronidation of 4-((hydroxymethyl)nitrosamino)-1-(3-pyridyl)-1-butanone, a metabolically activated form of 4-(methylnitrosamino)-1-(3-pyridyl)-1-butanone, by phenobarbital-treated rats. *Chem. Res. Toxicol.* 8, 772–9.

(250) Wiench, K., Frei, E., Schroth, P., and Wiessler, M. (1992) 1-c-glucuronidation of N-nitrosodiethylamine and N-nitrosomethyl-N-pentylamine in vivo and in primary hepatocytes from rats pretreated with inducers. *Carcinogenesis* 13, 867–872.

(251) Wiessler, M., and Rossnagel, G. (1987) Alpha-glucuronides of N-nitrosomethylbenzylamine, in *The Relevance of N-Nitroso Compounds to Human Cancer, Exposure and Mechanism* (Bartsch, H., O'Neill, I. K., and Schulte-Hermann, R., Eds.), pp 170–172. IARC Scientific Reports 84, Lyon, France.

(252) Bell-Parikh, L. C., and Guengerich, F. P. (1999) Kinetics of cytochrome P450 2E1-catalyzed oxidation of ethanol to acetic acid via acetaldehyde. *J. Biol. Chem.* 274, 23833–23840.

(253) Chowdhury, G., Calcutt, M. W., and Peter Guengerich, F. (2010) Oxidation of N-nitrosoalkylamines by human cytochrome p450 2a6: Sequential oxidation to aldehydes and carboxylic acids and analysis of reaction steps. *J. Biol. Chem.* 285, 8031–8044.

(254) Chowdhury, G., Calcutt, M. W., Nagy, L. D., and Guengerich, F. P. (2012) Oxidation of methyl and ethyl nitrosamines by cytochromes P450 2E1 and 2B1. *Biochemistry* 51, 9995–10007.

- (255) White, E. H., and Dolak, L. A. (1966) N-Nitroamides and N-nitrocarbamates. IV. Rates of decomposition. A case of steric acceleration. *J. Am. Chem. Soc.* 88, 3790–3795.
- (256) Darbeau, R. W., Pease, R. S., and Gible, R. E. (2001) A study of electronic effects on the kinetics of thermal deamination of N-nitrosoamides. *J. Org. Chem.* 66, 5027–5032.
- (257) Moss, R. A. (1966) The solvolysis of alkyl diazotates. I. Partition between carbonium ions and diazoalkanes in aqueous base. *J. Org. Chem.* 31, 1082–1087.
- (258) Loh, T.-P., Zhou, J.-R., Li, X.-R., and Sim, K.-Y. (1999) A novel reductive aminocyclization for the syntheses of chiral pyrrolidines: stereoselective syntheses of (S)-nornicotine and 2-(2'-pyrrolidyl)-pyridines. *Tetrahedron Lett.* 40, 7847–7850.
- (259) Loozen, H. J. J., Godefroi, E. F., and Besters, J. S. M. M. (1975) A novel and efficient route to 5-arylated gamma-lactones. *J. Org. Chem.* 40, 892–894.
- (260) Amin, S., Desai, D., Hecht, S. S., and Hoffmann, D. (1996) Synthesis of tobacco-specific N-nitrosamines and their metabolites and results of related bioassays. *Crit. Rev. Toxicol.* 26, 139–47.
- (261) Balsiger, R. W., and Montgomery, J. A. (1960) Synthesis of potential anticancer agents. XXV. Preparation of 6-alkoxy-2-aminopurines. *J. Org. Chem.* 25, 1573–1575.
- (262) Von Weymarn, L. B., Zhang, Q. Y., Ding, X., and Hollenberg, P. F. (2005) Effects of 8-methoxypsoralen on cytochrome P450 2A13. *Carcinogenesis* 26, 621–629.
- (263) Wong, H. L., Murphy, S. E., Wang, M., and Hecht, S. S. (2003) Comparative metabolism of N-nitrosopiperidine and N-nitrosopyrrolidine by rat liver and esophageal microsomes and cytochrome P450 2A3. *Carcinogenesis* 24, 291–300.
- (264) Stetter, H., and Schreckenberger, M. (1973) A new method for addition of aldehydes to activated double bonds. *Angew. Chemie Int. Ed. English* 12, 81.

- (265) McKennis, H., Turnbull, L. B., Wingfield, H. N., and Dewey, L. J. (1958) Metabolites of nicotine and a synthesis of nornicotine. *J. Am. Chem. Soc.* 80, 1634–1636.
- (266) Wingfield Jr., H. N. (1959) 4-(3-Pyridyl)-4-ketobutyric Acid. *J. Org. Chem.* 24, 872–873.
- (267) White, E. H. (1955) The chemistry of the N-alkyl-N-nitrosamides. I. methods of preparation. *J. Am. Chem. Soc.* 77, 6008–6010.
- (268) Corey, E. J.; Seebach, D. (1965) Carbanions of 1,3-dithianes. Reagents for C-C bond formation by nucleophilic displacement and carbonyl addition. *Angew. Chemie Int. Ed. English* 4, 1075–1077.
- (269) Appel, R. (1975) Tertiary phosphane/tetrachloromethane, a versatile reagent for chlorination, dehydration, and P-N linkage. *Angew. Chemie Int. Ed. English* 14, 801–811.
- (270) Corey, E. J., and Erickson, B. W. (1971) Oxidative hydrolysis of 1, 3-dithiane derivatives to carbonyl compounds using N-halosuccinimide reagents. *J. Org. Chem.* 36, 3553–3560.
- (271) Wong, H. L., Murphy, S. E., and Hecht, S. S. (2005) Cytochrome P450 2A-catalyzed metabolic activation of structurally similar carcinogenic nitrosamines: N'-Nitrosonornicotine enantiomers, N-nitrosopiperidine, and N-nitrosopyrrolidine. *Chem. Res. Toxicol.* 18, 61–69.
- (272) Stetter, H., and SchreckenBerg, M. (1974) A new method for the addition of aldehydes to activated double bonds III. Addition of aromatic and heterocyclic aldehydes to alpha,beta-unsaturated nitriles. *Chem. Ber.* 107, 210.
- (273) Nguyen, T., Dagne, E., Gruenke, L., Bhargava, H., and Castagnoli, N. J. (1981) The tautomeric structures of 5-hydroxycotinine, a secondary mammalian metabolite of nicotine. *J. Org. Chem.* 46, 758–760.
- (274) Basha, A., Lipton, M., and Weinreb, S. M. (1977) A mild, general method for

conversion of esters to amides. *Tetrahedron Lett.* 18, 4171–4172.

(275) Lipton, Michael F., Basha, Anwer, Weinreb, S. M. (1979) Conversion of esters To amides with dimethylaluminum amides: N,N-dimethylcyclohexanecarboxamide. *Org. Synth.* 59, 49.

(276) Carlson, E. S., Upadhyaya, P., Villalta, P. W., Ma, B., and Hecht, S. S. (2018) Analysis and identification of 2'-deoxyadenosine-derived adducts in lung and liver DNA of F-344 rats treated with the tobacco-specific carcinogen 4-(methylnitrosamino)-1-(3-pyridyl)-1-butanone and enantiomers of its metabolite 4-(methylnitrosamino)-1-(3-p. *Chem. Res. Toxicol.* 31, 358–370.

(277) Rom, W. N., and Markowitz, S. B. (Eds.). (2007) N-Nitrosamines, in *Environmental and Occupational Medicine* 4th ed., pp 1226–1239. Lippincott Williams & Wilkins, Philadelphia, PA.

(278) Engel, J. D. (1975) Mechanism of the dimroth rearrangement in adenosine. *Biochem. Biophys. Res. Commun.* 64, 581–586.

(279) Fujii, T., and Saito, T. (1985) Purines. XXVI. The dimroth rearrangement of 9-substituted 1-methyladenines: accelerating effect of a b-D-ribofuranosyl group at the 9-position. *Chem. Pharm. Bull.* 33, 3635–3644.

(280) Fujii, T., Saito, T., and Terahara, N. (1986) Purines XXVII. Hydrolytic deamination versus dimroth rearrangement in the 9-substituted adenine ring: effect of an omega-hydroxyalkyl group at the 1-position. *Chem. Pharm. Bull.* 34, 1094–1107.

(281) Barlow, T., Ding, J., Vouros, P., and Dipple, A. (1997) Investigation of hydrolytic deamination of 1-(2-hydroxy-1-phenylethyl)adenosine. *Chem. Res. Toxicol.* 10, 1247–1249.

(282) Fujii, T., Saito, T., Hisata, H., and Shinbo, K. (1990) Purines. XLVII. Dimroth rearrangement versus hydrolytic deamination of 1-ethyladenine. *Chem. Pharm. Bull.* 38,

3326–3330.

(283) Saito, T., Murakami, M., Inada, T., Hayashibara, H., and Fujii, T. (1992) Purines. LIII. Deamination of 1-(omega-hydroxyalkyl)adenine derivatives by nucleophiles. *Chem.Pharm.Bull.(Tokyo)* 40, 3201–3205.

(284) Selzer, R. R., and Elfarra, A. A. (1996) Characterization of N1- and N6-adenosine adducts and N1-inosine adducts formed by the reaction of butadiene monoxide with adenosine: evidence for the N1-adenosine adducts as major initial products. *Chem. Res. Toxicol.* 9, 875–881.

(285) Barlow, T., Takeshita, J., and Dipple, A. (1998) Deamination and dimroth rearrangement of deoxyadenosine-styrene oxide adducts in DNA. *Chem. Res. Toxicol.* 11, 838–845.

(286) Fujii, T., Saito, T., and Nakasaka, T. (1989) Purines. XXXIV. 3-Methyladenosine and 3-methyl-2'-deoxyadenosine: their synthesis, glycosidic hydrolysis, and ring fission. *Chem. Pharm. Bull.* 37, 2601–2609.

(287) Fujii, T., Saito, T., and Iguchi, K. (1994) Purines. LXI. An attempted synthesis of 2'-deoxy-7-methyladenosine: glycosidic hydrolyses of the N6-methoxy derivative and 2'-deoxy-Nx-methyladenosines. *Chem. Pharm. Bull.* 42, 495–499.

(288) Scholdberg, T. A., Merritt, W. K., Dean, S. M., Kowalczyk, A., Harris, C. M., Harris, T. M., Rizzo, C. J., Lloyd, R. S., and Stone, M. P. (2005) Structure of an oligodeoxynucleotide containing a butadiene oxide-derived N1 beta-hydroxyalkyl deoxyinosine adduct in the human N-ras codon 61 sequence. *Biochemistry* 44, 3327–3337.

(289) Hecht, S. S., Spratt, T. E., and Trushin, N. (1997) Absolute configuration of 4-(methylnitrosamino)-1-(3-pyridyl)-1-butanol formed metabolically from 4-(methylnitrosamino)-1-(3-pyridyl)-1-butanone. *Carcinogenesis* 18, 1851–1854.

- (290) Upadhyaya, P., and Hecht, S. S. (2008) Identification of adducts formed in the reactions of 5'-acetoxy- N'-nitrosornicotine with deoxyadenosine, thymidine, and DNA. *Chem. Res. Toxicol.* 21, 2164–2171.
- (291) Lao, Y., Yu, N., Kassie, F., Villalta, P. W., and Hecht, S. S. (2007) Formation and accumulation of pyridyloxobutyl DNA adducts in F344 rats chronically treated with 4-(methylnitrosamino)-1-(3-pyridyl)-1-butanone and enantiomers of its metabolite, 4-(methylnitrosamino)-1-(3-pyridyl)-1-butanol. *Chem. Res. Toxicol.* 20, 235–245.
- (292) Napoli, L. De, Messere, A., Montesarchio, D., Piccialli, G., and Varra, M. (1997) 1-Substituted 2'-deoxyinosine analogues. *J. Chem. Soc. Perkin Trans. 1* 2079–2082.
- (293) Dilauro, A. M., Seo, W., and Phillips, S. T. (2011) Use of catalytic fluoride under neutral conditions for cleaving silicon-oxygen bonds. *J. Org. Chem.* 76, 7352–7358.
- (294) Wickramaratne, S., Banda, D. M., Ji, S., Manlove, A. H., Malayappan, B., Nuñez, N. N., Samson, L., Campbell, C., David, S. S., and Tretyakova, N. (2016) Base excision repair of N6-deoxyadenosine adducts of 1,3-butadiene. *Biochemistry* 55, 6070–6081.
- (295) Pawłowicz, A. J., Munter, T., Zhao, Y., and Kronberg, L. (2006) Formation of acrolein adducts with 2'-deoxyadenosine in calf thymus DNA. *Chem. Res. Toxicol.* 19, 571–576.
- (296) Seneviratne, U., Antsyrovich, S., Goggin, M., Dorr, D. Q., Guza, R., Moser, A., Thompson, C., York, D. M., and Tretyakova, N. (2010) Exocyclic deoxyadenosine adducts of 1,2,3,4-diepoxybutane: synthesis, structural elucidation, and mechanistic studies. *Chem. Res. Toxicol.* 23, 118–133.
- (297) Kotapati, S., Wickramaratne, S., Esades, A., Boldry, E. J., Quirk Dorr, D., Pence, M. G., Guengerich, F. P., and Tretyakova, N. Y. (2015) Polymerase bypass of N6-deoxyadenosine adducts derived from epoxide metabolites of 1,3-butadiene. *Chem. Res. Toxicol.* 28, 1496–1507.

- (298) Chang, S. C., Seneviratne, U. I., Wu, J., Tretyakova, N., and Essigmann, J. M. (2017) 1,3-Butadiene-induced adenine DNA adducts are genotoxic but only weakly mutagenic when replicated in escherichia coli of various repair and replication backgrounds. *Chem. Res. Toxicol.* *30*, 1230–1239.
- (299) Dipple, A. (1999) DNA reactions, mutagenic action and stealth properties of polycyclic aromatic hydrocarbon carcinogens (Review). *Int. J. Oncol.* *14*, 103–111.
- (300) Bigger, C. A. H., Pontén, I., Page, J. E., and Dipple, A. (2000) Mutational spectra for polycyclic aromatic hydrocarbons in the supF target gene. *Mutat. Res. - Fundam. Mol. Mech. Mutagen.* *450*, 75–93.
- (301) Villalta, P. W., Hochalter, J. B., and Hecht, S. S. (2017) Ultrasensitive high-resolution mass spectrometric analysis of a DNA adduct of the carcinogen benzo[a]pyrene in human lung. *Anal. Chem.* *89*, 12735–12742.
- (302) Stepanov, I., and Hecht, S. S. (2005) Tobacco-specific nitrosamines and their pyridine-N-glucuronides in the urine of smokers and smokeless tobacco users. *Cancer Epidemiol. Biomarkers Prev.* *14*, 885–891.
- (303) McKennis, H., Schwartz, S. L., Turnbull, L. B., Tamaki, E., and Bowman, E. R. (1964) The metabolic formation of γ -(3-pyridyl)- γ -hydroxybutyric acid and its possible intermediary role in the mammalian metabolism of nicotine. *J. Biol. Chem.* *239*, 3981–3989.
- (304) McKennis, H., Schwartz, S. L., and Bowman, E. R. (1964) Alternate routes in the metabolic degradation of the pyrrolidine ring of nicotine. *J. Biol. Chem.* *239*, 3990–3996.
- (305) Schwartz, S. L., and McKennis, H. (1963) Studies on the degradation of the pyrrolidine ring of (—)-nicotine in vivo: formation of γ -(3-pyridyl)- γ -oxobutyric acid. *J. Biol. Chem.* *238*, 1807–1812.
- (306) Hecht, S. S., Hatsukami, D. K., Bonilla, L. E., and Hochalter, J. B. (1999)

Quantitation of 4-oxo-4-(3-pyridyl)butanoic acid and enantiomers of 4-hydroxy-4-(3-pyridyl)butanoic acid in human urine: A substantial pathway of nicotine metabolism. *Chem. Res. Toxicol.* 12, 172–179.

(307) Stepanov, I., Jensen, J., Hatsukami, D., and Hecht, S. (2006) Tobacco-specific nitrosamines in new tobacco products. *Nicotine Tob. Res.* 8, 309–313.

(308) Stepanov, I., Gupta, P. C., Dhumal, G., Yershova, K., Toscano, W., Hatsukami, D., and Parascandola, M. (2015) High levels of tobacco-specific N-nitrosamines and nicotine in Chaini Khaini, a product marketed as snus. *Tob. Control* 24, e271–e274.

(309) Carmella, S. G., Kagan, S. S., Kagan, M., Foiles, P. G., Palladino, G., Quart, A. M., Quart, E., and Hecht, S. S. (1990) Mass spectrometric analysis of tobacco-specific nitrosamine hemoglobin adducts in snuff dippers, smokers, and nonsmokers. *Cancer Res.* 50, 5438–5445.

(310) (2019) Urine 24-hour volume. *Medlin. Med. Encycl.* U.S. National Library of Medicine.

(311) Digard, H., Gale, N., Errington, G., Peters, N., and McAdam, K. (2013) Multi-analyte approach for determining the extraction of tobacco constituents from pouched snus by consumers during use. *Chem. Cent. J.* 7, 1–12.